

Intensity Attenuation in Indian Earthquakes

A Thesis Submitted
in Partial Fulfillment of the Requirements
for the Degree of

MASTER OF TECHNOLOGY

by

Sailender Kumar Chaubey
(Roll No. 9910324)



Department of Civil Engineering
Indian Institute of Technology Kanpur
August 2001

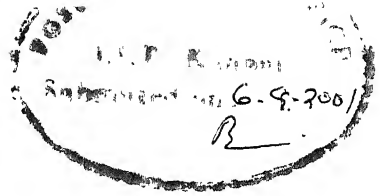
४ FEB 2009 / ०८
पुस्तकालय केन्द्र कर्पुसत्कालय
भारतीय ब्रिंदोगुकी संस्थान कानपुर

अवास्ति क्र० A_141861.....



A141861

CERTIFICATE



It is certified that the work contained in this thesis entitled "*Attenuation of Intensity in Indian Earthquakes*" by Mr. Sailender Kumar Chaubey (*Roll Number: 9910324*), has been carried out under our supervision and this work has not been submitted elsewhere for a degree.

(Mr. P. L. Narula)
Former Deputy Director General
Geological Survey of India
Faridabad


(Dr. Sudhir K. Jain)
Professor and Head
Department of Civil Engineering
Indian Institute of Technology, Kanpur

July, 2001

Abstract

India has experienced a large number of earthquakes in the past. The number of strong motion records from these earthquakes is very small, and is not sufficient to be used for the development of attenuation relationships and to evaluate seismic risk for a future earthquake. On the contrary, intensity maps are available for a substantial number of earthquakes and it is prudent to use these for the development of attenuation relationships.

In this study, 59 earthquakes from different parts of the country have been considered. The isoseismals are collected from different sources. All the isoseismals along with their intensity distance data are presented in a tabular form. The Indian subcontinent is divided into six attenuation provinces, *viz.*, Northwest, North, Northeast, Peninsular, Foredeep and Subduction. Different attenuation models are tried and best model has been found. For the first time, Indian subcontinent models relating magnitude and maximum intensity have been developed.

Intensity Attenuation relationships have been developed for each region. A single equation is also developed for entire Indian subcontinent. Epicentral as well as hypocentral distance has been used and relationships are developed along the major and minor axes of the fault in addition to that for average attenuation (considering average radius of intensity contour as distance parameter). The derived relationships are compared with that of India and other countries.

The approximate decay pattern of intensity for different provinces and distance up to which the intensity decay curve follows a particular trend has been found. It has been shown, whether it is prudent to use the relationships developed in other countries for seismic risk analysis in India.

Acknowledgement

I express my deep sense of gratitude to my thesis supervisor, Professor Sudhir K. Jain and Mr P. L. Narula, for their valuable and unbiased guidance, critical discussions, continuous encouragement, and support during the thesis program. Their constant surveillance and suggestions have helped me in the critical stages of the thesis. I am especially indebted to Professor Jain for keeping a special interest on the topic and helping me to complete my work well in time. Without the helpful guidance from Dr. Debasis Kundu, it would not have been possible for me to tackle the problems related to statistics.

I am also deeply indebted to C. V. R. Murthy for the constant support and encouragement provided throughout my course. I am thankful to Mr. Prabhar Pande of Geological survey of India, for providing me with the intensity data. I thank the faculty at IIT kanpur, without there help it would not have been possible for me to cover many of the unfamiliar territories in my subject.

The moments I spend with my friends Alok, Onkar, Sharvan, Dutta, Payal, Arindam, Brajesh, Sarna, Rakesh, Rajiv and many more will always be most memorable periods in my life. It would not have been possible for me to complete this endeavor without the great amount of help I got from Puneet, Jaswant, Anil, Vipin and Pathak. Its has been a pleasure to be with my juniors Santosh, Desai, Ajit, Murthy, Roopen, Kaustub, Ramesh.

I am gratefully acknowledging the help provided by officers of the Geological Survey of India, for providing intensity data.

S. K. Chaubey

TABLE OF CONTENT

CERTIFICATE	I
ABSTRACT	II
ACKNOWLEDGEMENTS	III
TABLE OF CONTENTS	IV
LIST OF TABLES	VIII
LIST OF FIGURES	XI
1 INTRODUCTION	1
1.1 GENI RAI	1
1.2 METHODS OF DESCRIBING SEISMIC INTENSITY LAW	2
1.3 SCOPE OF THE STUDY	3
2 REVIEW OF EXISTING ATTENUATION RELATIONSHIPS	5
2.1 INTRODUCTION	5
2.2 FACTORS AFFECTING THE INTENSITY ATTENUATION RELATIONSHIP	5
2.2.1 Focal Depth	5
2.2.2 Magnitude	6
2.2.3 Distance	6
2.3 MEDIUM OF PROPAGATION	7
2.3.1 Local Geological Conditions	7
2.3.2 Source Dimension	8
2.4 STEPS IN DEVELOPING INTENSITY ATTENUATION RELATIONSHIPS	9
2.4.1 Collection of Intensity Maps	9
2.4.2 Preparation of Database	9
2.4.3 Normalization of Intensity Scale	10
2.4.4 Division into Different Attenuation Provinces	10
2.4.5 Selection of Suitable Attenuation Relationship	10
2.4.6 Set Initial Epicentral Intensity (I_0) Values	10
2.4.7 Regression Analysis	11
2.4.8 Method of Regression Analysis	12
2.4.8.1 Method of Least Square	12
2.4.8.2 Validity of Results	12
2.4.8.2.1 Analysis of Residuals	12
2.4.8.2.2 Multiple Correlation Coefficient	12
2.4.8.2.3 Uncertainty in Prediction	13
2.5 DIFFICULTIES IN DERIVING THE ATTENUATION RELATIONSHIPS	13
2.5.1 Use of Different Intensity Scale	13
2.5.2 Maximum Intensity	13
2.5.3 Use of Intensity as a Whole Number	14
2.5.4 Source Dimension	14
2.5.5 Initial Epicentral Intensity (I_0)	14
2.6 LITERATURE REVIEW OF ATTENUATION RELATIONSHIPS	15
2.6.1 Egin (1969)	15
2.6.2 Rutledge (1972)	15
2.6.3 Gupta and Nutth (1976)	15
2.6.4 Anderson (1978)	15
2.6.5 Kaila and Sarkar (1978)	16
2.6.6 Chandra (1979)	17
2.6.7 Chandra et al (1979)	18
2.6.8 Malone and Bor (1979)	19
2.6.9 Vanmarcke and Lai (1980)	19
2.6.10 Chandra (1982a)	19

2 6 11 Chandra (1982b)	21
2 6 12 Rao et al. (1982)	23
2 6 13 Benjamin (1983)	24
2 6 14 Yarar et al (1983)	24
2 6 15 Burton et al (1985)	25
2 6 16 Lee and Trifunac (1985)	25
2 6 17 Tilford and Chandra (1985)	26
2 6 18 Drakopoulos and Stamelou (1986)	26
2 6 19 Gupta (1986)	27
2 6 20 Grandori et al (1987)	28
2 6 21 Chavez and Castro (1988)	29
2 6 22 Grandori et al. (1988)	30
2 6 23 Gupta and Trifunac (1988)	31
2 6 24 Pietrafesa et al (1990)	31
2 6 25 Prasad (1991)	32
2 6 26 Tao and Zheng (1991)	33
2 6 27 Timovska (1992)	35
2 6 28 Maugeri and Motta (1993)	36
2 6 29 Pantea (1994)	37
2 6 30 Teramo et al. (1995)	37
2 6 31 Wang et al (1995)	38
2 6 32 Gupta et al (1999)	38
2 7 NEED FOR THE PRESENT STUDY	39
CHAPTER 3	46
3 REVIEW OF EARTHQUAKE INTENSITY DATABASE	46
3 1 INTRODUCTION.....	46
3.2 EARTHQUAKES INTENSITY-DISTANCE DATABASE	47
3 2 1 Northwest Province	47
3 2 1 1 Kashmir Earthquake (1885)	47
3 2 1 2 Kangra Earthquake (1905)	48
3 2 1 3 Baluchistan Earthquake (1909)	49
3 2 1 4 North West Himalayan Earthquake (1929)	49
3.2 1 5 Mach Earthquake (1931)	49
3 2 1 6 Sharigh Earthquake (1931).....	50
3.2.1.7 Quetta Earthquake (1935).	50
3.2 1 8 Hindukush Earthquake (1937).....	51
3.2 1 9 Pamir Earthquake (1939)	51
3 2 1 10 Chamba Earthquake (1945).....	52
3.2.1 11 Badgom Earthquake (1963).	52
3 2 1 12 Anantnag Earthquake (1967)	52
3 2.1.13 Kinnaur earthquake (1975).....	53
3 2 1 14 Dharamsala Earthquake (1978)	54
3 2 1 15 Kathua Earthquake-1 (Jammu) (1980)	54
3.2 1 16 Kathua Earthquake-2 (Jammu) (1980)	55
3 2 1 17 Dharamsala Earthquake (1986)	55
3 2 1 18 Srinagar Earthquake (1988)	55
3.2.1 19 Chamba Earthquake (1995)	56
3 2 2 Northern Province	56
3 2 2 1 Delhi Earthquake (1960)	56
3.2 2 2 Calcutta Earthquake (1964)	57
3.2 2 3 Indo-Nepal Earthquake (1979)	57
3 2 2 4 Dharichula-Bajang Earthquake (1980)	57
3 2 2 5 Uttarkashi Earthquake (1991)	58
3 2 2 6 Delhi Earthquake (1994)	58
3.2 2 7 Bhind Earthquake (1994)	59
3.2 2 8 Chamoli Earthquake (1996)	59
3 2 2 9 Garhwal Earthquake (1996)	59
3.2 2 10 Indo-Nepal Earthquake (1997)	59
3 2 2 11 Chamoli Earthquake (1999)	60
3 2.3 Foredeep Earthquakes	60
3 2 3 1 Kathmandu Earthquake (1833)	60

3 2 3 2 Bihar-Nepal earthquake (1934)	61
3 2 3 3 Bulandshahar Earthquake (1956)	61
3 2 3 4 Roorkee Earthquake (1975)	62
3 2 3 5 Bihar-Nepal Earthquake (1988)	63
3 2 4 Northeastern Province	64
3 2 4.1 Assam Earthquake (1897)	64
3 2 4 2 Calcutta Earthquake (1906)	65
3 2 4 3 Shrimangal Earthquake (1918)	65
3 2 4 4 Dhubri Earthquake (1930)	66
3 2 4 5 Cachar Earthquake (1984)	66
3.2.5 Subduction Earthquakes	67
3 2 5 1 Assam Earthquake (1950)	67
3 2 5 2 Assam Earthquake (1975)	67
3 2 5 3 Nagaland Earthquake (1970)	68
3 2 5 4 Burma-India Earthquake (1988)	68
3 2 6 Peninsular Earthquakes	69
3 2 6 1 Kutch Earthquake (1819)	69
3 2 6 2 Coimbatore Earthquake (1900)	69
3 2 6 3 Satpura Earthquake (1938)	70
3 2 6 4 Anjar Earthquake (1956)	70
3 2 6 5 Koyna Earthquake (1967)	71
3 2 6 6 Bhadrachalam Earthquake (1969)	71
3 2 6 7 Broach Earthquake (1970)	71
3 2 6 8 Koyna Earthquake (1973)	72
3 2 6 9 Shimoga Earthquake (1975)	72
3 2 6 10 Jaisalmer Earthquake (1991)	73
3 2 6 11 Saurastra Earthquake (1993)	73
3 2 6 12 Killari (Latur) Earthquake (1993)	73
3 2 6 13 Bonaigar Earthquake (1995)	74
3 2 6 14 Jabalpur Earthquake (1997)	74
3 2 6 15 Bhuj earthquake (2001)	75
CHAPTER 4	169
4 DEVELOPMENT OF ATTENUATION RELATIONSHIPS	169
4 1 INTRODUCTION.	169
4 2 MODEL AND SHAPE OF ISOSISMAL.....	169
4.3 ATTENUATION Relationships of EPICENTRAL INTENSITY.....	169
4 4 ATTENUATION PROVINCES	174
4.5 DEVELOPMENT OF ATTENUATION RELATIONSHIPS.....	174
4 5 1 Selection of Parameters	174
4 5.2 Earthquake Parameters	174
4 5 3 Independent Variables	175
4 5 4 Source Mechanism	175
4 5 5 Propagation Parameters	175
4 5 6 Site Parameters	176
4 5 7 Type of Equation Used	176
4 5 8 Preliminary Analysis of the Data	177
4.6 DEVELOPMENT OF INTENSITY ATTENUATION RELATIONSHIPS.....	177
4.7 ADEQUACY OF THE MODEL	178
4 7.1 Analysis of Residue	178
4 7.2 Significance Testing of Coefficients	178
4.8 SQUARED MULTIPLE R	179
CHAPTER 5	198
5 DISCUSSION AND CONCLUSIONS.	198
5 1 INTRODUCTION...	198
5.2 DISCUSSION OF RESULTS	198
5 2.1 Type of Equations and Earthquake Parameters Used	198
5 2 2 Selection of the Best Equation.	199
5 2 3 Regional Dependency	200
5 2.4 Magnitude Dependency	200

5.2.5 Choice of Distance	200
5.2.6 Effect of Isoseismal Modeling	201
5.2.7 Approximate Decay Pattern	201
5.3 ATTENUATION FOR DIFFERENT PROVINCES	202
5.3.1 Equation Involving Magnitude	202
5.3.2 Equation Involving Maximum Intensity	202
5.3.3 Equation Involving Epicentral Intensity	203
5.4 COMPARISON OF ATTENUATION PATTERN OF WHOLE INDIA SUBCONTINENT WITH UNITED STATES .	203
5.5 COMPARISON WITH THE BHUJ 2001 EARTHQUAKE (M 7.9, IMAX 10)	204
5.6 CONCLUSIONS	204
5.7 SCOPE FOR FUTURE STUDIES	205
REFERENCES	226

List of Tables

TABLE 2.1 AVAILABLE EQUATIONS FOR INDIAN PROVINCES	41
TABLE 2.2 AVAILABLE EQUATIONS FOR UNITED STATES	41
TABLE 2.3 RELATIVE DIFFERENCE IN EXPECTED INTENSITY LEVELS FOR GEOLOGICAL MAPS UNITS AS SHOWN IN THE GEOLOGICAL MAP OF CALIFORNIA [EVERNDEN AND THOMSON, 1985] (TAKEN FROM REITER 1991). ..	41
TABLE 2.4 CONVERSION TABLE FOR INTENSITY PREPARED BY KAILA AND SARKAR (1978).....	42
TABLE 3.1 KASHMIR EARTHQUAKE (1885).....	77
TABLE 3.2 KANGRA EARTHQUAKE (1905).....	77
TABLE 3.3 BALUCHISTAN EARTHQUAKE (1909).....	77
TABLE 3.4 HIMALAYAN EARTHQUAKE (1929).....	77
TABLE 3.5 MACH EARTHQUAKE (1931).....	78
TABLE 3.6 SARIGH EARTHQUAKE (1931).....	78
TABLE 3.7 QUETTA EARTHQUAKE (1935).....	78
TABLE 3.8 HINDUKUSH EARTHQUAKE (1937).....	78
TABLE 3.9 PAMIR EARTHQUAKE (1939)	79
TABLE 3.10 CHAMBA EARTHQUAKE (1945)	79
TABLE 3.11 BADGOM EARTHQUAKE (1963)	79
TABLE 3.12 ANANTNAG EARTHQUAKE (1967)	79
TABLE 3.13 KINNAUR EARTHQUAKE (1975).....	80
TABLE 3.14 DHARAMSALA EARTHQUAKE (1978).....	80
TABLE 3.15 JAMMU-1 EARTHQUAKE (1980).....	80
TABLE 3.16 JAMMU-2 EARTHQUAKE (1980).....	81
TABLE 3.17 DHARAMSALA EARTHQUAKE (1986).....	81
TABLE 3.18 SRINAGAR EARTHQUAKE (1988)	81
TABLE 3.19 CHAMBA EARTHQUAKE (1995)	81
TABLE 3.20 DELHI EARTHQUAKE (1960).....	81
TABLE 3.21 INDO-NEPAL EARTHQUAKE (1978).....	81
TABLE 3.22 NEPAL EARTHQUAKE (1980).....	82
TABLE 3.23 UTTARKASHI EARTHQUAKE (1991).....	82
TABLE 3.24 DELHI EARTHQUAKE (1994).....	82
TABLE 3.25 BHIND EARTHQUAKE (1994)	82
TABLE 3.26 CHAMOLI EARTHQUAKE (1996).....	83
TABLE 3.27 GHARWAL EARTHQUAKE (1996)	83
TABLE 3.28 INDO-NEPAL EARTHQUAKE (1997).....	83
TABLE 3.29 CHAMOLI EARTHQUAKE (1999).....	83
TABLE 3.30 KATHMANDU EARTHQUAKE (1833).....	83
TABLE 3.31 BIHAR-NEPAL EARTHQUAKE (1934)	84
TABLE 3.32 BULANDSHAHAR EARTHQUAKE (1956)	84
TABLE 3.33 ROORKEE EARTHQUAKE (1975)	84
TABLE 3.34 BIHAR-NEPAL EARTHQUAKE (1988)	84
TABLE 3.35 ASSAM EARTHQUAKE (1897)	85
TABLE 3.36 CALCUTTA EARTHQUAKE (1906)	85
TABLE 3.37 SRIMANGAL EARTHQUAKE (1918)	85
TABLE 3.38 DUBIBRI EARTHQUAKE (1930)	86
TABLE 3.39 CACHAR EARTHQUAKE (1984)	86
TABLE 3.40 ASSAM EARTHQUAKE (1950)	86
TABLE 3.41 ASSAM EARTHQUAKE (1975)	86
TABLE 3.42 NAGALAND EARTHQUAKE (1970)	87
TABLE 3.43 BURMA-INDIA EARTHQUAKE (1988)	87
TABLE 3.44 KUTCH EARTHQUAKE (1819)	87
TABLE 3.45 COIMBATORE EARTHQUAKE (1900)	87
TABLE 3.46 SATPURA EARTHQUAKE (1938).....	87
TABLE 3.47 ANJAR EARTHQUAKE (1956).....	88
TABLE 3.48 CALCUTTA EARTHQUAKE (1964)	88
TABLE 3.49 KOYNA EARTHQUAKE (1967).....	88
TABLE 3.50 BHADRACHALAM EARTHQUAKE (1969)	88
TABLE 3.51 BROACH EARTHQUAKE (1970)	89

TABLE 3.52 KOYNA EARTHQUAKE (1973).....	89
TABLE 3.53 SHIMOGA EARTHQUAKE (1975).....	89
TABLE 3.54 JAISALMER EARTHQUAKE (1991).....	89
TABLE 3.55 SAURASHTRA EARTHQUAKE (1993).....	89
TABLE 3.56 KILLARI EARTHQUAKE (1993).....	90
TABLE 3.57 BONAIGARH EARTHQUAKE (1995).....	90
TABLE 3.58 JABALPUR EARTHQUAKE (1997).....	90
TABLE 3.59 BHUJ EARTHQUAKE (2001).....	90
TABLE 3.60 EARTHQUAKE DETAILS OF NORTHWEST PROVINCE.....	91
TABLE 3.61 EARTHQUAKE DETAILS OF NORTHERN PROVINCE	91
TABLE 3.62 EARTHQUAKE DETAILS OF FOREDEEP PROVINCE.....	92
TABLE 3.63 EARTHQUAKE DETAILS OF NORTHEAST PROVINCE.....	92
TABLE 3.64 EARTHQUAKE DETAILS OF SUBDUCTION PROVINCE	92
TABLE 3.65 EARTHQUAKE DETAILS OF PENINSULAR PROVINCE	93
TABLE 4.1 VALUES OF CONSTANTS, CONFIDENCE BAND, T-STATISTIC VALUES, STANDARD DEVIATION, STANDARD ERROR OF THE EQUATION AND R ² VALUES OF THE MODEL (EQUATION 3 WITH HYPOCENTRAL DISTANCE).....	180
TABLE 4.2 VALUES OF CONSTANTS, CONFIDENCE BAND, T-STATISTIC VALUES, STANDARD DEVIATION, STANDARD ERROR OF THE EQUATION AND R ² VALUES OF THE MODEL (EQUATION 3 WITH EPICENTRAL DISTANCE).....	180
TABLE 4.3 VALUES OF CONSTANTS, CONFIDENCE BAND, T-STATISTIC VALUES, STANDARD DEVIATION, STANDARD ERROR OF THE EQUATION AND R ² VALUES OF THE MODEL (EQUATION 6 WITH HYPOCENTRAL DISTANCE).....	181
TABLE 4.4 VALUES OF CONSTANTS, CONFIDENCE BAND, T-STATISTIC VALUES, STANDARD DEVIATION, STANDARD ERROR OF THE EQUATION AND R ² VALUES OF THE MODEL (EQUATION 6 WITH EPICENTRAL DISTANCE).....	181
TABLE 4.5 VALUES OF CONSTANTS, CONFIDENCE BAND, T-STATISTIC VALUES, STANDARD DEVIATION, STANDARD ERROR OF THE EQUATION AND R ² VALUES OF THE MODEL (EQUATION 10 WITH HYPOCENTRAL DISTANCE).....	182
TABLE 4.6 VALUES OF CONSTANTS, CONFIDENCE BAND, T-STATISTIC VALUES, STANDARD DEVIATION, STANDARD ERROR OF THE EQUATION AND R ² VALUES OF THE MODEL (EQUATION 10 WITH EPICENTRAL DISTANCE).....	182
TABLE 4.7 VALUES OF CONSTANTS, CONFIDENCE BAND, T-STATISTIC VALUES, STANDARD DEVIATION, STANDARD ERROR OF THE EQUATION AND R ² VALUES OF THE MODEL (EQUATION 7 WITH HYPOCENTRAL DISTANCE).....	183
TABLE 4.8 VALUES OF CONSTANTS, CONFIDENCE BAND, T-STATISTIC VALUES, STANDARD DEVIATION, STANDARD ERROR OF THE EQUATION AND R ² VALUES OF THE MODEL (EQUATION 7 WITH EPICENTRAL DISTANCE).....	183
TABLE 4.9 VALUES OF CONSTANTS, CONFIDENCE BAND, T-STATISTIC VALUES, STANDARD DEVIATION, STANDARD ERROR OF THE EQUATION AND R ² VALUES OF THE MODEL (EQUATION 3 WITH HYPOCENTRAL DISTANCE).....	184
TABLE 4.10 VALUES OF CONSTANTS, CONFIDENCE BAND, T-STATISTIC VALUES, STANDARD DEVIATION, STANDARD ERROR OF THE EQUATION AND R ² VALUES OF THE MODEL (EQUATION 3 WITH EPICENTRAL DISTANCE).....	185
TABLE 4.11 VALUES OF CONSTANTS, CONFIDENCE BAND, T-STATISTIC VALUES, STANDARD DEVIATION, STANDARD ERROR OF THE EQUATION AND R ² VALUES OF THE MODEL (EQUATION 6 WITH HYPOCENTRAL DISTANCE).....	186
TABLE 4.12 VALUES OF CONSTANTS, CONFIDENCE BAND, T-STATISTIC VALUES, STANDARD DEVIATION, STANDARD ERROR OF THE EQUATION AND R ² VALUES OF THE MODEL (EQUATION 6 WITH EPICENTRAL DISTANCE).....	187
TABLE 4.13 VALUES OF CONSTANTS, CONFIDENCE BAND, T-STATISTIC VALUES, STANDARD DEVIATION, STANDARD ERROR OF THE EQUATION AND R ² VALUES OF THE MODEL (EQUATION 7 WITH HYPOCENTRAL DISTANCE).....	188
TABLE 4.14 VALUES OF CONSTANTS, CONFIDENCE BAND, T-STATISTIC VALUES, STANDARD DEVIATION, STANDARD ERROR OF THE EQUATION AND R ² VALUES OF THE MODEL (EQUATION 7 WITH EPICENTRAL DISTANCE).....	189
TABLE 4.15 VALUES OF CONSTANTS, CONFIDENCE BAND, T-STATISTIC VALUES, STANDARD DEVIATION, STANDARD ERROR OF THE EQUATION AND R ² VALUES OF THE MODEL (EQUATION 10 WITH HYPOCENTRAL DISTANCE).....	190

TABLE 4.16 VALUES OF CONSTANTS, CONFIDENCE BAND, T-STATISTIC VALUES, STANDARD DEVIATION, STANDARD ERROR OF THE EQUATION AND R^2 VALUES OF THE MODEL (EQUATION 10 WITH EPICENTRAL DISTANCE)	191
TABLE 4.17 VALUES OF THE REGRESSION CONSTANTS OF THE EQUATION $I_{max} = e + f M$ CONSIDERING ALL EARTHQUAKES OF MAGNITUDE MORE THAN OR EQUAL TO 6.....	192
TABLE 4.18 VALUES OF THE REGRESSION CONSTANTS OF THE EQUATION $I_{max} = e + f M$ CONSIDERING ALL EARTHQUAKES OF MAGNITUDE LESS THAN 6.	192
TABLE 4.19 VALUES OF THE REGRESSION CONSTANTS OF THE EQUATION $I_o = e + f M + g I_{max}$ CONSIDERING ALL EARTHQUAKES OF MAGNITUDE MORE THAN OR EQUAL TO 6	192
TABLE 4.20 VALUES OF THE REGRESSION CONSTANTS OF THE EQUATION $I_o = e + f M + g I_{max}$ CONSIDERING ALL EARTHQUAKES OF MAGNITUDE LESS THAN 6.....	192
TABLE 5.1 POSSIBILITY OF COMBINING THE REGIONS AS PER T-TEST VALUES FOR THE COMPARISON OF CONSTANTS OF EQUATION 10 FOR HYPOCENTRAL DISTANCE (IN BRACKET ARE THOSE OF EQUATION 7).	206
TABLE 5.2 POSSIBILITY OF COMBINING THE SMALLER AND LARGER EARTHQUAKES GROUP, AS PER T-TEST VALUES FOR THE COMPARISON OF CONSTANTS, OF EQUATION 10 FOR HYPOCENTRAL DISTANCE (IN BRACKET ARE THOSE OF EQUATION 7).....	206
TABLE 5.3 BEST DISTANCE PARAMETER FOR DIFFERENT TYPE OF EQUATIONS.	206
TABLE 5.4 TABLE SHOWING STANDARD DEVIATIONS AND R^2 VALUES FOR DIFFERENT PROVINCES AS PER EQUATION 8, 9 AND 10 RESPECTIVELY, FOR AVERAGE ATTENUATION.....	207
TABLE 5.5 TABLE SHOWING STANDARD DEVIATIONS AND R^2 VALUES FOR DIFFERENT PROVINCES AS PER EQUATION 8, 9 AND 10 RESPECTIVELY, FOR LONGITUDINAL ATTENUATION	207
TABLE 5.6 TABLE SHOWING STANDARD DEVIATIONS AND R^2 VALUES FOR DIFFERENT PROVINCES AS PER EQUATION 8, 9 AND 10 RESPECTIVELY, FOR TRANSVERSE ATTENUATION.	208
TABLE 5.7 GENERAL TREND OF ATTENUATION PATTERN FOR DIFFERENT ATTENUATION PROVINCES.....	208
TABLE 5.8 APPROXIMATE PATTERN OF TYPE OF ATTENUATION PATTERNS WITH DISTANCE.	209

List of Figures

FIGURE 2.1 FIGURE SHOWING GRAPHICAL METHOD OF ESTIMATING EPICENTRAL INTENSITY	43
FIGURE 2.2 COMPARISON OF INTENSITY ATTENUATION OF PAST RELATIONS OF INDIAN PROVINCES WITH THOSE OF UNITED STATES	43
FIGURE 2.3 A COMPARISON OF SEISMIC INTENSITY SCALES (AFTER MURPHU AND O'BRIEN, 1977; AND RICHTER, 1958) (TAKEN FROM REITER, 1991)	44
FIGURE 2.4 DIFFERENT DEFINITIONS OF DISTANCES USED IN THE ATTENUATION RELATIONSHIPS [CAMPBELL, 1985]	45
FIGURE 3.1 ISOSEISMAL OF KASHMIR EARTHQUAKE (M 7) OF 30 TH MAY 1885 FOLLOWING MALLETT'S SCALE AFTER JONES (1885)	94
FIGURE 3.2 ISOSEISMAL OF KASHMIR EARTHQUAKE (M 7) OF 30 TH MAY 1885 AND BADGAM EARTHQUAKE (M 5.5) OF 2 ND SEPTEMBER 1963 FOLLOWING MM SCALE AFTER GOSAIN AND ARYA (1967)	95
FIGURE 3.3 ISOSEISMAL OF BALUCHISTAN EARTHQUAKE OF 21 ST OCTOBER 1906 FOLLOWING RF SCALE AFTER HARON (1910)	96
FIGURE 3.4 ISOSEISMAL OF NORTHWEST HIMALAYAN EARTHQUAKE (M 7.1) OF 1 ST FEBRUARY 1929 FOLLOWING RF SCALE AFTER COULSON (1930)	97
FIGURE 3.5 ISOSEISMAL OF NORTHWEST HIMALAYAN EARTHQUAKE (M 7.1) OF 1 ST FEBRUARY 1929 FOLLOWING MM SCALE AFTER MUKHERJEE (1950)	98
FIGURE 3.6 ISOSEISMAL OF MACHI EARTHQUAKE (M 7.5) OF 27 TH AUGUST 1931 FOLLOWING RF SCALE AFTER WEST (1934)	99
FIGURE 3.7 ISOSEISMAL OF SHARIGII EARTHQUAKE (M 7) OF 25 TH AUGUST 1931 FOLLOWING RF SCALE AFTER WEST (1934)	100
FIGURE 3.8 ISOSEISMAL OF QUILIA EARTHQUAKE (M 7.5) OF 31 ST MAY 1935 FOLLOWING RF SCALE AFTER WEST (1936)	101
FIGURE 3.9 ISOSEISMAL OF HINDKUSH EARTHQUAKE (M 7.2) OF 14 TH NOVEMBER 1937 FOLLOWING RF SCALE AFTER COULSON (1938)	102
FIGURE 3.10 ISOSEISMAL OF PAMIR EARTHQUAKE (M 6.9) OF 21 ST NOVEMBER 1939 FOLLOWING MM SCALE AFTER COULSON (1940)	103
FIGURE 3.11 ISOSEISMAL OF CHAMBA EARTHQUAKE (M 6.5) OF 22 ND JULY 1945 FOLLOWING MM SCALE AFTER KAPILA (1959)	104
FIGURE 3.12 ISOSEISMAL OF BADGUM EARTHQUAKE (M 5.5) OF 2 ND SEPTEMBER 1963 FOLLOWING MM SCALE AFTER WAKHAI LOO (1977)	105
FIGURE 3.13 ISOSEISMAL OF ANANTNAG EARTHQUAKE (M 5.7) OF 20 TH FEBRUARY 1967 FOLLOWING MM SCALE: AFTER WAKHAI LOO (1977)	106
FIGURE 3.14 ISOSEISMAL OF ANANTNAG EARTHQUAKE (M 5.7) OF 20 TH FEBRUARY 1967 FOLLOWING MM SCALE: AFTER GOSAIN AND ARYA (1967)	107
FIGURE 3.15 ISOSEISMAL OF JAMMU EARTHQUAKE (M 5.5, 5.4) OF 24 TH AUGUST 1980 FOLLOWING MM SCALE: AFTER KRISHNAMURTHY ET AL. (1990)	108
FIGURE 3.16 ISOSEISMAL MAP OF SRINAGAR EARTHQUAKE (M 3.2) OF 8 TH FEBRUARY 1988 FOLLOWING MSK SCALE AFTER GUPTA (1988)	109
FIGURE 3.17 ISOSEISMAL MAP OF CHAMBA EARTHQUAKE (M 4.5) OF 24 TH MARCH 1995 FOLLOWING MSK SCALE: AFTER PANDE AND SHARDA (1995)	110
FIGURE 3.18 ISOSEISMAL MAP OF KATHMANDU EARTHQUAKE OF 26 TH AUGUST 1833 FOLLOWING MM SCALE TAKEN FROM DASGUPTA ET AL. (2000)	111
FIGURE 3.19 ISOSEISMAL OF KANGRA EARTHQUAKE (M 8.6) OF 4 TH APRIL 1905 FOLLOWING RF SCALE AFTER MIDDLEMISS (1910)	112
FIGURE 3.20 ISOSEISMAL MAP OF BIHAR-NEPAL EARTHQUAKE (M 8.4) OF 15 TH JANUARY 1934 FOLLOWING MM SCALE AFTER GSI (1939)	113
FIGURE 3.21 ISOSEISMAL MAP OF BULANDSHAHAR EARTHQUAKE (M 6.5) OF 10 TH OCTOBER 1956 FOLLOWING MM SCALE: AFTER TANDON (1975)	114
FIGURE 3.22 ISOSEISMAL MAP OF DELHI EARTHQUAKE (M 6) OF 27 TH AUGUST 1956 FOLLOWING MM SCALE: AFTER MUKTINATH ET AL. (1969)	115
FIGURE 3.23 ISOSEISMAL OF KINNAUR EARTHQUAKE (M 7) OF 19 TH JANUARY 1975 FOLLOWING MM SCALE: AFTER HUKKU ET AL. (1975)	116
FIGURE 3.24 ISOSEISMAL OF KINNAUR EARTHQUAKE (M 7) OF 19 TH JANUARY 1975 FOLLOWING MM SCALE: AFTER GOSAVI ET AL. (1977)	117
FIGURE 3.25 ISOSEISMAL OF KINNAUR EARTHQUAKE (M 7) OF 19 TH JANUARY 1975 FOLLOWING MM SCALE: AFTER SINGH ET AL. (1975)	118

FIGURE 3.26 ISOSEISMAL OF DHARAMSHALA EARTHQUAKE (M 5) OF 15 TH JUNE 1978 FOLLOWING MM SCALE AFTER KUMAR ET AL. (1981)	119
FIGURE 3.27 ISOSEISMAL MAP OF ROORKEE EARTHQUAKE (M 4.7) OF 6 TH NOVEMBER 1975 FOLLOWING MM SCALE AFTER ARYA ET AL. (1977).....	120
FIGURE 3.28 ISOSEISMAL MAP OF NEPAL EARTHQUAKE (M 5.8) OF 21 ST MAY 1979 FOLLOWING MM SCALE AFTER KUMAR ET AL. (1981)	121
FIGURE 3.29 ISOSEISMAL MAP OF NEPAL EARTHQUAKE OF (M 6.1) 29 TH JULY 1980 FOLLOWING MM SCALE AFTER SRIVASTAVA ET AL. (1980).....	122
FIGURE 3.30 ISOSEISMAL MAP OF DHARAMSHALA EARTHQUAKE (M 5.7) OF 26 TH APRIL 1986 FOLLOWING MM SCALE AFTER GUPTA ET AL. (1986)	123
FIGURE 3.31 ISOSEISMAL MAP OF BIHAR-NEPAL EARTHQUAKE (M 6.4) OF 20 TH AUGUST 1988 FOLLOWING MM SCALE AFTER GSI (1993).	124
FIGURE 3.32 ISOSEISMAL MAP OF BIHAR-NEPAL EARTHQUAKE (M 6.4) OF 20 TH AUGUST 1988 FOLLOWING MM SCALE AFTER THAKKAR (1988).	125
FIGURE 3.33 ISOSEISMAL MAP OF UTTARKASHI EARTHQUAKE (M 6.6) OF 20 TH OCTOBER FOLLOWING MSK SCALE AFTER NARUI A ET AL. (1995).....	126
FIGURE 3.34 ISOSEISMAL MAP OF UTTARKASHI EARTHQUAKE (M 6.6) OF 20 TH OCTOBER FOLLOWING MSK SCALE AFTER RASTOGI AND CHADHA (1995).	127
FIGURE 3.35 ISOSEISMAL MAP OF UTTARKASHI EARTHQUAKE (M 6.6) OF 20 TH OCTOBER FOLLOWING MSK SCALE AFTER GSI (1992).	128
FIGURE 3.36 ISOSEISMAL MAP OF DELHI EARTHQUAKE (M 4) OF 28 TH JULY 1994 FOLLOWING MSK SCALE AFTER GUPTA AND SHARDA (1996).....	129
FIGURE 3.37 ISOSEISMAL MAP OF BHIND EARTHQUAKE (M 4.8) OF 1 ST SEPTEMBER 1994 FOLLOWING MSK SCALE AFTER PANDE ET AL. (1995).	130
FIGURE 3.38 ISOSEISMAL MAP OF CHAMOLI EARTHQUAKE (M 4.5) OF 23 RD JANUARY 1996 FOLLOWING MSK SCALE AFTER SINGH AND JOSHI (1996).	131
FIGURE 3.39 ISOSEISMAL MAP OF GARHWAL EARTHQUAKE (M 5) OF 26 TH MARCH 1996 FOLLOWING MSK SCALE AFTER PANDL AND GAIROLA (1996)..	132
FIGURE 3.40 ISOSEISMAL MAP OF INDO-NEPAL EARTHQUAKE (M 5.5) OF 5 TH JANUARY 1997 FOLLOWING MM SCALE AFTER DASGUPTA ET AL. (2000).	133
FIGURE 3.41 ISOSEISMAL MAP OF CHAMOLI EARTHQUAKE (M 6.3) OF 29 TH MARCH 1999 FOLLOWING MSK SCALE TAKEN FROM SHANKER AND NARULA (1999).	134
FIGURE 3.42 ISOSEISMAL MAP OF ASSAM EARTHQUAKE (M 8.7) OF 12 TH JUNE 1897 FOLLOWING OLHAM'S SCALE AFTER OLDHAM (1899)	135
FIGURE 3.43 ISOSEISMAL MAP OF ASSAM EARTHQUAKE (M 8.7) OF 12 TH JUNE 1897 FOLLOWING MSK AFTER NARUI A AND SHARDA (1997).	136
FIGURE 3.44 ISOSEISMAL MAP OF CALCUTTA EARTHQUAKE OF 29 TH SEPTEMBER 1906 FOLLOWING MM SCALE AFTER MIDDLEMISS (1907).....	137
FIGURE 3.45 ISOSEISMAL MAP OF SRIMANGAL EARTHQUAKE (M 7.6) OF 8 TH JULY 1918 FOLLOWING MM SCALE AFTER STAURT (1918)	138
FIGURE 3.46 ISOSEISMAL MAP OF DHUBRI EARTHQUAKE (M 7.1) OF 3 RD JULY 1930 FOLLOWING MM SCALE AFTER GEE (1934) TAKEN FROM KAILA AND SARKAR (1978)	139
FIGURE 3.47 ISOSEISMAL MAP OF ASSAM EARTHQUAKE (M 8.7) OF 15 TH AUGUST 1950 FOLLOWING MM SCALE AFTER PODDAR (1950).	140
FIGURE 3.48 ISOSEISMAL MAP OF ASSAM EARTHQUAKE (M 8.7) OF 15 TH AUGUST 1950 FOLLOWING MM SCALE TAKEN FROM DASGUPTA ET AL. (2000).	141
FIGURE 3.49 ISOSEISMAL MAP OF ASSAM EARTHQUAKE (M 6.7) OF 8 TH JULY 1975 FOLLOWING MM SCALE AFTER GOSAVI ET AL. (1977)	142
FIGURE 3.50 ISOSEISMAL MAP OF NAGALAND EARTHQUAKE (M 6.4) OF 29 TH JULY 1970 FOLLOWING MM SCALE AFTER GUHA AND GOSAVI (1974).	143
FIGURE 3.51 ISOSEISMAL MAP OF CACHAR EARTHQUAKE (M 5.5) OF 31 ST DECEMBER 1984 FOLLOWING MM SCALE AFTER NARUI A [TAKEN FROM DASGUPTA ET AL. (2000)].	144
FIGURE 3.52 ISOSEISMAL MAP OF BURMA EARTHQUAKE (M 6.8) OF 6 TH AUGUST 1988 FOLLOWING MM SCALE AFTER KUMAR (1992)	145
FIGURE 3.53 ISOSEISMAL MAP OF KUTCH EARTHQUAKE OF 16 TH JUNE 1819 FOLLOWING MM SCALE TAKEN FROM DASGUPTA ET AL. (2000).	146
FIGURE 3.54 ISOSEISMAL MAP OF COIMBATORE EARTHQUAKE (M 6) OF 8 TH FEBRUARY 1900 FOLLOWING MM SCALE AFTER BASU (1964) TAKEN FROM KAILA AND SARKAR (1978).	147
FIGURE 3.55 ISOSEISMAL MAP OF SATPURA EARTHQUAKE (M 6.2) OF 14 TH MARCH 1938 FOLLOWING MM SCALE AFTER MUKHERJI E (1942) TAKEN FROM DASGUPTA ET AL. (2000).	148

FIGURE 3.56 ISOSEISMAL MAP OF ANJAR EARTHQUAKE (M 7) OF 21 ST JULY 1956 FOLLOWING MM SCALE AFTER TANDON (1959).	149
FIGURE 3.57 ISOSEISMAL MAP OF ANJAR EARTHQUAKE (M 7) OF 21 ST JULY 1956 FOLLOWING MM SCALE TAKEN FROM DASGUPTA ET AL. (2000).	150
FIGURE 3.58 ISOSEISMAL MAP OF CALCUTTA EARTHQUAKE (M 5.5) OF 15 TH AUGUST 1964 FOLLOWING MM SCALE AFTER JHINGRAN ET AL. (1969) TAKEN FROM KAILA AND SARKAR (1978).	151
FIGURE 3.59 ISOSEISMAL MAP OF KOYNA EARTHQUAKE (M 5.2) OF 10 TH DECEMBER 1967 FOLLOWING MM SCALE AFTER CHATTHRI ET AL. (1967) TAKEN FROM KAILA AND SARKAR (1978).	152
FIGURE 3.60 ISOSEISMAL MAP OF BHADRACHALAM EARTHQUAKE (M 6.5) OF 13 TH APRIL 1969 FOLLOWING MM SCALE AFTER MUKHARI (1971) TAKEN FROM KAILA AND SARKAR (1978).	153
FIGURE 3.61 ISOSEISMAL MAP OF BHADRACHALAM EARTHQUAKE (M 6.5) OF 13 TH APRIL 1969 FOLLOWING MM SCALE TAKEN FROM DASGUPTA ET AL. (2000).	154
FIGURE 3.62 ISOSEISMAL MAP OF BROACH EARTHQUAKE (M 6.7) OF 23 RD MARCH 1970 FOLLOWING MM SCALE AFTER CHAUDHURY ET AL. (1970) TAKEN FROM KAILA AND SARKAR (1978).	155
FIGURE 3.63 ISOSEISMAL MAP OF BROACH EARTHQUAKE (M 6.7) OF 23 RD MARCH 1970 FOLLOWING MM SCALE TAKEN FROM DASGUPTA ET AL. (2000).	156
FIGURE 3.64 ISOSEISMAL MAP OF KOYNA EARTHQUAKE (M 5.2) OF 17 TH OCTOBER 1973 FOLLOWING MM SCALE AFTER GOSAVI ET AL. (1977).	157
FIGURE 3.65 ISOSEISMAL MAP OF SHIMOGA EARTHQUAKE (M 5) OF 12 TH MAY 1975 FOLLOWING MM SCALE AFTER GOSAVI ET AL (1977) TAKEN FROM KAILA AND SARKAR (1978)	158
FIGURE 3.66 ISOSEISMAL MAP OF JAISALMER EARTHQUAKE (M 5.5) OF 8 TH NOVEMBER 1991 FOLLOWING MM SCALE TAKEN FROM DASGUPTA ET AL. (2000).	159
FIGURE 3.67 ISOSEISMAL MAP OF SAURASTRA COAST EARTHQUAKE OF 24 TH AUGUST 1993 FOLLOWING MM SCALE TAKEN FROM DASGUPTA ET AL. (2000).	160
FIGURE 3.68 ISOSEISMAL MAP OF KILLARI (LATOR) EARTHQUAKE (M 6.2) OF 30 TH SEPTEMBER 1993 FOLLOWING MM SCALE TAKEN FROM DASGUPTA ET AL. (2000).	161
FIGURE 3.69 ISOSEISMAL MAP OF KILLARI (LATOR) EARTHQUAKE (M 6.2) OF 30 TH SEPTEMBER 1993 FOLLOWING MM SCALE TAKEN FROM NARULA ET AL. (1996A).	162
FIGURE 3.70 ISOSISMAL MAP OF BONAIGARH EARTHQUAKE (M 4.4) OF 27 TH MARCH 1995 FOLLOWING MSK SCALE TAKEN FROM DASGUPTA ET AL. (2000).	163
FIGURE 3.71 ISOSEISMAL MAP OF JABALPUR EARTHQUAKE (M 6) OF MAY 1997 FOLLOWING MSK SCALE TAKEN FROM DASGUPTA ET AL. (2000).	164
FIGURE 3.72 ISOSEISMAL MAP OF JABALPUR EARTHQUAKE (M 6) OF MAY 1997 FOLLOWING MSK SCALE AFTER CHATURVEDI ET AL. (2000).	165
FIGURE 3.73 ISOSEISMAL MAP OF BIUJ EARTHQUAKE (M 7.9) OF 26 TH JANUARY 2001 FOLLOWING MSK SCALE AFTER NARULA AND CHAUBEY (2001).	166
FIGURE 3.74 ISOSEISMAL MAP OF BIUJ EARTHQUAKE (M 7.9) OF 26 TH JANUARY 2001 FOLLOWING MSK SCALE AFTER GSI (2001).	167
FIGURE 3.75 PLOT OF EARTHQUAKES CONSIDERED IN THE PRESENT STUDY	168
FIGURE 4.1 DATA PLOTS FOR NORTHWEST PROVINCE EARTHQUAKES.	193
FIGURE 4.2 DATA PLOTS FOR PENINSULAR PROVINCE EARTHQUAKES.	193
FIGURE 4.3 DATA PLOTS FOR NORTHI EARTHQUAKES.	194
FIGURE 4.4 DATA PLOTS FOR FOREDEEP EARTHQUAKES.	194
FIGURE 4.5 DATA PLOTS FOR SUBDUCTION EARTHQUAKES.	195
FIGURE 4.6 DATA PLOTS FOR NORTHEAST EARTHQUAKES.	195
FIGURE 4.7 PLOTS OF RESIDUALS OF THE REGRESSION ANALYSIS FOR NORTHERN PROVINCE CONSIDERING ALL EARTHQUAKES.	196
FIGURE 4.8 PLOTS OF RESIDUALS OF THE REGRESSION ANALYSIS FOR NORTHWEST PROVINCE CONSIDERING ALL EARTHQUAKES	196
FIGURE 4.9 PLOTS OF RESIDUALS OF THE REGRESSION ANALYSIS FOR NORTHEAST PROVINCE CONSIDERING ALL EARTHQUAKES.	197
FIGURE 4.10 PLOTS OF RESIDUALS OF THE REGRESSION ANALYSIS FOR PENINSULAR PROVINCE CONSIDERING ALL EARTHQUAKES.	198
FIGURE 5.1 ATTENUATION OF INTENSITY WITH HYPOCENTRAL DISTANCE FOR DIFFERENT PROVINCES	210
FIGURE 5.2 ATTENUATION OF INTENSITY WITH HYPOCENTRAL DISTANCE FOR DIFFERENT PROVINCES USING EQUATION 10 CONSIDERING EARTHQUAKES OF MAGNITUDE GREATER THAN OR EQUAL TO 6.	210
FIGURE 5.3 ATTENUATION OF INTENSITY WITH HYPOCENTRAL DISTANCE FOR DIFFERENT PROVINCES USING EQUATION 10 CONSIDERING EARTHQUAKES OF MAGNITUDE LESS THAN 6.	211

FIGURE 5.4 PLOT OF ATTENUATION RATES OF DIFFERENT EARTHQUAKE GROUP FOR NORTHERN PROVINCE AS PER EQUATION 10	212
FIGURE 5.5 PLOT OF ATTENUATION RATES OF DIFFERENT EARTHQUAKE GROUP FOR NORTHWEST PROVINCE AS PER EQUATION 10.	212
FIGURE 5.6 PLOT OF ATTENUATION RATES OF DIFFERENT EARTHQUAKE GROUP FOR PENINSULAR PROVINCE AS PER EQUATION 10.	212
FIGURE 5.7 ATTENUATION PATTERN FOR DIFFERENT PROVINCES WITH EPICENTRAL AND HYPOCENTRAL DISTANCE FOR M7.0 .. .	213
FIGURE 5.8 PLOT OF ATTENUATION ALONG AVERAGE, LONGITUDINAL AND TRANSVERSE DIRECTION FOR	214
FIGURE 5.9 ATTENUATION PATTERN FOR DIFFERENT ATTENUATION PROVINCES WITH DISTANCE AS PARAMETER (EQUATIONS 8, 9 AND 10) .. .	215
FIGURE 5.10 PLOT OF ATTENUATION WITH DIFFERENT DISTANCE PARAMETERS FOR NORTH PROVINCE CONSIDERING EARTHQUAKES OF M<6 (EQUATIONS 8, 9 AND 10).	216
FIGURE 5.11 PLOT OF ATTENUATION WITH DIFFERENT DISTANCE PARAMETERS FOR NORTHWEST PROVINCE CONSIDERING EARTHQUAKES OF M<6 (EQUATIONS 8, 9 AND 10).	216
FIGURE 5.12 PLOT OF ATTENUATION WITH DIFFERENT DISTANCE PARAMETERS FOR PENINSULAR PROVINCE CONSIDERING EARTHQUAKES OF M<6 (EQUATIONS 8, 9 AND 10).	216
FIGURE 5.13 PLOT OF ATTENUATION WITH DIFFERENT DISTANCE PARAMETERS FOR NORTH PROVINCE CONSIDERING EARTHQUAKES OF M≥6 (EQUATIONS 8, 9 AND 10).	217
FIGURE 5.14 PLOT OF ATTENUATION WITH DIFFERENT DISTANCE PARAMETERS FOR NORTHWEST PROVINCE CONSIDERING EARTHQUAKES OF M≥6 (EQUATIONS 8, 9 AND 10).	217
FIGURE 5.15 PLOT OF ATTENUATION WITH DIFFERENT DISTANCE PARAMETERS FOR PENINSULAR PROVINCE CONSIDERING EARTHQUAKES OF M≥6 (EQUATIONS 8, 9 AND 10).	217
FIGURE 5.16 PLOT OF AVERAGE ATTENUATION FOR DIFFERENT PROVINCES FOR MAGNITUDE 8.5, 7.0 AND 5.5 USING EQUATION 3.	218
FIGURE 5.17 PLOT OF AVERAGE ATTENUATION FOR DIFFERENT PROVINCES FOR MAXIMUM INTENSITY 11, 9 AND 6.	220
FIGURE 5.18 COMPARISON OF ATTENUATION PATTERN OF INDIA TO THAT OF UNITED STATES AS GIVEN BY CHANDRA (1979).	222
FIGURE 5.19 COMPARISON OF ATTENUATION PATTERN OF INDIA TO THAT OF OTHERS AS GIVEN BY GUPTA AND NUTTI (1976).	222
FIGURE 5.20 COMPARISON OF INTENSITY PATTERNS OF INDIA WITH THAT OF UNITED STATES (CHANDRA 1982).	223
FIGURE 5.22 COMPARISON OF BHUJ 2001 EARTHQUAKE DATA WITH THAT OF DERIVED EQUATION FOR PENINSULAR PROVINCE (EQUATIONS 3, 6, AND 7).	224
FIGURE 5.23 COMPARISON OF BHUJ 2001 EARTHQUAKE DATA WITH THAT OF DERIVED EQUATION FOR INDIAN SUBCONTINENT (EQUATIONS 3, 6, AND 7).	224

Chapter 1

Introduction

1.1 General

Seismic risk analysis for important projects like nuclear power plants, important bridges, and high dams, requires attenuation relationships which relate seismological data with parameters of engineering interest, such as peak ground acceleration, velocity, or response spectral ordinates. This implies that instrumental records of ground motions covering reasonable time spans be made available for the region of interest. However, for India enough strong motion database is not available and hence earthquake intensity maps of past earthquakes have to be used. The attenuation relations of intensity with distance can be obtained (*e.g.*, Howell and Schultz, 1975), and combining those with ground motion to intensity correlation from regions with abundant data, one can estimate the seismic ground motion parameters for the region of interest (*e.g.*, Rao *et. al.*, 1982).

Empirical intensity data from past earthquakes have often been used to predict ground motion for a given future earthquake with similar size and location [Malone and Bor, 1979]. Intensity data have also been widely used to determine the location of earthquake, which occurred prior to modern seismological instrumentation (*e.g.*, Malone and Bor, 1979). The intensity distribution can also be used to estimate focal depths, near field energy absorption coefficient, and other related parameters to assess the size of an event (*e.g.*, Ambraseys, 1985). Very little research has been conducted in India. For seismic risk analysis of major projects like nuclear plants, important bridges and high dams, attenuation relations developed in other places like North America and California are still used.

Many factors affect the attenuation of seismic intensity with distance. These include magnitude of earthquake, depth of focus, epicentral distance, rupture model of

source fault, topography and condition of the medium in which seismic waves propagate [Maugeri and Motta, 1993]. Due to these factors the earthquakes have regional characteristics and the attenuation laws of seismic intensity are different for different regions. Unless two regions have similar conditions of geology, tectonics, topography, earthquake source *etc.*, one may not be able to apply the attenuation law obtained in one region to another region [Maugeri and Motta, 1993].

1.2 Methods of Describing Seismic Intensity Law

The attenuation law of seismic intensity depends on many factors, amongst which the magnitude of earthquake M (or epicentral intensity I_o) and hypocentral distance Δ (or the epicentral distances R) are most important. Accordingly, many expressions describing attenuation laws of seismic intensity have been developed. The following three are most frequently used:

1. If the strength of the earthquake is represented by the magnitude M , and assuming that there is a linear relation between the seismic intensity I and the magnitude M , and linear and logarithmic relation with the of distance R , the attenuation law of seismic intensity can be written in the following form,

$$I = a + b M + c R + d \ln(R + D) \quad (1.1)$$

where a , b , and c are regression constants and D is a constant concerning the size of the earthquake source. In general, the term “ $c R$ ” can be neglected and the formulation of the above can be written as,

$$I = a + b M + d \ln(R + D) \quad (1.2)$$

2. Strength of an earthquake can be represented by the “imaginary” intensity I_o at the earthquake epicenter instead of the magnitude M . In this case, the attenuation law of seismic intensity can be written as follows,

$$I = a + b I_o + c \ln(R + D) \quad (1.3)$$

where I_o is the imaginary intensity (higher than the maximum assigned intensity) at the epicenter of the earthquake, and D is a suitably assumed constant concerning size of the earthquake source.

3. Equations 1.2 and 1.3 show that the decay of seismic intensity is independent of strength I_o . However, it has been observed that the rate of attenuation of intensity with distance is faster for small earthquakes than that for large earthquakes. Considering this, a different relationship for seismic intensity attenuation is proposed [Maugeri and Motta, 1993].

$$\iota = I_o - I = \left(\frac{I}{\ln(\psi)} \right) \ln \left[1 + \frac{(\psi - 1)}{\psi_o} \frac{R}{(R_i - I)} \right] \quad (1.4)$$

where I_o is the intensity of the epicenter area, R_i is the equivalent radius of the highest mapped isoseismal line, R is the equivalent radius corresponding to intensity I , and ψ , ψ_o are two constant obtained as follows,

$$\psi = \frac{R_{k+1} - R_k}{R_k - R_{k-1}}, \quad K \geq 2 \quad \text{and} \quad (1.5)$$

$$\psi_o = \frac{R_2 - R_1}{R_1}, \quad (1.6)$$

where R_k is the equivalent radius of the k^{th} isoseismal line (the boundary line of the area with intensity I_k).

In all the three methods, R can be the epicentral distance or the hypocentral distance $d = \sqrt{R^2 + h^2}$, where h is the depth of the earthquake focus.

1.3 Scope of the Study

In this study, earthquake data from past 59 Indian earthquakes have collected from many sources and different attenuation relationships are developed for Indian subcontinent. Keeping in mind geological conditions, the entire Indian subcontinent is

divided into six attenuation provinces, namely Northeast, Northern, Northwest, Peninsular, Foredeep, and Subduction province.

Adopting the deterministic method and one step iterative regression analysis, attenuation equations are developed for each region. Different equations are developed involving magnitude, epicentral intensity, maximum intensity and the combination of them to arrive at the best-fit equation. Based on these, attenuation characteristic of different regions have been compared. Important results are obtained like, how much would be the maximum damaged area if a particular strength of earthquake strikes the concerned place, at what distances the intensity drops by one unit at a particular place, whether intensity attenuation in India is similar to that of United States or not and which type of attenuation equation is best suited for a particular province.

• • •

Chapter 2

Review of Existing Attenuation Relationships

2.1 Introduction

This chapter is aimed at bringing out the research carried out in the past on intensity attenuation. The attenuation relationships found in the literature have been reviewed. There are several attenuation relationships, showing intensity attenuation with the epicentral distance and magnitude. Many researchers have tried to correlate the epicentral intensity with earthquake parameters such as focal depth, magnitude [Kaila and Sarkar, 1978]. Some researchers have also tried to consider the effect of local geological conditions (*e.g.*, Lee and Trifunac, 1985). The basic equation is found to be in the form of either $I - I_o = a + b R + c \log_{10}(R)$ or $I = a + b M + c R + d \log_{10}(R)$, where I is the intensity at epicentral distance R , I_o is the epicentral intensity and a , b and c are the regression constants. The intensity attenuation relationships developed for India and United States in the past are presented in Tables 2.1 and 2.2.

2.2 Factors Affecting the Intensity Attenuation Relationship

2.2.1 Focal Depth

The extent of the affected areas and shapes of isoseismals depend on the focal depth [Rao, *et. al.*, 1982]. For any earthquake the directional variation of the intensity is due to the variation in the sub-surface geology, whereas change in decay rate from one earthquake to another is likely to be due to the depth of focus. The greater the focal depth, slower is the fall of intensity with distance [Kaila and Sarkar, 1978]. For the same size or energy of earthquakes, the epicentral intensity (I_o) depends on the focal depth of the earthquake and high magnitude (high epicentral intensity) is generally correlated with small focal depth [Burton *et. al.*, 1985].

2.2.2 Magnitude

Magnitude is a measure of the size of earthquake. It is measured from amplitude of the earthquake waves and it represents the energy released at the source. A smaller magnitude earthquake can have same epicentral intensity as that of larger one, but then it will have smaller felt area depending upon the source dimension and the focal depth.

2.2.3 Distance

The variable that is generally used to characterize the propagation parameter is distance. The intensity or damage potential of an earthquake attenuates with distance from the macroseismic hypocenter or focus. The earthquake rupture can be extended over tens to hundred of kilometers, and a number of distance measurements have come into use. The various distance measures used in the literature are (Figure 2.4): (a) epicentral distance, R , (b) hypocentral distance, Δ , (c) distance to zone of energy release, R_z , (d) closest distance to rupture, R_{rup} , and (e) closest distance to surface projection of rupture, R_{jb} . In literature, the intensity attenuation relationships are expressed in terms of either epicentral distance or hypocentral distance. In deriving the intensity attenuation relationships, it is assumed that the seismic energy radiates from a point source and hence hypocentral distance should be used instead of the epicentral distance. The epicentral distance can be used as an approximation for hypocentral distance for shallow focus earthquakes whose fault length is not large.

Earthquakes whose fault length is large will have large difference in attenuation along the transverse and longitudinal directions since energy is radiated from a line source instead of a point source. The difference in the value of intensity drop can be as high as one unit [Chandra, 1982(a)]. In the present work, epicentral as well as hypocentral distance is used and attenuation is expressed in both longitudinal and transverse directions of the fault.

2.3 Medium of Propagation

The amplitude of ground motion depends on both the properties and configuration of the near surface strata through which seismic waves propagate. The properties having maximum effect on the ground motion are impedance and absorption. Impedance is the resistance to the particle motion and is defined as the product of density, seismic wave velocity, and the cosine of the angle of incidence [Reiter, 1991]. Particle velocity is inversely proportional to the square root of impedance. As seismic waves propagate through a medium of increasing impedance, the increase in resistance to motion decreases the particle velocity and amplitude of seismic wave to preserve the energy. Keeping other factors constant, effect of an earthquake will be more on a low-density medium than on a high-density one [Reiter, 1991].

Absorption is also termed as damping or inelastic attenuation, which tends to be substantially greater for soft soils than for hard rocks [Chandra, 1982(a)]. At higher frequencies the impact of absorption is found to be very severe while at low frequencies it is less. These effects appear to balance out at frequencies dominating the peak ground accelerations and most empirical studies show that there is very little difference in peak ground acceleration recorded on rock or soil. If ground motion is dominated by high frequencies, such as in small earthquakes, the lower absorption of hard rock can allow higher peaks than other types of site [Reiter, 1991].

2.3.1 Local Geological Conditions

The distortion of isoseismal shape from concentric circles is mainly due to the local geological conditions. The character of the upper few hundred meters of strata beneath any site may, under certain conditions, have a more profound effect on the level of earthquake shaking than the effect of earthquake magnitude. The different intensity scales make little or no effort to take the local geological conditions into account [Reiter, 1991]. An examination of Modified Mercalli intensity scale shows that, considerable

damage to building could define intensity VII, VIII and IX, depending upon whether the buildings were “poorly built or badly designed”, and “ordinary substantial buildings”, or “structures built especially to withstand earthquakes”. No mention is made, however, of whether these structures are on hard rock, deep sediments, or loosely consolidated sands.

Many investigators (*e.g.*, Malone and Bor, 1979) have estimated generic corrections in expected intensity as a function of local site conditions. Evernden and Thomson (1985) used specific corrections to an average intensity to correlate with surface geology (taken from Reiter, 1991), as it appears on the geological map of California (Table 2.3). From the studies of Tilford *et. al.* (1985), it was concluded that sites located on the soil foundations appear to be subjected to an intensity of ground shaking about one unit higher on the MM scale than the sites located on rock foundations (Table 2.3).

2.3.2 Source Dimension

In deriving the intensity attenuation relationship it is assumed that the energy is radiated from a point source through a space of simple geometry (*e.g.*, a uniform hemisphere or layers) [Howell and Schultz, 1975]. Such type of source under uniform and isotropic soil conditions gives rise to an isoseismal pattern in the form of concentric circles. It has been often observed that isoseismals are elliptical in nature with their longitudinal axis along the length of the fault. To accommodate this fact different attenuation rates can be assumed along the major and minor axes of the elliptical isoseismals (*e.g.*, Tilford *et. al.*, 1985).

An earthquake with a small source dimension may have a large observed or mapped epicentral intensity, although the total felt area might be rather small. On the other hand, an earthquake with a large source dimension may have the same mapped epicentral intensity but a much larger felt area. The earthquake in later case is of larger

magnitude. The calculated epicentral intensity (I_o) values represent the strength of an equivalent point source.

2.4 Steps in Developing Intensity Attenuation Relationships

2.4.1 Collection of Intensity Maps

In deriving the intensity attenuation relationship the isoseismal maps of the past earthquake are required. In India most of the isoseismal maps are available with the Geological Survey of India in Memoirs of GSI. The other sources include Indian Meteorological Department, National Geophysical Research Institute (Hyderabad) and many Indian journals.

2.4.2 Preparation of Database

The pattern of isoseismals would be concentric circles, with highest intensity near the epicenter, if the earthquake energy is released from a point source and propagates through a uniform isotropic soil. Since these conditions are not satisfied in reality, the real patterns of the isoseismals are irregular. The preparation of database is entirely dependent on the pattern of isoseismal maps, *i.e.*, either elliptical or irregular. To prepare the database one can convert the mapped isoseismal areas into equivalent circles and obtain their radius for the corresponding intensity. Many researchers have adopted this approach because of its simplicity.

Sometimes the trend of isoseismals is elliptical, with longitudinal axis along the length of the fault. In this case many researchers (*e.g.*, Tilford and Chandra, 1985) have assumed different attenuation along major and minor axes, and data points were obtained in both the directions along and normal to the fault rupture. In case of irregular shapes, data points can be read along any number of desired directional lines and then averaged to get the average attenuation (*e.g.*, Chandra, 1979).

2.4.3 Normalization of Intensity Scale

Over the years, various researchers have developed different intensity scales. Hence, for comparison and uniformity, the different scales have to be converted to one scale. In this study, the various intensities are converted to one scale using the conversion available in the literature [Reiter, 1991].

2.4.4 Division into Different Attenuation Provinces

There are many factors affecting the intensity-attenuation relations, such as strength of earthquake, focal depth, and epicentral distance, rupture model of source fault, topography and medium of propagation. However, earthquakes have regional character. Unless two regions have similar conditions of geology, tectonics, topography, earthquake source *etc.*, the attenuation law obtained in one region cannot be applied to another region [Maugeri and Motta, 1993]. Hence, the concerned area has to be divided into the different zones so that a particular equation is adequate to describe the attenuation relationship. In present study the Indian subcontinent is divided into six attenuation provinces, *viz.*, Northeast, Northern, Northwest, Peninsular, Foredeep, and Subduction province.

2.4.5 Selection of Suitable Attenuation Relationship

Many attenuation relationships are available in the literature as described in the Section 2.6. There are basically three methods of describing the intensity attenuation as described in the Section 1.2. Suitable attenuation relationships should be selected depending on the region and the adequacy of the relationship to the region.

2.4.6 Set Initial Epicentral Intensity (I_o) Values

Intensity attenuation relationship is more sensitive to the epicentral intensity rather than the maximum intensity. Many studies have shown that the assumed initial high value of epicentral intensity (I_o) will result in a relationship with high rate of intensity attenuation relation and vice versa (*e.g.*, Burton *et. al.*, 1985, Lee and Trifunac, 1985). Hence the initial values of epicentral intensity (I_o) should be selected appropriately.

There are two methods to arrive at the appropriate epicentral intensity (I_o) values. These

are,

1. **Graphical Method:** Following the parallelism of the intensity lines for different earthquakes, a smooth curve is drawn, using this curve as the reference, for a particular earthquake, I_o at each isoseismal intensity point was estimated and then averaged. Most of the authors use this method because this give quite good approximates.

Figure 2.1 shows intensity-distance curves for average distance for the three earthquakes. Following the general parallelism of the intensity lines for different earthquakes, a smooth curve has been shown by dashed line. The intensity at zero distance for the dashed curve is 8.7. Using the dashed curve as a reference, for a particular earthquake, I_o at each isoseismal, intensity point was estimated and then averaged. For example, the five points for the earthquake event 1, in order of increasing distance occur at 0.50, 0.58, 0.23, 0.43 and 0.43 intensity units above the intensity 8.7 (dashed) curve. Therefore, from these three points, I_o for earthquake event 1 will be inferred as 9.20, 9.28, 8.93, 9.13 and 9.13, respectively, and the average I_o is be estimated as 9.13. Similarly I_o for the other events are calculated.

2. **Empirical Method:** If the magnitude of the earthquake is accurately known (from reliable source), one can use the epicentral intensity-magnitude relationship to get the epicentral intensity. Due to non-availability of instrumental records of past earthquakes, it is difficult to rely on the magnitude. Hence this method is scarcely used.

2.4.7 Regression Analysis

After setting the initial value of the epicentral intensity, iterative regression analysis has to be performed between drop of intensity ($I_o - I$) values and the

corresponding distance (Δ or R). Using the regression expression, the epicentral intensity for each data point of an earthquake is found and averaged to get the new epicentral intensity. This procedure is repeated until no significant improvement is observed for the drop of intensity ($I_o - I$) values.

2.4.8 Method of Regression Analysis

In literature many methods of regression analysis are available such as method of least square, two step regression analysis, and method of maximum likelihood. One-step method of least square is generally used (e.g., Gupta *et. al.*, 1999, Chandra, 1979, Yarar *et. al.*, 1984).

2.4.8.1 Method of Least Square

This procedure minimizes the sum of the squared error $\sum_{i=1}^n w_i (y_i - \hat{y}_i)^2$, where \hat{y}_i

is the predicted value of y_i , and w_i is the weight assigned to each observation y_i .

2.4.8.2 Validity of Results

2.4.8.2.1 Analysis of Residuals

Different methods for regression analyses are derived on the assumption that the random error term (ε_i) is normally distributed. This error term is represented by the residuals obtained after regression. The normality assumption of the residual is checked by χ^2 (chi-square) test. The adequacy of the model with respect to the fitted variables is then checked by plotting the residuals versus the independent variables (I_o , R). If these plots do not show any apparent trend, the model can be assumed adequate [Roshan, 2000].

2.4.8.2.2 Multiple Correlation Coefficient

The adequacy of the fit can be evaluated by the multiple correlation coefficients. The expression for correlation coefficient is (e.g., Timiovska, 1992),

$$r = \frac{\sum (I_{obs} - \bar{I}_{obs}) \sum (I_{est} - \bar{I}_{est})}{\sum (I_{obs} - \bar{I}_{obs})^2 \sum (I_{est} - \bar{I}_{est})^2}, \quad (2.1)$$

where I_{obs} is the observed intensity, \bar{I}_{obs} is the mean of the observed intensity, I_{est} is the estimated intensity level, and \bar{I}_{est} is the mean of the estimated intensity level. The value of the correlation coefficient should be in between 0 to 1 [Timiovska, 1992].

2.4.8 2.3 Uncertainty in Prediction

In addition to median intensity estimates, the uncertainty (standard deviation) is also important for seismic risk analyses. The uncertainty in the prediction is represented with the help of standard deviation (σ) of the predicted values. The predicted dependence of standard deviation is different for different models, since it depends on the data set.

2.5 Difficulties in Deriving the Attenuation Relationships

2.5.1 Use of Different Intensity Scale

Over the years several intensity scales like Oldham, RF, MM and MSK were used. To develop intensity attenuation relationships, one has to convert the available isoseists of different intensity scales to one scale. Some difficulty arises in assigning the maximum intensity. For example, intensity VIII on RF scale is equivalent to VII on MM scale, but for an earthquake of maximum intensity VIII on RF scale, does not mean that it will have maximum intensity of VII on MM scale. In such case the maximum intensity reaches VIII on MM scale on a separate isoseist to be drawn inside the innermost isoseismal. Hence careful examination is needed while converting intensities from one intensity scale to another.

2.5.2 Maximum Intensity

The empirical equations found in literature, show that intensity-attenuation relationship is quite sensitive to the maximum intensity. The maximum intensity is distributed on a relatively small area, and is more sensitive to population and building

density than estimate of smaller intensities at greater distance. Since the intensity scale is not finely divided and does not take all factors in account, the maximum intensity may be incorrectly estimated [Anderson, 1978].

2.5.3 Use of Intensity as a Whole Number

The available intensity scales designate different levels of shaking with whole numbers. Since the estimates of intensity near the epicenter of an earthquake are sensitive to population and building density, there is a high probability that the epicentral intensity can be inappropriately estimated [Anderson, 1978]. Sometimes ambiguity in assigning the intensity level is dealt by assigning a dual intensity level, such as MMI VII-VIII (7.5), or VII.V (7.5). However, this type of practice is very rare and whether its adequacy is debatable [Reiter, 1991].

2.5.4 Source Dimension

In deriving the intensity attenuation relationship it is assumed that the energy is radiated from a point source through a space of simple geometry (e.g., a uniform hemisphere or layers). The equations do not give good results where distance is not large compared to the source dimension [Howell and Schultz, 1975]. An alternative approach postulates that the intensity-distance relation is the sum of two attenuation rates, one at short distance, the other at large distances [Kaila and Sarkar, 1978]. Some of the researchers have assumed that the different attenuation rate exists along the major and minor axes of the isoseismals [Tilford and Chandra, 1985].

2.5.5 Initial Epicentral Intensity (I_o)

The level of the attenuation curve is quite sensitive to the initial epicentral intensity set selected for the analysis. The empirical relationship shows a high rate of attenuation if the initial epicentral intensity (I_o) set contains high values for different earthquakes, and low rate of attenuation if the initial epicentral intensity set contains low

values [Chandra, 1979]. Hence to avoid such ambiguity, a graphical method, as described in the Section 2.2.7 has been adopted by many researches to arrive at the initial set of I_o .

2.6 Literature Review of Attenuation Relationships

2.6.1 Ergin (1969)

The observed intensity-distance relation for a number of earthquakes that occurred in Turkey and elsewhere was studied and found that the curve, given by the

$$\text{formula } I - I_o = n \log_{10} \frac{\sqrt{R^2 + h^2}}{h} + \text{absorption term}, \text{ best fits for either } n \text{ equal to 3 or 5,}$$

where h is the focal depth.

2.6.2 Rutledge (1972)

The macroseismic areas for all earthquakes of MM Intensity IV or greater which occurred in the United States (east of the longitude 106° W) from 1928 to 1969 have been examined. A regression equation between the epicentral distance, R , and the epicentral intensity, I_o , was fit. The equation used was of the form,

$$\log_{10}(R) = -3.14 + 1.05 I_o. \quad (2.2)$$

2.6.3 Gupta and Nuttli (1976)

A deterministic approach was adopted to derive the intensity attenuation relationship for central United States by considering eight earthquakes, and adopting the method of least square for the regression analysis. The equation derived was,

$$I - I_o = 3.7 - 0.0011 R - 2.7 \log_{10}(R) \quad \text{for } R \geq 20 \text{ km.} \quad (2.3)$$

This equation was also used in estimating the topographical error of an earthquake whose maximum intensity is not known reliably.

2.6.4 Anderson (1978)

A probabilistic approach was adopted to develop the attenuation of shaking intensity with distance for the United States earthquakes. The best fitting parameters were

found for a Gaussian distribution function to fit the observed distributions of $\log_{10}(R)$ for each of combination of epicentral intensity and the intensity bounded by the counters.

2.6.5 Kaila and Sarkar (1978)

A comprehensive atlas of isoseismal maps of 26 major earthquakes in India was prepared. These isoseismals were also superimposed on the geological map of India. Intensity-distance relations for these earthquakes for different directions were studied. Assuming that the logarithm of intensity varies linearly with the epicentral distance a single attenuation relationship for entire India was derived. The equation was,

$$\frac{I}{I_o} = \exp^{-\left(\frac{1564}{h^2} + 0.0011\right)} \quad \text{for } 15 < h < 240 \text{ km,} \quad (2.4a)$$

where I_o is the epicentral intensity in MM, I is intensity at an epicentral distance Δ , and h is the focal depth in km. The derived empirical relation connecting maximum intensity, I_o , magnitude, M , and focal depth, h , of an earthquake was as follows,

$$I_o = 1.5 M - 4.1 \log_{10}(h) + 4.5 \quad \text{for } 8 < h < 70 \text{ km.} \quad (2.4b)$$

A linear relationship was proposed between magnitude and inverse of the square of focal depth was,

$$\frac{I}{h^2} = -1.1706 M - 0.005. \quad (2.4c)$$

It was found that in some cases (Koyna, Kangra, Anjar, and Srimangal earthquakes) the intensity data fits a pair of straight lines instead of one, indicating thereby two rates of intensity decay, faster for the near distance and slower for the larger distance range. The reason behind this is attributed to the fact that the fault plane may be extending quite deep and as a consequence of which, two ends of the fault may be acting as two independent source of energy. There can be another possibility that the two intensity decay slopes are

in reality due to two independent earthquakes occurring almost simultaneously, separated by a few seconds, one with shallow focus and the other with a comparatively deep focus.

2.6.6 Chandra (1979)

Attenuation relationships were obtained using data from 31 earthquakes in and around the United States. As proposed by Howell and Schultz (1975), the region was divided into three attenuation provinces. A graphical method for the estimation of an initial set of epicentral intensities (I_o), from the intensity-distance plot for different earthquake was used, thus avoiding the need to equate the maximum reported or mapped intensity (I_{max}) with the epicentral distance. Using an iterative least-square fit procedure the attenuation relations were determined, wherein an initial approximate estimate of I_o for each earthquake is successively improved. The standard equation of the type $I - I_o = a + b(R + D) + c \log_{10}(R + D)$ was used for regression. The value of D was taken to be equal to the average focal depth of the concerning region. The empirical relations between felt area (A) and epicentral intensities were also obtained. The equations derived were,

San Andreas Province

$$I - I_o = 2.065 - 0.00594 R - 2.065 \log_{10}(R + 10) \quad (2.5a)$$

$$\sigma = 0.266 \quad R < 330\text{km.}$$

$$\log_{10}(A) = 1.61 + 0.724 I_o \quad (2.5b)$$

$$7.2 \leq I_o \leq 10.0, \quad \sigma_a = 0.19$$

Cordilleran Province

$$I - I_o = 2.819 - 0.00503 R - 2.017 \log_{10}(R + 25) \quad (2.5c)$$

$$\sigma = 0.245 \quad R < 335\text{km.}$$

$$\log_{10}(A) = 1.94 + 0.448 I_o \quad (2.5d)$$

$$6.8 \leq I_o \leq 9.2, \quad \sigma_a = 0.22$$

Eastern Province

$$I - I_o = 3.374 - 0.00164 R - 2.414 \log_{10}(R + 25) \quad (2.5e)$$

$$\sigma = 0.363 \quad R < 475 \text{ km.}$$

$$\log_{10}(A) = 2.20 + 0.453 I_o \quad (2.5f)$$

$$6.9 \leq I_o \leq 10.2, \quad \sigma_a = 0.48$$

Central United States

$$I - I_o = 3.534 - 0.00164 R - 2.528 \log_{10}(R + 25) \quad (2.5g)$$

$$\sigma = 0.243 \quad R < 1600 \text{ km.}$$

$$\log_{10}(A) = 3.76 + 0.285 I_o \quad (2.5h)$$

$$6.1 \leq I_o \leq 817, \quad \sigma_a = 0.30$$

2.6.7 Chandra *et al.* (1979)

Data from 12 earthquakes from Iran was considered and equations were obtained for parallel and transverse to the direction of fault rupture, and for average attenuation. The average curve method to get the initial epicentral (I_o) values, with one step iterative iteration method was adopted. The equations derived were,

Along major axis

$$I - I_o = 4.8724 - 0.00548 R - 3.708 \log_{10}(R + 20) \quad R < 160 \text{ km} \quad (2.6a)$$

Along minor axis

$$I - I_o = 8.729 - 0.01158 R - 6.709 \log_{10}(R + 20) \quad R < 160 \text{ km and} \quad (2.6b)$$

Average attenuation

$$I - I_o = 6.453 - 0.00121 R - 4.960 \log_{10}(R + 20) \quad R < 120 \text{ km.} \quad (2.6c)$$

2.6.8 Malone and Bor (1979)

This study was aimed towards prediction of intensities at various observation sites, which was then compared to the actually observed intensity. The difference between the predicted and observed intensity was then used as site correction factors. The empirical relations of Everndon (1975) were used to determine the size and depth for each earthquake and the local attenuation factor (k), for two physiographic parts of the United States. The value of k in the Puget Sound region and Northern Canada is 1.75, while 1.5 is more appropriate for Eastern Washington and Northern Oregon.

2.6.9 Vanmarcke and Lai (1980)

With data from 83 earthquakes in the Philippines, an intensity attenuation equation was derived in the form,

$$I - I_o = 4.01 - 0.015 R - 2.10 \log_{10}(R). \quad (2.7)$$

This compares very well with results for a tectonically similar region, the San Andreas region, derived by Howell and Schultz (1975).

2.6.10 Chandra (1982a)

Isoseismal maps for past 57 earthquakes from different parts of Greece were analyzed to develop relationships between intensity, magnitude and distance. The region under consideration was divided into six attenuation provinces, namely Hellenic, Peloponnese, Corinth-Saronikos, North Greece, Northwest Greece and Albania, and Northeast Greece province. Also, the earthquakes associated with the Hellenic province were grouped into two categories. Hellenic province (shallow focus), which includes shallow focus earthquakes showing rapid attenuation of intensity with distance, and Hellenic subduction zone (intermediate focus), which includes intermediate focal depth earthquakes, about 120 km deep, showing a rather slow attenuation of intensity with epicentral distance. Equation of the type $I = a + b M + c (R + D) + d \log_{10}(R + D)$ was

used. The values of the regression constants a , b , and c were found by multiple linear regression fit of the data. The equations derived were,

Hellenic province (Shallow focus)

Along Major Axis

$$I = 5.22 + 1.154 M - 0.00394 (R + 15) - 3.3 \log_{10} (R + 15) \quad (2.8a)$$

$$\sigma_a = 0.392, \quad \sigma_b = 0.384, \quad \sigma_c = 0.549 \quad \text{for } R \leq 250 \text{ km}.$$

Along minor Axis

$$I = 5.96 + 0.890 M - 0.00565 (R + 15) - 3.3 \log_{10} (R + 15) \quad (2.8b)$$

$$\sigma_a = 0.500, \quad \sigma_b = 0.528, \quad \sigma_c = 0.727 \quad \text{for } R \leq 165 \text{ km}.$$

Average

$$I = 5.52 + 1.030 M - 0.00489 (R + 15) - 3.3 \log_{10} (R + 15) \quad (2.8c)$$

$$\sigma_a = 0.395, \quad \sigma_b = 0.418, \quad \sigma_c = 0.395, \quad \text{for } R \leq 200 \text{ km}.$$

Hellenic subduction zone (Intermediate focus)

Parallel to the Hellenic arc

$$I = 7.11 + 1.041 M - 0.00351 R - 3.3 \log_{10} (R) \quad (2.8d)$$

$$\sigma_a = 0.697, \quad \sigma_b = 0.511, \quad \sigma_c = 0.864 \quad \text{for } R \leq 460 \text{ km}.$$

Transverse to the Hellenic arc

$$I = 6.87 + 1.213 M - 0.01222 R - 3.3 \log_{10} (R) \quad (2.8e)$$

$$\sigma_a = 0.796, \quad \sigma_b = 0.689, \quad \sigma_c = 1.053 \quad \text{for } R \leq 300 \text{ km}.$$

Average

$$I = 6.85 + 1.137 M - 0.00713 R - 3.3 \log_{10} (R + 15) \quad (2.8f)$$

$$\sigma_a = 0.731, \quad \sigma_b = 0.594, \quad \sigma_c = 0.942 \quad \text{for } R \leq 375 \text{ km}.$$

Peloponnese province

$$I = 6.95 + 0.906 M - 0.001369 (R + 15) - 3.3 \log_{10} (R + 15) \quad (2.8g)$$

$$\sigma_a = 0.226, \quad \sigma_b = 0.254, \quad \sigma_c = 0.340 \quad \text{for } R \leq 80 \text{ km}.$$

Corinth-Saronikos province

$$I = 3.97 + 1.374 M - 0.01157 (R + 15) - 3.3 \log_{10} (R + 15) \quad (2.8h)$$

$$\sigma_a = 0.465, \quad \sigma_b = 0.615, \quad \sigma_c = 0.770 \quad \text{for } R \leq 165 \text{ km}.$$

North Greece province

$$I = 5.99 + 1.014 M - 0.01037 (R + 15) - 3.3 \log_{10} (R + 15) \quad (2.8i)$$

$$\sigma_a = 0.432, \quad \sigma_b = 0.320, \quad \sigma_c = 0.538 \quad \text{for } R \leq 160 \text{ km}.$$

Northwest Greece and Albania province

$$I = 6.29 + 0.993 M - 0.01512 (R + 15) - 3.3 \log_{10} (R + 15) \quad (2.8j)$$

$$\sigma_a = 0.362, \quad \sigma_b = 0.137, \quad \sigma_c = 0.387 \quad \text{for } R \leq 105 \text{ km}.$$

Northeast Greece province

$$I = 5.14 + 1.204 M - 0.00647 (R + 15) - 3.3 \log_{10} (R + 15) \quad (2.8k)$$

$$\sigma_a = 0.368, \quad \sigma_b = 0.191, \quad \sigma_c = 0.415 \quad \text{for } R \leq 190 \text{ km}.$$

This study of seismic risk in Greece, suggested that the strength of the maximum potential earthquakes from various seismic sources, could be more appropriately expressed in terms of magnitude, rather than epicentral intensity.

2.6.11 Chandra (1982b)

Based on the general consideration of the regional geology and tectonics, the region (Indian subcontinent) under investigation was broadly divided into eight attenuation provinces. These are Makran, Quetta, Hindukush-Pamir, Jammu and Kashmir-Himachal Pradesh, Ganga basin, Peninsular province, Northeast province, and Burma province. A total of 24 earthquakes were considered. The deterministic method of analysis was used. Equation used is of the type $I - I_o = a \log_{10} (D) + b R + c \log_{10} (R + D)$.

Where the term D is suitably assumed to be equal to the average focal depth of earthquakes in a particular province. The introduction of the term D in the above equation will eliminate the singularity of the equation at distance $R = 0$. One step regression analysis was performed to obtain the expression for each province. Initial set of epicentral intensity (I_o) values were found by the graphical method. The equations derived are,

Makran Coast

$$I - I_o = 3.321 - 0.00369 R - 2.553 \log_{10}(R + 20) \quad (2.9a)$$

$$\sigma = 0.054 \quad R < 600 \text{ km.}$$

Quetta Province

$$I - I_o = 2.987 - 0.00737 R - 2.296 \log_{10}(R + 20) \quad (2.9b)$$

$$\sigma = 0.429 \quad R < 325 \text{ km.}$$

Hindu Kush - Pamir

$$I - I_o = 6.985 - 0.00590 R - 2.982 \log_{10}(R + 220) \quad (2.9c)$$

$$\sigma = 0.301 \quad R < 550 \text{ km.}$$

Jammu and Kashmir - Himachal Pradesh

$$I - I_o = 3.975 - 0.00100 R - 3.055 \log_{10}(R + 20) \quad (2.9d)$$

$$\sigma = 0.472 \quad R < 650 \text{ km.}$$

Ganga Basin

$$I - I_o = 3.470 - 0.00210 R - 2.667 \log_{10}(R + 20) \quad (2.9e)$$

$$\sigma = 0.193 \quad R < 1110 \text{ km.}$$

Northeast Province

$$I - I_o = 2.501 - 0.00452 R - 1.922 \log_{10}(R + 20) \quad (2.9f)$$

$$\sigma = 0.244 \quad R < 1050 \text{ km.}$$

Peninsular Province

$$I - I_o = 4.987 - 0.00204 R - 3.833 \log_{10}(R + 20) \quad (2.9g)$$

$$\sigma = 0.338 \quad R < 400 \text{ km.}$$

Burma Province

$$I - I_o = 2.116 - 0.001425 R - 1.626 \log_{10}(R + 20) \quad (2.9h)$$

$$\sigma = 0.350 \quad R < 375 \text{ km.}$$

It was concluded that the decay of intensity is least for the Hindu Kush province. This was attributed to the larger focal depths in this province (generally around 200-250 km). The peninsular and Burma provinces show the highest attenuation rate.

2.6.12 Rao *et al.* (1982)

One-step regression analysis was performed to obtain the attenuation relations using data from eight Indian earthquakes. A linear relation between logarithm of intensity and the epicentral distance similar to that by Kaila and Sarkar (1978) was assumed. For each earthquake the slope of the best-fit curve was obtained. To draw the intensity attenuation characteristic curve for different focal depths, the relationship derived by Kaila and Sarkar (1978) was used. Relationship between acceleration and intensity are also derived. The epicentral acceleration was plotted on a semi-logarithmic scale and intensity on a linear scale, and the best fit straight lines obtained were as follows,

$$\log_{10}(A) = 0.333 I - 0.05, \quad \text{for firm ground, and} \quad (2.10a)$$

$$\log_{10}(A) = 0.288 I - 0.06, \quad \text{for unconsolidated Alluvial.} \quad (2.10b)$$

Where acceleration, A , is in the percentage of acceleration due to gravity and intensity, I , is on MM Scale. This study mainly resulted in the preparation of master curves involving the focal depth, intensity, and average peak ground acceleration of earthquake in the absence of strong motion data.

2.6.13 Benjamin (1983)

Based on the assumption that the earthquake energy is radiated from a point source and subsequently transmitted through a homogeneous media, the attenuation of the Rossi-Forel intensity with respect to both epicentral and hypocentral distances was studied for the Philippine region. The data consisted of earthquakes from years 1913 to 1980. They tried to fit many equation of the form $I_o = a + b M$. The equations derived were,

$$I = -2.53 + 1.26 M - 0.009 \Delta, \quad (2.11a)$$

$$I = 3.64 + 1.17 M - 1.46 \ln(\Delta), \quad (2.11b)$$

$$I = 0.91 + 1.25 M - 0.86 \ln(\Delta) - 0.004 \Delta, \quad (2.11c)$$

$$I = -1.82 + 1.11 M - 0.007 R, \quad (2.11d)$$

$$I = 4.54 + 1.08 M - 1.51 \ln(R), \text{ and} \quad (2.11e)$$

$$I = 1.31 + 1.13 M - 0.77 \ln(R) - 0.004, \quad (2.11f)$$

The Equation 2.11c is found to be the best suited for the Philippine region.

2.6.14 Yarar *et al.* (1983)

In this study fourteen earthquakes from Turkey were considered. The non-isotropic characteristic of the intensity distributions was accounted for, by separately, treating the earthquakes associated with strike slip faulting and those associated with Graben type. For the derivation of intensity attenuation relationships associated with strike-slip events, sets of intensity versus distance data points were obtained for each isoseismal contour, along the perpendicular and transverse axis fault rupture. One-step regression analysis was performed. The following results were obtained for the attenuation of intensity in transverse direction to the strike slip faults,

$$I_o - I = 1.237 + 0.004 R + 1.216 \ln(R) \quad \sigma = 0.53, \text{ and} \quad (2.12a)$$

$$I = 0.34 + 1.54 M - 0.001 R - 1.27 \ln(R) \quad \sigma = 0.63 \quad (2.12b)$$

For earthquakes associated with Graben type faulting, exhibiting more or less circular intensity distributions, the attenuation of intensities in radial direction from the macroseismic epicenter was derived as,

$$I_o - I = 2.465 + 0.0003 R + 1.235 \ln(R) \quad \sigma = 0.54, \text{ and} \quad (2.12c)$$

$$I = 0.568 + 1.534 M - 0.001 R - 1.235 \ln(R) \quad \sigma = 0.64 \quad (2.12d)$$

where I_o and I represent, the epicentral intensity and mean intensity at a distance R in transverse direction to the fault respectively, and σ is the standard deviation of the dependent variable.

2.6.15 Burton *et al.* (1985)

A set of 101 earthquakes between years 1727-1979 in Britain was considered. They investigated intensity attenuation with distance and focal depth, and inferred that the equation of the type $I_o - I = a \log_{10} \left(\frac{R}{h} \right) + b (R - h)$ fits best for the British earthquakes and the equation derived was,

$$I_o - I = 3 \log_{10} \left(\frac{r}{h} \right) + 0.0089 (R - h). \quad (2.13)$$

In deriving the equation one-step iterative regression analysis and average graphical method were adopted to get the initial I_o values.

2.6.16 Lee and Trifunac (1985)

Four regression equations describing the attenuation of MM intensity in terms of local earthquake magnitude, M , epicentral distance, R , focal depth, H , fault size, s , and the local geological conditions at the recording site ($S = 0$ for alluvium, $S = 2$ for basement rock, and $S = 1$ for intermediate sites) have been investigated. The equation used was of the form,

$$I = 1.5 M - A - B \ln(A) - \frac{C \Delta}{100} - D s, \quad (2.14)$$

where I is the MM intensity and $\Delta = \sqrt{R^2 + H^2 + S^2}$. For $R = 0$, $H = 10$ to 15 km and $S = 0$, the results of this equation become equivalent to $I = 1.5 M - 1.5$, proposed by Gutenberg and Richter (1956). The predicted intensity I was found to be, about one half-intensity level higher for alluvium sites than that of basement rock sites.

2.6.17 Tilford and Chandra (1985)

Data from three earthquakes of Greece was considered to obtain the intensity attenuation relationship. One-step iterative regression analysis was used and average graphical method to get the initial set of I_o values was adopted. The intensity residual method was used to capture the effect of local geology on the observed values of intensity. It was observed that under similar circumstances, sites located on soil experiences about one intensity unit more shaking than sites located on rock. The equation derived were,

Longitudinal attenuation

$$I - I_o = 2.150 - 0.00750 R - 2.150 \log_{10}(R+10) \quad (2.15a)$$

$$\sigma = 0.359 \quad R < 300 \text{ km.}$$

Transverse attenuation

$$I - I_o = 3.180 - 0.00458 R - 3.180 \log_{10}(R+10) \quad (2.15b)$$

$$\sigma = 0.234 \quad R < 215 \text{ km.}$$

Average attenuation

$$I - I_o = 2.541 - 0.00727 R - 2.541 \log_{10}(R+10) \quad (2.15c)$$

$$\sigma = 0.233 \quad R < 250 \text{ km.}$$

2.6.18 Drakopoulos and Stamelou (1986)

Intensity-distance relations along major and minor axis of proposed elliptical isoseismals in Western Greece considering past 41 earthquakes were developed. The western Greece earthquakes were divided into two attenuation provinces depending upon

the range of focal depths, one with focal depth in the range 0-15 km and the other in the range 16-41 km. The equation of the type $I - I_o = a + b R + c \log_{10}(R + D)$ was used. The values of regression constants a , b , and c were determined by least square fit between $(I - I_o)$ and R . Here, I is the intensity at an epicentral distance R , D is a constant to be taken equal to the approximate average focal depth. The graphically estimated epicentral intensity set (I_o) was used as first approximation. The attenuation coefficient (γ) was also calculated using the formula,

$$I_o - I = \gamma \log_{10} \sqrt{1 + \frac{A_i^2}{h^2}} . \quad (2.16a)$$

The intensity-distance relations under the assumption of equivalent circle and along the major and minor axis for earthquakes with focal depth in the range 0-15 km were as follows,

$$I - I_o = 3.906 - 0.004 R - 3.883 \log_{10}(R + 10.5) \quad \text{for } R_{mean} \gamma = 3.34 , \quad (2.16b)$$

$$I - I_o = 1.487 - 0.013 R - 1.950 \log_{10}(R + 5.78) \quad \text{for } R_{max} \gamma = 3.48 \text{ and} \quad (2.16c)$$

$$I - I_o = 2.667 - 0.009 R - 3.163 \log_{10}(R + 6.94) \quad \text{for } R_{min} \gamma = 3.25 . \quad (2.16d)$$

For earthquakes with focal depths from 16-40 km:

$$I - I_o = 9.289 - 0.003R - 6.545 \log_{10}(R + 26.3) \quad \text{for } R_{mean} \gamma = 3.68 , \quad (2.16e)$$

$$I - I_o = 2.414 - 0.011 R - 1.885 \log_{10}(R + 20.1) \quad \text{for } R_{max} \gamma = 3.96 \text{ and} \quad (2.16f)$$

$$I - I_o = 9.152 - 0.004 R - 6.733 \log_{10}(R + 22.86) \quad \text{for } R_{min} \gamma = 3.53 . \quad (2.16g)$$

2.6.19 Gupta (1986)

A probabilistic model, which makes use of MM intensity data, was developed for evaluating seismic risk for Northern India. This model predicts the probability of exceedance of any specified earthquake ground motion amplitude from the entire earthquake expected during a selected future period in the region around the site of

interest, and does not use more than one single design earthquake. The intensity attenuation model used was of the form given below, which represents the probability of the intensity I , being observed at an epicentral distance less than or equal to R .

$$P(R) = \frac{1}{\sqrt{2\pi}\sigma} \int_{-\infty}^{\log R} \exp\left[-\frac{1}{2}\left(\frac{\mu - x}{\sigma}\right)^2\right] dx, \quad (2.17a)$$

where μ is the mean and σ the standard deviation of $\log_{10}R$. The probability of observing an intensity value I_1 at a distance R is given by,

$$P\{I = I_1\} = P\{I \leq I_1\} - P\{I \leq (I_1 - I)\}. \quad (2.17b)$$

In this study 18 past Indian earthquakes were considered. The intensity attenuation relationship with distance were found to be as follows,

For mean

$$I - I_o = 2.256 - 0.0099 R - 1.798 \log_{10} R. \quad (2.17c)$$

For mean plus one standard deviation

$$I - I_o = 3.475 - 0.0048R - 2.080 \log_{10} R. \quad (2.17d)$$

2.6.20 Grandori *et al.* (1987)

To develop the intensity-epicentral distance relationships, data from past 19 Italian earthquakes were considered. The epicentral distance R was considered instead of the hypocentral distance Δ because earthquakes were of shallow focal depth range. They used equation of the type,

$$I_o - I = \frac{1}{\ln(\psi)} \left[I + \frac{\psi - 1}{\psi_o} \left(\frac{R_i}{R_o} - 1 \right) \right], \quad (2.18a)$$

where

$$\psi_o = \frac{R_i - R_o}{R_o} = Constant, \quad (2.18b)$$

$$\psi = \frac{R_{i+1} - R_i}{R_i - R_{i-1}} = Constant = \psi \quad i \geq 1 . \quad (2.18c)$$

The values found were as follows,

$$\psi_0 = 1.07 , \quad \psi = 1.58 , \quad D_{0(I_a=10)} = 9.3$$

where R_i is the average radius of the i^{th} isoseismal.

2.6.21 Chavez and Castro (1988)

Two relations were proposed to predict the attenuation of Modified Mercalli intensity (I) with epicentral distance (D) for Mexican earthquakes. These are,

$$\ln(I) = B_0 + B_1 \ln\left(\frac{D}{D'}\right) + B_2 (D - D') + B_3 \ln(M_s), \text{ and} \quad (2.19a)$$

$$\ln(I) = B_0 + B_1 \left(\frac{D}{D'} \right) + B_2 \ln(D - D') + B_3 \ln(M_s), \quad (2.19b)$$

where M_s is the surface-wave magnitude, D' is a distance related to the maximum intensity mapped for an earthquake. The coefficients B_i , for $i=0,1,2,3$ were obtained by least-square fit, for the information contained in the intensity maps of 32 events of the region. The earthquakes were classified in three groups according to their epicentral location, focal mechanism, and focal depth. They are,

Group 1: 18 earthquakes belonging to subduction zone, with thrust mechanisms and depths between 15 and 20 km. The equations derived were,

$$\ln(I) = 1.1090 - 0.1399 \ln\left(\frac{D}{D'}\right) - 0.0011 (D - D') + 0.5209 \ln(M_s) \quad \sigma = 0.71 \quad (2.20a)$$

$$\ln(I) = 1.3891 - 0.0475 \left(\frac{D}{D'} \right) - 0.0220 \ln(D - D') + 0.3627 \ln(M_s) \quad \sigma = 0.67 \quad (2.20b)$$

Group (2): 10 intermediate-depth earthquakes in south-central Mexico, with normal faulting mechanisms and depths varying from 65 to 150 km. The equations derived were,

$$\ln(I) = 1.5188 - 0.0627 \ln\left(\frac{D}{D'}\right) - 0.0021(D - D') + 0.3314 \ln(M_s) \quad \sigma = 0.95$$

(2.20c)

$$\ln(I) = 0.6013 - 0.0337\left(\frac{D}{D'}\right) - 0.0224 \ln(D - D') + 0.7745 \ln(M_s) \quad \sigma = 0.80$$

(2.20d)

Group (3): Four earthquakes with epicenters located on the Trans-Mexican Volcanic belt, with reverse and normal mechanisms and depths shallower than about 20 km. The equation derived was,

$$\ln(I) = 3.0021 - 0.3057 \ln\left(\frac{D}{D'}\right) + 0.0019(D - D') - 0.325 \ln(M_s) \quad \sigma = 0.83$$

(2.20e)

$$\ln(I) = 2.0922 - 0.0881\left(\frac{D}{D'}\right) - 0.0233 \ln(D - D') + 0.0351 \ln(M_s) \quad \sigma = 0.79$$

(2.20f)

2.6.22 Grandori *et al.* (1988)

It was observed that the intensity attenuation of the form $I - I_o = a + bR + c \log_{10}(R)$, does not comply very well with Italian data, as it is implicitly based on the assumption that energy is radiated from a point source. This approach is not reliable, where distance is not large compared to the source dimensions. Moreover, in the following formula the intensity decay ($I_o - I$) does not depend on the epicentral intensity I_o , while the average trend of Italian earthquakes shows that the rate of attenuation is fast for small earthquakes. The drop of intensity relation used was,

$$i = I_o - I_i = \frac{1}{\ln(\psi)} \left[I + \frac{\psi - 1}{\psi_o} \left(\frac{R_i}{R_o} - 1 \right) \right], \quad (2.21a)$$

where

$$\psi = \left(\frac{R_{i+1} - R_i}{R_i - R_{i-1}} \right)$$

$$\frac{R_{i+1} - R_i}{R_i} = \psi_o$$

where I_i is the intensity at an epicentral distance of R_i , ψ is a constant and is independent of both i and epicentral intensity (I_o), R_o is the minimum epicentral distance of the isoseismal, and R_k is the equivalent radius of the k^{th} isoseismal line (the boundary line of the area with intensity).

2.6.23 Gupta and Trifunac (1988)

A probabilistic method was adopted to derive the intensity attenuation relationships for Indian earthquakes. The distribution of epicentral distance R to a given isoseismal I , during an earthquake with epicentral intensity I_o , is assumed to be approximated by a Gaussian probability density function. The equation of the type $I - I_o = a + b R + c \log_{10}(R)$ was used. Data from 30 major earthquakes from Indian subcontinent were used. The equations derived for mean and mean plus one standard deviation for the northern India are,

$$I - I_o = 2.256 - 0.0099 R - 1.798 \log_{10}(R), \text{ and} \quad (2.22a)$$

$$I - I_o = 3.474 - 0.0048 R - 2.080 \log_{10}(R). \quad (2.22b)$$

2.6.24 Pietrafesa *et al.* (1990)

The heterogeneous set of intensity data the equation given below is the best fit, while the other available equations show a good fit for Calabro-Sicilian region.

$$I_o - I = \frac{1}{\ln(\psi)} \left[1 + \frac{\psi - 1}{\psi_o} \left(\frac{R_i}{R_o} - 1 \right) \right], \quad (2.23a)$$

where R_o and R_i represent, respectively, the equivalent radii of the first and the i^{th} isoseismal lines. R_o must be evaluated with respect to epicentral intensity (I_o) and the other terms are represented by the following ratios,

$$\psi_o = \frac{R_i - R_o}{R_o} = \text{Constant}, \text{ and} \quad (2.23b)$$

$$\psi_i = \frac{R_{i+1} - R_i}{R_i - R_{i-1}} = \text{Constant} = \psi \quad i \geq 1. \quad (2.23c)$$

2.6.25 Prasad (1991)

It was proposed that in most of the cases, a straight line fit the intensity data points for Indian earthquake. This study is similar to Kaila and Sarkar (1978). The slope of these lines indicates decay rate of intensity with epicentral distance. The intensity-distance follows the relation,

$$\ln(I) = \ln(I_o) - s \Delta, \quad (2.24a)$$

$$\text{which gives } \frac{I}{I_o} = \exp^{-s \Delta}, \quad (2.24b)$$

where I is the intensity at an epicentral distance of Δ , I_o is the epicentral intensity. Intensity-distance relations were obtained for 6 earthquakes of India. These relationships are as follows,

Assam earthquake (1897)

$$\frac{I}{I_o} = \exp^{-0.000934 \Delta} \quad (2.24c)$$

Bihar-Nepal earthquake (1934)

$$\frac{I}{I_o} = \exp^{-0.0010396 \Delta} \quad (2.24d)$$

Anjar earthquake (1956)

$$\frac{I}{I_o} = \exp^{-0.0034922 \cdot I} \quad (2.24e)$$

Koyna earthquake (1967)

$$\frac{I}{I_o} = \exp^{-0.0098187 \cdot I} \quad (2.24f)$$

Guwahati earthquake (1975)

$$\frac{I}{I_o} = \exp^{-0.0017933 \cdot I} \quad (2.24g)$$

Dharamsala earthquake (1986)

$$\frac{I}{I_o} = \exp^{-0.00119263 \cdot I}. \quad (2.24h)$$

It was concluded that intensity attenuation for Dharamsala earthquake is high because of hard subsurface structure. The intensity decay of Koyna earthquake is also high which is attributed to the harder nature of Deccan trap.

2.6.26 Tao and Zheng (1991)

The attenuation relationships used in seismic zonation of China were reviewed. Some recently suggested results were introduced and ongoing research using the artificial neural network technique to establish the relationships was reported. The seismic zonation in China is proposed to be guided by two principles: (1) at certain locality, the highest earthquake intensity experienced in the past would be also expected in the future; (2) regions of similar tectonic structures would be subjected to similar intensity. A total of 566 isoseismals from 199 earthquakes were chosen as database for regression analysis with earthquakes having magnitude not less than 5. The attenuation relationships fitted for Eastern and Western parts of China were as follows.

For eastern part of China

Longitudinal direction

$$I - I_o = 6.046 + 1.480 M - 2.081 \ln(R + 25) \quad \sigma = 0.49, \quad (2.25b)$$

Transverse direction

$$I - I_o = 2.617 + 1.435 M - 1.441 \ln(R + 7) \quad \sigma = 0.56, \quad (2.25c)$$

For western part of China

Longitudinal direction

$$i = 5.643 + 1.538 M - 2.1091 \ln(R + 25) \quad s = 0.64, \quad (2.25d)$$

Transverse direction

$$I - I_o = 2.941 + 1.363 M - 1.494 \ln(R + 7) \quad \sigma = 0.61 \quad (2.25e)$$

Some recently suggested results

1. Probability models of intensity attenuation: Instead of commonly used empirical formulae, conditional probability $P(I = i | i_o, r^o)$ can be adopted to describe the attenuation for given i_o and r^o , where i_o is epicentral intensity and r^o is epicentral distance and written in the form of,

$$P(I = i | i_o, r^o) = F_i(r^o | i_o, i+1) - F_i(r^o | i_o, i), \quad (2.27a)$$

where F_i is the conditional probability distribution function of r^o for given i_o and i , which are chosen as lognormal.

2. A united regression analysis method: The form of the regression equation was taken as,

$$i = A + B M - C_1 \ln(r_a + r_{oa}) - C_2 \ln(r_b + r_{ob}) + \varepsilon, \quad (2.27b)$$

where r_a and r_b are the distances for the semi-major axes and semi-minor, i.e. a and b mentioned above respectively; r_{oa} and r_{ob} are the predetermined coefficients for the two axes, and two sets of data can be obtained by the limitation of $r_b = 0$ if $r_a \neq 0$ and $r_a = 0$ if $r_b \neq 0$ from an isoseismal contour.

3. Aimed at the criticism on geological defect in the uncertainty correction procedure currently used in the seismic risk analysis for macroseismic intensity. The following form of regression equation was suggested

$$y = \ln(r + r_0) = A + B M - C, \quad (2.27c)$$

The intensity term was moved to the right hand side of the equation and the term associated with distance was moved to the left-hand side as a dependent variable. It was done as the intensity with a decimal may not be widely accepted and VII-VI ≠ VIII-VII, so that the sum of squares of remaining errors would be thought meaningless. In regression analysis the dependent variable must be continuous and it should be taken as part of independent variable. Thus it is more appropriate to chose distance as the dependent variable instead of intensity. Results showed that by this concept the attenuation at greater distance is faster than the conventional equations.

4. Using the intensity-distance data, one can develop attenuation relationship by using the intensity-distance data; by neural network using the error back propagation approach, which can eliminate the error caused by smoothening of the isoseismal.

2.6.27 Timiovska (1992)

The data from past Macedonian earthquakes, during the years 1905 to 1985, was used to obtain the attenuation relation. An iterative regression analysis was used to obtain relation between epicentral intensity, I_o , epicentral distance, R, and local geological conditions at the recording site, S, ($S = 0, 1$ or 2 for soft, medium and hard geological site condition). The equation derived was of the form,

$$I - I_o = 0.162 - 0.023 R - 0.577 \log_{10}(R) - 0.52 S. \quad (2.28a)$$

The quality of fit was tested and the correlation coefficient computed from

$$r = \frac{\sum (I_{obs} - \bar{I}_{obs}) \sum (I_{est} - \bar{I}_{est})}{\sqrt{\sum (I_{obs} - \bar{I}_{obs})^2} \sqrt{\sum (I_{est} - \bar{I}_{est})^2}} \quad (2.28b)$$

where \bar{I}_{obs} is the mean of the observed intensity I_{obs} , and \bar{I}_{est} is the mean of the estimated intensity level I_{est} . This study shows that the intensities recorded on sediments ($S = 0$) tend to be about one intensity level higher than the intensities recorded on the basement rock site ($S = 2$).

2.6.28 Maugeri and Motta (1993)

In this study 22 earthquakes from Sicily and Calabria were considered and divided into two groups. First group contains earthquakes with focal depth greater than or equal to 15 km, while earthquakes with focal depths less than 15 km were kept in the second group. The following three type of equations were used to describe the attenuation law of seismic intensity.

$$I = a + b M + c \ln(R + D) \quad (2.29a)$$

$$I = a + b I_o + c \ln(R + D) \quad \text{and} \quad (2.29b)$$

$$i = I_o - I = \left(\frac{1}{\ln(\psi)} \right) \ln \left[1 + \frac{(\psi - 1)}{\psi_o} \frac{R}{(R_i - I)} \right], \quad (2.29c)$$

where I_o is the intensity of the epicentral area, R_i is the equivalent radius of the highest mapped isoseismal line, R is the equivalent radius corresponding to intensity I , and ψ, ψ_o are two constants obtained as follows

$$\psi = \frac{R_{k+1} - R_k}{R_k - R_{k-1}} \quad \text{for} \quad k \geq 2, \quad (2.29d)$$

$$\psi_o = \frac{R_2 - R_1}{R_1} \quad (2.29e)$$

where R_k is the equivalent radius of the k^{th} isoseismal line (the boundary line of the area with intensity).

2.6.29 Pantea (1994)

Macroseismic intensity attenuation relationships for Romanian territory and adjacent areas were developed considering 18 earthquakes with epicentral intensities in the range of V to X on MSK intensity scale. The attenuation was analyzed as a function of distance and azimuth from the three main attenuation formulae: logarithmic, exponential, and power-law of which the last one was preferred, as it best fits the observed data. To account for the asymmetry of the isoseismal lines, the attenuation relationships along the following azimuths: N, NE, E, SE, SW, W and NW were sampled. The hypocentral distance was used where the depth of the focus was available and the epicentral distance in other cases.

It was concluded that even for the zones that are adjacent to each other, there is noticeable difference among their rates of attenuation. Thus, future work is needed to verify the results obtained since it was the first approach of the macroseismic intensity attenuation for normal depth source on the Romanian territory.

2.6.30 Teramo *et al.* (1995)

In this study an anisotropic attenuation relationship of the macroseismic intensity was deduced. Results obtained after analyzing a set of earthquakes in Eastern Sicily and Southern Calabria, showed a greater adaptability to the observed data as compared with those deduced using isotropic attenuation laws modified to take anisotropy into account.

The proposed approach is based on a suitable mechanical modeling of the macroseismic field, which allows a quantitative characterization of its anisotropy. Taking into account each irregular isoseismal area and the resistance offered in the direction of energy propagation, it is possible to describe this resistance with the moment of inertial function of the generic isoseismal area A_i , delimited by the two successive isoseismals, ($i-1$)th and i th, with reference to a coordinate system (O_{xy}), with the origin in its baricentre (epicenter) and with respect to the respect to the x -axis, is equal to the,

$$\lambda_i = \int_{A_i} \mu dA_i y^2 , \quad (2.30a)$$

where λ_i is moment of inertia of the area A_i , A_i is the isoseismal area delimited by the two successive $(i-1)^{th}$ and i^{th} isoseismal, dA_i is the infinitesimal element of the isoseismal area A_i , y is the distance of dA_i from x -axis and μ is constant.

The equation deduced was

$$I_i = I_o - \alpha \log\left(\frac{\lambda_i}{\lambda_o}\right) \quad (2.30b)$$

where α is the attenuation coefficient.

2.6.31 Wang *et al.* (1995)

Using the 330 intensity points from 19 historical events ($M_s=3.0$ to 7.8) in and near Jammica, a least-square regression analysis was used to develop intensity attenuation relationship.

$$I = 2.043 + 0.99 M_s - 1.22 \log_{10}(R) - 0.01 R , \quad (2.31)$$

where I represents MM intensity, M_s is the earthquake surface-wave magnitude, and R the epicentral distance in km. The focal depth term was not considered as the island was in a strike-slip plate boundary zone, so the earthquakes are almost exclusively shallow events (0 to 50 km).

2.6.32 Gupta *et al.* (1999)

The MM intensity data was used to study the regional attenuation characteristics of strong ground motion in the peninsular India, using a lognormal probability distribution. The best possible values of the parameters of this distribution were obtained, by using the isoseismal map of fifteen important earthquakes in the Peninsular India. One-step iterative regression analysis was performed to evaluate the attenuation relationship. The equation derived was,

$$I - I_o = 1.8704 - 2.5423 R - 0.001956 \log_{10}(R), \quad (2.32)$$

where intensity (I) was measured on MM scale. It was observed that the trend of attenuation for the peninsular India is almost parallel to that for the Eastern United States, with some flat intensity-distance slope for smaller distance (horizontal translation). The horizontal translation of the curve for peninsular India towards smaller distance was attributed towards the shallower average focal depth.

2.7 Need for the Present Study

In India where large numbers of strong motion records are not available one has to rely on the isoseismals of the past earthquakes to predict the estimated ground motion at a particular site. The attenuation relation can be used to assess the attenuation of damage potential of earthquakes from epicenter. Till date very little work has been done in India. Only few researchers like Kaila and Sarkar (1978), Chandra (1982), Gupta (1986) and Gupta *et al.* (1999) have done some studies. These are the points, which evoke the need for the present study

- 1 The equations fitted in the past are mostly based on the epicentral intensity (Table 2.1). Sometimes equations involving magnitudes fit better than the epicentral intensity (Tao and Zheng, 1991). No studies have been made to ascertain the various equations based on different parameters such as magnitude and maximum intensity or both, and to find which is the most suitable for the Indian subcontinent. In the present study, equations involving magnitude, maximum intensity, epicentral intensity or their combination have been derived and their adequacy for the Indian subcontinent has been checked.
2. In the past, equations were developed using either magnitude or epicentral intensity. But epicentral intensity is an imaginary intensity and magnitudes of past earthquakes are not much reliable as they were not measured directly from instrument. In the

present study, new attenuation relations have been developed considering the maximum intensity (intensity of innermost isoseist) and are compared with the conventional type of equations.

3. Earlier equations were derived only for the average attenuation, but there exists a large difference in the attenuation along the longitudinal and transverse direction of the fault (as large as one intensity unit). Considering this point, equations have been developed for longitudinal as well as for transverse direction along with the average attenuation.
4. The past relations describe only the mean attenuation and the deviations about the mean have not been taken into account. In the present study, equations have been developed for mean as well as mean plus one standard deviation.
5. The past relations were developed using data points from few earthquakes only, which may not be reliable in all cases (*e.g.*, Chandra, 1982(a)). In the present study data points from past 59 earthquakes have been considered which is expected to give results with more confidence.
6. In India, equations developed in United States are still used to evaluate the seismic risk at a particular site. Hence there is a need to compare the attenuation of both the regions (Table 2.4). The past equations show that attenuation in Indian subcontinent is quite different from those of United States (Figure 2.2).
7. The past equations do not directly show how damage area changes with drop of intensity and how the intensity drops differs from one province to other (Table 2.2). These things are incorporated in the present study.



Table 2.1 Available equations for Indian provinces

Province	Researcher	Type of equation used	σ	No of EQ.
North	Gupta 1986	$I - I_o = 2.256 - 0.00990 R - 1.798 \log R$	-	18
	Chandra 1982	$I - I_o = 3.470 - 0.00210 R - 2.667 \log R$	0.193	one
Northeast	Chandra 1982	$I - I_o = 2.501 - 0.00452 R - 1.922 \log R$	0.244	4
Northwest	Chandra 1982	$I - I_o = 3.975 - 0.00100 R - 3.055 \log R$	0.244	3
Peninsular	Chandra 1982	$I - I_o = 4.987 - 0.00204 R - 3.833 \log R$	0.193	5
	Gupta 1986	$I - I_o = 1.870 - 0.001956 R - 2.5432 \log R$	-	15

Table 2.2 Available equations for United States

Province	Type of equation used	σ	No of earthquake considered
San Andreas	$I - I_o = 2.065 - 0.00594 R - 2.065 \log(R + 10)$	0.266	10
Cordilleran	$I - I_o = 2.819 - 0.00503 R - 2.017 \log(R + 25)$	0.245	13
Eastern	$I - I_o = 3.374 - 0.00164 R - 2.414 \log(R + 25)$	0.363	8
Central	$I - I_o = 3.534 - 0.00164 R - 2.528 \log(R + 25)$	0.243	10

Table 2.3 Relative difference in expected intensity levels for geological maps units as shown in the geological map of California [Evernden and Thomson, 1985] (taken from Reiter 1991)

Geological Map Unit	Relative Intensity Compared to Granite Rock
Granitic and Metamorphic Rocks	0.0
Paleozoic Sedimentary Rocks	0.4
Early Mesozoic Sedimentary Rocks	0.8
Cretaceous through Eocene Sedimentary Rocks	1.2
Undivided Tertiary Sedimentary Rocks	1.3
Oligocene through Middle Pliocene Sedimentary Rocks	1.5
Pliocene-Pleistocene Sedimentary Rocks	2.0
Tertiary Volcanic Rocks	0.3

Table 2.4 Conversion table for intensity prepared by Kaila and Sarkar (1978)

Oldham scale	RF Scale
1	X
2	IX
3	VIII
4	VI-VII
5	IV-V
6	II-III
7	I-II

MM Scale	RF Scale
I	I
II	I-II
III	III
IV	IV-V
V	V-VI
VI	VI-VII
VII	VIII
VIII	VII-IX
IX	IX
X	X-XII

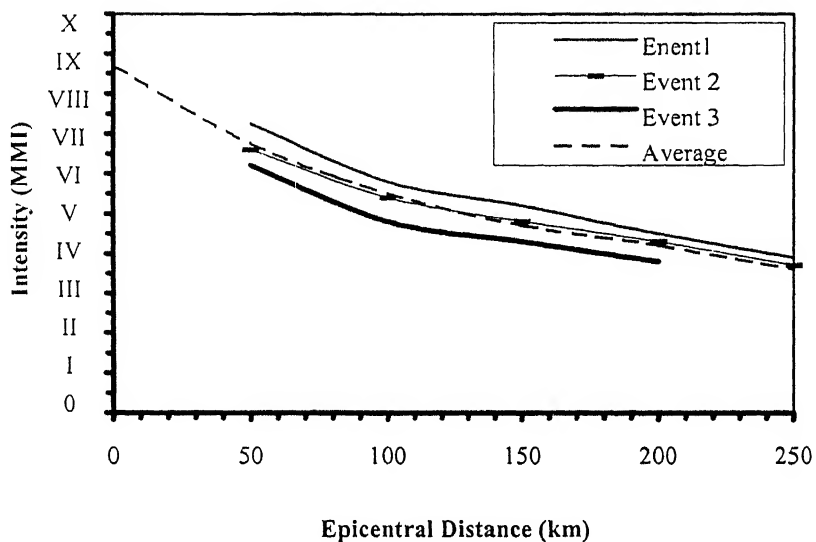


Figure 2.1 Figure showing graphical method of estimating epicentral intensity

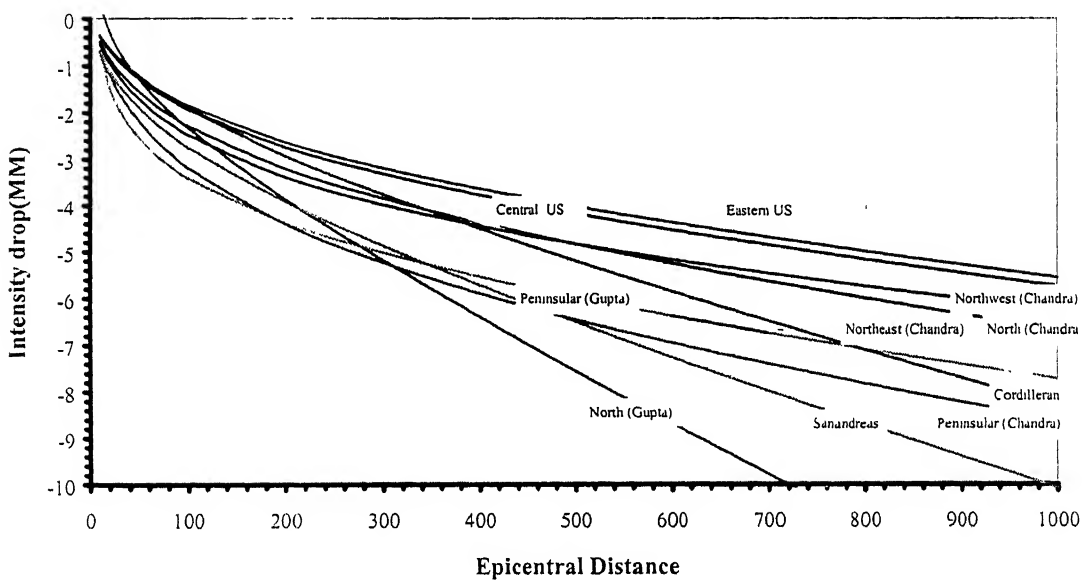


Figure 1.2 Comparison of intensity attenuation of past relations of Indian provinces with those of United States

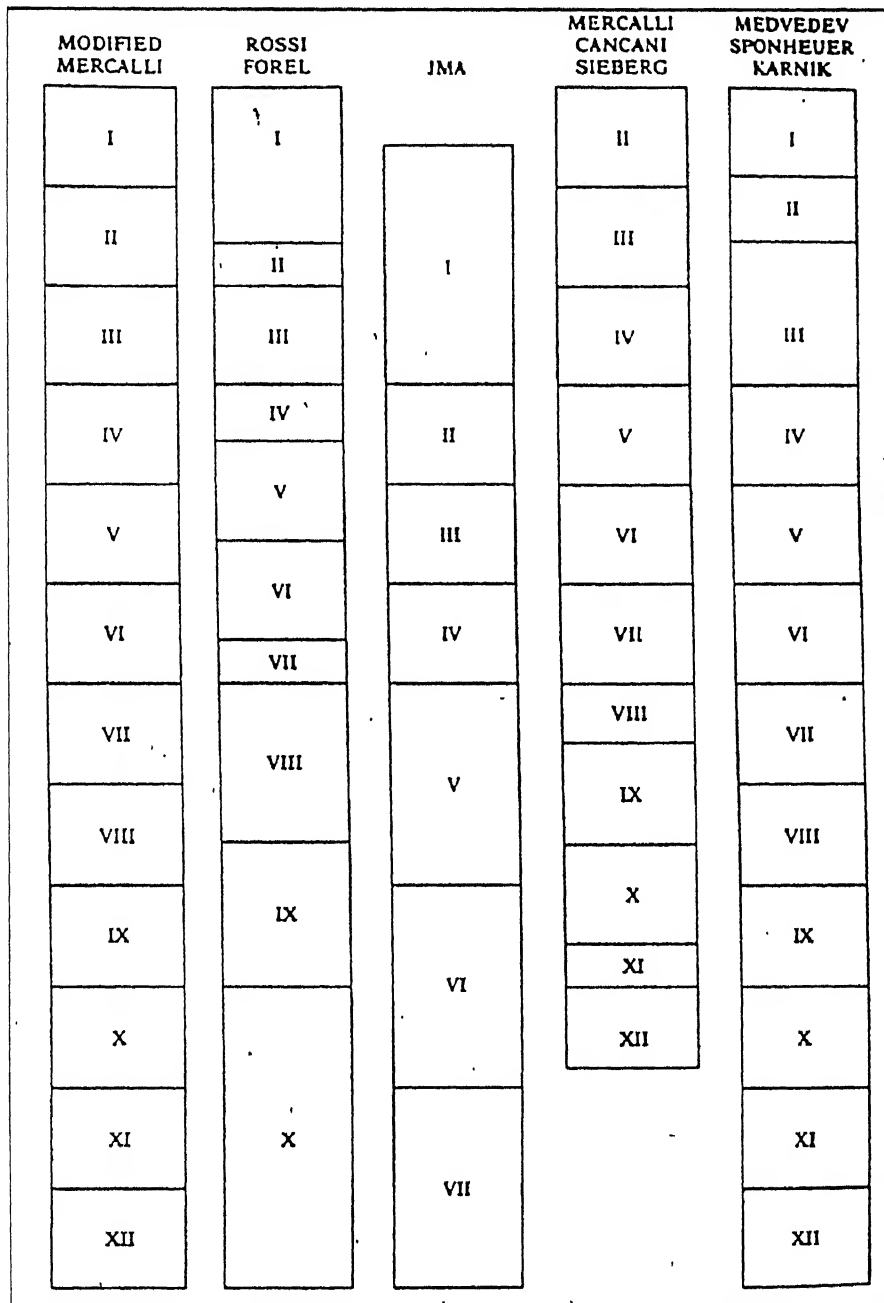


Figure 1.3 A comparison of seismic intensity scales (after Murphu and O'Brien, 1977; and Richter, 1958) (taken from Reiter, 1991).

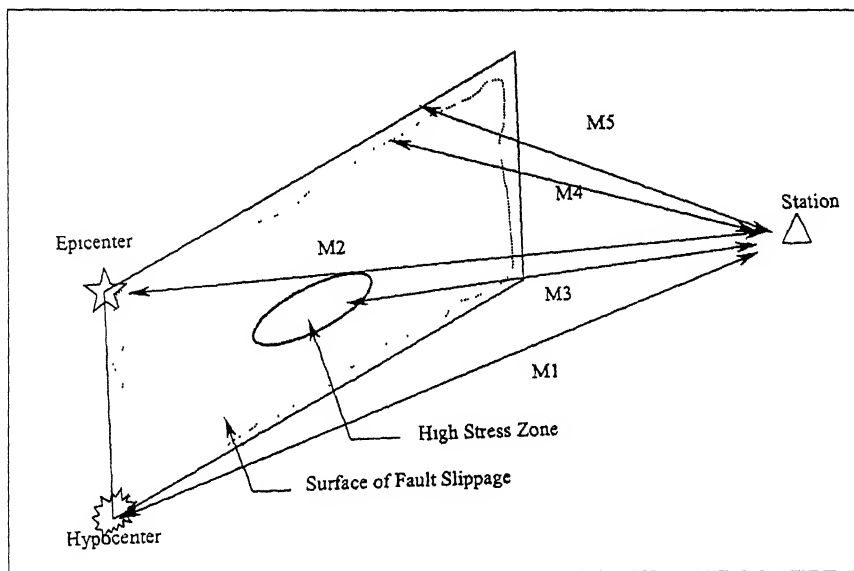


Figure 2.4 Different definitions of distances used in the attenuation relationships [Campbell, 1985]

Chapter 3

Review of Earthquake Intensity Database

3.1 Introduction

Isoseismal maps provide us valuable information about macro-seismic effects of large earthquakes. These are constrained by the field observation of the damage pattern and terrain changes soon after the earthquake. To develop the intensity attenuation relationship for Indian earthquakes, iso-seismal maps from past earthquakes are collected from various sources. Most of the iso-seismal maps are based on the field investigations performed by the Geological Survey of India (GSI). These have been published in Memoirs, Records and other publications of GSI. The publications of India Meteorology Department such as Indian Journal of Meteorology and Geophysics, also contain iso-seismal maps for a number of earthquakes. A few maps were also obtained from other sources like Bulletin of the Indian Society of Earthquake Technology and Bulletin of Seismological Society of America. Various workers have drawn the iso-seimals using different intensity scales. For the purpose developing intensity attenuation relationships, all the maps have been converted to MM scale.

In the present study the Indian sub-continent is divided into six provinces keeping in mind the general geology, tectonic setup, and the source mechanism of earthquakes. The six provinces are the Northwest province, Northern province, Northeastern province, Peninsular province, Foredeep province and Subduction province. The intensity-epicentral distance data for each Indian earthquake is presented in Tables 3.1 to 3.59 with converted intensity scale of MM. The data points considered for the present study have been plotted with respect to magnitude of the event in Figures 3.75 to 3.80.

3.2 Earthquakes Intensity-distance database

3.2.1 Northwest Province

This province consists of whole of northwest India, northeast of Pakistan, and the Kachhi plain in Pakistan. The earthquakes of this region show a mixed mechanism. The isoseismals of events near the Himalayas are elongated along the Main Central Thrust (MCT) and the Main Boundary Thrust, while those of Kachhi plains are elongated towards the south-southwest directions. Most of the isoseists are incomplete due to the very limited population in this region and the past isoseismals are drawn taking very few observation points. Some of the isoseists got accentuation due to the presence of thick alluvial in the Kachhi plain. The shape of isoseist are extrapolated and they are extended to form circles or ellipses and the corresponding distances are taken in the present study. The Kangra earthquake of 1905 is taken into this province because it does not fit well with that of north province earthquakes giving high errors.

3.2.1.1 Kashmir Earthquake (1885)

This earthquake struck the Kashmir valley on May 30, 1885 causing loss of over 3000 lives. Jones (1985) studied the earthquake and located the epicenter near Jampur (34.12°N : 74.61°W), situated about 19.5 km west of Srinagar with focal depth of 12 km. The general trend of the isoseismals is aligned in the NW-SE direction. The epicentral tract covers an area of about 2641 sq. km where the maximum damage occurred (Figure 3.1). The shock was accompanied by the sound of “a hundred canons going off at once”. The area over which the shock was sufficiently large to cause severe damage to buildings extended from the neighborhood of Srinagar on the south-east (Figure 3.2), around a little north of Sopur and Bramula down the Jhelum valley as far as the fort of Chikae near Garhi [Gosain and Arya, 1967].

Gosain and Arya (1967) reevaluated the damage pattern and assigned an intensity of IX in an area of 1902 sq. km (Figure 3.2). It appears that the maximum damage area

identified by Jones (Figure 3.1) encompasses the intensity IX and a part of intensity VIII. Jones (1885) had used the Maline scale to delineate the isoseismals, which is very rough and hence, this map is not used here and the isoseismals given by Gosain and Arya (1967) are used in the present study. The isoseismals given by Gosain and Arya (1967) are on MM scale but they have not explained how they have reevaluated the isoseismal map of Jones (1885).

3.2.1.2 Kangra Earthquake (1905)

This is one of the four great earthquakes in the Himalayan region, it took a toll of 20,000 human lives and caused colossal loss in the form of complete damage to buildings and caused numerous landslides and earth fissures. The earthquake occurred on April 4, 1905 and the epicenter was located in Himachal Pradesh (33.63°N : 76.2°E). The magnitude of the event was 8.6. Middlemiss (1905) studied the damage pattern on the basis of 10 point RF scale. The meizoseismal intensity, according to his interpretations, reached the maximum of X on RF scale (Figure 3.19) and focal depth was estimated to be in between 33 to 65 km.

The elongated epicentral tracts enclosed within the three higher isoseismals were closer towards WNW direction indicating a rapid decrease of intensity and were widely separated towards ESE direction indicating a slow rate of decrease. A small isolated ellipse of MM intensity VII-VIII was found to exist around Mussoorie area, which was attributed by Middlemiss to a separate focus. The isoseismals of the event can be obtained from Middlemiss (1910), Kaila and Sarkar (1978) or Dasgupta *et al.* (2000). Middlemiss prepared the basic map and Kaila and Sarkar (1978) have reproduced the same isoseismals intensity converted from RF scale to MM intensity scale. Dasgupta *et al.* (2000) had reproduced the isoseismals on the geological map of India with all geological and geotectonic information.

For the present study the isoseismals (Figure 3.19) prepared by Middlemiss (1910) are used because all other maps were derived from this only, and are converted to MM scale.

3.2.1.3 Baluchistan Earthquake (1909)

This earthquake struck the Kachhi plain, alluvium basin, on October 21, 1909 with its epicenter at 30°N : 68°E . The isoseismals are elliptical in shape with elongation towards southeast direction (Figure 3.3). The maximum intensity assigned was IX on RF scale. Elliptical shape of the isoseismal indicates that the strata beneath are uniform and homogeneous. The isoseismal map given by Haron (1912) has been utilized for the present study after converting it to MM scale.

3.2.1.4 North West Himalayan Earthquake (1929)

Macroseismic survey for this event was carried out by Coulson (1930), who assigned maximum intensity of VIII on RF scale, magnitude of 7.1 and computed a focal depth of around 200 to 250 km with its epicenter at 36.5°N : 70.5°E . The isoseismals are elliptical with WNW-ESE elongation (Figure 3.4). Mukherjee (1950) reevaluated the data of this event and constrained the isoseismals with NW-SE trend and almost uniform attenuation pattern in the NE as well as SW quadrants. The isoseismals given by Mukherjee (1950) (Figure 3.5) have been utilized in the present study since it is directly on MM scale and the elongation pattern of the isoseismals are similar to the that of most of the isoseismals of this region.

3.2.1.5 Mach Earthquake (1931)

The earthquake occurred on August 27, 1931, felt over a vast area of 9,58,300 sq. km and had epicenter location at 30.2°N : 67.7°E . West (1934) studied this earthquake and constrained the isoseismal on RF scale (Figure 3.6) and assigned a maximum intensity VIII on RF scale. The movement of the crust parallel to the isoseists might have caused the earthquake [West, 1934]. The isoseismal map shows how the isoseismal lines extend

northeast in the Indus valley. This is in accordance with the general observation that the alluvial soil experiences larger shaking than the hard rock. The irregular shape of the isoseismal IV, V and VI was attributed to severe manifestation of earthquake effects in the alluvial tracts [West, 1934]. The isoseismal map of the event prepared by West (1934) has been utilized in the present study after converting it to MM scale. The maximum intensity assigned to it on MM scale is VIII since there are evidence of exceeding intensity VIII on RF scale at some places.

3.2.1.6 Sharigh Earthquake (1931)

Sharigh earthquake of August 25, 1931 with epicentral location as 29.8°N: 67.7°E felt over a relatively small area of 960,000 sq. km and had the maximum mapped intensity of VIII on RF scale (Figure 3.7). West (1934) delineated the isoseismals on RF scale. The isoseismals show N-W elongation, which does not conform to the general trend in this region. The same isoseismals has been utilized for the present study with converted intensities on MM scale.

3.2.1.7 Quetta Earthquake (1935)

Macroseismic study for this earthquake of magnitude 7.5, maximum intensity of IX on RF scale, with epicentral location of 29.5°N: 66.8°E were conducted by West (1936). The isoseismals of this event represent the similar pattern as that of Mach earthquake 1931, with smaller felt area of about 259,000 sq. km (Figure 3.8). Both the earthquakes show epicentral elongation in the NE-SW directions because of the presence of alluvium. For the present study isoseismals given by West (1936) are used after converting it on MM scale. The maximum intensity assigned to this event is X on MM scale because there are evidences of reaching intensity X on RF scale at some places [West, 1936]. An isoseist of intensity X on MM scale is drawn inside the innermost isoseist by approximation. The outermost isoseist is neglected since it is very irregular in shape and does not follow the trend of higher isoseists.

3.2.1.8 Hindukush Earthquake (1937)

This earthquake occurred in the Hindukush region on November 14, 1937 and had magnitude of 7.2, maximum intensity of VIII on RF scale (Figure 3.9), epicentral location of 37.5°N : 71.5°E , and focal depth around 200 to 250 km. Coulson (1938) studied this earthquake and delineated the isoseismals on RF scale. Kaila and Sarkar (1978) reproduced the isoseismals on MM scale. The geological map for the earthquake along with the isoseismal is also available [Dasgupta, 2000]. For the present study the map given by Coulson (1938) has been utilized after converting it on MM scale. The cause of earthquake in this region is reported to be due to the great dislocation crossed by numerous secondary faults, which separate the tertiary formations from the ancient rocks. Forces responsible for these faults seemed to be responsible for the earthquake also [de Ballore, 1940]. The isoseismals are modeled as if they represent a family of half ellipses. The maximum assigned intensity is VIII after converting it to MM scale, since there are evidences of intensity reaching higher than VIII on RF scale. The isoseist VIII is drawn approximately inside the isoseist VII with similar shape.

3.2.1.9 Pamir Earthquake (1939)

The earthquake occurred on November 21, 1939. Its magnitude was 6.9 and induced similar intensities as the two earlier earthquakes in this region [Mach, 1931 and Quetta, 1935]. Coulson (1940) who studied this event estimated the focal depth to be 200 km and epicentral location as 36.5°N : 74°E . The maximum assigned intensity was VIII on RF scale (Figure 3.10). Immense dislocations at the sharp change in direction of the Himalayan chain, must be contributing to the instability of the region. Kaila and Sarkar (1978) had produced the same isoseismal on MM scale. For the present study the isoseismals given by West (1940) has been utilized after converting it to MM scale.

पुस्तकालय केन्द्रीय काशीनाथ

भारतीय बोधोग्रन्थी संस्थान कानपुर

141861

अवाप्ति क्र० A-----

3.2.1.10 Chamba Earthquake (1945)

Kapila (1959) studied the effects of this earthquake, delimited isoseismals of intensities IX, VIII, and VII on MM scale and located the epicenter at 32.75°N : 76.5°E . The earthquake had a magnitude of 6.5 and the isoseismals roughly have a north-south orientation, this does not conform to the general disposition of the structural elements of the region (Figure 3.11). Krishnaswamy (1962) explained this occurrence with the presence of nearly north-south trend of possible tear faults in the area. He further correlated the event with the origin of the Kangra orocline. Dasgupta *et al.* (2000) had reproduced the same isoseismals on the geological map of the region. The same isoseismals are considered in the present study.

3.2.1.11 Badgom Earthquake (1963)

The Badgom earthquake of magnitude 5.5 struck the Srinagar area on September 2, 1963. Wakhloo (1977) studied the earthquake on the basis of damage to the structures and other effects like development of earth fissures, and assigned a maximum intensity of VIII on MM scale (Figure 3.12). The epicenter of the event was located near the village Kolabug (33.98°N : 74.73°E). Wakhloo (1977) concluded that the dislocation along a fault with probable NNW-SSE trend, existing below Karewa sediments was the cause of the earthquake. The earthquake was felt over an area of approximately 100,000 sq. km. On account of the shallow focus (44 km), the shaking was less intense but it was strong enough to result in the collapse 2000 village houses mostly of mud construction [Gosain and Arya, 1967]. The isoseismals of the event are also available with Gosain and Arya (1967). For the present study the isoseismal given by Wakhloo (1977) has been utilized since it is based on the extensive field survey.

3.2.1.12 Anantnag Earthquake (1967)

This earthquake struck the entire district of Anantnag on February 20, 1967 and had a magnitude of 5.7, focal depth of around 24 km, and the epicenter at 33.60°N :

75.28°E. The shock was also felt in the south-eastern section of Srinagar district. The quake was accompanied by a deep rumbling sound (lasted for 20 seconds), which was described as the pealing of thunder by the local populace [Gosain and Arya, 1967]. The damage pattern was confined to VII isoseismal and is around the village Sop, where about 10% old and poorly constructed houses were wholly or partially wrecked. About 458 villages were affected and 786 houses were totally damaged in Anantnag district. Dasgupta *et al.* (2000) had produced the isoseismals given by Wakhloo (1977) on the geological map of the region. The isoseismals given by Gosain and Arya (1967) have been utilized for the present study since they constrain more isoseismals while the map by Wakhloo gives only the epicentral area and the next intensity (VII). The looping part of the isoseismals (Figure 3.14) on the western side has been neglected and the isoseismals are modeled as concentric ellipses.

3.2.1.13 Kinnaur earthquake (1975)

On January 19, 1975, the entire tribal belt of Kinnaur and Lehul Spiti was shocked by a strong event of magnitude around 7. It was felt over an area of about 0.25 million sq. km and had epicenter located at 32.45°N: 78.43°E. The isoseismals are elliptical in shape and oriented in the north-south direction, parallel to the Kaurik-Chango fault [Hukku *et al.*, 1975]. The earthquake caused considerable loss of life and different degrees of damage to various constructions in the area. The most common construction in stone masonry suffered extensive damage. Corrugated iron sheets nailed on timber arches and frames forming cylindrical shell and barrack type structures suffered little damage. Large size boulders rolling down the hill slopes resulted in severe damage to some of the buildings and highways [Singh *et al.*, 1977]. A ground fissure of about 18 km length was formed which appeared to be a surface expression of the fault causing the earthquake [Gosavi *et al.*, 1977].

Hukku *et al.* (1975) assigned a maximum intensity of X on MM scale (Figure 3.23) on the basis of the wide and extensive ground fissures of widths up to 1m; Singh *et al.* (1977) assigned a maximum intensity of IX on MM scale (Figure 3.25), as a few C-Type structures (RCC structures) existing in the area had not suffered damage suitable to assign intensity IX. Singh *et al.* (1977) calculated the magnitude as 6.7 and depth of focus as 25 km. Gosavi *et al.* (1977) also estimated maximum intensity IX on MM scale but their map contained a small isoseismal of X (Figure 3.25), which they attributed to local accentuation caused by loose foundation conditions. They estimated the magnitude of the event to be 6.2 and focal depth around 30 km. The possible sources of isoseismals are Hukku *et al.* (1975), Singh *et al.* (1977), Gosavi *et al.* (1977), Kaila and Sarkar (1978), Dasgupta (2000). Kaila and Sarkar (1978), and Dasgupta (2000) have reproduced the same isoseismal map. Out of all sources, the isoseismals of Hukku *et al.* (1975) of Geological Survey of India has been utilized for the present study.

3.2.1.14 Dharamsala Earthquake (1978)

This earthquake of magnitude 5 struck Himachal Pradesh (32.23°N : 76.61°E) on June 14, 1978. Kumar *et al.* (1981) studied the earthquake and assigned a maximum intensity of VI on MM scale. They had interpreted that the strike slip movement along an N-S tear, exposed west of Dharamsala, which have been displaced could have been responsible for the earthquake. However Dasgupta *et al.* (1982), after studying the focal mechanism indicated a thrust type of mechanism along more or less N-S trending nodal planes. The isoseismals are elongated towards N-S direction and are elliptical in shape. The isoseismal map (Figure 3.26) given by Kumar *et al.* (1981) is considered in the present study.

3.2.1.15 Kathua Earthquake-1(Jammu) (1980)

Two earthquake of magnsitude 5.5 and 5.4, triggering at an interval of 12 minutes, shook Kathua on August 24, 1980. These were named as Bhaddu-Dudwara and Lohai-

Malar shocks. Krishnamurthy *et al.* (1980), on the basis of macroseismic survey estimated the maximum intensity of the Bhaddu-Dudwara event to be VIII and that of Lohai-Malar shock to be VII on MM scale (Figure 3.15). Isoseismals delineated thus has a general NW-SE elongation, which more or less conform to the regional structural trends. For the present analysis both the events are considered separately because both sets of isoseismals can be separated.

3.2.1.16 Kathua Earthquake-2 (Jammu) (1980)

The details of this earthquake are described in the Section 3.2.15 since both the events took place simultaneously.

3.2.1.17 Dharamsala Earthquake (1986)

This earthquake had magnitude of 5.7 and epicenter location as 32.25°N: 76.3°E. It struck the Kangra region on April 26, 1986. Gupta *et al.* (1986) studied the earthquake and assigned maximum intensity of VIII on MM scale (Figure 3.30). The attenuation of intensity VII is quicker on the southeastern side than on the northwestern side while the reverse is true for intensities VI and V and once again the attenuation of intensity IV was rapid in the southeastern direction. From these intensity decay patterns Narula and Shome (1992) inferred that the source fault is aligned in the N55°W: S55°E direction along the general trend of the isoseismals but adjustments might have taken place along the north-south tear located west of Dharamsala township.

In this study the isoseismal map prepared by Narula and Shome (1992) is utilized. The reverse attenuation of isoseismals is neglected. The isoseismals are modeled as if they represent a family of concentric ellipses.

3.2.1.18 Srinagar Earthquake (1988)

Gupta (1988) prepared the isoseismals of the event of magnitude of 3.2. The epicenter of the earthquake was at 34.4°N: 75.3°E as per Indian Meteorology Department. The trend of the isoseismals corresponds to the Himalayan trend of NW-SE and longer

axis extended along the course of Jhelum River (Figure 3.16). The isoseismals of the event is taken from Dasgupta *et al.* (2000).

3.2.1.19 Chamba Earthquake (1995)

An earthquake of magnitude 4.5 rocked the Chamba region of Himachal Pradesh on March 24, 1995. Pande and Sharda (1995) studied the earthquake, assigned maximum intensity of VII on MSK scale, and focal depth around 10 km (Figure 3.17). The same isoseismal map was reproduced on the geological map by Dasgupta *et al.* (2000). For the present study the isoseismals are taken from Dasgupta *et al.* (2000).

3.2.2 Northern Province

This province consists of the whole Indo-Gangetic plain. The whole area is covered by very thick alluvium. The earthquakes of this region are of intermediate focal depth (10-30 km). The uniform and homogenous strata below give rise to elliptical isoseismals but sometime the alluvial deposits cause accentuation in the felt intensity. Preliminary analysis were carried out taking the foredeep and north Indian earthquakes into one category, but the results showed that the two should be separated. The final equations after separating the two give smaller errors and hence they are considered separately in the present study.

3.2.2.1 Delhi Earthquake (1960)

The earthquake of magnitude of 6.0 struck Delhi (28.2°N : 77.4°E) city on August 27, 1960, causing damage and minor casualties. Mukti Nath *et al.* (1969) studied the earthquake and assigned maximum mapped intensity of VII on MM scale (Figure 3.22). The depth of focus was calculated to be in between 5 to 6 km. The elliptical isoseismal VII indicates northeast-southwest feature parallel to the junction of Alwar quartzite and alluvium. The probable cause of the earthquake, as given by them, was the slippage of rocks along the weak regions of fault planes beneath the alluvium. As the isoseismal are

relationship of earthquake with the fault. The isoseismals also represent some isolated intensities of VI. For the present studies the isoseismal map (Figure 3.29) given by Srivastava *et al.* (1980) has been utilized. The isoseismals are modeled as if they represent a family of half-concentric ellipses and the isolated portions are neglected.

3.2.2.5 Uttarkashi Earthquake (1991)

A moderate earthquake of magnitude 6.6 (IMD) shook Garhwal Himalayan region on October 20, 1991. The shock was widely felt in the adjoining northern states of Punjab, Harayana, Himachal Pradesh, Jammu and Kashmir, and Delhi and caused extensive damage in the districts of Uttarkashi, Tehri, and Chamoli. The earthquake took a toll of 768 human lives and caused injuries to 5066 others. The strong ground motion lasting for over 45 seconds caused damages ranging from hairline crack to complete collapse of around “one hundred thousand” houses [Narula *et al.*, 1995]. The earthquake was assigned maximum intensity of IX on MSK scale. The isoseismals are elongated along WNW-ESE directions. The isoseists are generally elliptical in shape with some isolated isoseists of intensity VI and V. The direction of rupture propagation is indicated to be towards southeast from the widening of isoseismal in that direction.

The isoseismals of the event are available with Narula *et al.* (1995), Rastogi and Chadha (1995), GSI (1992), and Dasgupta *et al.* (2000). Narula *et al.* (1995) delineated the epicentral tract and isoseismals (Figure 3.33) of higher intensities on the basis of comprehensive damage surveys. Rastogi and Chadha (1995) have redrawn the isoseismal (Figure 3.34) on the basis of data given in GSI (1992). Dasgupta *et al.* (2000) had reproduced the map given by GSI on the geological map (Figure 3.35). For the present study the isoseismal given by GSI (1992) has been utilized.

3.2.2.6 Delhi Earthquake (1994)

A mild earthquake of magnitude 4 and focal depth of 4 km struck the national capital on July 28, 1994. Gupta and Sharada (1996) studied the earthquake and assigned a

maximum mapped intensity of V on MSK scale (Figure 3.36). The isoseismals are oval in shape and trending in NE-SW direction. The shape of the isoseismals indicates that a NE-SW trending fault might be responsible for the event.

3.2.2.7 Bhind Earthquake (1994)

This earthquake had a magnitude of 4.8 and shook the Bundelkhand and adjoining parts on September 1, 1994. The earthquake was studied and investigated by Pande *et al.* (1995). The general trend shown by the isosiesmals is elongation in ENE-WSW (Figure 3.37), indicating that a slip along that direction might be responsible for the event. The same isoseismals are used which has also been reproduced in Dasgupta *et al.* (2000).

3.2.2.8 Chamoli Earthquake (1996)

This earthquake had a magnitude of 4.5 and struck the Chamoli district on January 23, 1996. The isoseismals given by Singh and Joshi (1996) show general elongation towards N25°E-S25°W direction and had maximum mapped intensity of V on MSK scale (Figure 3.38). The earthquake had a focal depth around 20 km and a fault trending NE-SW might be responsible for it.

3.2.2.9 Garhwal Earthquake (1996)

A moderate earthquake of magnitude of 5.0 rocked the central part of Garhwal Himalayan region on March 26, 1996. Pande and Gairola (1996) conducted the field survey and assigned maximum intensity of VI on MSK scale (Figure 3.39). The general trend shown by the isosiesmals is elongation in NW-SE direction.

3.2.2.10 Indo-Nepal Earthquake (1997)

This earthquake had a magnitude of 5.5, focal depth of 16 km and struck the Indo-Nepal border area (29.8°N: 80.5°E) on January 5, 1997. The isoseismals of the event (Figure 3.40) are taken from Dasgupta *et al.* (2000). The earthquake had maximum mapped intensity of VI on MSK scale. The epicentral tract was elongated in the NE-SW direction following the general trend of earthquakes in this area.

3.2.2.11 Chamoli Earthquake (1999)

A recent earthquake of magnitude 6.3 rocked Garhwal-Kumau Himalayan region on March 29, 1999. The United States Geological Survey (USGS) located its epicenter at 30.512°N: 79.403°E near Gopeshwar, in Chamoli District of Uttar Pradesh, and depth of focus as 21 km. A joint study conducted by The National Society for Earthquake Technology (NSET), Nepal and department of earthquake engineering, Roorkee, studied the earthquake and drew the isoseismal using the MSK scale. The event has a maximum intensity of VIII on MSK scale (Figure 3.41). The elongation of isoseismal line of intensity VII in WSW-ENE direction depicts that the strike of the slip may be in WSW-ENE direction. The elongation and anti-clockwise rotation of the isoseismal line for intensity VI may be due to the effect of the Alaknanda river valley in the almost NE-SW direction. The pattern of damage *i.e.*, maximum damage in the strike direction, at some distance from the epicenter and not near the epicenter depicts that the slip has been on a low angle fault. The isoseismals of the event is taken from Shanker and Narula (1999).

3.2.3 Foredeep Earthquakes

This province consists of the Indo-Gangetic foredeep. The earthquakes in this region show quite different characteristic as those of Northern India province. The earthquakes of this province have focal depth generally larger than that of Northern India province. The isoseismal of this province are generally accentuated in the southern direction due to the presence of thick alluvial below and the northern portion are generally incomplete due to lack of population and difficult terrain.

3.2.3.1 Kathmandu Earthquake (1833)

The epicenter of the event lies close to Kathmandu. The magnitude of the event was reported to be in between 7.5 and 7.9 [Dasgupta *et al.*, 2000]. The earthquake struck at 11 A.M. by a loud subterranean noise comparable to the noise produced by a discharge of 100 pieces of artillery. The direction of the motion was variously stated. At Tirhoot it

was said to have been from east to west; at Buxer, from north to south [Oldham, 1883]; at Patna apparently east and west; at Calcutta, northeast to southwest; and at Kathmandu, apparently east to west. All shocks came from east to northeast. Each of the shock, lasted three or four seconds but some are stated to have lasted one minute [Oldham, 1883]. The event affected around a million square km region of north India, Nepal and Tibet and caused landslides, rockfalls and destruction of 4600 dwellings. It took around 500 lives. It has maximum mapped intensity of IX on MM scale (Figure 3.18). The isoseismals are elliptical in shape with the elongation towards NW-SE directions. The fall of intensity is faster towards the Himalayas but it was slower towards SW direction.

3.2.3.2 Bihar-Nepal earthquake (1934)

On January 15, 1934, north Bihar and Nepal were shaken by one of the severest earthquake in the history measuring 8.3 on the Richter scale. Its epicenter was located near Madhubani (26.3°N : 86.3°E), and maximum intensity observed was X on MM scale (Figure 3.20). The earthquake was studied by GSI (1939). The intensity was found to diminish rapidly with increase in the distance away from epicenter lying on the eastern edge of the region covered by isoseismal X. The high intensity region of the Nepal valley was attributed to the presence of unconsolidated alluvium. The elliptical shape of the isoseismals was supposed to be due to elongated nature of the fault rupture. The shock was felt over an area of 4,920,000 sq. km. Roy (1939) assigned depth of focus from seismometric study as 14.8 km while Richter (1958) kept the focus between 20-30 km depth.

3.2.3.3 Bulandshahar Earthquake (1956)

An earthquake of magnitude 6.5 struck the Bulandshahar and Khurja towns (28.2°N : 77.8°E) on October 10, 1956. The isoseismal map was taken from Tandon (1975). The depth of focus was calculated to be 20 km and radius of perceptibility 300 km. It was indicated that a strike slip motion along NNE-SSW was responsible for the

event. The isoseismals are elongated along southeast direction. The same isoseismals are considered in the present study. The earthquake was felt throughout northwest Uttar Pradesh and adjoining area and caused minor property damage at Bulandshahar and Khurja. It was strongly felt in Delhi where a large number of people rushed out in open for safety. Minor cracks also appeared in a few buildings. In Delhi the intensity was close to VI on MM scale (Figure 3.21).

3.2.3.4 Roorkee Earthquake (1975)

A moderate earthquake of magnitude 4.7 shook the area around Roorkee on November 6, 1975, with the epicenter at 29.85°N: 77.88°E. The earthquake was felt at Delhi, Dehradun, Bijnor, and other adjoining districts in the state of Uttar Pradesh. Different degrees of damage were caused mostly to the older constructions around Roorkee. Cracks along mortar joints and fall of plaster were commonly observed in a number of residential buildings. The earthquake was recorded on Multiple Structural Response Recorder installed at the premises of the School of Research and Training in Earthquake Engineering, University of Roorkee. This was for the first time that an earthquake had been recorded on a strong motion instrument installed in Roorkee [Arya *et al.*, 1977].

The area around Roorkee has a 300m thick cover of recent alluvium. The region north of the area consists of Terai and Bhabar formation, which are unconsolidated young deposits. Further to the north, the Indo-Gangetic plain is terminated by Quaternary tectonic movements. The geomorphologic evidences indicate the existence of two important faults near Roorkee in the unconsolidated young deposits namely, the Ganeshpur fault and Roorkee fault. The Roorkee fault runs just north of the terrace bluff of Roorkee. The apparent termination of the tilted terraces, sudden swing of regional drainage from N-S to W-E, apparent relative young age of the sediments in the zone north

of the fault and the terraces bluff are evidences of the existence of this fault which strikes nearly NW-SE direction [Arya *et al.*, 1977].

Arya *et al.* (1977) studied the earthquake and assigned a maximum mapped intensity of VI on MM scale. The elliptical isoseismals as given by Arya *et al.* (1977) are elongated towards NW-SE (Figure 3.27), which is parallel to the Roorkee fault. Kaila and Sarkar (1978) had reproduced the same isoseismals. The isoseismal given by Arya *et al.* (1977) has been utilized in the present study.

3.2.3.5 Bihar-Nepal Earthquake (1988)

This earthquake struck on August 21, 1988 (epicenter at 26.72°N: 86.63°E) and had magnitude of 6.4 (USGS). The earthquake severely rocked the entire north Bihar and adjacent areas of east Nepal, Sikkim and Darjeeling in West Bengal. The shock was felt almost all over north and eastern Indian from Rajasthan in the west to north eastern States in the east and from Himalayan foothills in the north to Chhotanagpur plateau in the south. Darbhanga and Madhubani were the worst affected districts. The earthquake killed about 300 people in north Bihar, 700 people in Nepal, and caused collapse of about 50,000 houses in the entire area. The reason for the damage being so extensive was that the quake struck close to thickly populated areas. Moreover, the alluvial soil of the Indo-Gangetic plains makes the region particularly vulnerable during earthquakes. The quake lasted for 40 seconds, and its impact was a catastrophic release of energy that struck the surface in ever-expanding concentric circles, leaving in its wake a trail of death and devastation [Duggal and Sato, 1989].

Sinha (1993) studied the earthquake and assigned a maximum intensity of IX on MM scale (Figure 3.31). The isoseismals contain an isolated isoseist of intensity VIII towards the south of Ganga river. The mechanism solution of the event by Banghar (1991) indicates two nodal planes, one striking N58°W: N88°E, and the other with

N30°E: N60°W. The isoseismal map prepared by Thakkar *et al.* (1993) is symmetrical (Figure 3.32) and quite different from that of Sinha (1993). They assigned maximum intensity of VIII on MM scale. For the present study the isoseismal map given by Sinha (1991) has been utilized since it looks quite realistic and reliable since alluvial soil may cause local failure, which distort the shape of isoseismal from general elliptical shape. Kumar (1990) has also given a preliminary isoseismal map. The isoseismals are modeled as if they represent a family of half-concentric circles and the isolated isoseists are neglected because of local effects encountered.

3.2.4 Northeastern Province

The earthquakes of this province are of intermediate focal depth and the isoseismals are generally elliptical in shape. The soil beneath is thick alluvial of Brahmaputra river plain. The isoseists sometimes get accentuated due the presence of thick alluvium. Preliminary survey were conducted keeping the northeast and the subduction earthquakes together but the results showed that the two should be separated. The final equations after separating the two give lesser errors and hence they are considered separately in the present study.

3.2.4.1 Assam Earthquake (1897)

The Assam earthquake of 1897 comes amongst the greatest earthquakes of the world. It struck Shilong (26°N: 91°W) on June 12, 1897 and had a magnitude of 8.7 and epicentral intensity of XII on MM scale (Figure 3.42). Oldham (1899) determined the focal depth in between 180 and 320 km. Oldham (1899) attributed cause of this earthquake to a movement along thrust plane(s) and along secondary thrust and fault planes. He observed dislocation up to 10.66m along Chedrang fault and only 3 cm along comparatively minor Samin fault. The elliptical shape of the isoseismal, given by Oldham (1899) were closely spaced in the east and southeast directions but widely spaced in the west and southwest directions. The approximately elliptical shapes suggest that as

if the soil underneath is homogeneous. The inner irregular isoseismals were due to the geological conditions, the alluvial causing a higher degree of damage. Oldham (1899) estimated the felt area of the event to be not less than 3,120,000 square km.

The isoseismals of the events can be obtained from many sources like Oldham (1899), Kaila and Sarkar (1978), Narula and Sharda (1997), and Dasgupta *et al.* (2000). Oldham (1899) first prepared the isoseismal map of the event on the basis of field observations on Oldham intensity scale. Kaila and Sarkar (1978) had reproduced the map (Figure 3.43) with converted scale of intensity from Oldham to MM intensity scale. Narula and Sharda (1997) reviewed the field data available [Oldham, 1899] and regenerated the isoseismals on MSK scale and assigned maximum intensity of XI on MSK scale (Figure 3.43). Dasgupta *et al.* (2000) reproduced isoseismal map (Oldham, 1899) on the geological map of the region with all geological and geotectonic information. For the present study the isoseismal prepared by Narula and Sarkar (1978) has been utilized since it is directly on MM scale.

3.2.4.2 Calcutta Earthquake (1906)

Middlemiss (1907) delineated the isoseismals (Figure 3.44) and located the epicenter at 27°N: 91°E. There is no record of estimate of magnitude of the earthquake. The epicentral area was elongated NS and coincided roughly with the course of Bhagirathi River down to its junction with Hooghly River. Kaila and Sarkar (1978) have reproduced the same isoseismal map on MM scale.

3.2.4.3 Shrimangal Earthquake (1918)

This earthquake had a magnitude of 7.6 and epicenter at 24.5°N: 91°E. The earthquake was studied in detail by Stuart and used Oldham intensity scale to draw the isoseismals. It was suggested that the cause of earthquake was the subsidence along the southern side of a fault running below the Sylhet valley alluvium, approximately under the major axis of the epicentral tract. The calculated focal depth was around 13 to 14.5

km. The isoseismals were found to be very regular with the apex towards northwest. The isoseismals (Figure 3.45) of the event are available with Stuart (1926), Kaila and Sarkar (1978), and Dasgupta (2000). For the present study the isoseismal map given by Stuart (1926) is used because it is derived from the actual field observations. Kaila and Sarkar (1978) have reproduced the same isoseismals with converted intensity scale to MM scale, while Dasgupta (2000) had produced the same isoseismals on the geological map of the region. For the present study the isoseismals given by Staurt (1918) has been utilized after converting to MM scale.

3.2.4.4 Dhubri Earthquake (1930)

This earthquake had a magnitude of 7.1 and epicentral location at 25.5°N: 90.9°E. It was studied in detail by Gee (1934). The maximum mapped intensity was IX on MM scale (Figure 3.46). The intensity of the event decreases rapidly northwards across the strike of the Himalayan. Gee suggested a considerable depth of focus, as there was no rapid decrease in intensity in the vicinity of the epicentral area. Kaila and Sarkar (1978) also drew the isoseismal map on MM scale and the same is utilized in the present study.

3.2.4.5 Cachar Earthquake (1984)

This earthquake struck the northeast India on December 31, 1984. It had a magnitude of 5.5 and focal depth of 2 km. The isoseismals are taken from Dasgupta *et al.* (2000). The isoseismals are elliptical in shape. The epicentral tract is elongated in NE-SW direction following the general tectonic trend in the region. The epicentral tract was assigned a maximum mapped intensity of VII on MM scale (Figure 3.51). Mud houses were badly damaged and their collapse caused 13 deaths. The Assam type construction (made with bamboos for earthquake resistant) using brick masonry had mainly suffered damage to masonry portions. The light timber construction had generally tilted due to absence of diagonal bracing and not burying the timber posts into the ground [Agarwal, 1985].

3.2.5 Subduction Earthquakes

Subduction earthquakes have high focal depth (60 to 100 km). The high focal depth is mainly attributed to the subduction of Indian plate with that of Burma plate. The earthquakes near the Dauki and Halflong fault with high focal depth are considered in this province. The Assam earthquake of 1975 is also considered in this province because it has large focal depth and its epicenter is near the Dauki and Halflong fault and hence is considered in this province, but past literature does not mention whether it is subduction earthquake or not.

3.2.5.1 Assam Earthquake (1950)

This earthquake struck on August 15, 1950 and the epicenter was near the northeastern border of India (28.5°N : 96.5°E). The earthquake was studied by many researchers. The reports are available in a Central Board of Geophysics publication entitled “A Compilation of Papers on Assam Earthquake”. The magnitude of the shock was 8.7 and focal depth of 30 km (Poddar, 1953). Ray (1953) reported that the maximum intensity at the epicenter might have reached the value XII (Figure 3.48). The isoseismals elongated towards southwest might indicate the presence of a causative fault trending NE-SW. The isoseismals of the event are also available with Dasgupta *et. al.* (2000) and the same are utilized in the present study since they are based on the extensive field investigations conducted by GSI.

3.2.5.2 Assam Earthquake (1975)

This earthquake was studied by Gosavi *et al.* (1977). It took place on July 8, 1975, had a magnitude of 6.7, epicenter at 21.5°N : 94.7°E and focal depth at about 60 km. The earthquake was felt over an area of 500 km radius. The maximum mapped intensity assigned to it was VII on MM scale. The isoseismals are elliptical in shape with epicentral elongation towards NE-SW direction (Figure 3.49), as shown by other earthquake in this

region. The isoseismal given by Gosavi *et al.* (1977) has been utilized for the present study.

3.2.5.3 Nagaland Earthquake (1970)

On July 29, 1970, north eastern part of India, near India-Burma border was struck by an earthquake of magnitude 6.4, with a focal depth of 59 km. the epicentre was located at 26°N: 95.4°E. Guha and Gosavi (1974) prepared the isoseismal map and the same is considered for analysis in the present study. The maximum intensity assigned was VII on MM scale to area around Margherita and Digboi (Figure 3.50), where some damage to housing property occurred. The epicentral tract runs NE-SW and indicates possible tectonic adjustment along Haflong-Dissang thrust fault. Distribution of earthquake intensities show the influence or regional geology and local foundation conditions such as at Imphal where local accentuation in ground vibrations could be attributed to thick sedimentary cover [Guha and Gosavi, 1974].

3.2.5.4 Burma-India Earthquake (1988)

This earthquake had a magnitude of 6.8 and rocked the northeastern states on August 6, 1988. Kumar (1992) on the basis of field investigation prepared the isoseismal map and assigned a maximum mapped intensity of VII on MM scale (Figure 3.52). The isoseismals are elliptical in shape. The elliptical shape of the isoseismal with its major axis having NW-SE trend do not show a close association with the existing major lineaments in the region. Berlongfer and Diphu villages had highest and second highest peak ground accelerations of 0.337g and 0.331g respectively. It was reported that the earthquake was also felt at distant places like parts of West Bengal, and Bihar [Kumar, 1992]. The earthquake was felt strongly in northeast. Buildings in Guwahati, Jorhat, Sibsagar, Diphu, Silchar in Assam and other parts of northeastern states also suffered damage. The earthquake caused landslides at several places including National Highway 37 and Lumding-Diphu section of meter gauge railroad in Assam.

3.2.6 Peninsular Earthquakes

3.2.6.1 Kutch Earthquake (1819)

This earthquake struck the Kutch region on June 16, 1819. This earthquake had magnitude of 8.3 [Jain, 1998]. It was one of the largest intra-plate earthquakes to have occurred in the world. The shock was felt over a radius of 1600 km and was perceptible all over the country as far as Calcutta and Madras. It provided the earliest clear and circumstantially occurrence of faulting. It caused fault scrap of about 90 km long and about 6-9 m high, trending roughly E-W and was later called as "Allah Bund (wall of God)" [Jain, 1998 and Dasgupta *et al.*, 2000], and caused a tsunami from Arabian Sea to surged across the Rann. The dislocation model based on deformation data suggests rupture along a reverse fault. The location of the epicenter of this earthquake is equivocal. According to many researchers the epicenter lies in the south of the Allah Bund, while a few consider it to be lie north of it [Dasgupta *et al.*, 2000]. The isoseismal map is taken from Dasgupta *et al.* (2000). The maximum mapped intensity was IX on MM scale (Figure 3.53). Isoseists corresponding to intensity IX, VIII and II only were shown in the map. The isoseist II is very close to other isoseismal on western side and very far towards southeastern side. The epicentral area was very large as compared to that of other earthquakes in this region. Due to these reasons this event is not considered in the present study.

3.2.6.2 Coimbatore Earthquake (1900)

This is one of the oldest peninsular shield earthquakes. It occurred on February 8, 1900 and epicenter was located at 10.75°N: 76.75°E. It was studied by Basu (1964) and assigned a maximum intensity of VII on MM scale (Figure 3.54). The depth of the focus was around 70 km and the magnitude was 6. From the isoseismal pattern, it was concluded that a fault striking north-northwest on the western coast was responsible for the earthquake. The isoseismal map also contains an isolated isoseist of intensity VI. For

in the present study the isolated isoseist is neglected assuming the existence of particularly localized weak strata. Kaila and Sarkar (1978) and Dasgupta (2000) have reproduced the same isoseismals.

3.2.6.3 Satpura Earthquake (1938)

This earthquake struck the Satpura region on July 14, 1938. It had a magnitude of around 6 and epicentral location of 21.53°N : 75.83°E . The earthquake was studied by Mukherjee (1942). The focal depth was determined to be 43 km and maximum intensity was VII on MM scale (Figure 3.55). The epicentral tract is elongated along NE-SW direction as if fault plane movement has occurred in that direction. For the present study isoseismals are taken from Dasgupta *et al.* (2000).

3.2.6.4 Anjar Earthquake (1956)

On July 21, 1956 earthquake of magnitude 7.0 and depth of focus around 13 to 18 km, struck near Anjar town (23.3°N : 70°E) of the Kutch region. The maximum mapped intensity was IX on MM scale. The earthquake was felt as far away as Bombay in the south, Hyderabad and Thar Parkar districts of Pakistan in the north, Lorwada railway station in east, and the extreme western end of Kutch in the west. The area of maximum damage was confined to about 2,000 sq. km in the central mainland of Kutch. The elliptical isoseismals given by Tandon (1959) have the major axis in the northeast-southwest direction (Figure 3.56), indicating that the probable fault was in this direction. Tandon (1959) observed that the damage to the eastern portion of the Anjar town was more severe than to the western part. He attributed this to the fact that the eastern part of the town was built on soft ground whereas the western part was on hard trap rocks. This earthquake caused 115 fatalities and hundreds were injured. About 1350 houses were destroyed in Anjar town alone and almost 200 houses were partially damaged. The quake also resulted in landslides, which dislocated railway services and snapped communication

and telegraph lines. The earthquake had radius (Figure 3.57) of perceptibility around 300 km [Dasgupta *et al.*, 2000].

3.2.6.5 Koyna Earthquake (1967)

This was one of the most destructive earthquakes in the peninsular region and took place on December 10, 1967. Its epicenter was located at 17.2°N : 73.72°E . Chatterji *et al.* (1969) have given the isoseismal map (Figure 3.59), prepared from the field investigations conducted by GSI. Central Water and Power Research Station (CWPRS), India has also prepared an isoseismal map. The maximum mapped intensity was IX on MM scale. The pattern of the isoseismals is elliptical and aligned nearly north south which probably indicated the strike of the causative fault. The magnitude of the event ranges from 6 to 7.5 given by different agencies and focal depth around 10 km.

3.2.6.6 Bhadrachlam Earthquake (1969)

The earthquake took place on the peninsular shield area on April 13, 1969. Mukherjee (1971) studied the earthquake, determined the focal depth around 40 km and magnitude as 6.5. The epicenter of the event is located at 17.9°N : 80.6°E . The elliptical isoseismals were having their major axis trending almost east-west indicating that the causative fault may be striking in that direction. The isoseismal map is also available with Raju *et al.* (1975), Kaila and Sarkar (1978), Varma *et al.* (1970) and Dasgupta (2000) (Figure 3.61). The isoseismal (Figure 3.60) prepared by Mukherjee (1971) has been used in this study.

3.2.6.7 Broach Earthquake (1970)

The earthquake took place on March 23, 1970, had a magnitude of around 6 and maximum mapped intensity of VII on MM scale. The epicenter of the event was located at 21.68°N : 73.2°E . The isoseismal map (Figure 3.62) was given by Chaudhury *et al.* (1972) and reported depth of focus was in between 15 to 25 km. The same isoseismals are considered in the present study. The isoseismals are almost elliptical in shape with their

elongation in the NE-SW direction indicating as if a fault movement had taken place in that direction. The isoseismals of this event are also available with Chaudhury *et al.* (1972) and Dasgupta *et al.* (2000). A ground fissure of about 15 km in length in alluvial tract was formed along the southern bank of the river Narmada. Spouting of fresh and cool water fissured through ground, very loud sounds in the epicentral zone, disturbance in the Narmada river water, extreme rotatory motion experienced by residents of Broach were noticed in this earthquake. Thick alluvial bed of the northern bank of Narmada had considerably accentuated the seismic movements and contributed to these extreme local phenomena at the epicenter although the earthquake was of magnitude 6 only [Varma *et al.*, 1970].

3.2.6.8 Koyna Earthquake (1973)

Gosavi *et al.* (1977) studied this earthquake at Koyna, it took place on October 17, 1973. It had magnitude of 5.2 and maximum intensity of VI on MM scale. It was felt over an area of 150 km radius and had a focal depth of 10 km. The epicenter of the event was located at 17.7°N: 73.9°E. The isoseismal pattern is almost elliptical in shape and elongated in NE-SW direction. For the present studies the isoseismal map (Figure 3.64) given by Gosavi *et al.* (1977) is considered and the outer isoseist are extended to make full elliptical shape.

3.2.6.9 Shimoga Earthquake (1975)

There were no past records of earthquake activity in region surrounding Shimoga before the Shimoga earthquake of May 12, 1975. The shock was studied by Gosavi *et al.* (1977). They assigned a magnitude of 5.0 and maximum mapped intensity of V on MM scale (Figure 3.65). The epicenter was located at 13.8°N: 75.3°E. The isoseismals were found to of crescent shape with the concave side facing north-northeast. Focal depth and felt radius as reported by them were 35 km and 140 km respectively.

3.2.6.10 Jaisalmer Earthquake (1991)

This earthquake struck the Rajasthan state on September 8, 1991 and the epicenter was located at 26.4°N : 70.66°E . It had a magnitude of 5.5 and focal depth around 30 km. The isoseismals (Figure 3.66) used in this study are taken from Dasgupta *et al.* (2000). The isoseimals given are elliptical in shape with elongation towards NW-SE directions. The intensity falls rapidly from intensity level VIII to VII but slowly from VII to V. The maximum mapped intensity assigned was VIII on MM scale.

3.2.6.11 Saurastra Earthquake (1993)

This earthquake struck the Saurastra coast on August 24, 1993. The epicenter was located at 20.7°N : 71.44°E with focal depth of 29 km. The isoseismals (Figure 3.68) used in this study are taken from Dasgupta *et al.* (2000). The epicentral tract is elongated towards NE-SW direction but the lesser isoseists are elongated towards E-W direction. The maximum mapped intensity was V on MM scale.

3.2.6.12 Killari (Latur) Earthquake (1993)

A devastating earthquake of magnitude 6.4 (USGS) occurred in the early morning of September 30, 1993 in the southern part of the Latur District of Maharashtra State. It had epicenter at 18.07°N : 76.62°E , and focal depth around 12 km (IMD). The earthquake caused widespread damage in some 80 villages and took a toll of more than 11,000 lives. Historically, no earthquake is reported to have occurred in this area [Gupta, 1994]. With death toll exceeding 8933 human lives, the Latur earthquake is globally the deadliest earthquake in the stable continental crust to have occurred in the recorded history. The focal Mechanism solution obtained by NGRI with first motion directions from regional and teleseismic stations indicates reverse faulting with NW-SE orientation of the nodal planes [Ramakrishnan *et al.*, 1995].

Ramakrishnan *et al.* (1995) has drawn the isoseismals on the basis of extensive field investigation conducted by Geological Survey of India. The maximum mapped

intensity assigned was IX on MSK scale. The higher isoseists are closer towards NE and wider on SW direction. Dasgupta *et al.* (2000), Figure 3.68, and Narula *et al.* (1996), Figure 3.69, have also given the isoseismal map. Sinvhal *et al.* (1994) had given preliminary isoseismals of the earthquake. For the present study the isoseismals given by Ramakrishnan *et al.* (1995) are used since it is based on the of extensive field investigation conducted by Geological Survey of India.

3.2.6.13 Bonaigar Earthquake (1995)

This earthquake had a magnitude of 4.4, focal depth around 21 km and epicenter at 21.66°N: 85.59°E. The isoseismals (Figure 3.70) used in this study are taken from Dasgupta *et al.* (2000). The maximum mapped intensity was V on MSK scale. The epicentral tract is elongated towards NE-SW directions. The intensity falls rapidly in NE direction but slowly in SW direction.

3.2.6.14 Jabalpur Earthquake (1997)

This earthquake struck the Jabalpur city on May 22, 1997. Its epicenter was located at 23.083°N: 80.081°E (USGS). The focus was at a depth of 36 km. This earthquake was first to hit any populous city in India. This earthquake caused considerable damage and loss of life. Jabalpur city and several villages located within a radius of about 15 km around the epicenter suffered heavy damage [Rai *et al.*, 1997]. Jabalpur is situated in Narmada rift valley, which is bounded, by Narmada north and Narmada south faults passes through the southern part of Jabalpur city along the Narmada river course. The deep seated earth settlement (37 to 43 km) below the surface for crust part of earth along the fault zone, has been considered as the reason for Jabalpur earthquake.

Rai *et al.* (1997) studied the earthquake and assigned maximum intensity of VIII on MM scale (Figure 3.71). The epicentral tract was elongated in NEN-SWS direction. The shape of the isoseismal depicts shallow nature of the earthquake. The change in the

orientation of the major axis of elliptical isoseismal lines from NEN-SWS to ENE-WSW with the decrease in intensity can be attributed to the effect of local geology and rupture direction [Rai *et al.*, 1997]. Chaturvedi *et al.* (2000) obtained the isoseismal map (Figure 3.73) based on the extensive field survey conducted by GSI. The isoseismals show NE-SW elongation with maximum intensity of VIII on MSK scale. For the present study the isoseismal map prepared by Chaturvedi *et al.* (2000) is used since it is based on the extensive field survey.

3.2.6.15 Bhuj earthquake (2001)

A devastating earthquake of magnitude 7.7 struck Kutch region of Gujarat on January 26, 2001. The earthquake has taken huge toll of life and property in the meizoseismal area as well as in cities of Ahmedabad, Bhavnagar, and Surat located at large distances from the epicenter. The maximum intensity was X on MSK scale. The epicentral tract was elliptical with an area of about 2100 sq. km, which was characterized by adobe, brick and stone masonry buildings and many reinforced cement concrete buildings. The epicentral region had suffered damage of grade 4 to 5 (MSK damage grades). Wide ground fissures and collapses of low height road embankments were observed. The long axis of the epicentral tract was aligned in ENE-WSW to E-W direction.

This earthquake was first to hit major metropolitan cities and the modern industrial construction of the country. In Ahmedabad, 69 RCC buildings collapsed while cities of Rapar, Anjar, Bachho and Gandhidham were completely destroyed. Widespread liquefaction was observed in the Rann of Kutch, the Little Rann of Kutch as well as the coastal areas in the vicinity of Gandhidham, Kandla, and between Malya and Samakhiali. The liquefaction was recorded profoundly in isoseist VIII to X. The distribution deviated from the general E-W elongation consistent with higher isoseismal, to almost north-south

patter along the area occupied by deep seated Quaternary and Cenozoic cover sediments along the Cambay Graben. The accentuation of the motions because of these thick covers has resulted in modification of boundaries (Figure 3.75) of isoseist VII [Narula and Chaubey, 2001]. The isoseismals of the event are available with Narula and Chaubey (2001) and GSI (2001), (Figure 3.76). For the presents study the isoseismal given by Narula and Chaubey (2001) are used. There are modifications in the depositions and trend of VII isoseist of this earthquake because of the presence of thick alluvial in the Cambay Graben, which has resulted in intensity of more than VII in Ahemadabad. For working out the attenuation the average radius of this has been considered in which the effect of accentuation is not there.



Earthquakes Intensity Data

Symbols used

In. : Intensity in MM scale

Rad. : Equivalent radius of circle

Long. : Distance in longitudinal direction of isoseismal from geometric center

Tran. : Distance in transverse direction of isoseismal from geometric center

So. : Source of the isoseismal

North-West Earthquakes Intensity Data

Table 3.1 Kashmir earthquake (1885)

Kashmir- 1885 (M7)	So.	Jones (1885)				Gosain and Arya (1967)			
	In.	Area	Rad	Long	Tran	Area	Rad	Long	Tran
	IX	2641	29	45	20	1902	25	63	39
	VIII	13678	66	65	73	4070	36	92	57
	VII	284487	301	363	235	-	-	-	-

Table 3.2 Kangra earthquake (1905)

Kangra- 1905 (M8.6)	So.	Middlemiss 1910			
	In.	Area	Rad	Long	Tran
	XI	520	13	10	10
	VIII.V	4659	40	46	25
	VII	12868	64	74	40
	V.V	548912	418	480	365
	IV	1368478	660	725	600
	II.V	4154756	1150	1250	950

Table 3.3 Baluchistan earthquake (1909)

Baluchistan 1909 (M7)	So.	Haron 1912			
	In.	Area	Rad	Long	Tran
	IX	511	13	31	6
	VII.V	908	17	41	8
	VII	3216	32	60	17
	VI	5540	42	75	24

Table 3.4 Himalayan earthquake (1929)

Himalayan 1929 (M7.1)	So.	Coulson 1930				Mukherjee 1950			
	In.	Area	Rad	Long	Tran	Area	Rad	Long	Tran
	VIII.V	45973	121	269	103	85487	165	266	98
	VII.V	244421	279	450	300	339877	329	461	316
	V.V	-	-	-	-	912236	539	771	363
	III	-	-	-	-	2226147	842	1134	611

Table 3.5 Mach earthquake (1931)

Mach 1931 (M7.4)	So.	West 1934			
	In.	Area	Rad	Long	Tran
	VIII	2827	30	56	13
	VII.V	4536	38	93	21
	VI.V	66052	145	232	75
	V.V	113411	190	304	97
	I	301593	310	400	240

Table 3.6 Sarigh earthquake (1931)

Sarigh (1931) (M7)	So.	West 1934			
	In.	Area	Rad	Long	Tran
	VII	531	13	12	13
	V.V	19597	79	111	72
	I	78387	158	231	108

Table 3.7 Quetta earthquake (1935)

Quetta 1935 (M7.5)	So.	West 1936			
	In.	Area	Rad	Long	Tran
	X	1662	23	40	12
	VIII.V	2733	29.5	52	16
	VII	8556	52.2	93	29
	I	256840	286	273	273

Table 3.8 Hindukush earthquake (1937)

Hindukush 1937 (M7.2)	So.	Coulson 1938			
	In.	Area	Rad	Long	Tran
	VIII	18627	77	98	60
	VII	45239	120	150	98
	V.V	282743	300	375	262
	IV.V	679291	465	525	413
	III	1552603	703	825	600
	II.V	2505260	893	1013	786

Table 3.9 Pamir earthquake (1939)

Pamir 1939 (M6.9)	So.	Coulson 1940			
	In.	Area	Rad	Long	Tran
	VIII	5027	40	52	30
	VII	85530	165	250	108
	VI	282743	300	370	240
	V	425447	368	422	320
	IV	622114	445	480	410
	III	817128	510	520	500

Table 3.10 Chamba earthquake (1945)

Chamba 1945 (M6.5)	So.	Kapila 1959			
	In.	Area	Rad	Long	Tran
	X	50	3.98	4	3.8
	IX	201	8	8	8
	VIII	9157	54	55	53
	VII	35282	106	106	104

Table 3.11 Badgom earthquake (1963)

Badgom 1963 (M5.5)	So.	Wakhloo 1977				Gosain and Arya 1967			
	In.	Area	Rad	Long	Tran	Area	Rad	Long	Tran
	VIII	3	0.84	1	0.6	13	2	3	1.5
	VII	39	3.48	5	2.5	88	5	7	4
	VI	-	-	-	-	1357	21	24	18
	V	-	-	-	-	6685	46	56	38
	IV	-	-	-	-	22217	84	104	68

Table 3.12 Anantnag earthquake (1967)

Anantnag 1967 (M5.7)	So.	Wakhloo 1977				Gosain and Arya 1967			
	In.	Area	Rad	Long	Tran	Area	Rad	Long	Tran
	VII	5	1.16	1.16	1	616	14	22	9
	VI	453	12	12	4	2827	30	48	19
	V	-	-	-	-	4301	37	55	25
	IV	-	-	-	-	11310	60	80	44

Table 3.13 Kinnaur earthquake (1975)

	So.	Hukku et al. 1975				Singh et al. 1977			
		In.	Area	Rad	Long	Tran	Area	Rad	Long
Kinnaur 1975 (M7)	X	154	7	5	7	201	8	5	7
	IX	962	17.5	8	19	1018	18	8	20
	VIII	2826	30	20	50	3216	32	22	50
	VII	8821	53	38	71	9157	54	40	75
	VI	24317	88	72	105	24872	89	75	108
	V	62427	141	140	135	70650	150	145	140
	IV	160379	226	222	200	166106	230	232	209

	Gosain and Arya 1967			
In.	Area	Rad	Long	Tran
X	2827	30	35	26
IX	4536	38	46	33
VIII	7854	50	63	43
VII	11310	60	71	52
VI	25447	90	105	79
V	31416	100	122	88
IV	101788	180	194	172
III	196350	250	253	243
II	502655	400	424	388

Table 3.14 Dharamsala earthquake (1978)

	So.	Kumar et al. 1981			
		In.	Area	Rad	Long
Dharamsala 1978 (M5.7)	V	33	3.24	6	2
	IV	688	14.8	18	12

Table 3.15 Jammu-I earthquake (1980)

	So.	Krishnamurthy et al. 1980			
		In.	Area	Rad	Long
Jammu-I 1980 (M5.5)	VIII	41	3.6	6	2
	VII	114	6	9	3
	VI	314	10	19	7
	V	804	16	30	9

Table 3.16 Jammu-2 earthquake (1980)

Jammu-2 1980 (M5.4)	So.	Krishnamurthy et al. 1980			
	In.	Area	Rad	Long	Tran
	VII	37	3.4	4	2
	VI	255	9	10	7
	V	2641	29	38	17

Table 3.17 Dharamsala earthquake (1986)

Dharamshala 1986 (M5.7)	So.	Gupta et al. 1986			
	In.	Area	Rad	Long	Tran
	VII	201	8	9	6
	VI	1520	22	25	19
	V	4776	39	43	35
	IV	18137	76	126	49

Table 3.18 Srinagar earthquake (1988)

Srinagar 1988 (M4.5)	So.	Gupta 1988			
	In.	Area	Rad	Long	Tran
	IV	314	10	16	6
	III	2462	28	40	20

Table 3.19 Chamba earthquake (1995)

Chamba 1995 (M4.5)	So.	Pande and Sharda 1995			
	In.	Area	Rad	Long	Tran
	VII	7	1.4	1.4	1.4
	VI	255	9	10	7
	V	1809	24	28	21

Table 3.20 Delhi earthquake (1960)

Delhi 1960 (M6)	So.	Muthinath et al. 1969			
	In.	Area	Rad	Long	Tran
	VII	168	7.3	14	3
	VI	1256	20	22	20
	V	4535	38	49	31

Table 3.21 Indo-Nepal earthquake (1978)

Indo-Nepal 1978 (M4.5)	So.	Kumar et al. 1981			
	In.	Area	Rad	Long	Tran
	VI	2123	26	7	3
	V	7850	50	15	7
	IV	14520	68	19	14
	III	44466	119	-	-

Table 3.22 Nepal earthquake (1980)

Nepal 1980 (M5.8)	So.	Srivastava et al. 1980			
	In.	Area	Rad	Long	Tran
	VIII	531	13	41	16
	VII	4070	36	84	28
	VI	17195	74	94	42
	V	93978	173	143	88

Table 3.23 Uttarkashi earthquake (1991)

Uttarkashi 1991 (M6.6)	So.	GSI 1992				Narula et al. 1995			
	In.	Area	Rad	Long	Tran	Area	Rad	Long	Tran
	IX	347	10.5	10	10	565	13	15	12
	VIII	453	12	21	11	1062	18	26	13
	VII	3630	34	40	33	5730	43	48	38
	VI	26577	92	113	71	28981	96	123	75

Narula et al. 1995			
Area	Rad	Long	Tran
415	11	12	11
939	17	23	13
5089	40	45	36
30140	98	123	78
137071	209	271	161

Table 3.24 Delhi earthquake (1994)

Delhi 1994 (M4)	So.	Gupta and Sharda 1996			
	In.	Area	Rad	Long	Tran
	V	59	4.3	4.3	4
	IV	453	12	12	9

Table 3.25 Bhind earthquake (1994)

Bind 1994 (M4.8)	So.	Pande et al. 1995			
	In.	Area	Rad	Long	Tran
	VII	113	6.5	7	6
	VI	1810	24	28	20
	V	7854	50	60	42
	IV	28353	95	95	95

Table 3.26 Chamoli earthquake (1996)

Chamoli 1996 (M4.5)	So.	Singh and Joshi 1996			
	In.	Area	Rad	Long	Tran
	VI	452	12	20	7
	V	1257	20	30	14
	IV	5542	42	50	36

Table 3.27 Gharwal earthquake (1996)

Gharwal 1996 (M5)	So.	Pande and Gajrola 1996			
	In.	Area	Rad	Long	Tran
	VI	113	6	8	4
	V	452	12	16	8
	IV	3217	32	27	37

Table 3.28 Indo-Nepal earthquake (1997)

Indo-Nepal 1997 (M5.5)	So.	Dasgupta et al. 2000			
	In.	Area	Rad	Long	Tran
	VI	2827	30	44	20
	V	11310	60	83	44

Table 3.29 Chamoli earthquake (1999)

Chamoli 1999 (M6.3)	So.	GSI			
	In.	Area	Rad	Long	Tran
	VIII	1810	24	40	14
	VII	18146	76	115	50

Table 3.30 Kathmandu earthquake (1833)

Kathmandu 1833	So.	Dasgupta et al. 2000			
	In.	Area	Rad	Long	Tran
	IX	16278	72	75	63
	VIII	149226	218	225	200
	VI	358727	338	483	267
	VI	520138	407	533	308
	V	970688	556	788	388
	IV	1775683	752	1033	500

Table 3.31 Bihar-Nepal earthquake (1934)

Bihar-Nepal 1934 (M8.4)	So.	GSI 1939			
	In.	Area	Rad	Long	Tran
	X	2827	30	60	15
	IX	32669	102	140	65
	VIII	70650	150	175	138
	VII	262256	289	256	279
	VI	794449	503	694	368
	V	2039858	806	921	591
	IV	3974063	1125	1058	898
	II	7302463	1525	1340	1234

Table 3.32 Bulandshahar earthquake (1956)

Bulandsahar 1956 (M6.5)	So.	Tandon 1975			
	In.	Area	Rad	Long	Tran
	VIII	1320	20.5	20	17
	VII	6359	45	53	38
	VI	18618	77	88	65
	V	244421	279	333	230

Table 3.33 Roorkee earthquake (1975)

Roorkee 1975 (M4.7)	So.	Arya et al. 1977			
	In.	Area	Rad	Long	Tran
	VI	59	4.3	6.5	3
	V	314	10	16	7
	IV	707	15	20	12

Table 3.34 Bihar-Nepal earthquake (1988)

Bihar- Nepal 1988 (M6.4)	So.	GSI 1993				Thakkar et al. 1993			
	In.	Area	Rad	Long	Tran	Area	Rad	Long	Tran
	IX	3019	31	42	23	-	-	-	-
	VIII	17671	75	108	50	35151	106	167	67
	VII	38013	110	160	75	101747	180	233	139
	VI	80425	160	215	115	189545	246	311	194

Table 3.35 Assam earthquake (1897)

Assam 1897 (M8.7)	So.	Narula and Sarkar 1997			
	In.	Area	Rad	Long	Tran
	XI	14527	68	90	50
	X	70686	150	192	120
	IX	180956	240	312	180
	VIII	384845	350	402	300
	VII	679291	465	540	400

So.	Oldham 1899				
	In.	Area	Rad	Long	Tran
	XI	118177	194	213	172
	VIII.V	323549	321	410	287
	VII.V	678947	465	616	418
	VI	1719464	740	820	673
	IV	3350659	1033	1148	944

Table 3.36 Calcutta earthquake (1906)

Calcutta 1906	So.	Middlemiss 1907			
	In.	Area	Rad	Long	Tran
	VI	12070.2	62	88	44
	IV	79382.3	159	190	111
	II	180864	240	278	187

Table 3.37 Srimangal earthquake (1918)

Srimangal 1918 (M7.6)	So.	Stuart 1918			
	In.	Area	Rad	Long	Tran
	X	460	12	15	8
	VIII.V	4070	36	44	30
	VII.V	18377	77	90	67
	VI	40808	114	134	103
	IV	836044	516	744	492
	II.V	2371206	869	1020	820

So.	Struat 1920				
	In.	Area	Rad	Long	Tran
	X	-	-	-	-
	VIII.V	-	-	-	-
	VII.V	-	-	-	-
	VI	22156	84	125	76
	IV	855600	522	750	491

Table 3.38 Duhbri earthquake (1930)

Dhubri 1930 (M7.1)	So.	Gee 1934			
	In.	Area	Rad	Long	Tran
	IX	1134	19	12	15
	VII	15829	71	70	91
	VII	62427	141	170	110
	VI	174886	236	273	190
	IV	602391	438	430	381

Table 3.39 Cachar earthquake (1984)

Cachar 1984 (M5.5)	So.	Dasgupta et al 2000			
	In.	Area	Rad	Long	Tran
	VII	20	2.52	4	1.5
	VI	238	8.7	15	6
	V	1018	18	25	17

Table 3.40 Assam earthquake (1950)

Assam 1950 (M8.7)	So.	Poddar 1950			
	In.	Area	Rad	Long	Tran
	XI	6362	45	65	30
	X	90746	170	310	95
	IX	212264	260	460	154
	VIII	384650	350	602	207
	VII	638680	451	802	251
	VI	1460490	682	951	351
	V	2178812	833	1112	482
	II	4635347	1215	1410	889

Table 3.41 Assam earthquake (1975)

Assam 1975 (M6.7)	So.	Gosavi et al. 1977			
	In.	Area	Rad	Long	Tran
	VI	3847	35	59	18
	V	29545	97	131	70
	IV	153361	221	288	174
	III	530412	411	505	344

Table 3.42 Nagaland earthquake (1970)

	So.	Guha and Gosain 1974			
		In.	Area	Rad	Long
Nagaland 1970 (M6.4)	VI	27158	93	130	70
	V	146500	216	280	155
	IV	446286	377	470	215
	III	919019	541	625	365
	II	1650463	725	830	618

Table 3.43 Burma-India earthquake (1988)

	So.	BIECT			
		In.	Area	Rad	Long
Burma- India 1988 (M6.8)	VII	1256	20	32	18
	VI	6359	45	58	32
	V	20096	85	110	70

Table 3.44 Kutch earthquake (1819)

	So.	Dasgupta et al. 2000			
		In.	Area	Rad	Long
Kutch 1819	IX	169007	232	257	201
	VIII	352387	335	389	320
	II	3415846	1043	1111	840

Table 3.45 Coimbatore earthquake (1900)

	So.	GSI (Atlas)			
		In.	Area	Rad	Long
Coimbat- ore 1900 (M6)	VII	11684	61	80	45
	VI	40808	114	148	84
	V	119399	195	194	98
	IV	307623	313	274	231
	III	816714	510	510	400

Table 3.46 Satpura earthquake (1938)

	So.	Mukherjee 1942			
		In.	Area	Rad	Long
Satpura 1938 (M6.2)	VII	21632	83	96	75
	VI	120627	196	218	191
	V	278845	298	328	239
	IV	492403	396	464	300
	III	684800	467	546	382
	I.V	1016610	569	870	700

Table 3.47 Anjar earthquake (1956)

Anjar 1956 (M7)	So.	Tandon 1956				Dasgupta et al. 2000			
	In.	Area	Rad	Long	Tran	Area	Rad	Long	Tran
	IX	154	7	11	7	327	10	13	8
	VIII	1662	23	23	24	1806	24	25	23
	VII	4070	36	38	38	4775	39	40	38
	VI	11684	61	72	51	12959	64	75	55
	V	35950	107	131	90	41186	114	138	95
	IV	110981	188	215	169	123700	198	225	175
	III	294018	306	343	284	307876	313	350	280

Table 3.48 Calcutta earthquake (1964)

Calcutta 1964 (M5.5)	So.	Jhingram et al. 1969			
	In.	Area	Rad	Long	Tran
	VIII	11304	60	70	30
	VII	24872	89	95	68
	VI	53066	130	135	89
	IV	101736	180	230	124
	II	180864	240	280	158

Table 3.49 Koyna earthquake (1967)

Koyna 1967 (M7)	So.	Chatterji et al. 1967			
	In.	Area	Rad	Long	Tran
	VIII	79	5	7	4.5
	VII	1134	19	17	12
	VI	1963	25	31	21
	V	133250	206	238	145
	IV	509965	403	463	310

Table 3.50 Bhadrachalam earthquake (1969)

Bhadrac- -halam 1969 (M6)	So.	Mukherjee 1971				Dasgupta et al. 2000			
	In.	Area	Rad	Long	Tran	Area	Rad	Long	Tran
	VII	42984	117	115	90	51472	128	165	100
	VI	121861	197	250	155	132025	205	258	163
	V	232310	272	331	240	280862	299	358	250
	II	1023769	571	700	384	-	-	-	-

Table 3.51 Broach earthquake (1970)

	So.	GSI (Atlas)				Chaubhury et al. 1970			
		In.	Area	Rad	Long	Tran	Area	Rad	Long
Broach 1970 (M6.7)	VII	64	4.5	12	5	-	-	12	5
	VI	1018	18	27	20	1809	24	26	21
	V	3630	34	62	39	7235	48	60	41
	IV	18137	76	96	77	24317	88	98	79
	III	-	-	-	-	48281	124	139	111
	II	-	-	-	-	102870	181	206	158

Table 3.52 Koyna earthquake (1973)

	So.	Gosavi et al 1977			
		In.	Area	Rad	Long
Koyna 1973 (M5.2)	V	616	14	16	9
	IV	3317	32.5	38	28
	III	18137	76	91	68
	II	88624	168	205	141

Table 3.53 Shimoga earthquake (1975)

	So.	Gosavi et al. 1977			
		In.	Area	Rad	Long
Shimoga 1975 (M5)	V	-	-	-	-
	IV	7235	48	70	25
	III	28939	96	112	64
	II	76416	156	173	122

Table 3.54 Jaisalmer earthquake (1991)

	So.	Dasgupta et al. 2000			
		In.	Area	Rad	Long
Jaisalmer 1991 (M5.5)	VIII	114	6	3	3
	VII	908	17	45	6
	VI	13267	65	96	37
	V	36625	108	129	88

Table 3.55 Saurashtra earthquake (1993)

	So.	Dasgupta et al. 2000			
		In.	Area	Rad	Long
Saurashtra 1993	V	7540	49	70	37
	IV	36625	108	125	80
	III	64210	143	177	127

Table 3.56 Killari earthquake (1993)

Killari 1993 (M6.2)	So.	GSI (Atlas)			
	In.	Area	Rad	Long	Tran
	IX	154	7	5	3
	VIII	453	12	9	5
	VII	616	14	16	11
	VI	8168	51	57	38
		VI	14520	68	148
					100

Table 3.57 Bonaigarh earthquake (1995)

Bonaigarh 1995 (M4.4)	So.	Dasgupta et al. 2000			
	In.	Area	Rad	Long	Tran
	V	1520	22	19	23
	IV	6645	46	47	41
	III	15829	71	76	65

Table 3.58 Jabalpur earthquake (1997)

Jabalpur 1997 (M6)	So.	Rai et al. 1997				Dasgupta et al. 2000			
	In.	Area	Rad	Long	Tran	Area	Rad	Long	Tran
	VIII	320	10	12	9	360	12	14	11
	VII	2262	27	36	20	2642	29	42	18
	VI	8708	53	84	33	10568	58	92	35
	V	74374	154	178	133	84496	164	188	143

Table 3.59 Bhuj earthquake (2001)

Bhuj 2001 (M7.9)	So.	Narula and Chaubey 2001				GSI 2001			
	In.	Area	Rad	Long	Tran	Area	Rad	Long	Tran
	X	2324	27	42.5	18	1005	18	20	16
	IX	11011	59	90	42	11517	- 61	78	47
	VIII	30049	98	170	85	41639	115	141	94
	VII	-	-	-	-	104458	182	266	125

Table 3.60 Earthquake details of Northwest province

Sl. No	Name	Date	Mag.	Foc. Dep.	Max. int.	Co-ordinate		Source
1	Kashmir	30-May-1885	7	12	I/MS	34.1	74.61	Jones 1885
					VIII/MSK			Gosain and Aiyar 1967
2	Kangra	4-Apr-1905	8.6	32.6-62		X/MMI	33.6	76.2
3	Baluchistan	21-Oct-1909	-	200-250	IX/MMI	30	68	Middlemiss 1910
4	Himalaya	1-Feb-1929	7.1		VIII/RF	36.5	70.5	Coulson 1930
					VIII/RF			Mukerjee 1950
5	Mach	25-Aug-1931	7.4	-	VIII/RF	30.2	67.7	West 1934
6	Sharigh	27-Aug-1931	7	-	VIII/RF	29.8	67.7	West 1934
7	Quetta	31-May-1935	7.5	-	X/MMI	29.5	66.8	West 1936
8	Hindukush	14-Nov-1937	7.2	200-250	VIII/RF	37.5	71.5	Coulson 1938
9	Pamir	21-Nov-1939	6.9	200-250	VIII/MMI	36.5	74	Coulson 1940
10	Chamba	22-Jul-1945	6.5	60	IX/RF	32.5	76	Kapila 1959
11	Badgom	2-Sep-1963	5.5	-	VIII/MMI	33.59	74.44	Wakhaloo 1977
12	Anantnag	20-Feb-1967	5.7	24	VII/MMI	33.7	75.28	Wakhaloo 1977
			5.5	20	VII/MMI			Gosain and Arya 1967
13	Kinnaur	19-Jan-1975	-	-	X/MMI	32.5	78.43	Gosavi et al. 1977
			6.8	30	X/MMI			Singh et al. 1977
			7	1	X/MMI			Hukku et al. 1977
14	Dharamsala	15-Jun-1978	5	-	VI/MMI	32.2	76.61	Kumar et al. 1981
15a	Jammu-1	24-Aug-1980	5.5	-	VIII/MMI	-	-	Krishnamurthy et al. 1990
16	Jammu-2	24-Aug-1980	5.4	-	VII/MMI			Krishnamurthy et al. 1990
17	Dharamsala	26-Apr-1986	5.7	23	VIII/MMI	32.3	76.3	Gupta 1986
18	Srinagar	8-Feb-1988	3.2	-	IV/MSK	34.4	75.3	Gupta 1988
19	Chamba	24-Mar-1995	4.5	10	VI/MSK	-	-	Pande and Sharda 1995

Table 3.61 Earthquake details of Northern province

Sl. No	Name	Date	Magnitude	Focal depth	Max. inten	Co-ordinate		Source
20	Delhi	27-Aug-1960	6	-	VII/MMI	28.2	77.4	Muktinath et al. 1969
21	Indo-Nepal	21-May-1979	5.8	13-16	IV/MMI	30	80.3	Kumar et al. 1981
22	Nepal	29-Jul-1980	6.1	-	VIII/MMI	29.6	81.07	Srivastava et al. 1980
23	Utterkashi	20-Oct-1991	6.6	-	VIII/MMI			Thakkar 1993
					IX/MSK			GSI 1992
					IX/MSK			Narula et al. 1995
24	Calcutta	15-Apr-1964	5.5	36	VIII/MMI	21	88.5	Jhingran et al. 1969
25	Delhi	28-Jul-1994	4	4	V/MSK	-	-	Gupta and Sharda 1996
26	Bhind	1-Sep-1994	4.8	-	7/MSK	-	-	Pande et al. 1995
27	Chamboli	23-Jan-1996	4.5	20+5	VI/MSK	-	-	Singh and Joshi 1996
28	Garhwal	26-Mar-1996	5	-	VI/MSK	-	-	Pande and Gairola 1996
29	Indo-Nepal	5-Jan-1997	5.5	16	VI/MSK	29.8	80.5	Kumar et al. 1981
30	Chamboli	29-Mar-1999	6.3	21	VIII/MSK	30.5	79.4	Dasgupta et al. 2000

Table 3.62 Earthquake details of Foredeep province

31	Kathmandu	26-Aug-1833	-	-	IX/MMI	-	-	Dasgupta <i>et al</i> 2000
32	Bihar-Nepal	15-Jan-1934	8.4	20-30	X/MMI	26.5	86.5	Gsi 1939
33	Bulandshahar	10-Oct-1956	6.5	20	VIII/MMI	28.2	77.8	Tandon 1975
34	Roorkee	6-Nov-1975	4.7	-	VI/MMI	32.4	78.5	Arya <i>et al</i> 1977
35	Bihar-Nepal	21-Aug-1988	6.4	65	IX/MMI	26.7	86.63	GSI 1993

Table 3.63 Earthquake details of Northeast province

Sl. No	Name	Date	Mag.	F.D.	Max. int.	Co-ordinate		Source
36	Assam	12-Jun-1897	8.7	155-310	XII/MMI	26	91	Oldham 1899
								Narula and Sarkar 1997
37	Calcutta	29-Sep.-06	-	-	VI/MMI	27	97	Middlemiss 1907
38	Shrimangal	8-Jul-1918	7.6	12.4-14	X/MMI	24.5	91	Staart 1918
39	Dhubri	3-Jul-1930	7.1	-	IX/MMI	25.5	90.9	Gee 1934
40	Cachar	31-Dec-1984	5.5	2	VII/MMI	24.7	92.85	Dasgupta <i>et al</i> . 2000

Table 3.64 Earthquake details of Subduction province

41	Assam	15-Aug-1950	8.7	46.5	X/MMI	28.5	96.5	Poddar 1950
					X/MMI			Dasgupta <i>et al</i> 2000
42	Assam	8-Jul-1975	6.7	60	VII/MMI	21.5	94.7	Gosavi <i>et al</i> 1977
43	Nagaland	29-Jul-1970	6.4	59	VII/MMI	26	95.4	Guha and Gosavi 1974
44	Burma-India	6-Aug-1988	6.8	-	VII/MMI	-	-	BIEST

Table 3.65 Earthquake details of Peninsular province

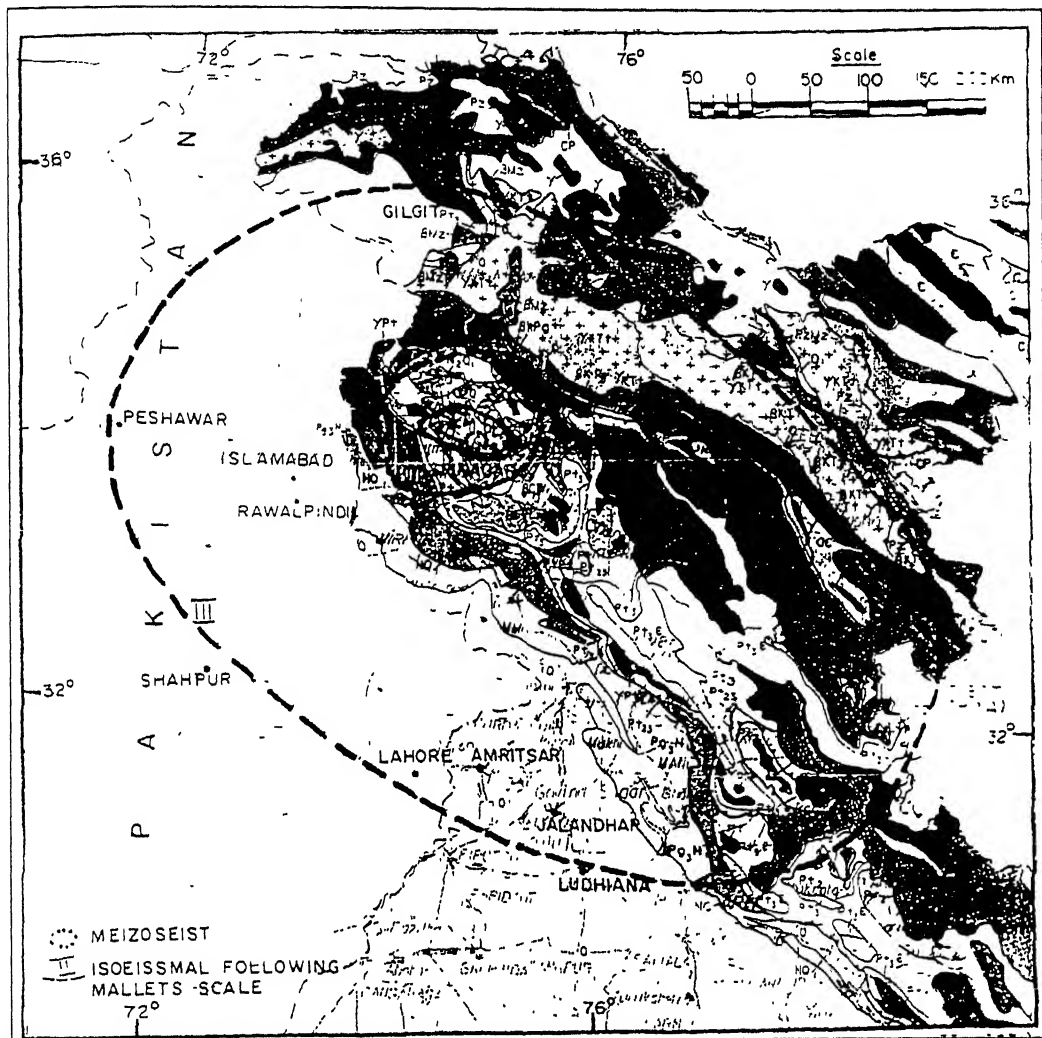


Figure 3.1 Isoseismal of Kashmir earthquake (M 7) of 30th May 1885 following Mallet's scale after Jones (1885).

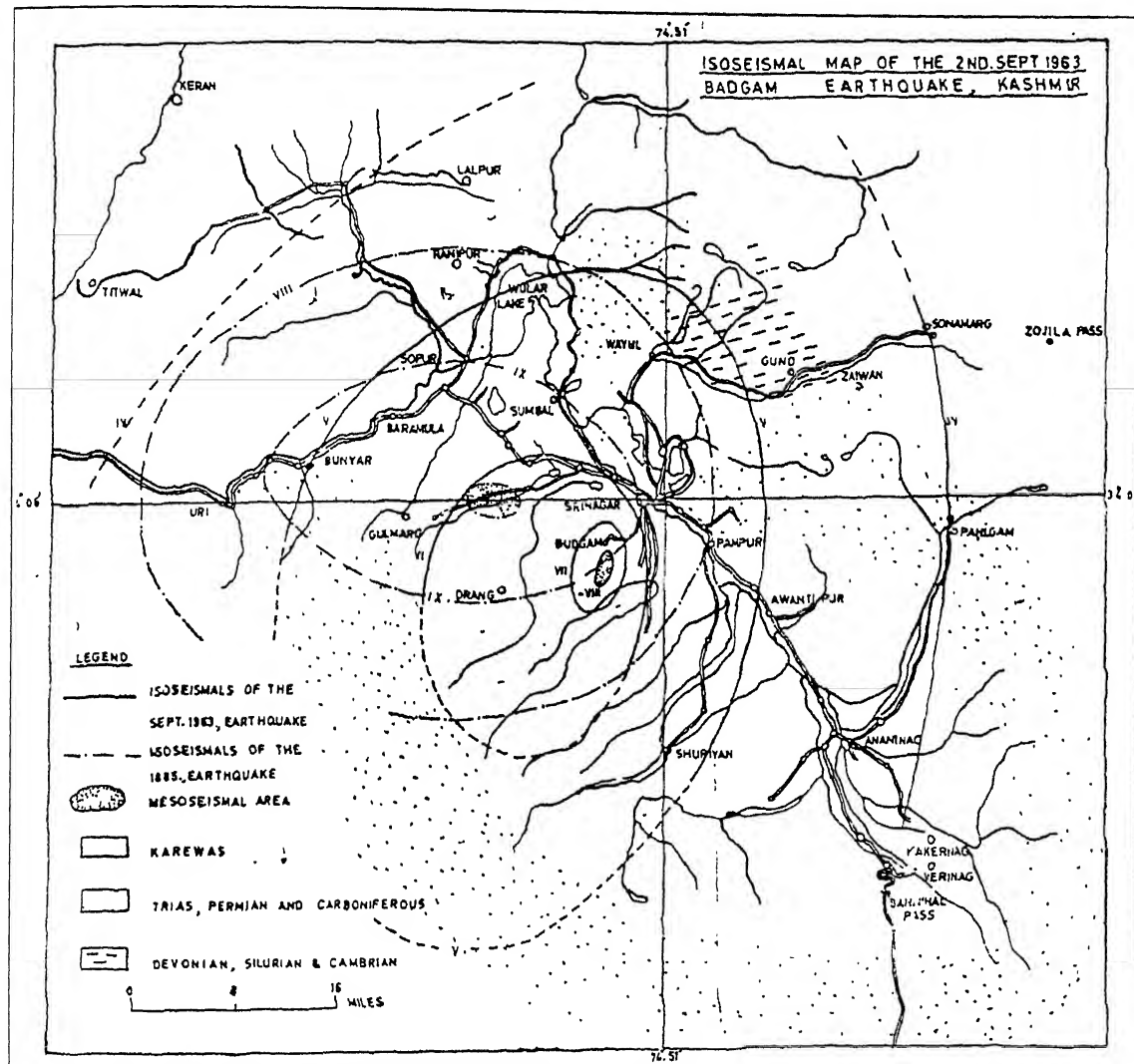


Figure 3.2 Isoseismal of Kashmir earthquake (M 7) of 30th May 1885 and Badgam earthquake (M5.5) of 2nd September 1963 following MM scale after Gosain and Arya (1967).

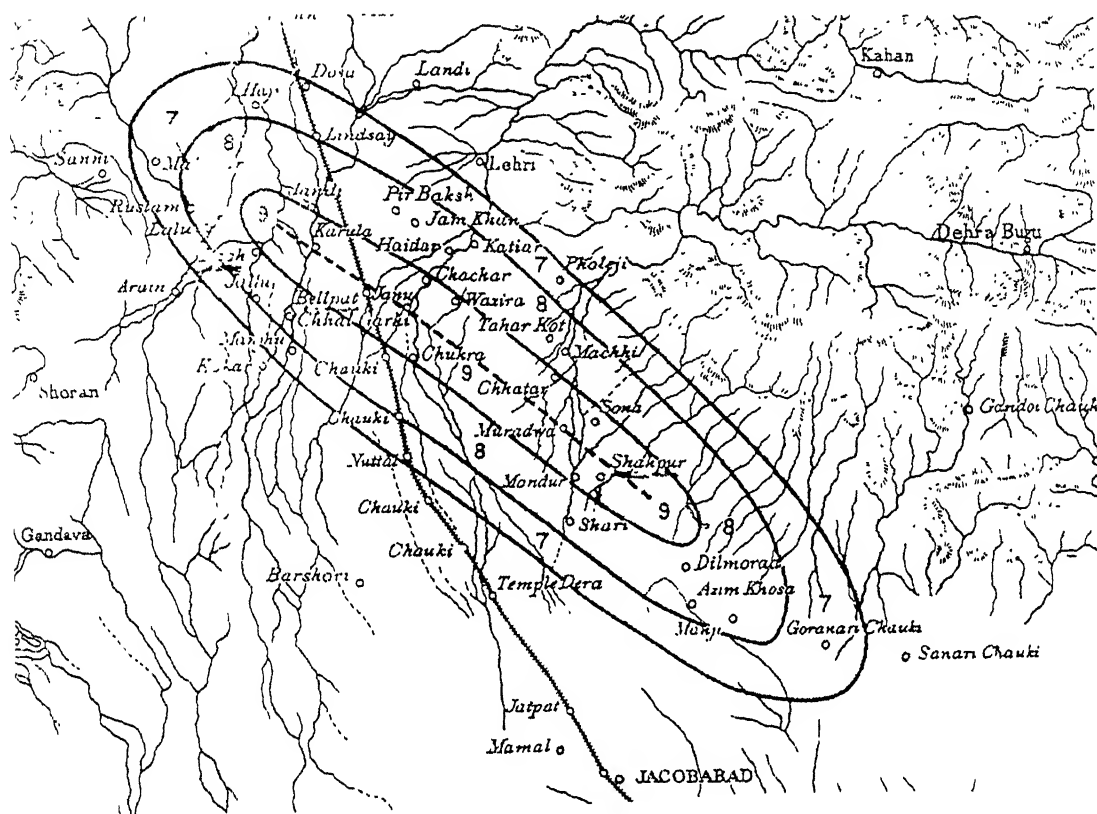


Figure 3.3 Isoseismal of Baluchistan earthquake of 21st October 1906 following RF scale after Haron (1910).

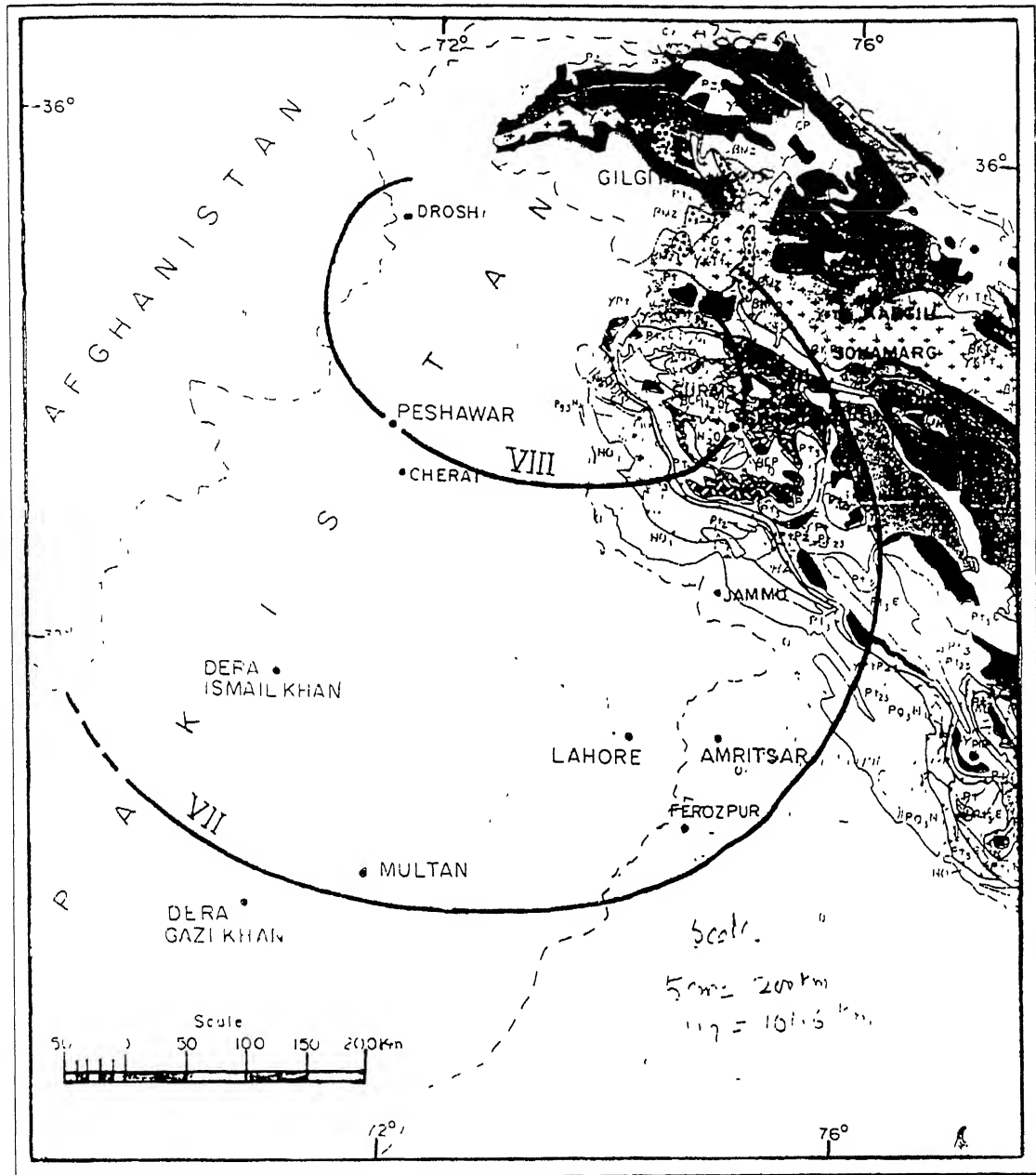


Figure 3.4 Isoseismal of Northwest Himalayan earthquake (M 7.1) of 1st February 1929 following RF scale after Coulson (1930).

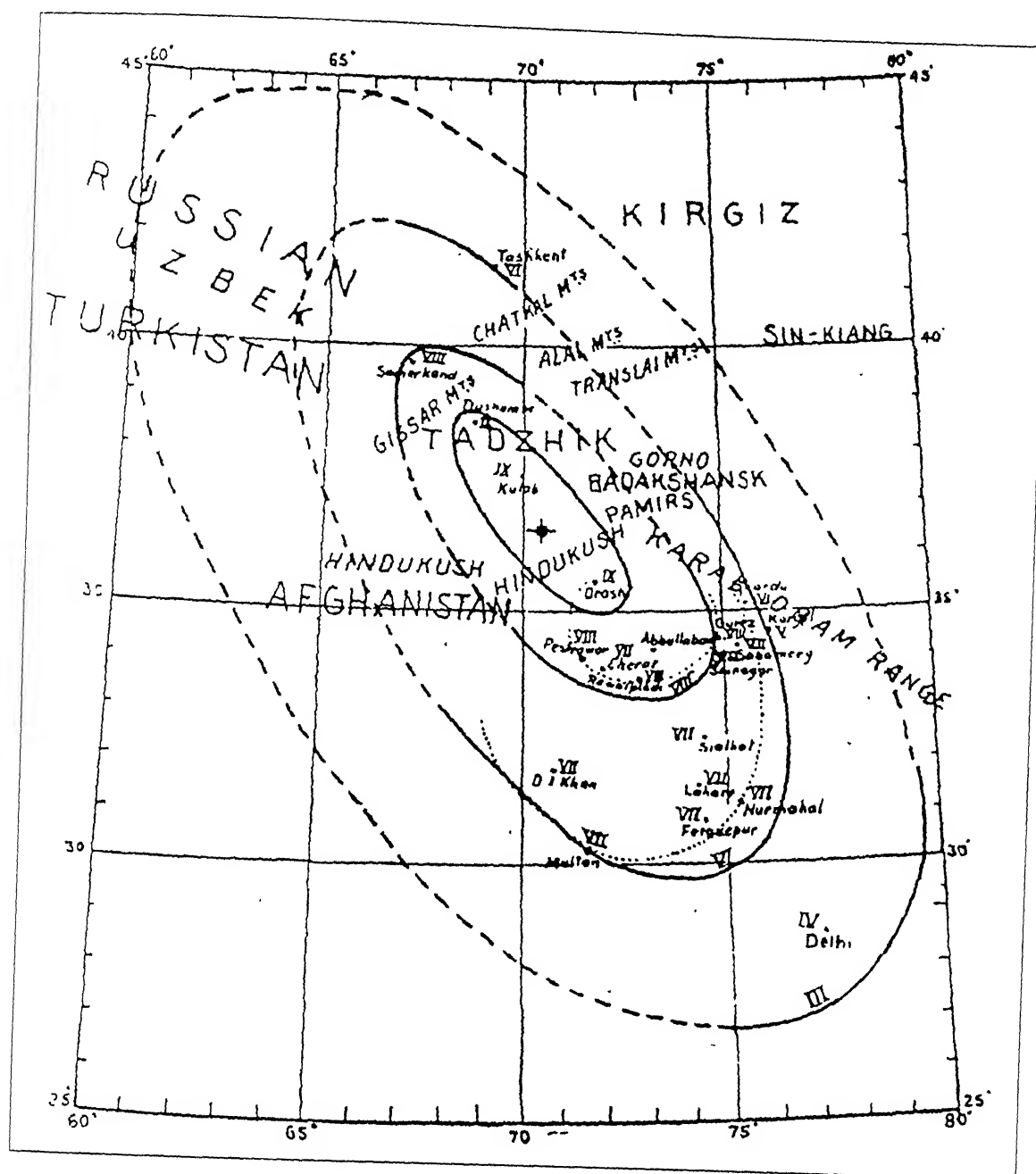


Figure 3.5 Isoseismal of Northwest Himalayan earthquake (M 7.1) of 1st February 1929 following MM scale after Mukherjee (1950).

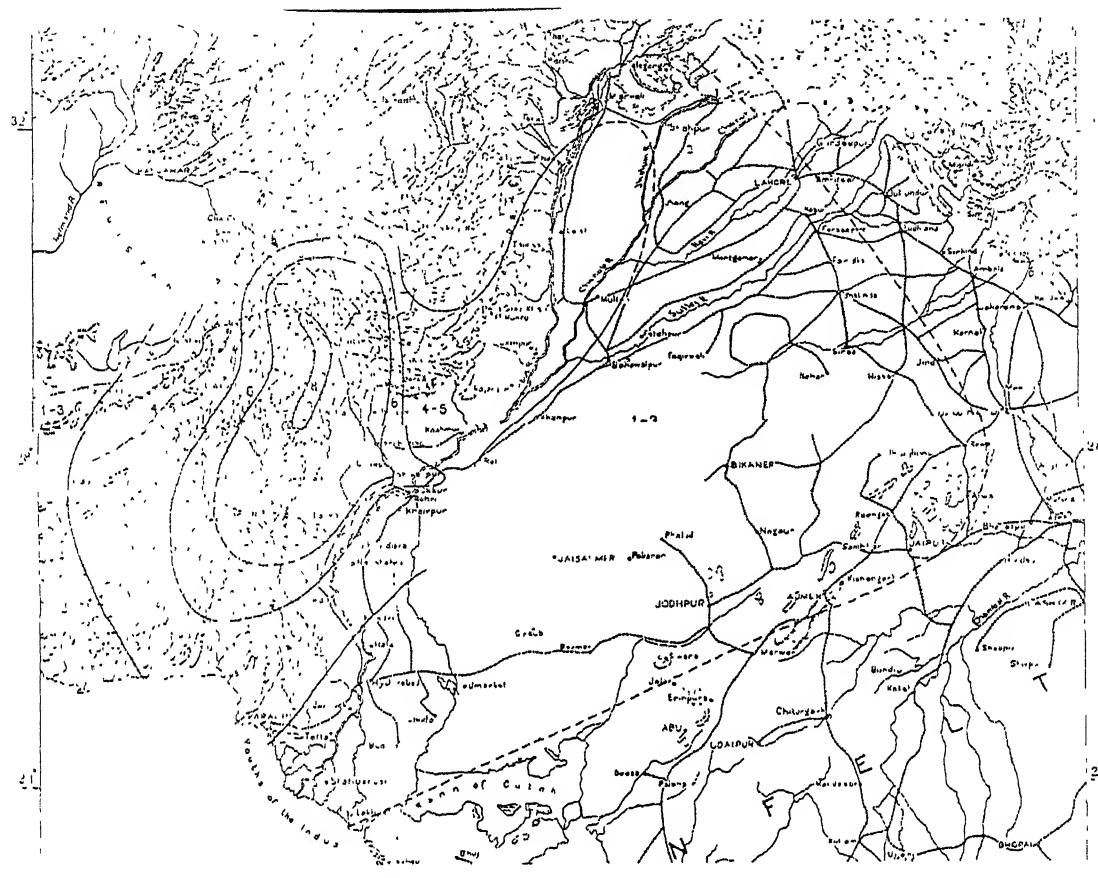


Figure 3.6 Isoseismal of Mach earthquake (M 7.5) of 27th August 1931 following RF scale after West (1934).

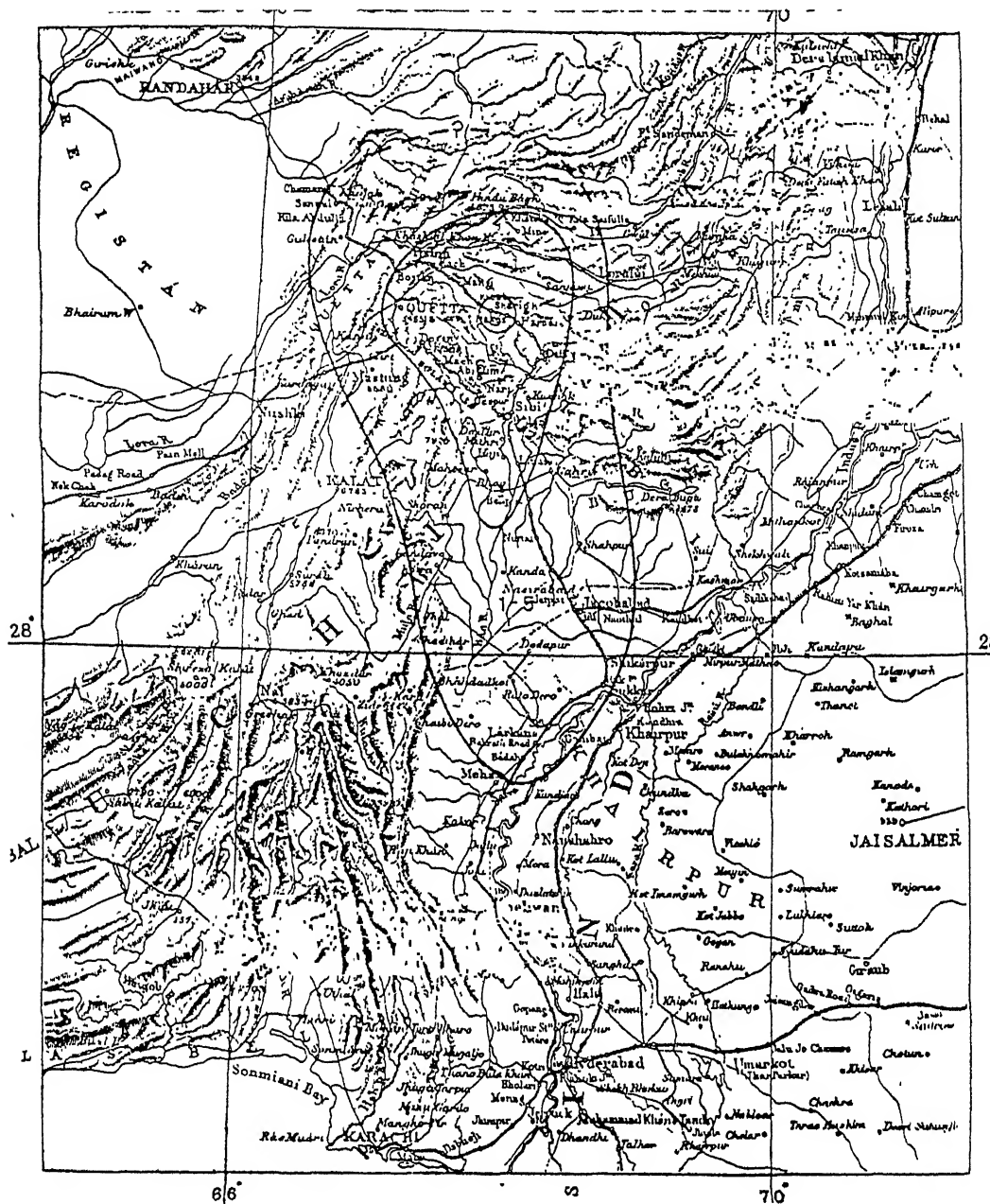


Figure 3.7 Isoseismal of Sharigh earthquake (M 7) of 25th August 1931 following RF scale after West (1934).

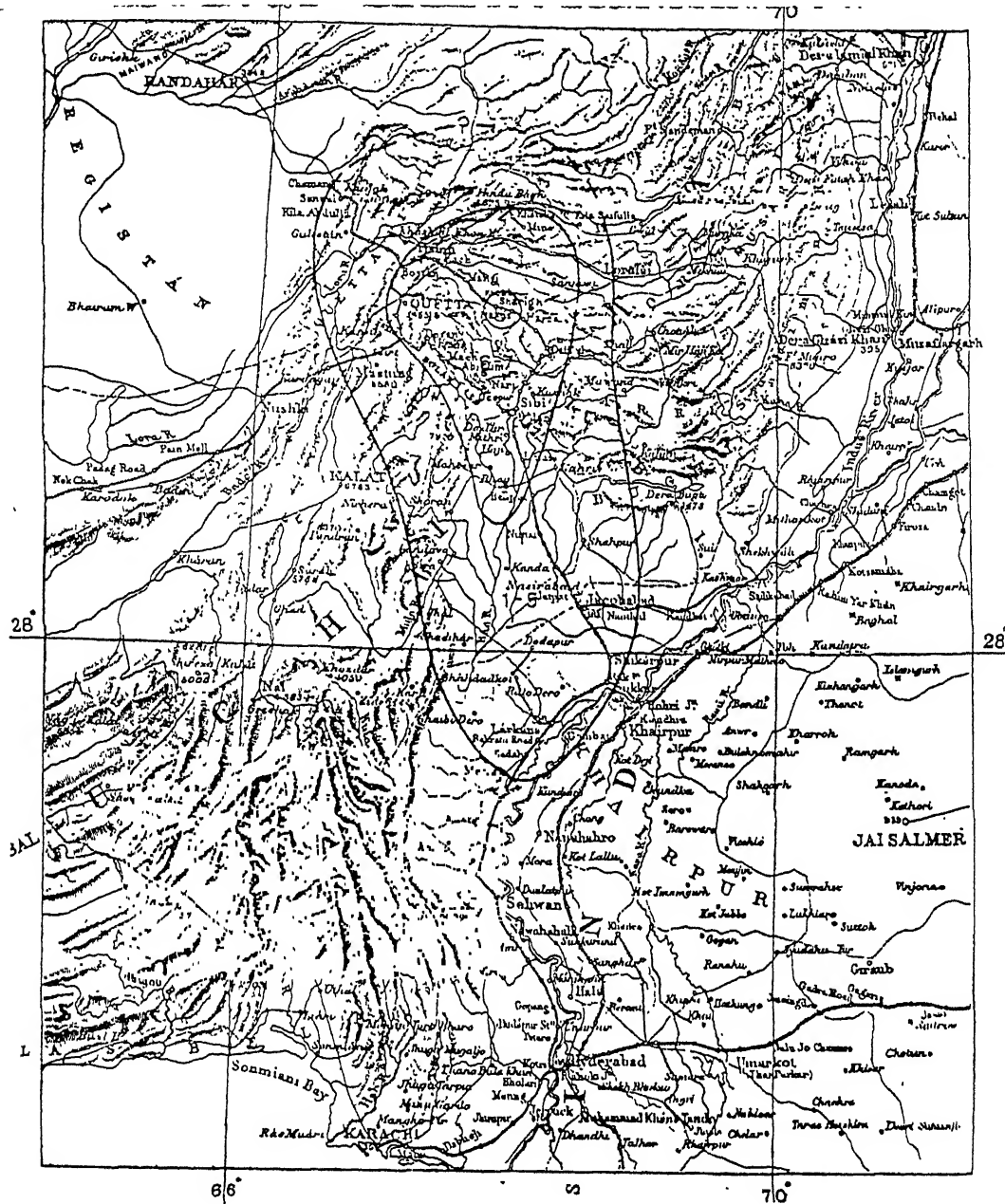


Figure 3.7 Isoseismal of Sharigh earthquake (M 7) of 25th August 1931 following RF scale after West (1934).

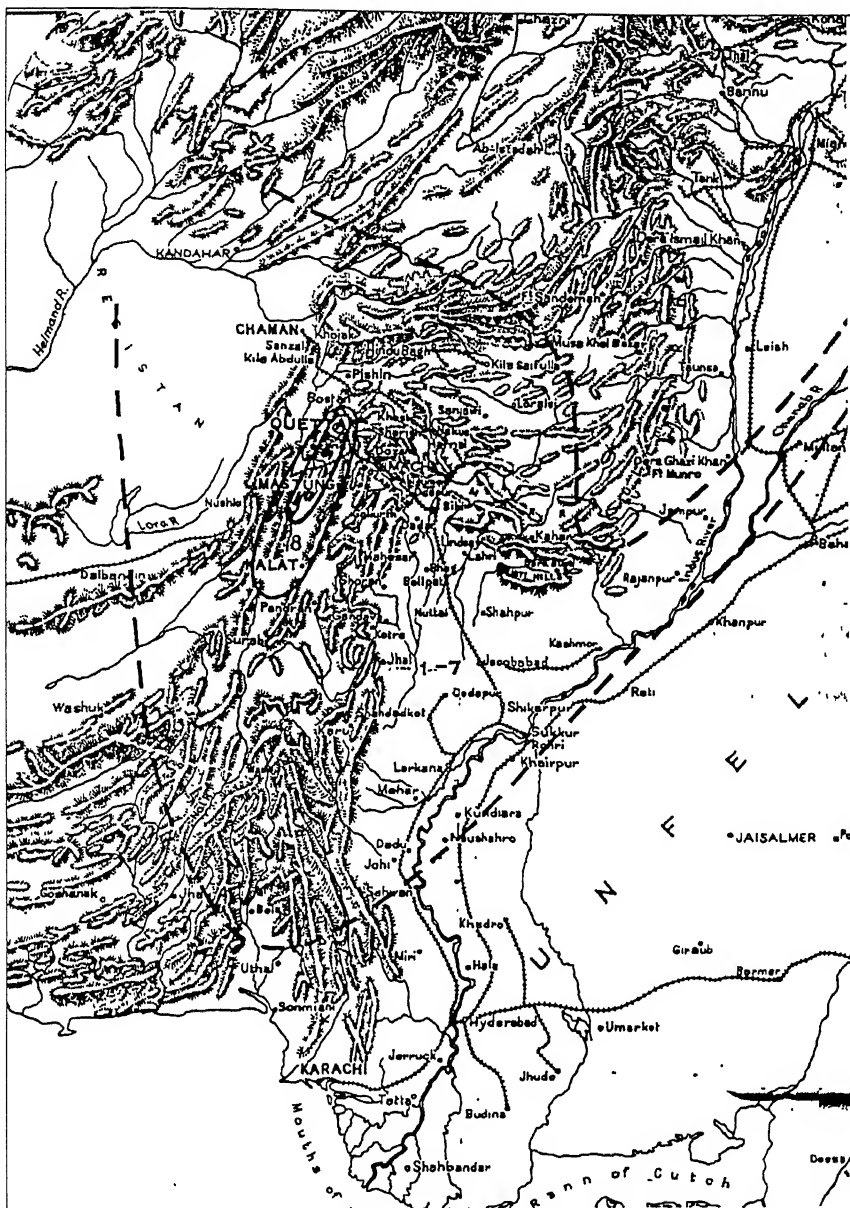


Figure 3.8 Isoseismal of Quetta earthquake (M 7.5) of 31st May 1935 following RF scale after West (1936).

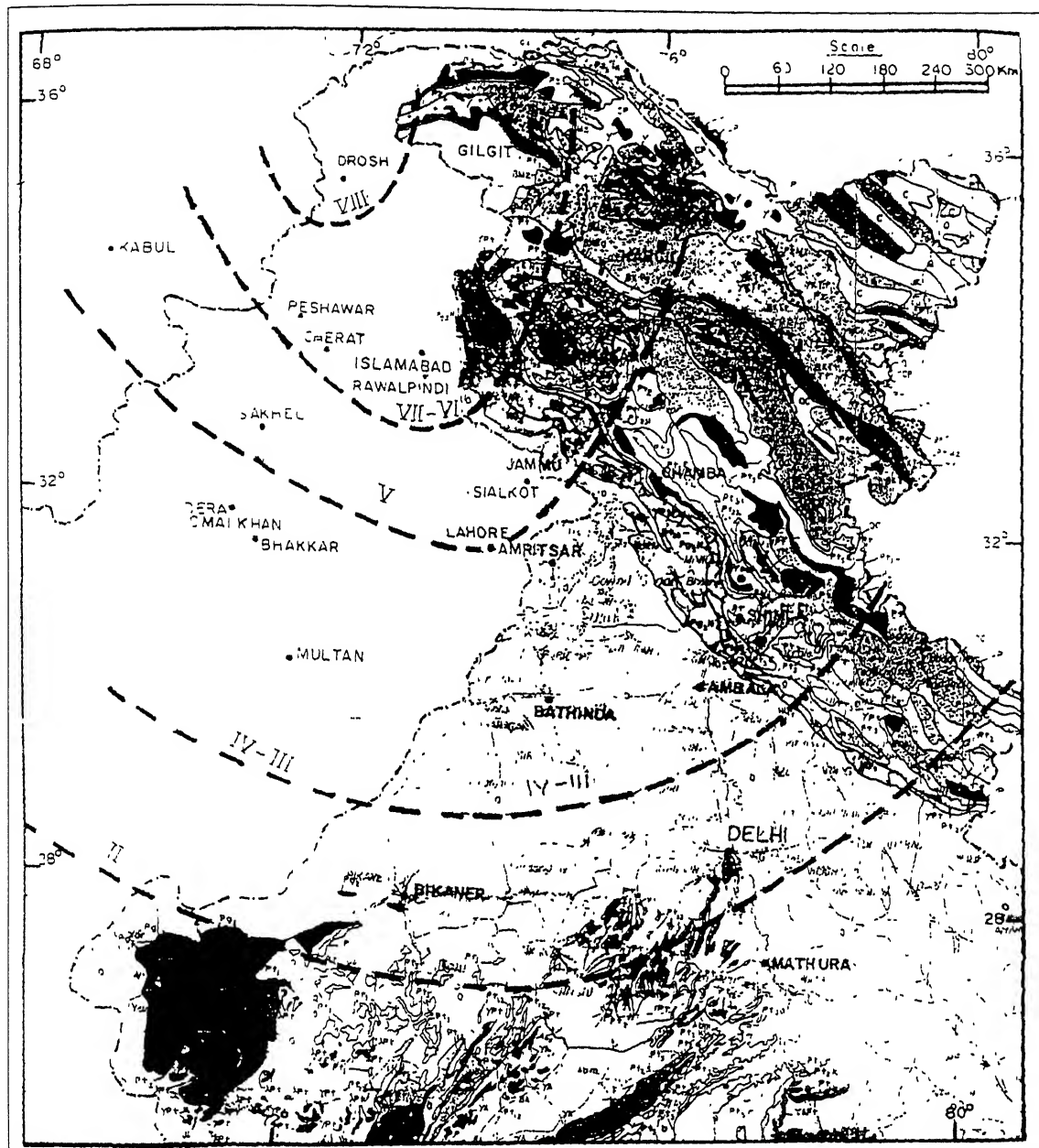


Figure 3.9 Isoseismal of Hindkush earthquake (M 7.2) of 14th November 1937 following RF scale after Coulson (1938).

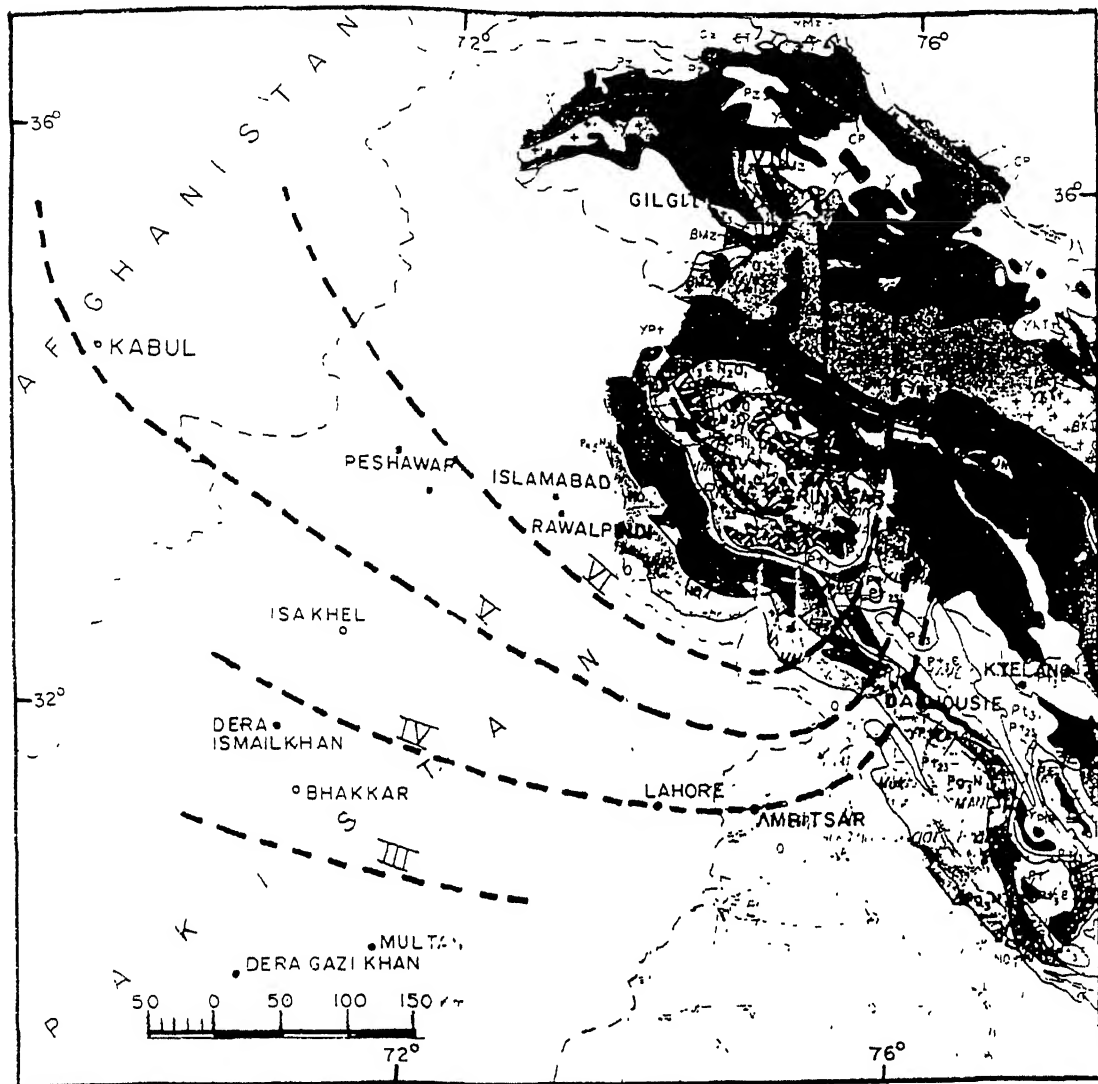


Figure 3.10 Isoseismal of Pamir earthquake (M 6.9) of 21st November 1939 following MM scale after Coulson (1940).

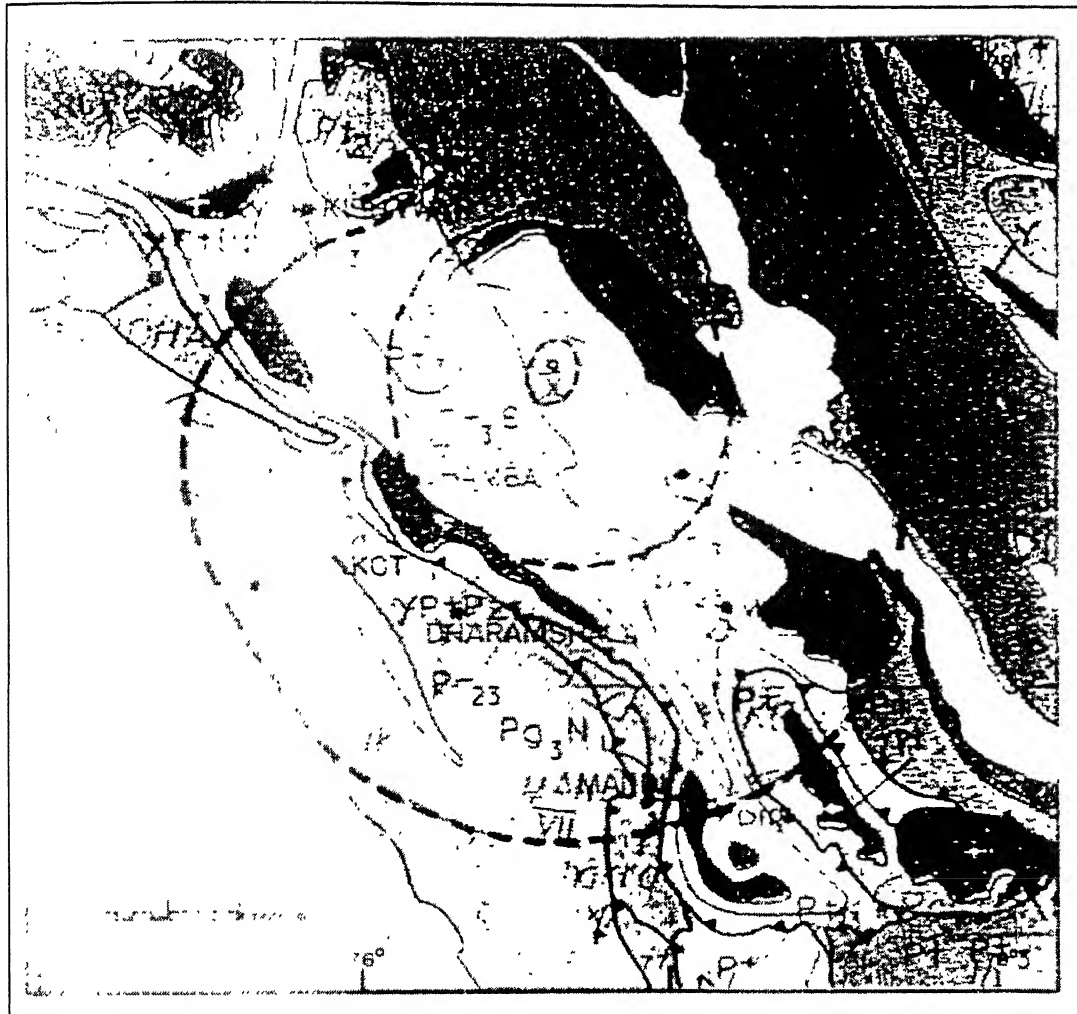


Figure 3.11 Isoseismal of Chamba earthquake (M 6.5) of 22nd July 7 1945 following MM scale after Kapila (1959).

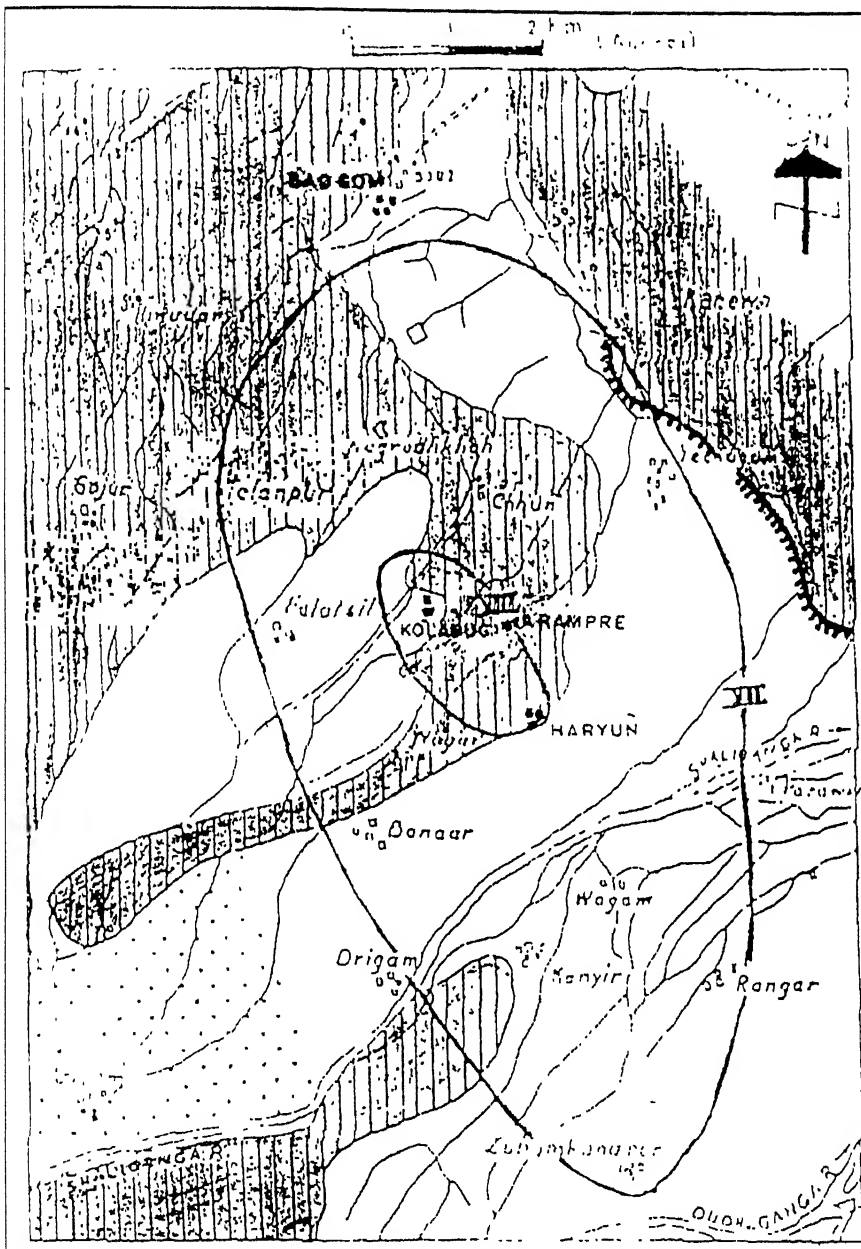


Figure 3.12 Isoseismal of Badgum earthquake (M 5.5) of 2nd September 1963 following MM scale after Wakhloo (1977).

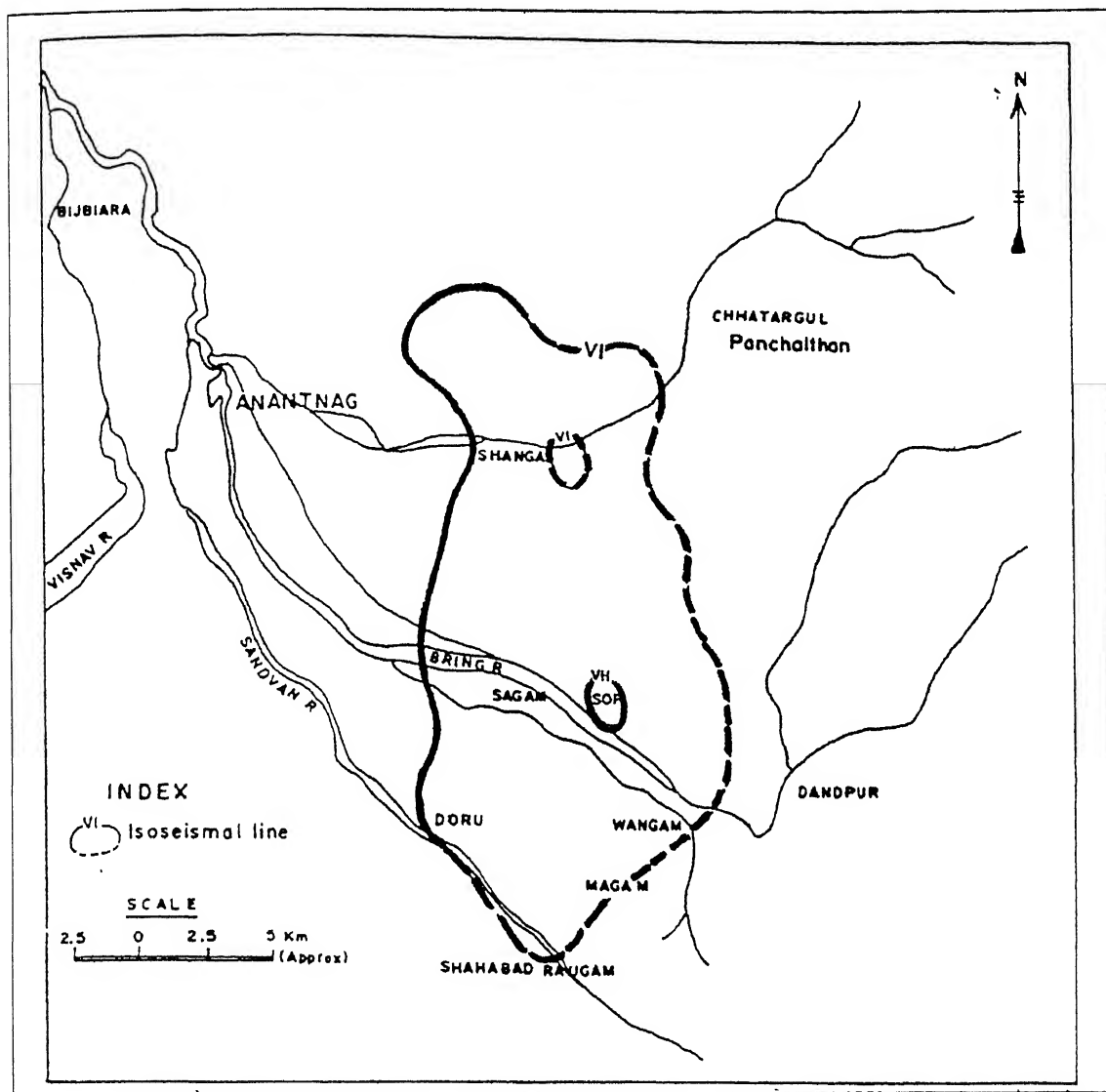


Figure 3.13 Isoseismal of Anantnag earthquake (M 5.7) of 20th February 1967 following MM scale after Wakhloo (1977).

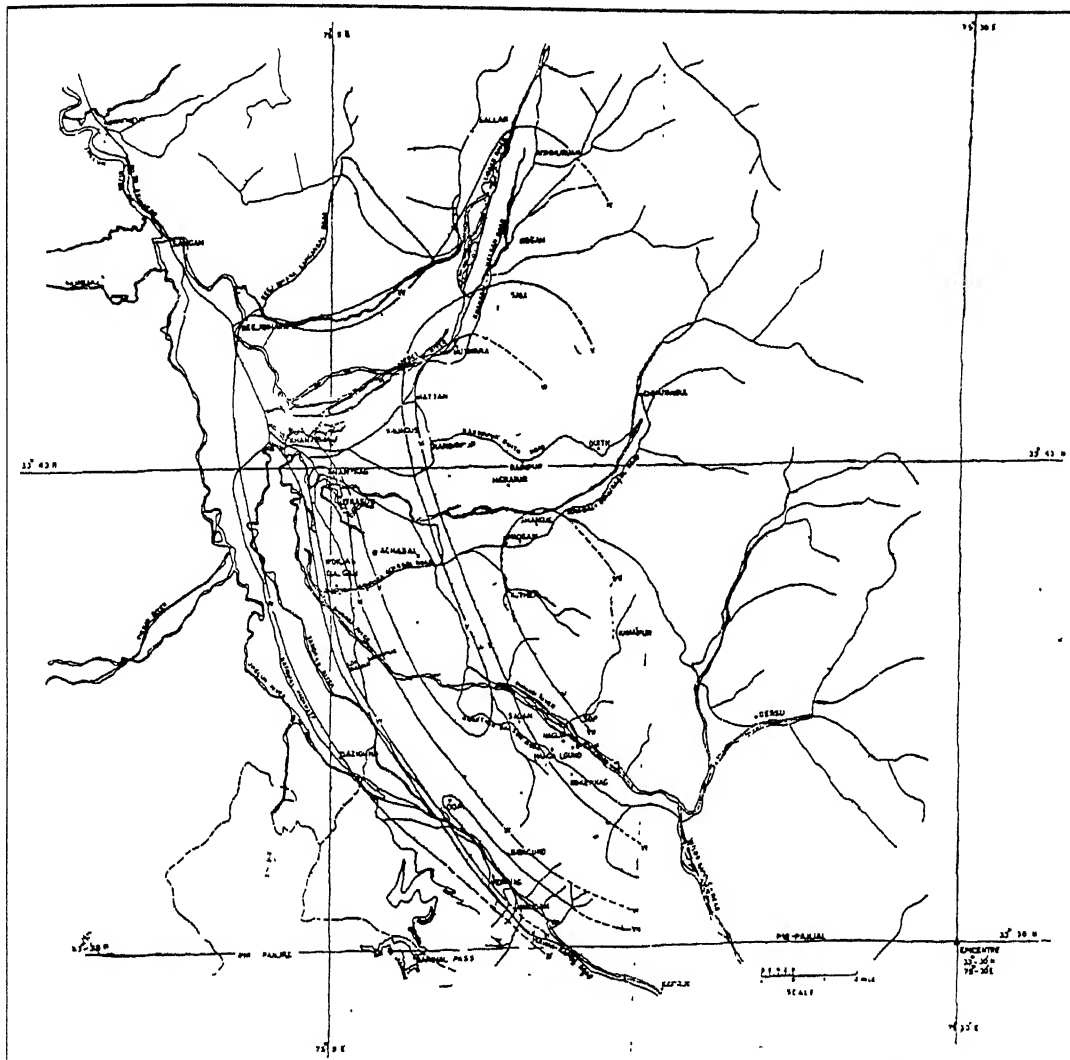


Figure 3.14 Isoseismal of Anantnag earthquake (M 5.7) of 20th February 1967 following MM scale after Gosain and Arya (1967).

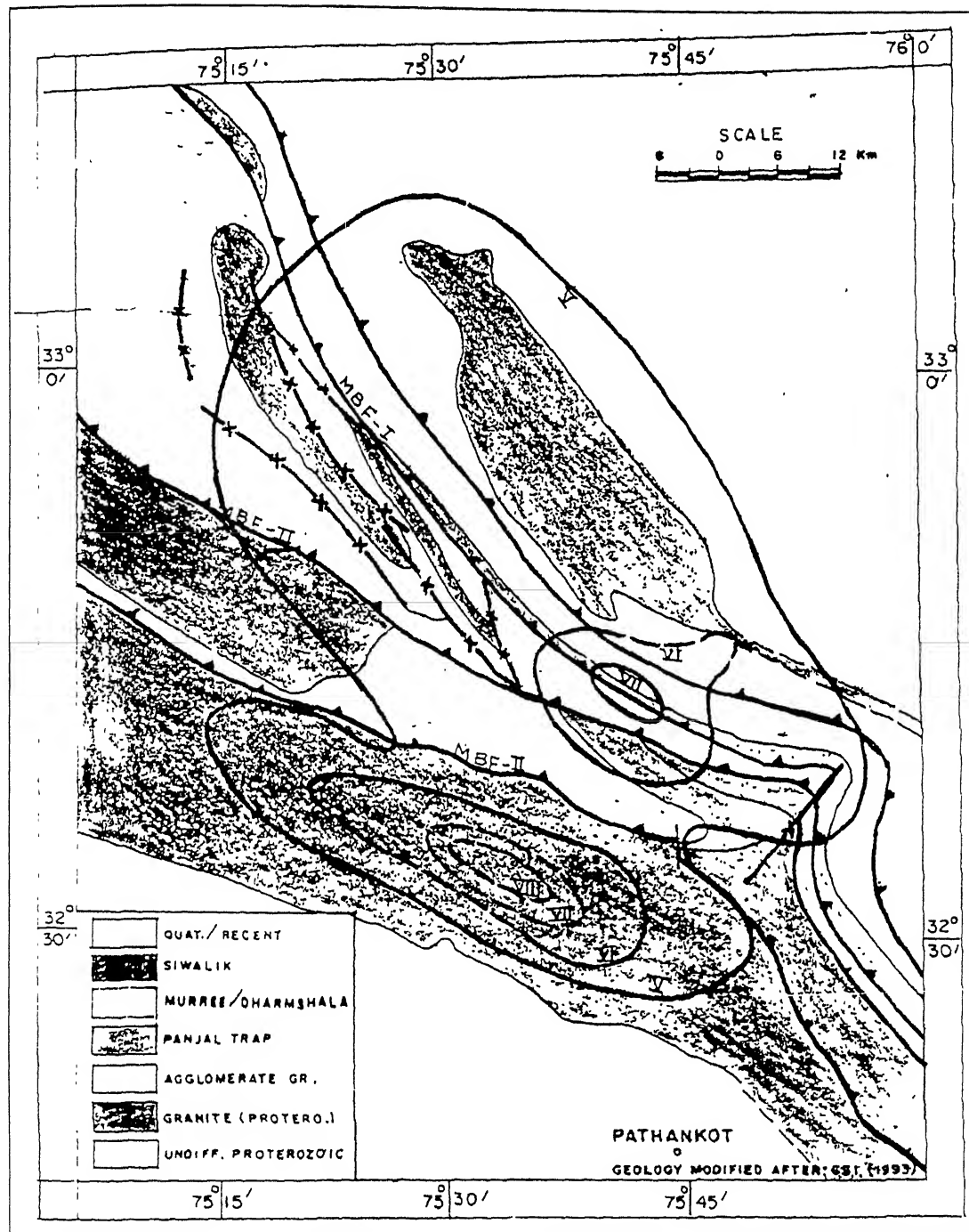


Figure 3.15 Isoseismal of Jammu earthquake (M 5.5, 5.4) of 24th August 1980 following MM scale after Krishnamurthy *et al.* (1990).

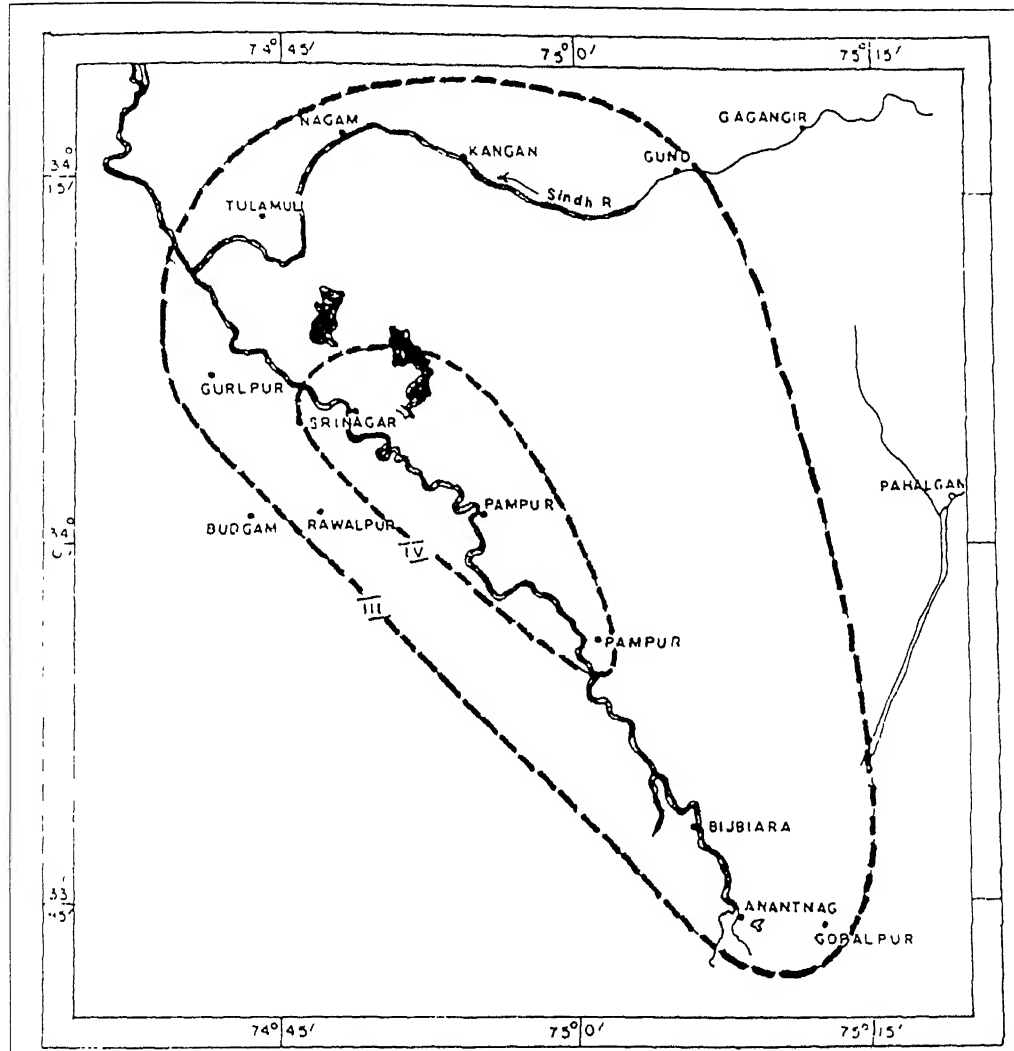


Figure 3.16 Isoseismal map of Srinagar earthquake (M 3.2) of 8th February 1988 following MSK scale after Gupta (1988).

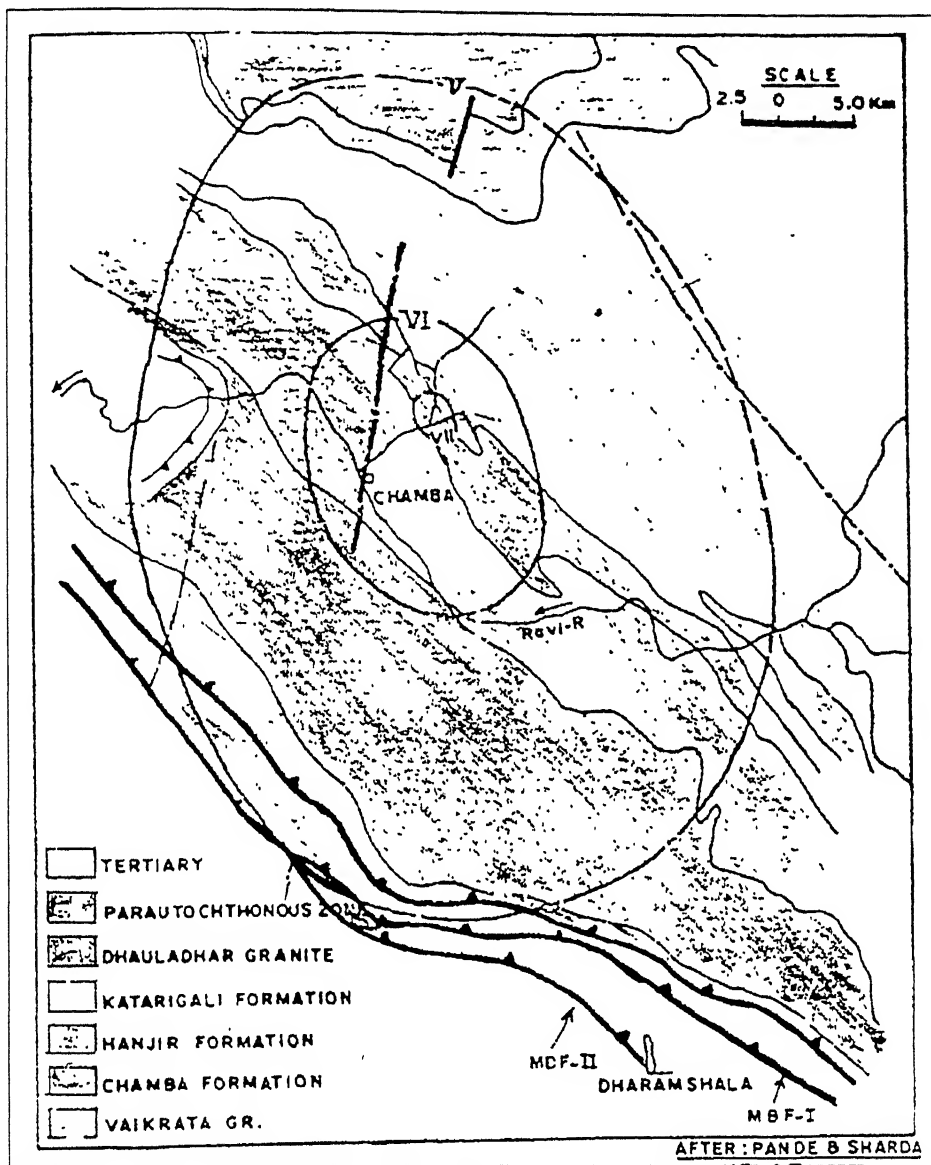


Figure 3.17 Isoseismal map of Chamba earthquake (M 4.5) of 24th March 1995 following MSK scale after Pande and Sharda (1995).

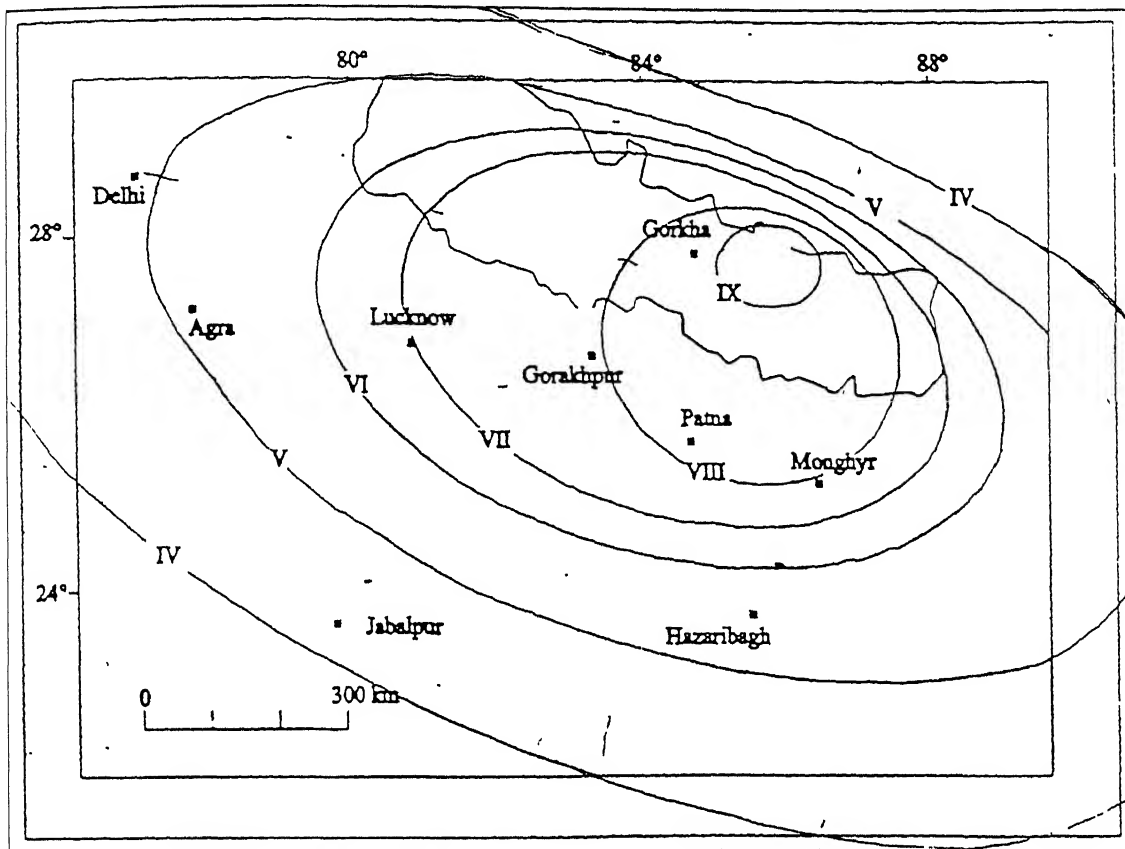


Figure 3.18 Isoseismal map of Kathmandu earthquake of 26th August 1833 following MM scale taken from Dasgupta *et al.* (2000).

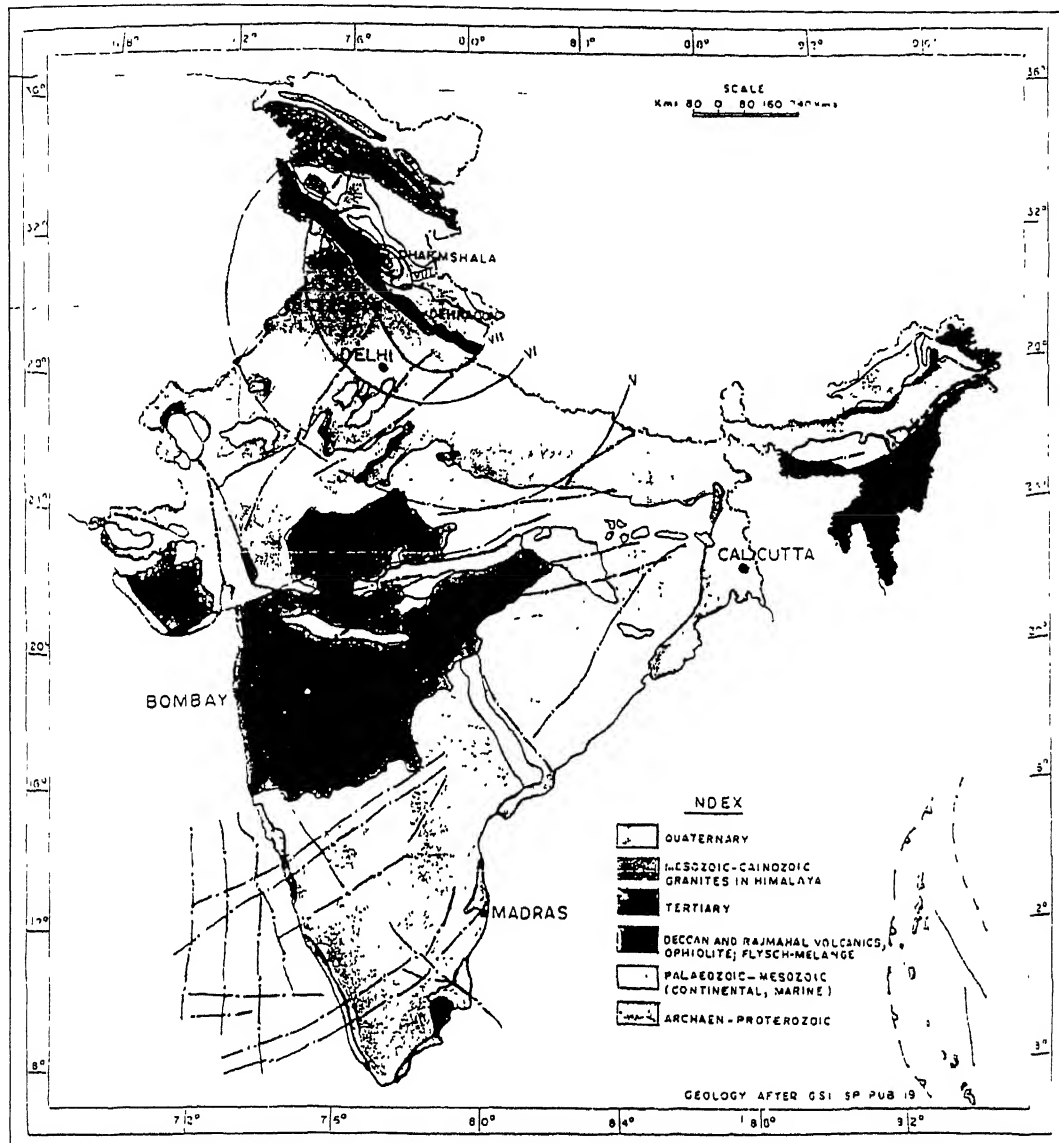


Figure 3.19 Isoseismal of Kangra earthquake (M 8.6) of 4th April 1905 following RF scale after Middlemiss (1910).

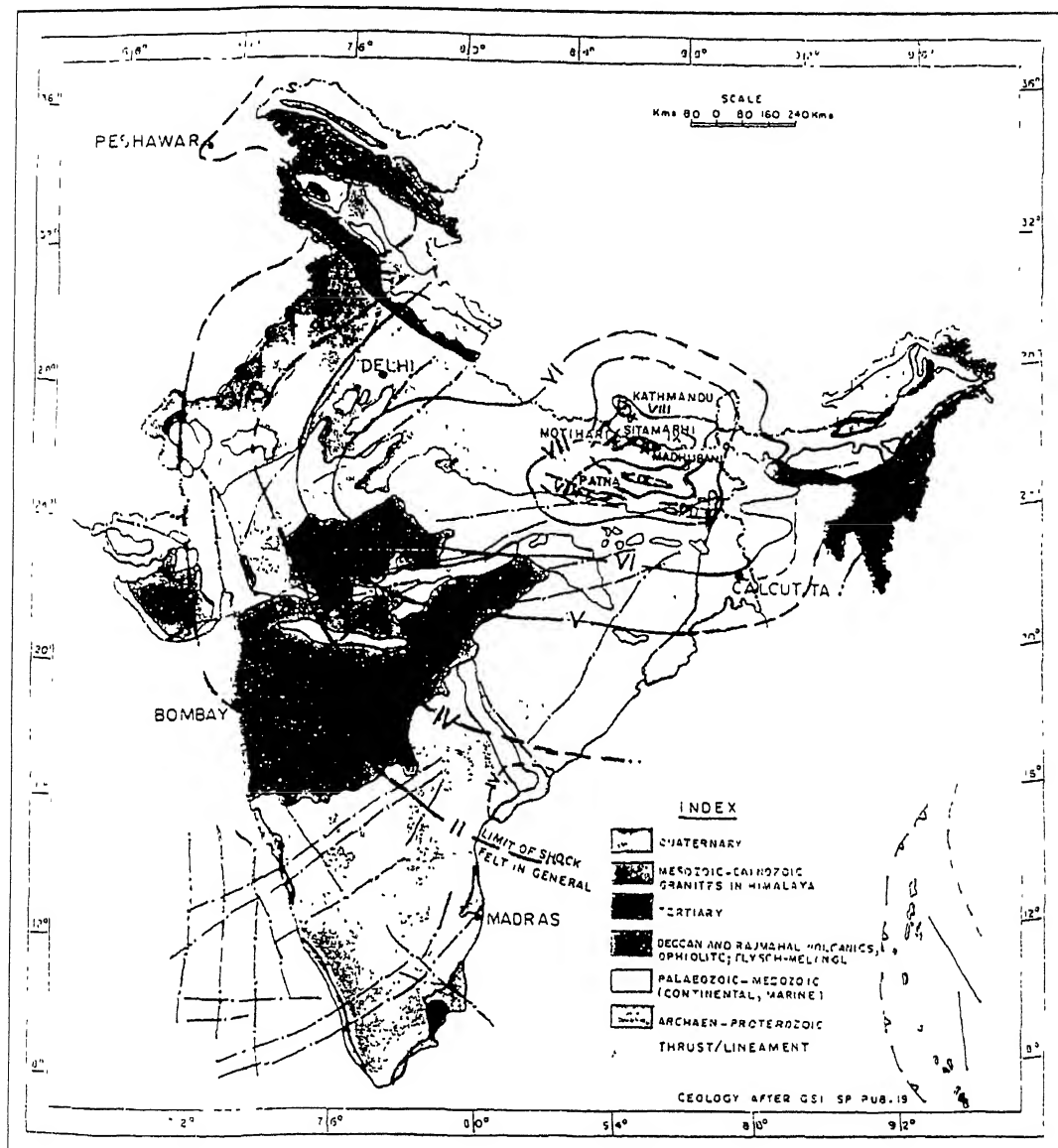


Figure 3.20 Isoseismal map of Bihar-Nepal earthquake (M 8.4) of 15th January 1934 following MM scale after GSI (1939).

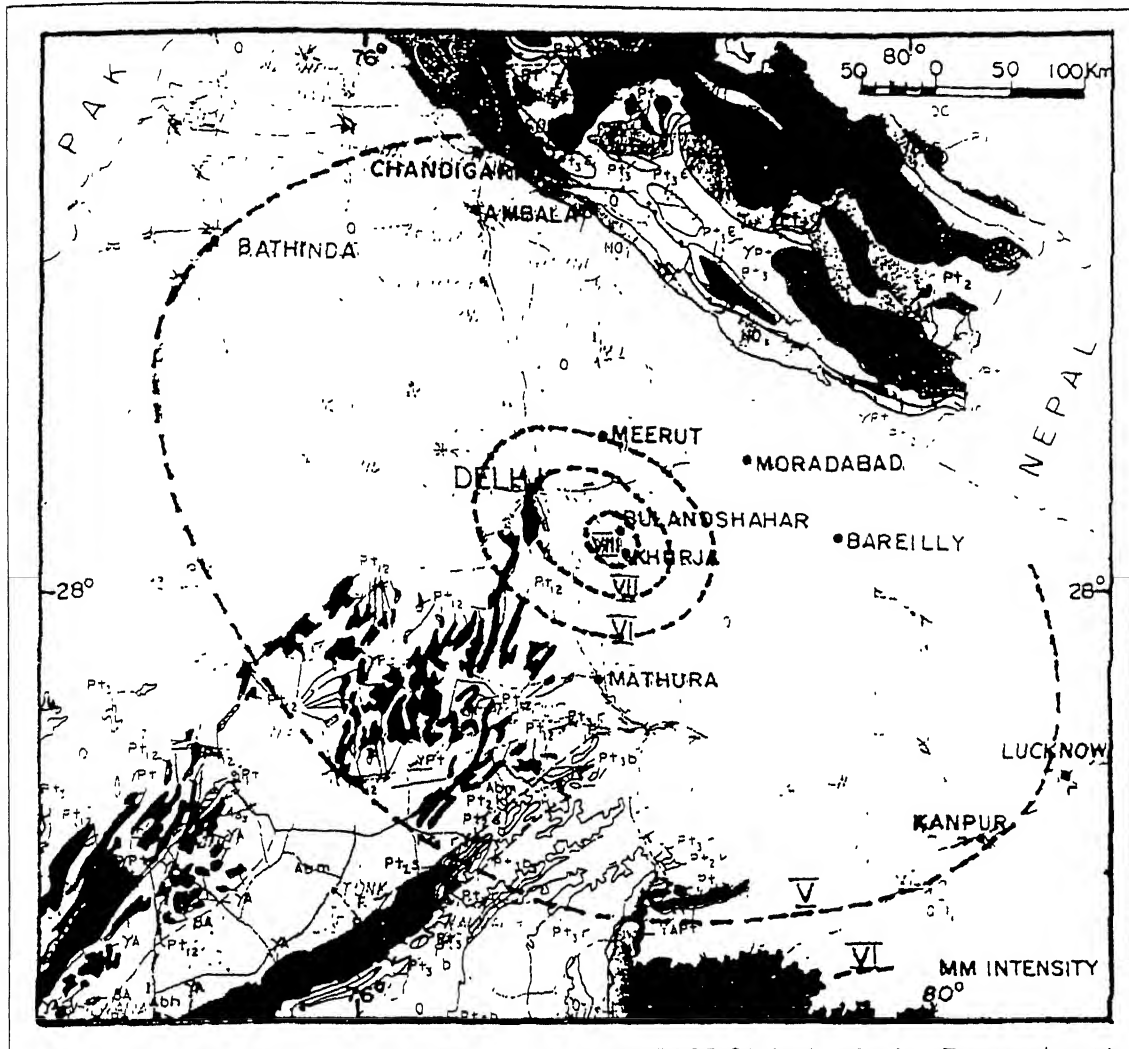


Figure 3.21 Isoseismal map of Bulandshahar earthquake (M 6.5) of 10th October 1951 following MM scale after Tandon (1975).

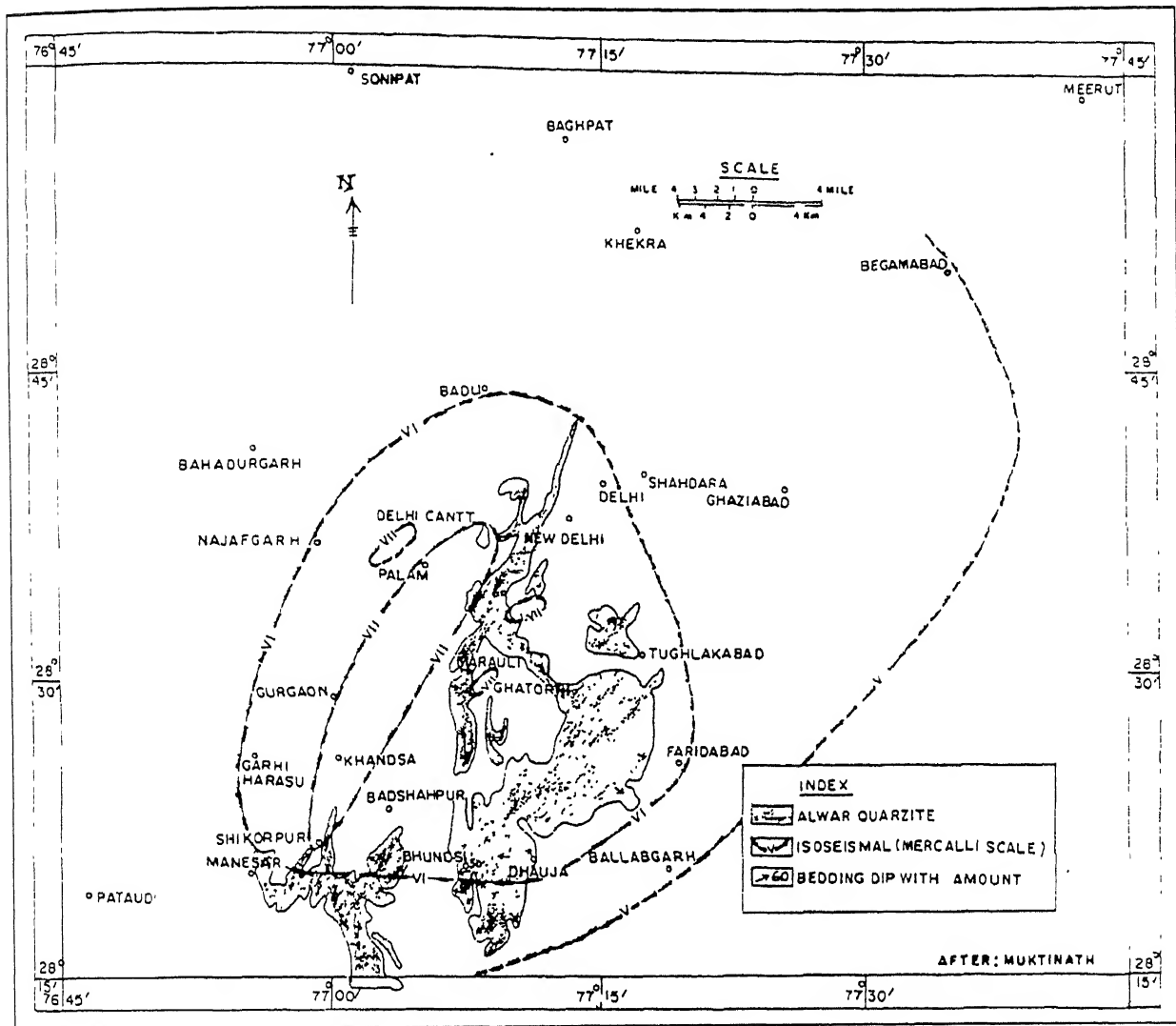


Figure 3.22 Isoseismal map of Delhi earthquake (M 6) of 27th August 1956 following MM scale after Muktinath *et al.* (1969).

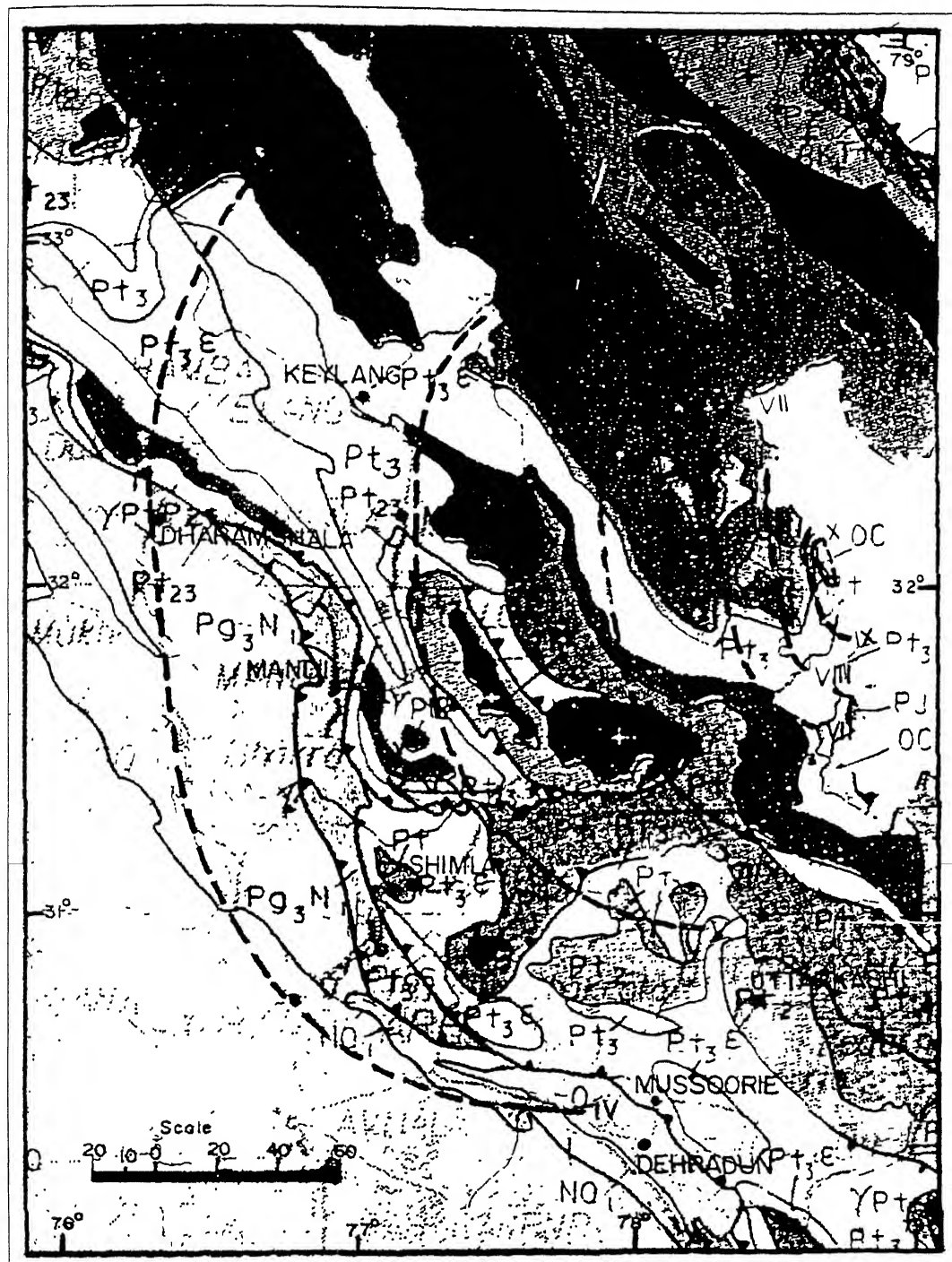


Figure 3.23 Isoseismal of Kinnar earthquake (M 7) of 19th January 1975 following MM scale after Hukku *et al.* (1975).

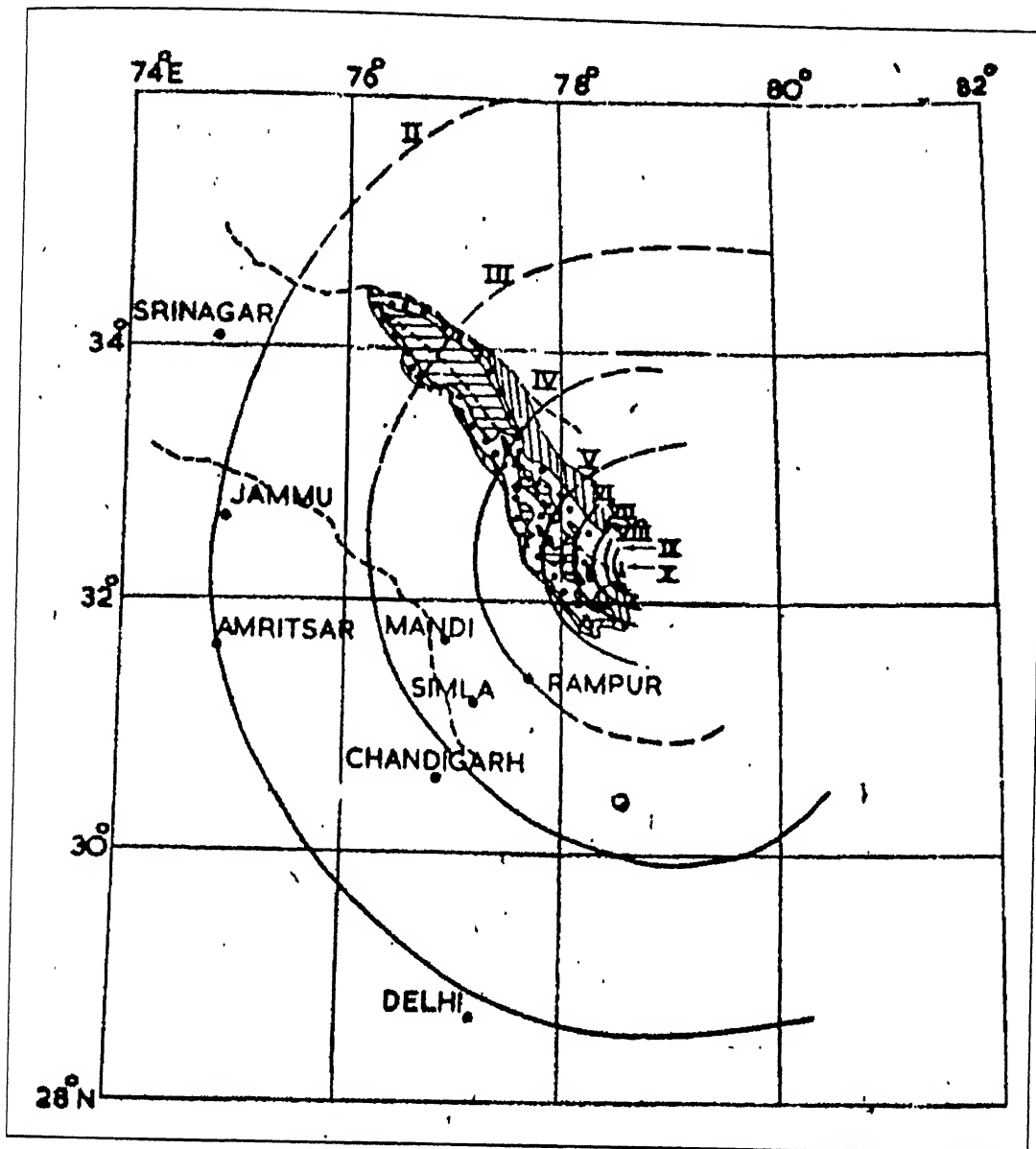


Figure 3.24 Isoseismal of Kinnaur earthquake (M 7) of 19th January 1975 following MM scale after Gosavi *et al.* (1977).

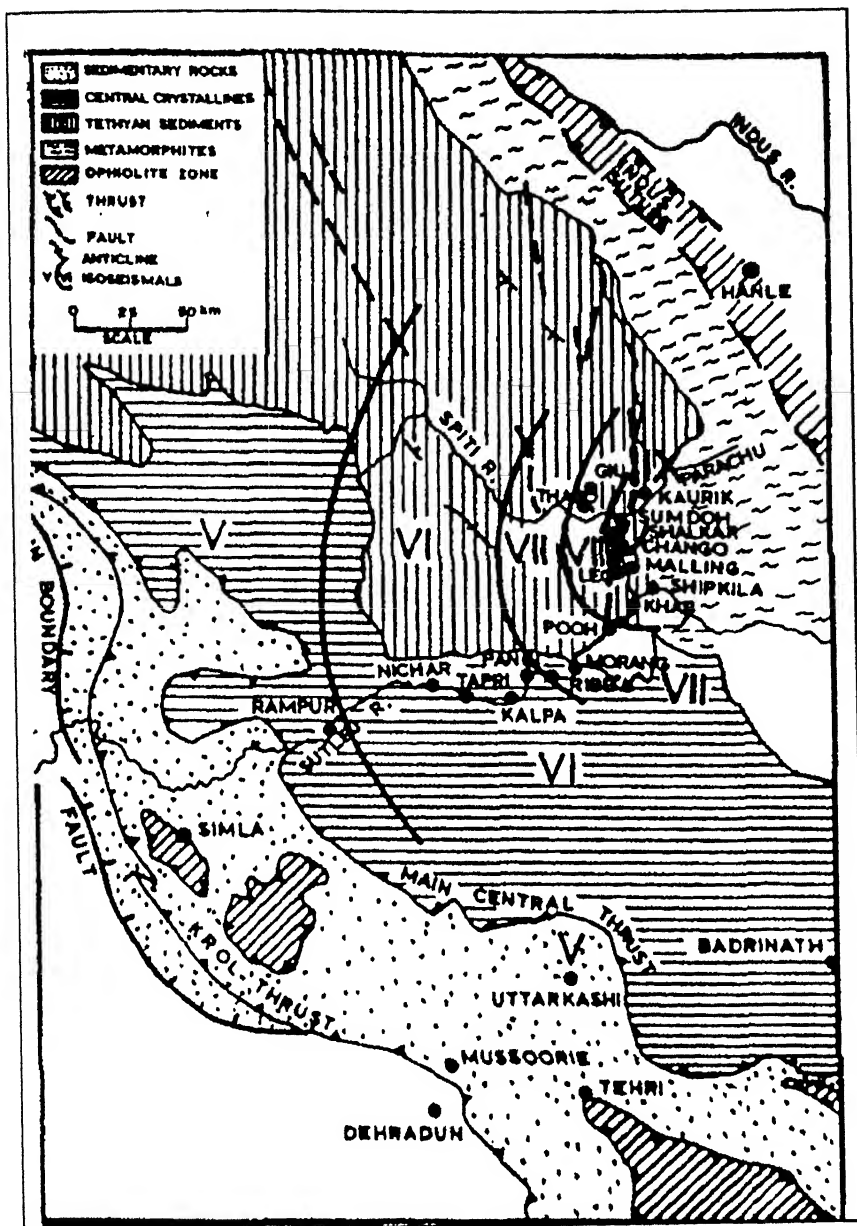


Figure 3.25 Isoseismal of Kinnaur earthquake (M 7) of 19th January 1975 following MM scale after Singh *et al.* (1975).

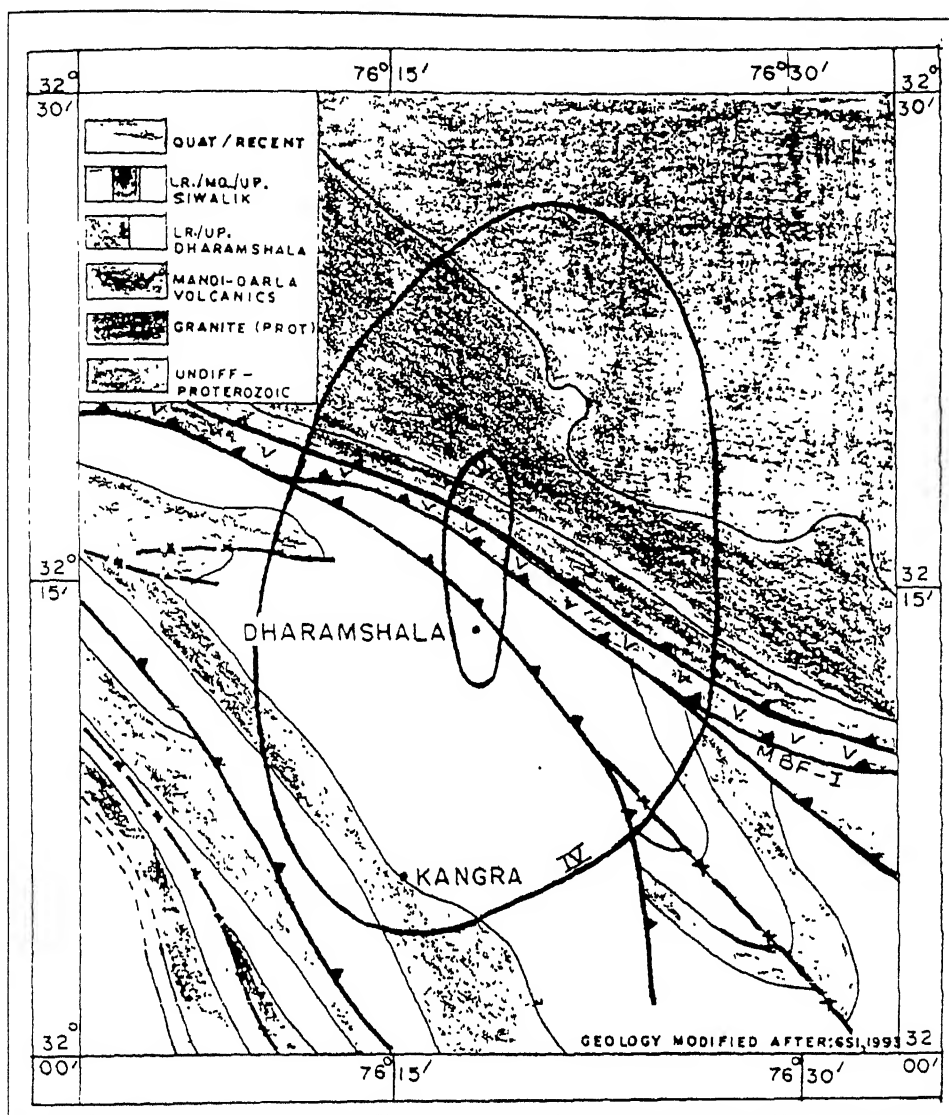


Figure 3.26 Isoseismal of Dharamshala earthquake (M 5) of 15th June 1978 following MM scale after Kumar *et al.* (1981).

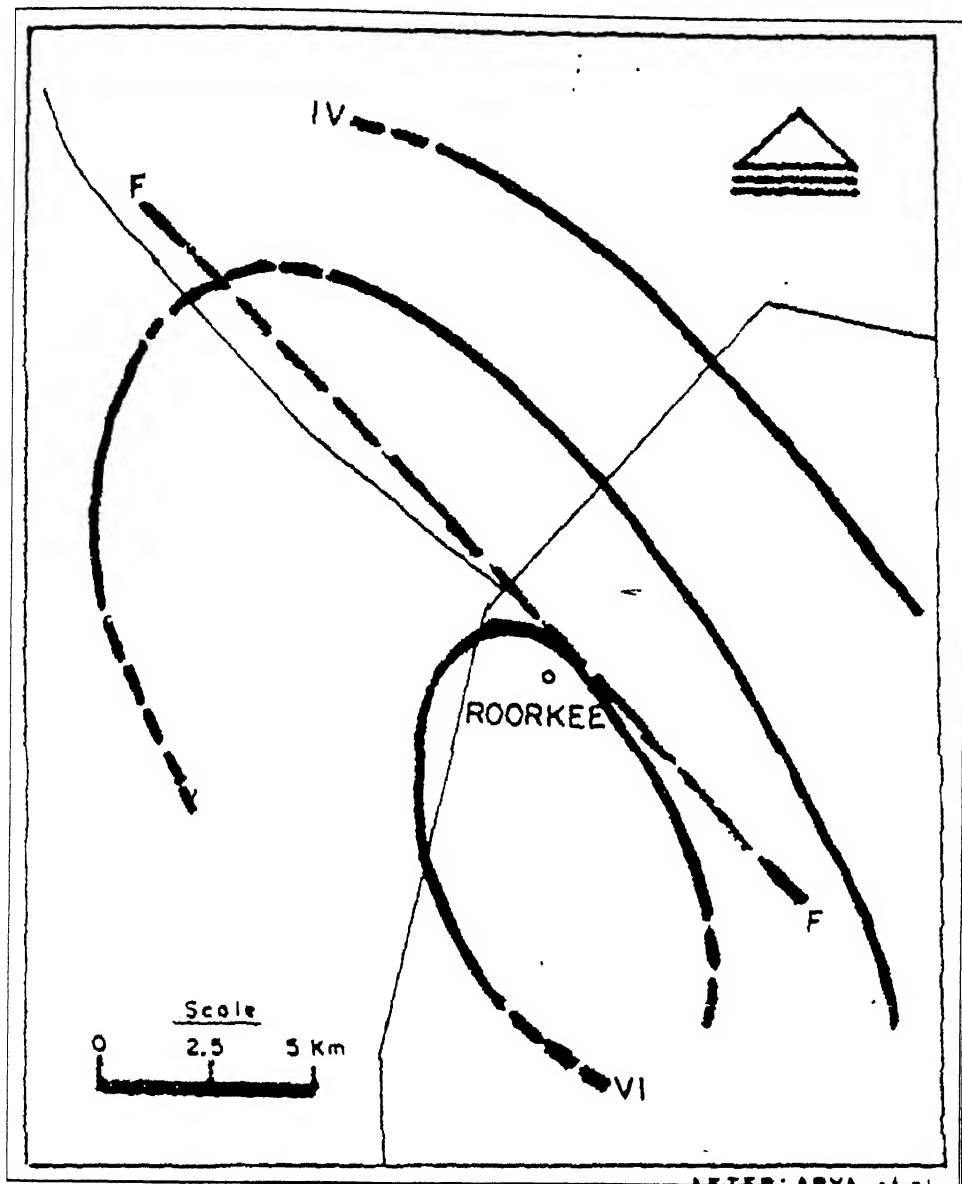


Figure 3.27 Isoseismal map of Roorkee earthquake (M 4.7) of 6th November 1975 following MM scale after Arya *et al.* (1977).

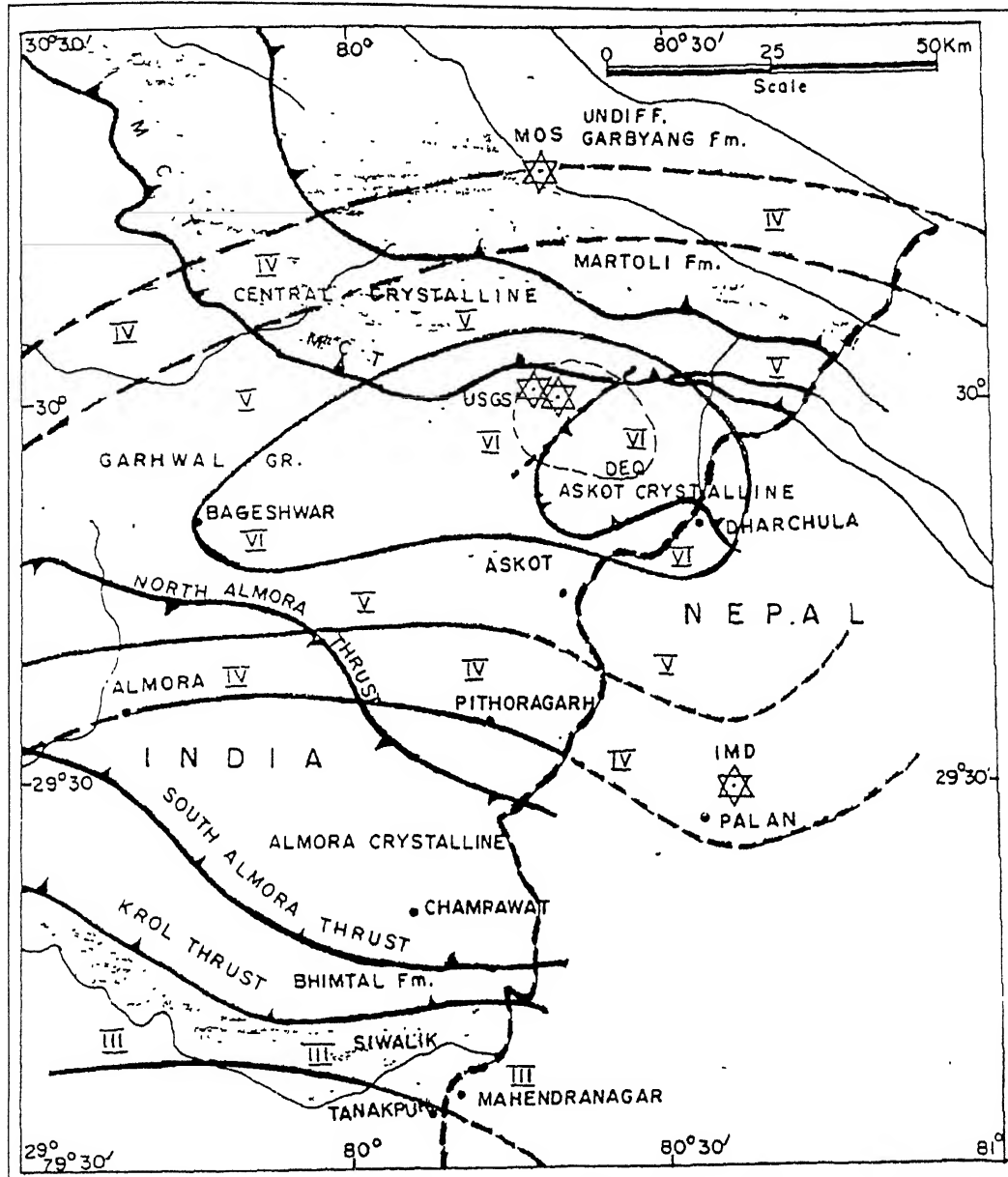


Figure 3.28 Isoseismal map of Nepal earthquake (M 5.8) of 21st May 1979 following MM scale after Kumar *et al.* (1981).

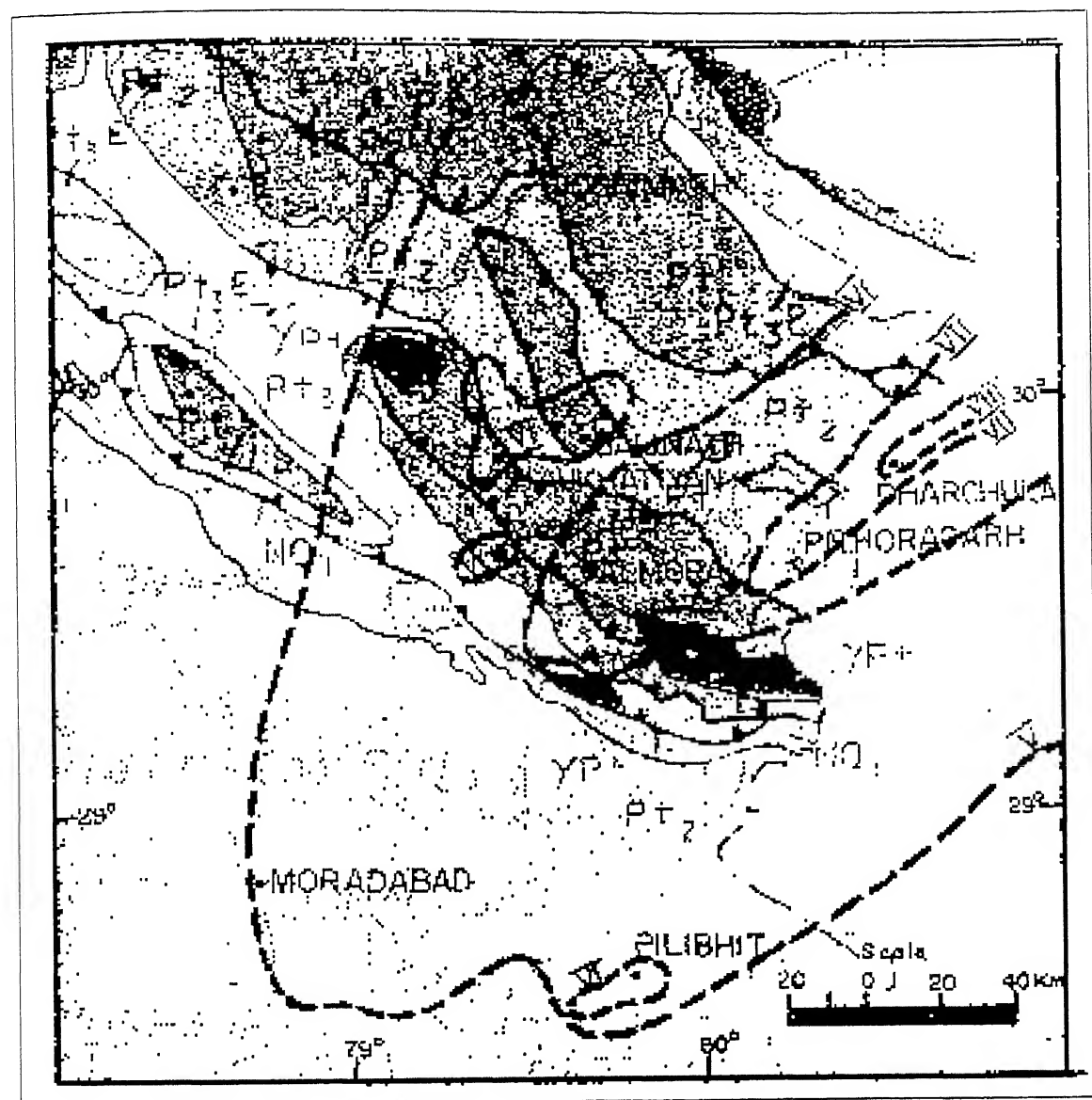


Figure 3.29 Isoseismal map of Nepal earthquake of (M 6.1) 29th July 1980 following MM scale after Srivastava *et al.* (1980).



Figure 3.30 Isoseismal map of Dharamshala earthquake (M 5.7) of 26th April 1986 following MM scale after Gupta *et al.* (1986).

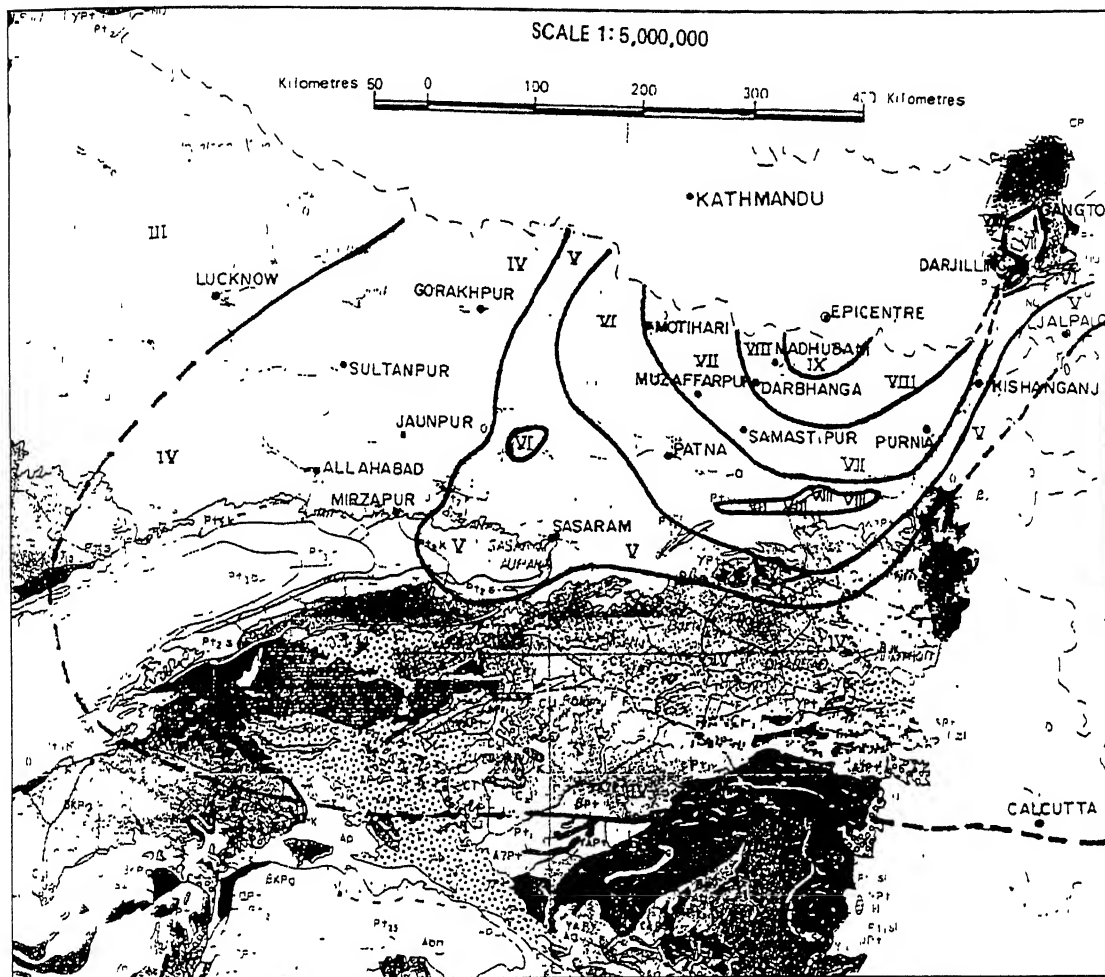


Figure 3.31 Isoseismal map of Bihar-Nepal earthquake (M 6.4) of 20th August 1988 following MM scale after GSI (1993).

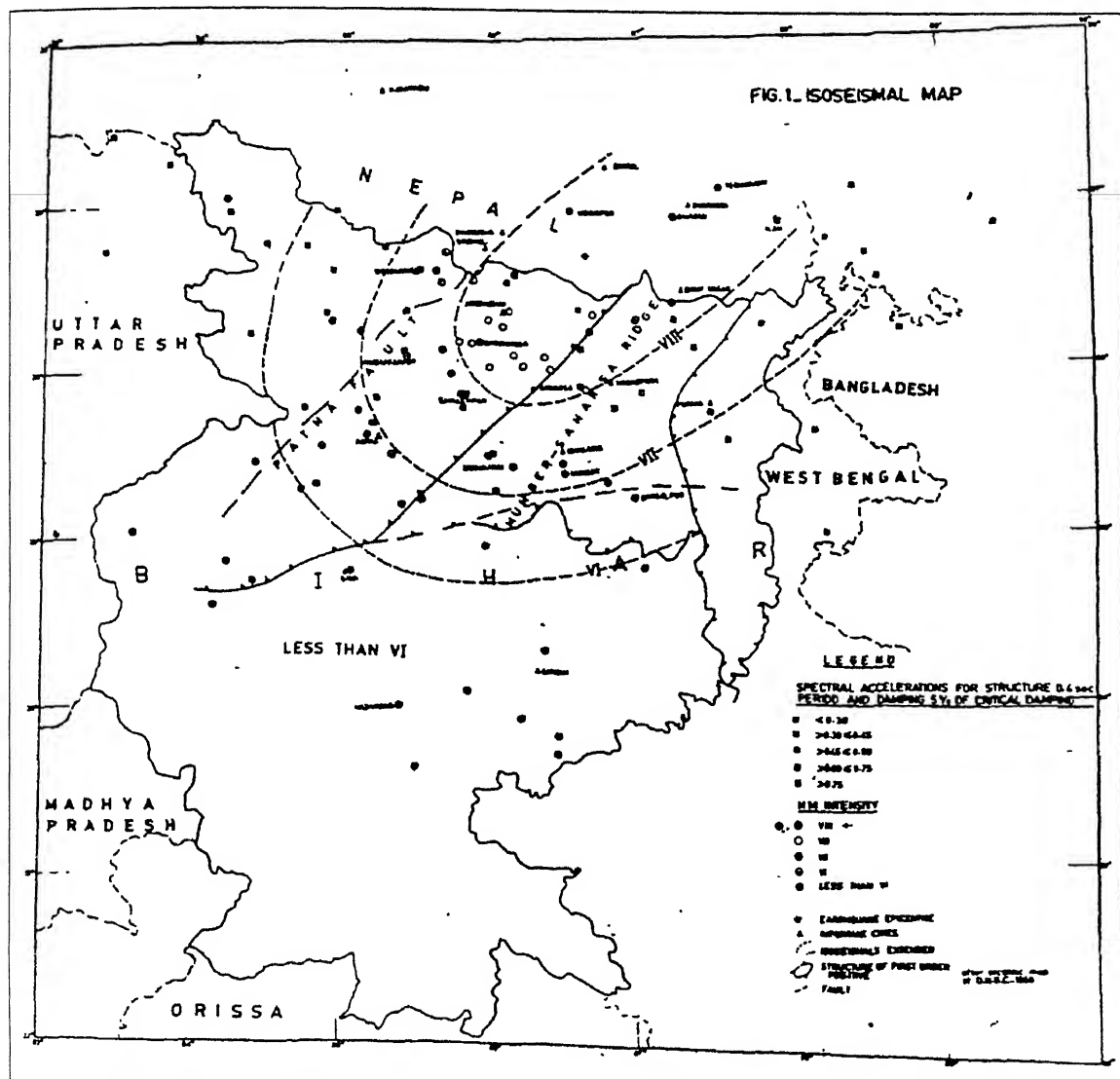


Figure 3.32 Isoseismal map of Bihar-Nepal earthquake (M 6.4) of 20th August 1988 following MM scale after Thakkar (1988).

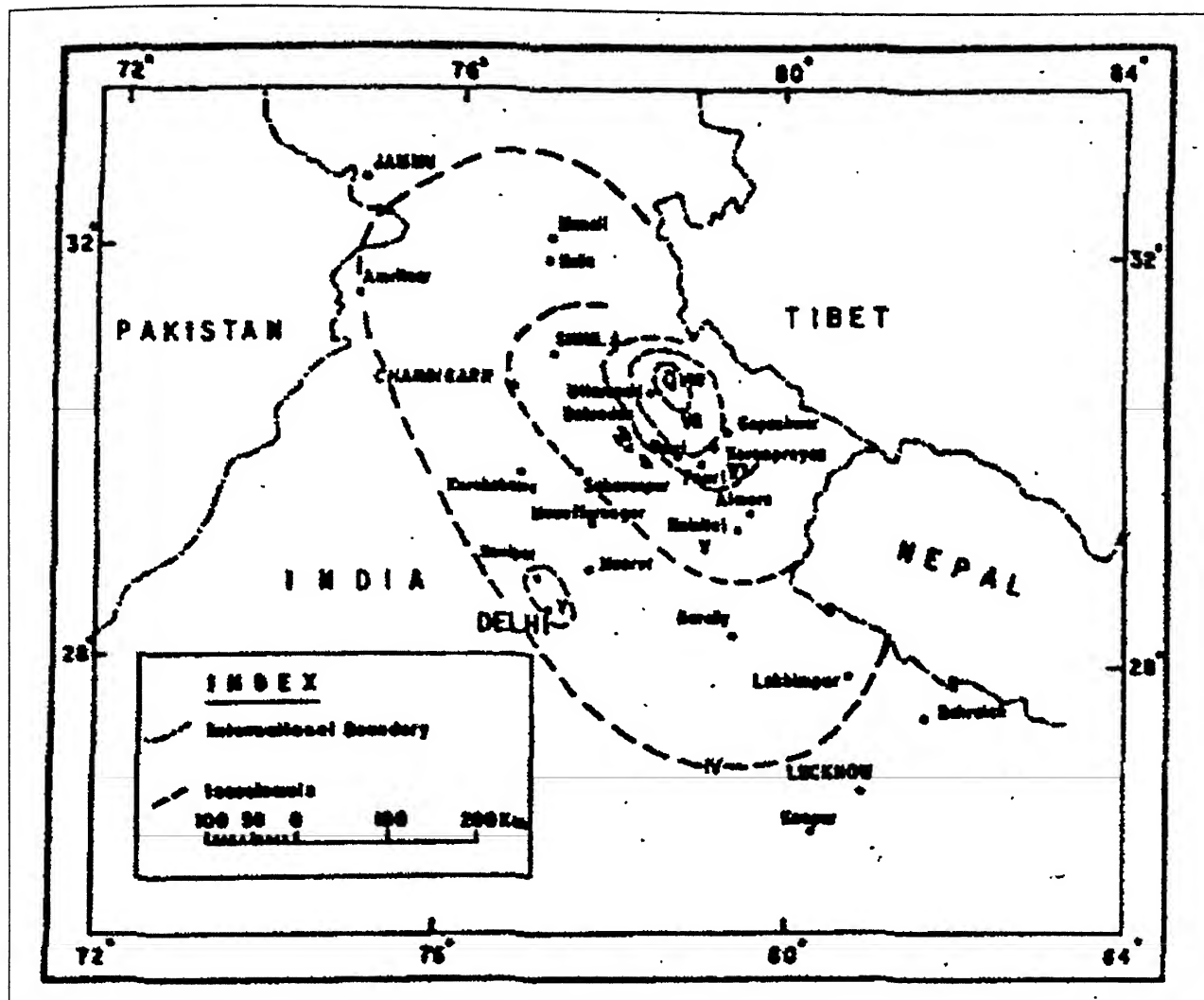


Figure 3.33 Isoseismal map of Uttarkashi earthquake (M 6.6) of 20th October following MSK scale after Narula *et al.* (1995).

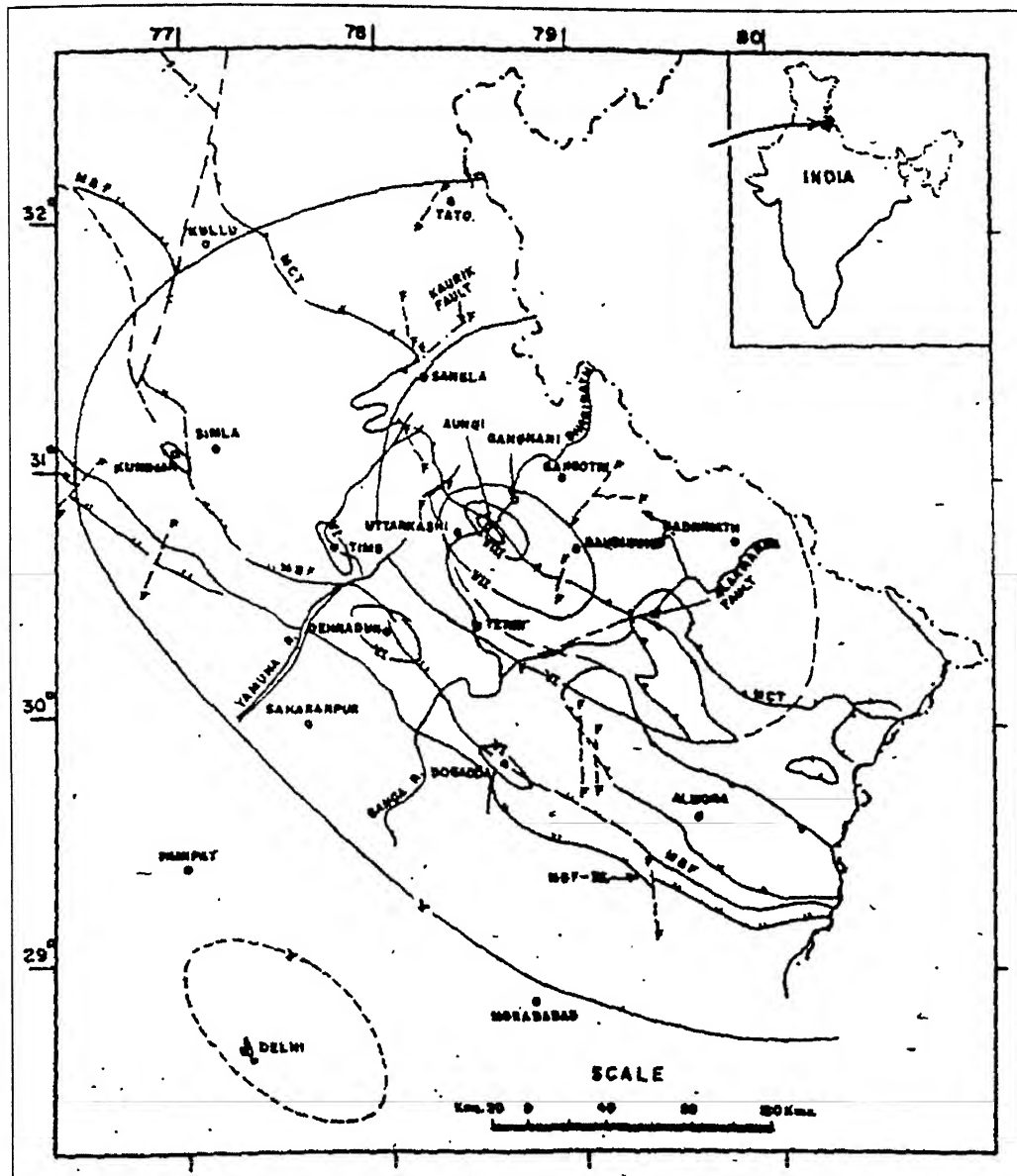


Figure 3.34 Isoseismal map of Uttarkashi earthquake (M 6.6) of 20th October following MSK scale after Rastogi and Chadha (1995).

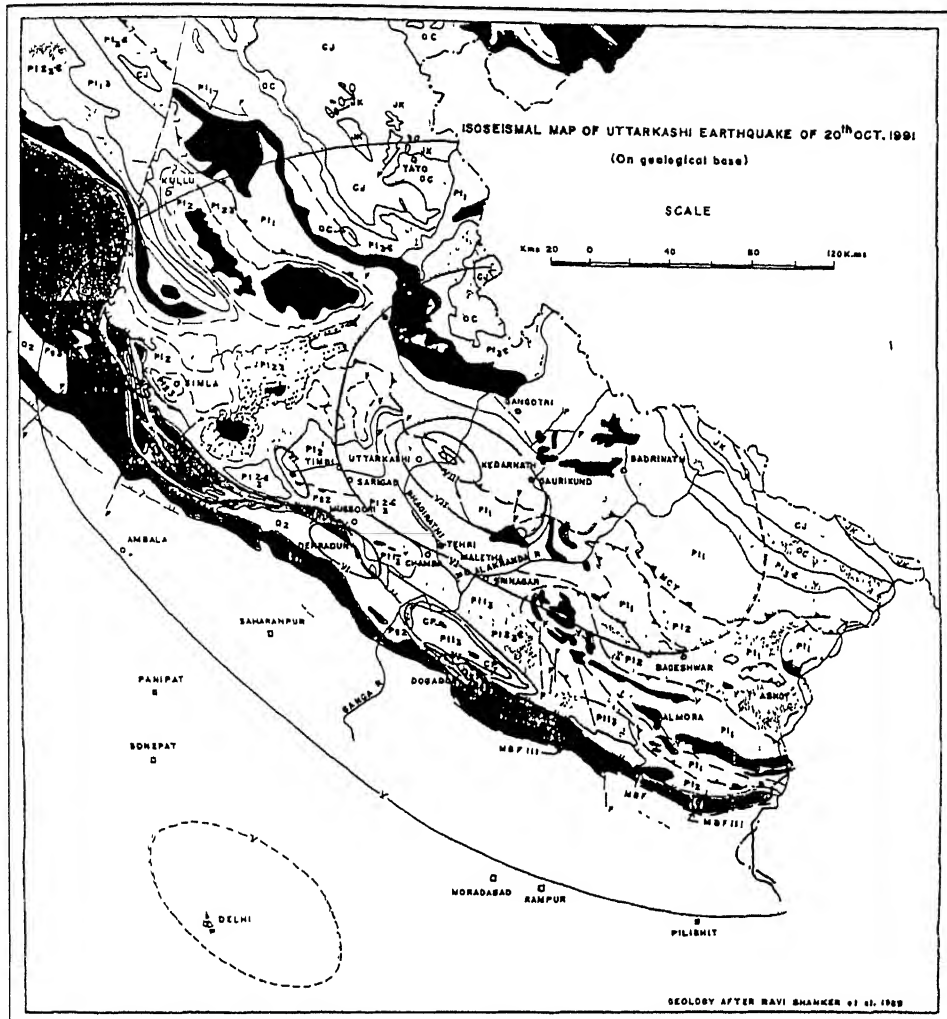


Figure 3.35 Isoseismal map of Uttarkashi earthquake (M 6.6) of 20th October following MSK scale after GSI (1992).

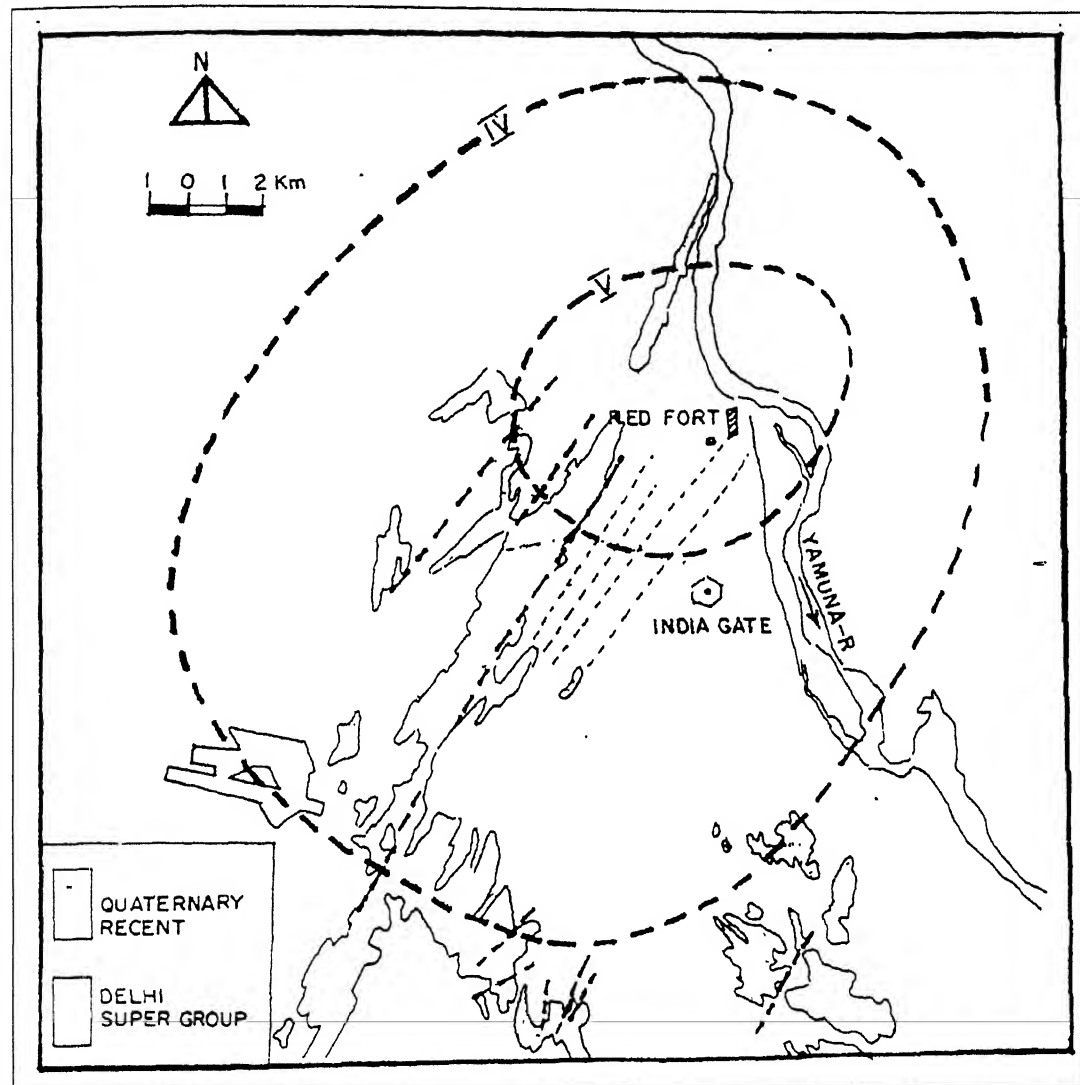


Figure 3.36 Isoseismal map of Delhi earthquake (M 4) of 28th July 1994 following MSK scale after Gupta and Sharda (1996).

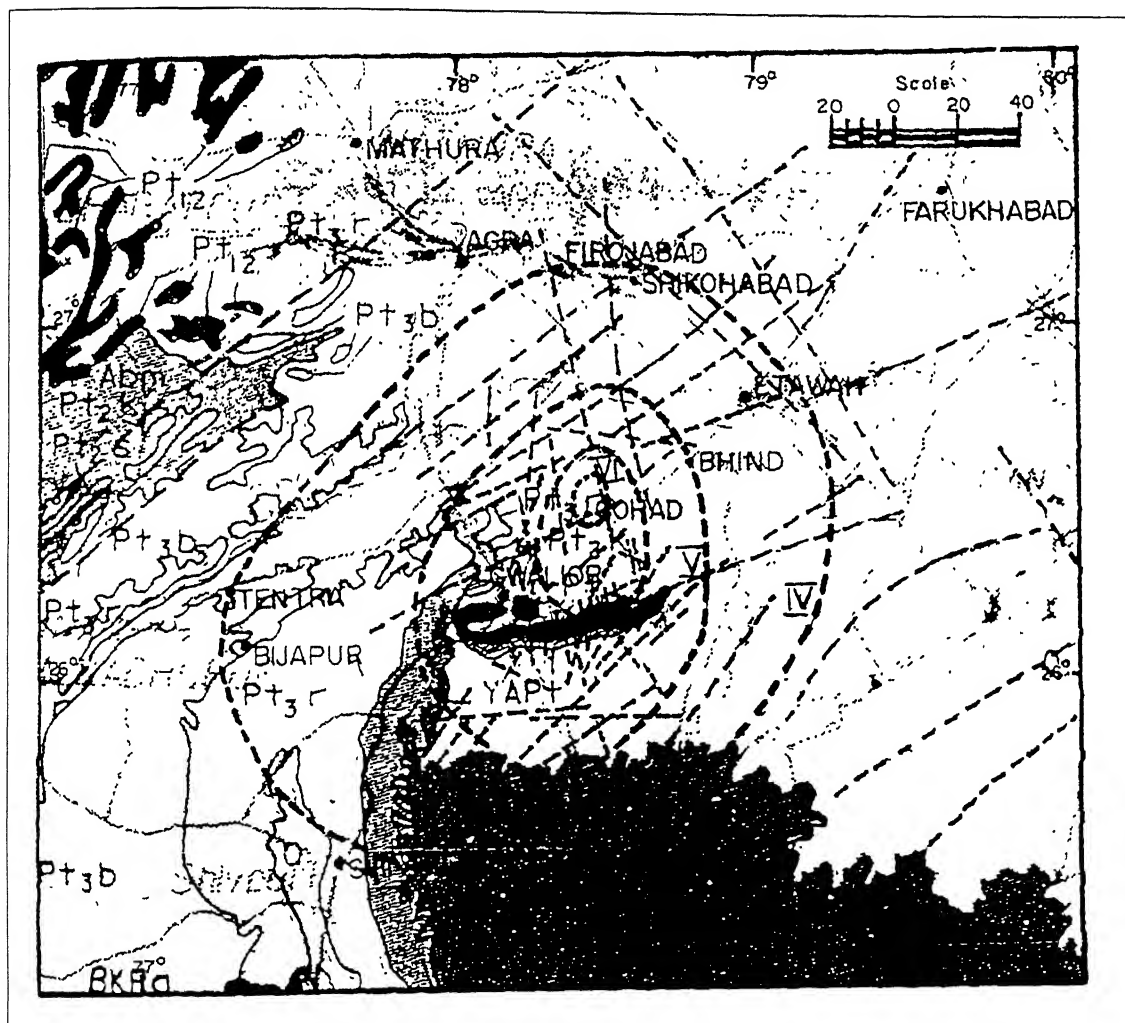


Figure 3.37 Isoseismal map of Bhind earthquake (M 4.8) of 1st September 1994 following MSK scale after Pande *et al.* (1995).

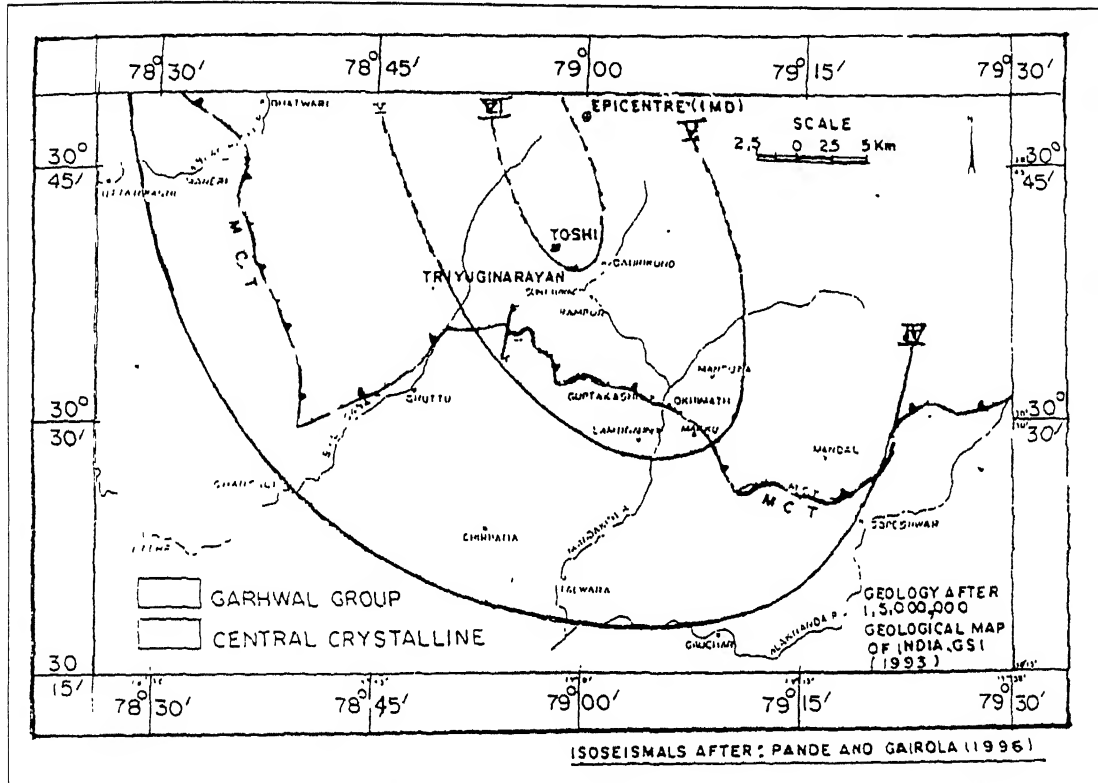


Figure 3.39 Isoseismal map of Garhwal earthquake (M 5) of 26th March 1996 following MSK scale after Pande and Gairola (1996).

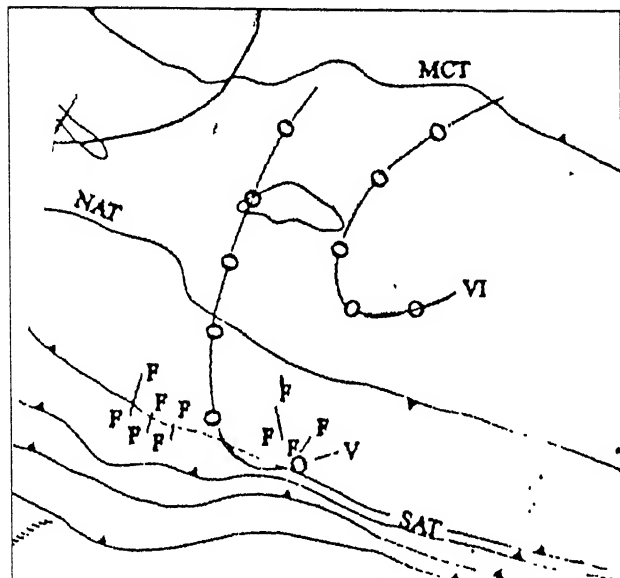


Figure 3.40 Isoseismal map of Indo-Nepal earthquake (M 5th) of 5th January 1997 following MM scale after Dasgupta *et al.* (2000).

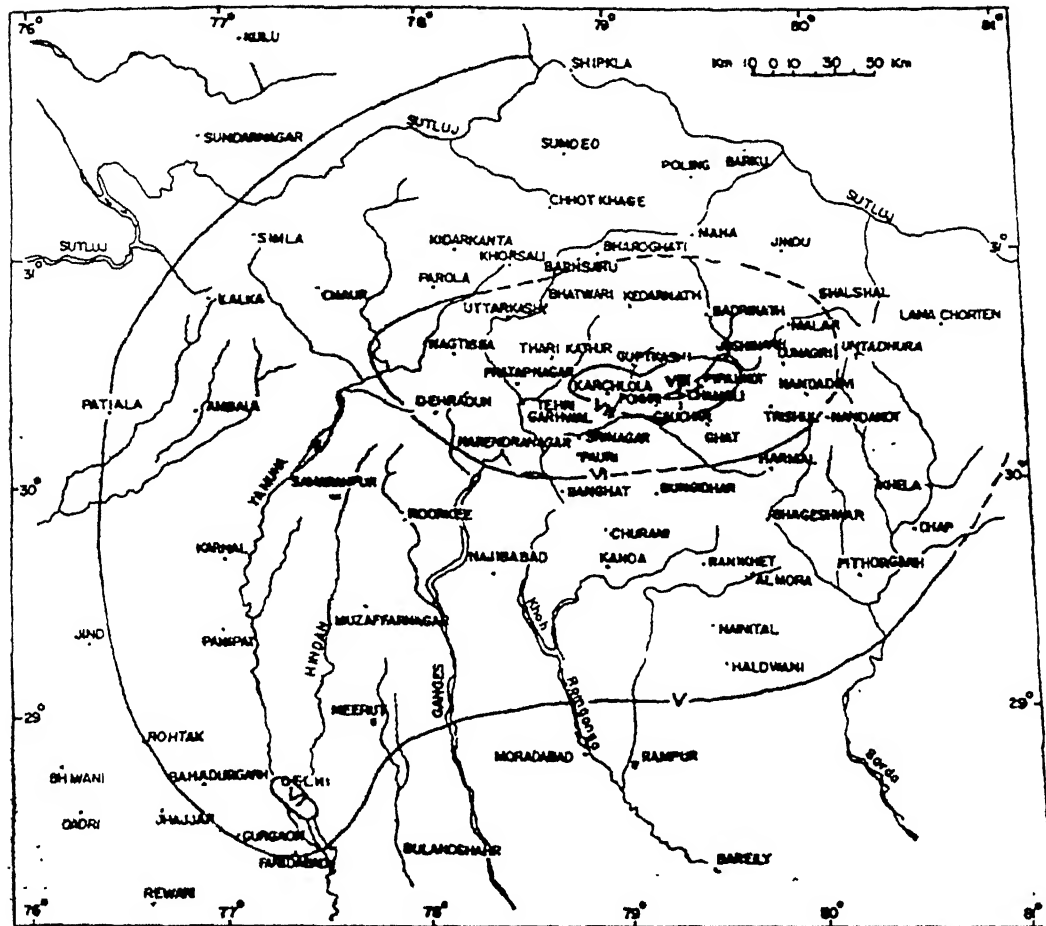


Figure 3.41 Isoseismal map of Chamoli earthquake (M 6.3) of 29th March 1999 following MSK scale taken from Shanker and Narula (1999).

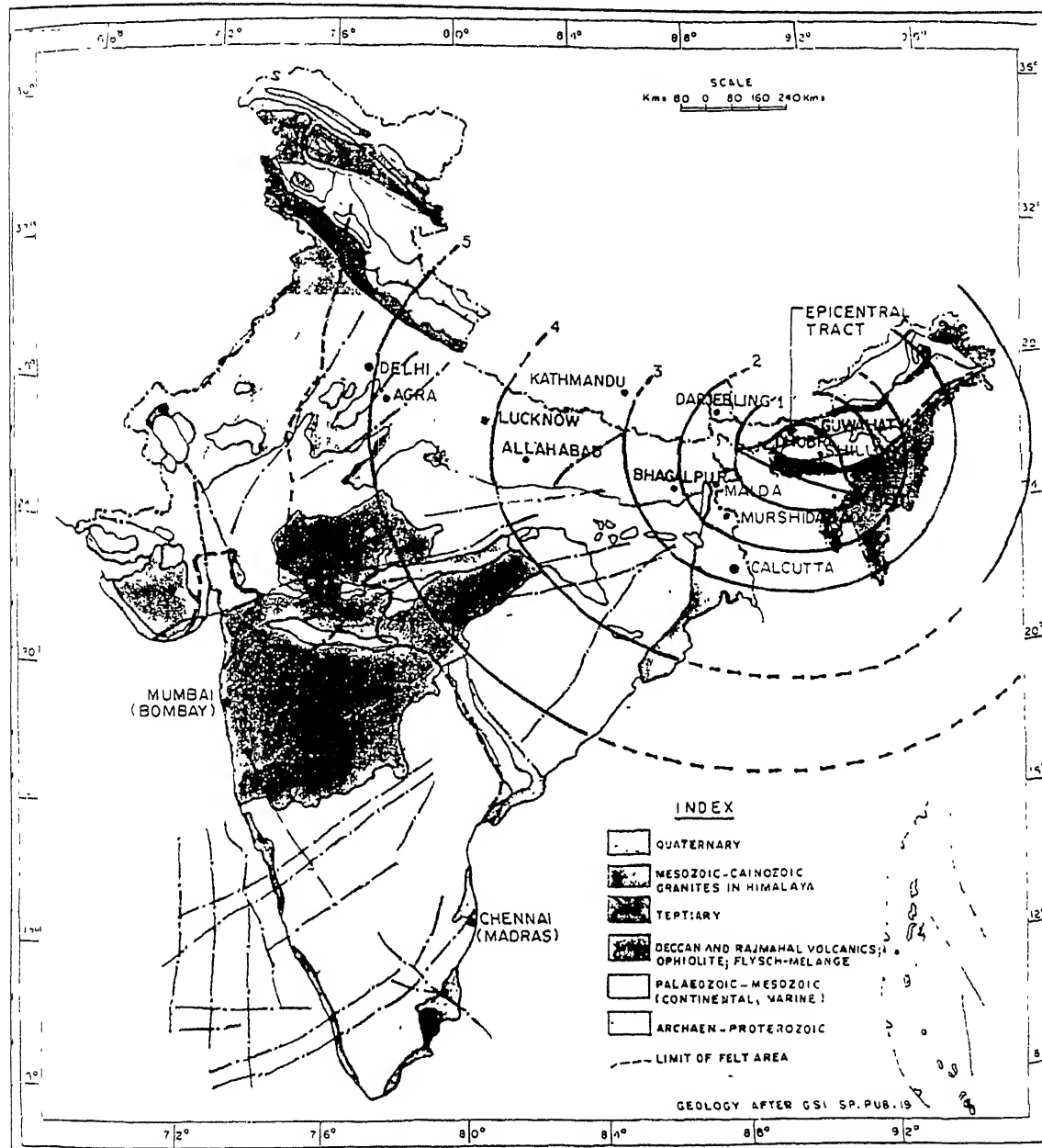


Figure 3.42 Isoseismal map of Assam earthquake (M 8.7) of 12th June 1897 following Olaham's scale after Oldham (1899).

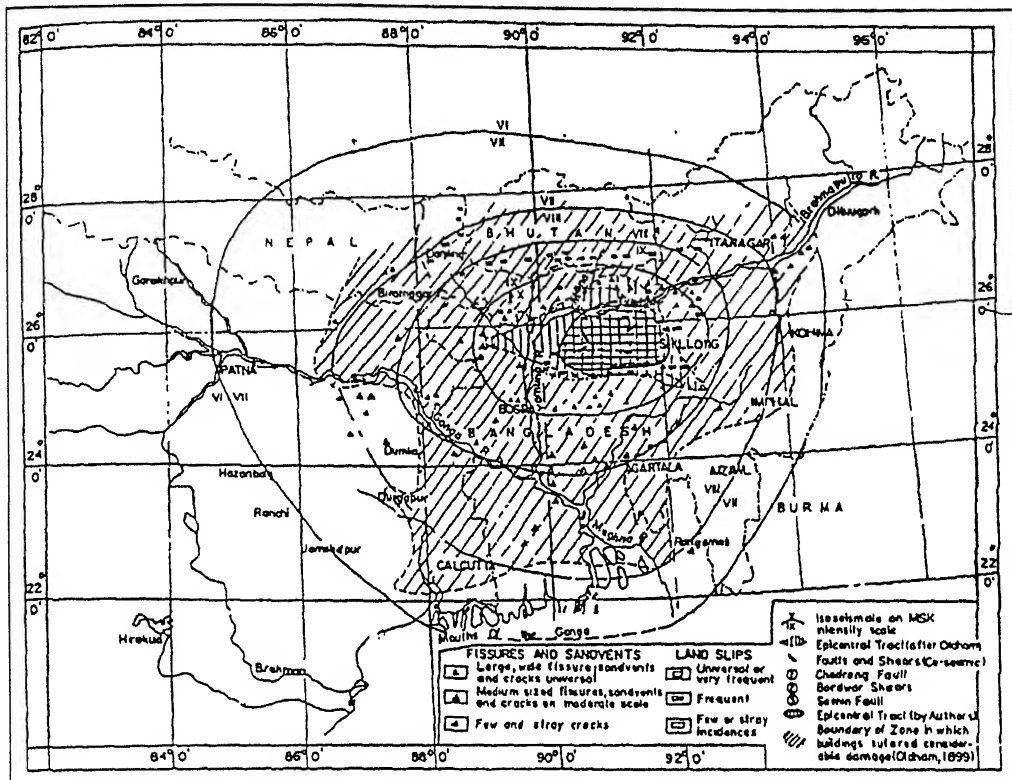


Figure 3.43 Isoseismal map of Assam earthquake (M 8.7) of 12th June 1897 following MSK after Narula and Sharda (1997).

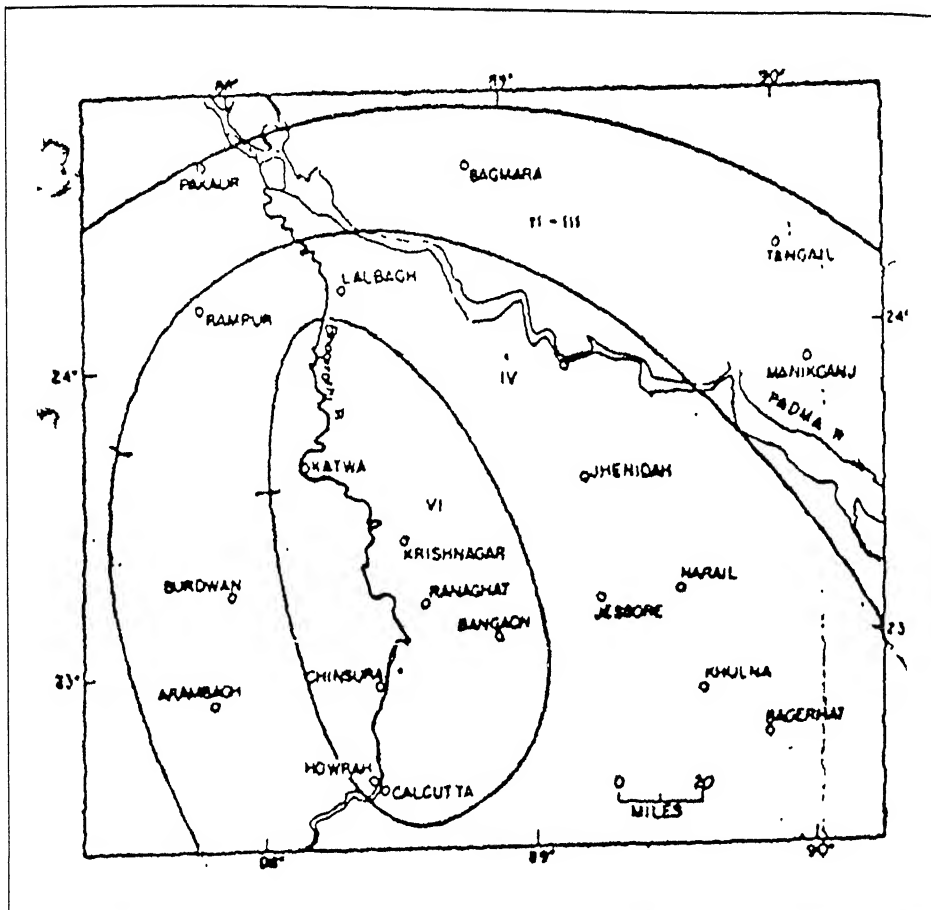


Figure 3.44 Isoseismal map of Calcutta earthquake of 29th September 1906 following MM scale after Middlemiss (1907).

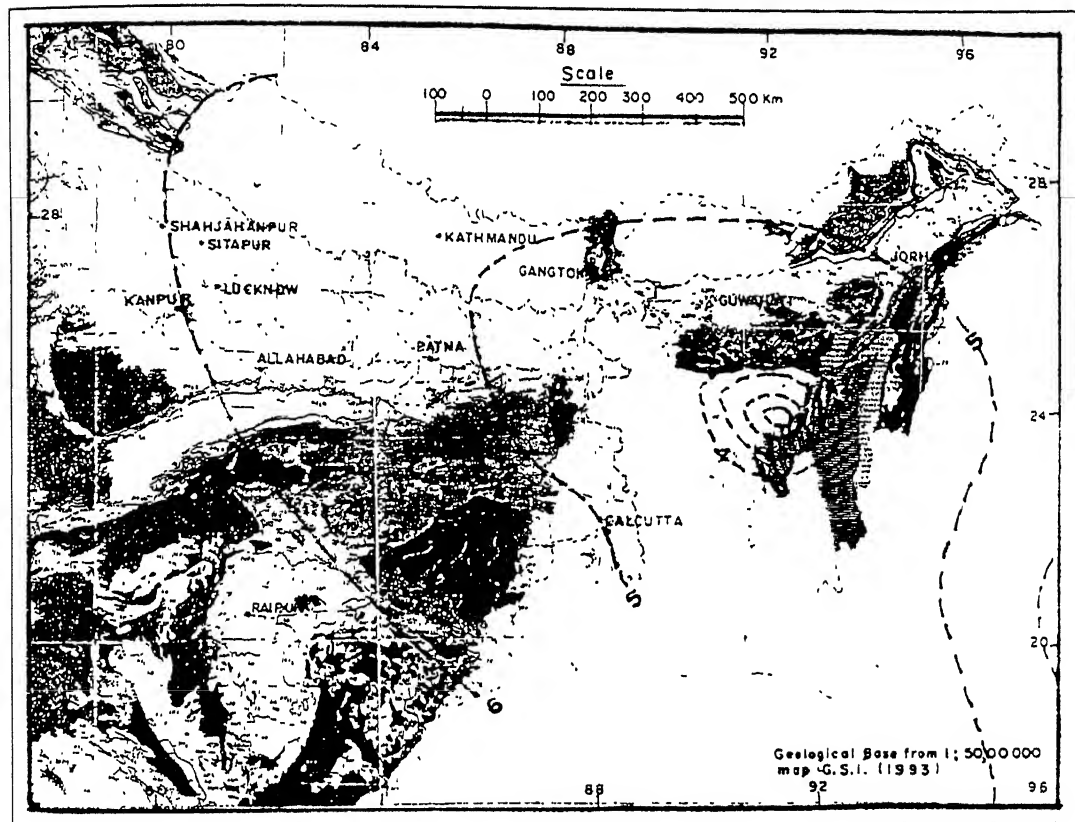


Figure 3.45 Isoseismal map of Srimangal earthquake (M 7.6) of 8th July 1918 following MM scale after Staurt (1918).

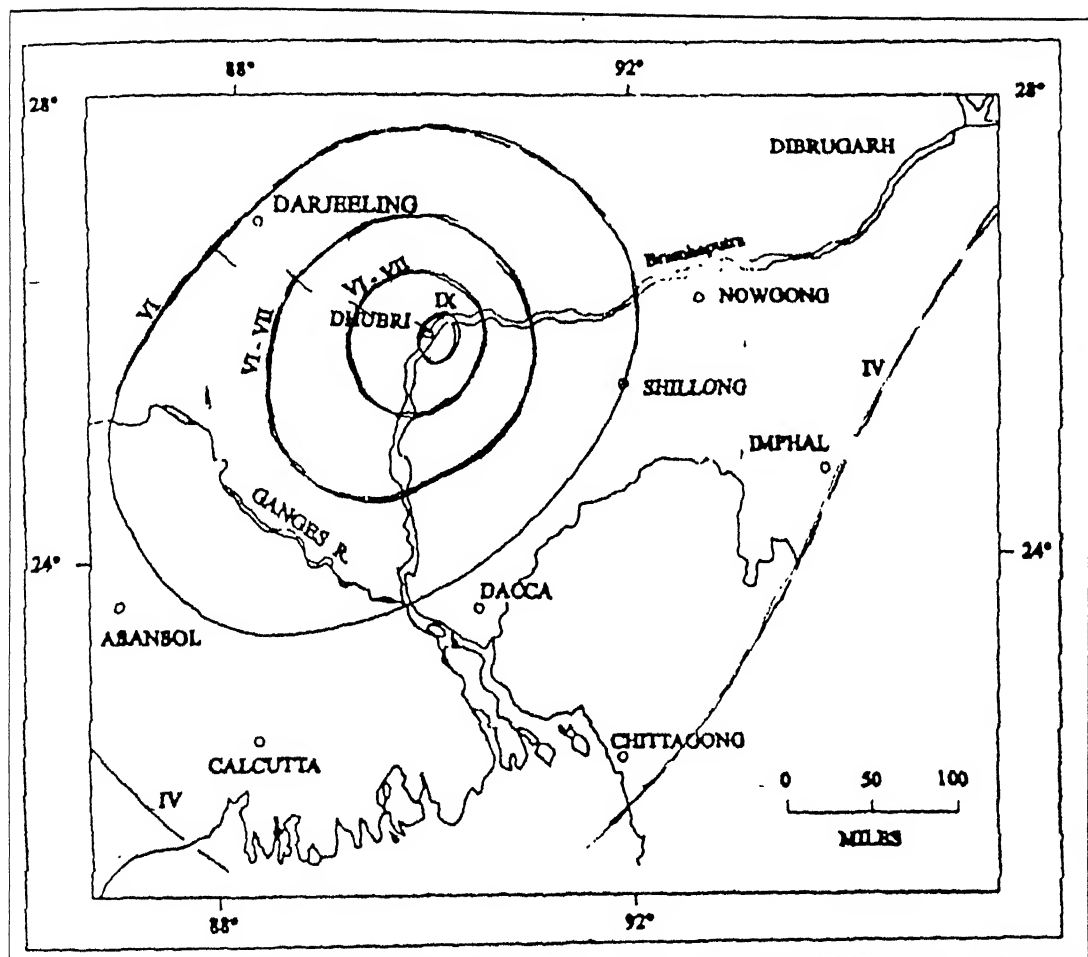


Figure 3.46 Isoseismal map of Dhubri earthquake (M 7.1) of 3rd July 1930 following MM scale after Gee (1934) taken from Kaila and Sarkar (1978).

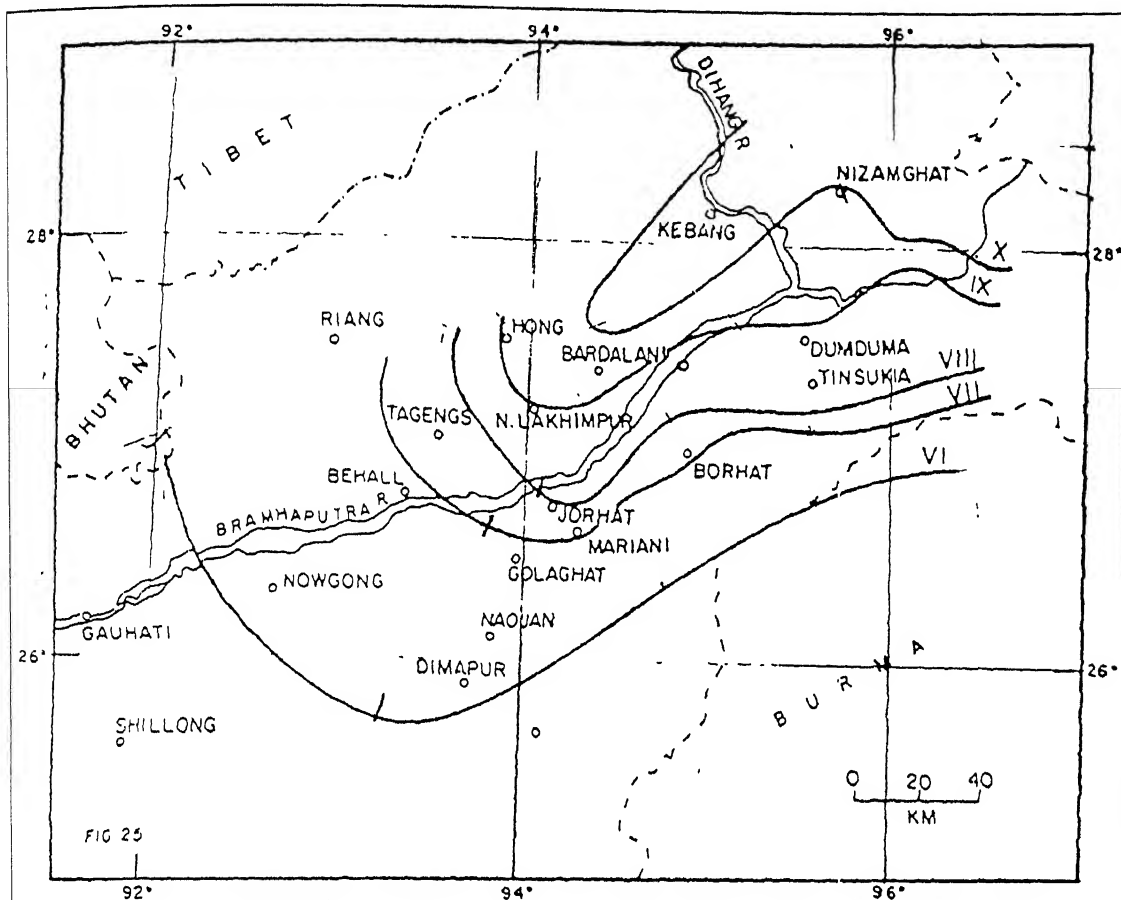


Figure 3.47 Isoseismal map of Assam earthquake (M 8.7) of 15th August 1950 following MM scale after Poddar (1950).

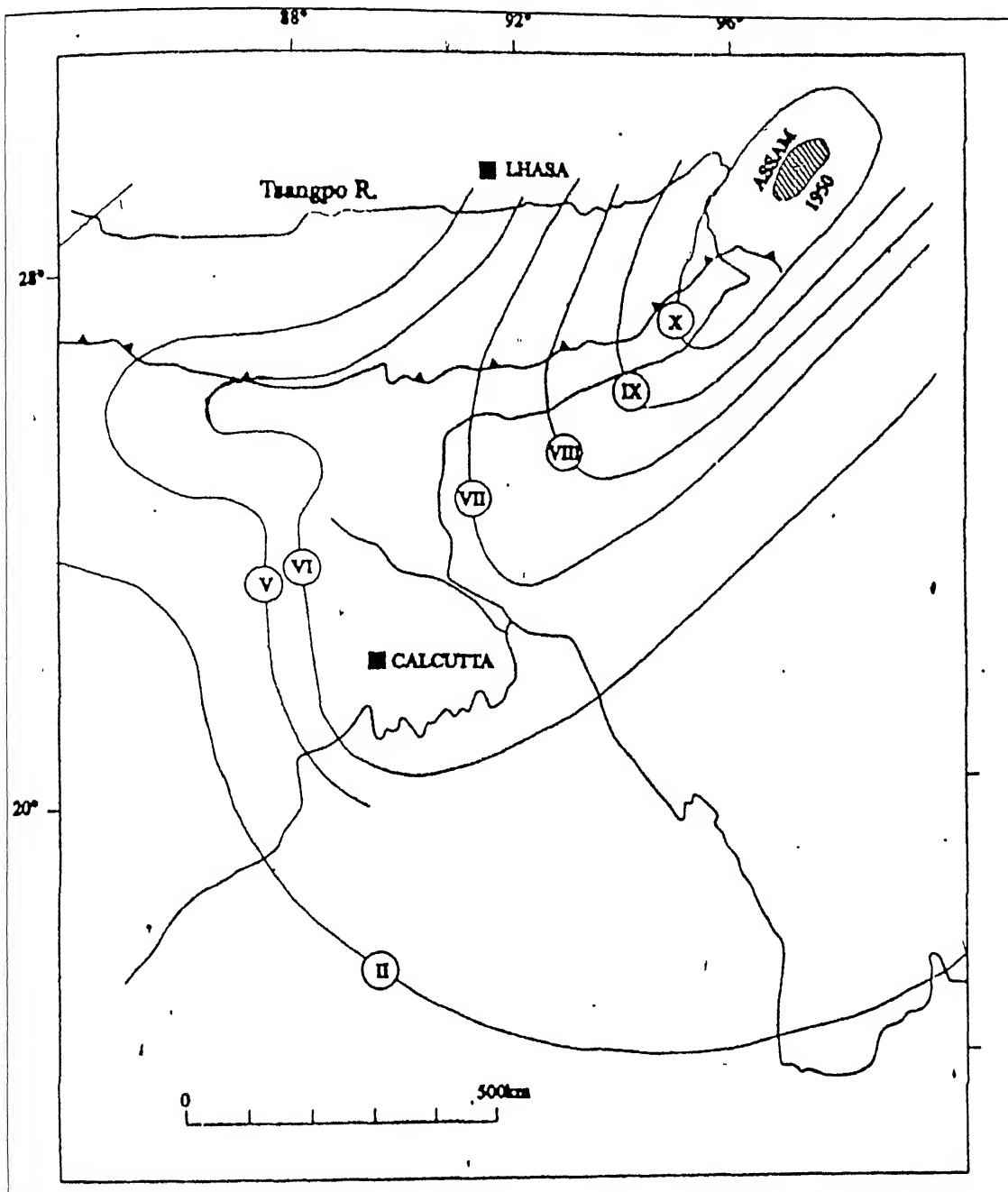


Figure 3.48 Isoseismal map of Assam earthquake (M 8.7) of 15th August 1950 following MM scale taken from Dasgupta *et al.* (2000).

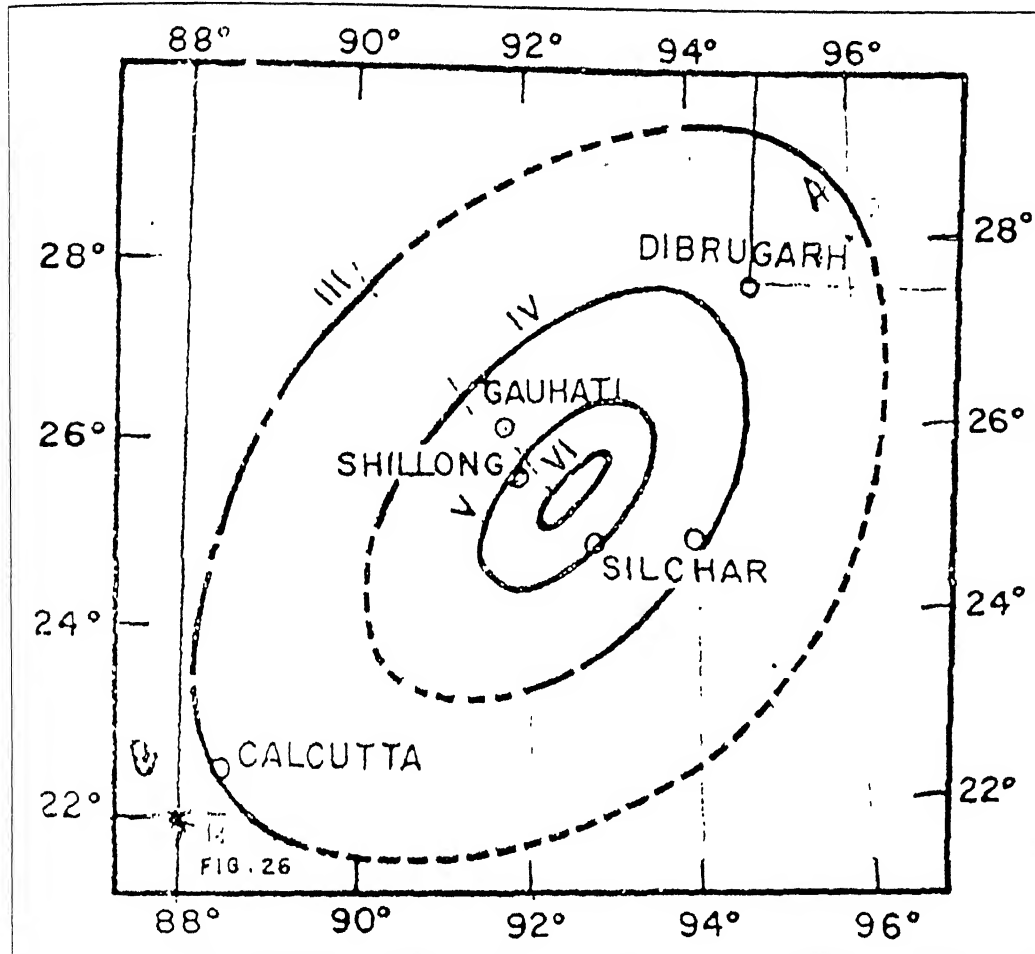


Figure 3.49 Isoseismal map of Assam earthquake (M 6.7) of 8th July 1975 following MM scale after Gosavi *et al.* (1977).

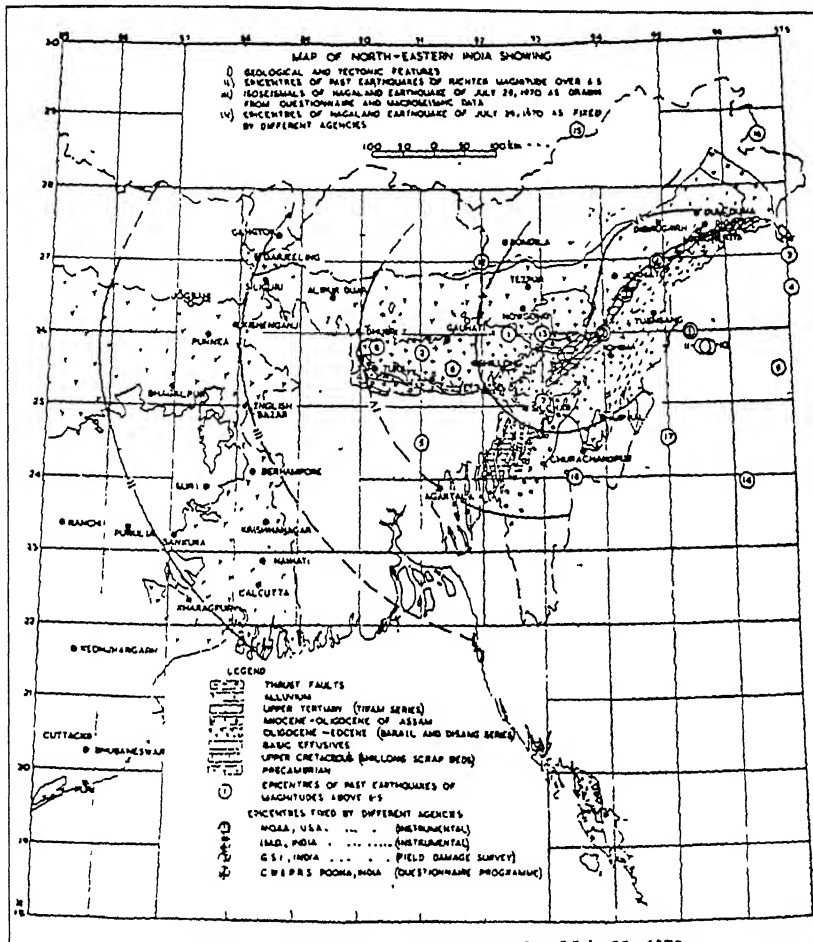


Figure 3.50 Isoseismal map of Nagaland earthquake (M 6.4) of 29th July 1970 following MM scale after Guha and Gosavi (1974).

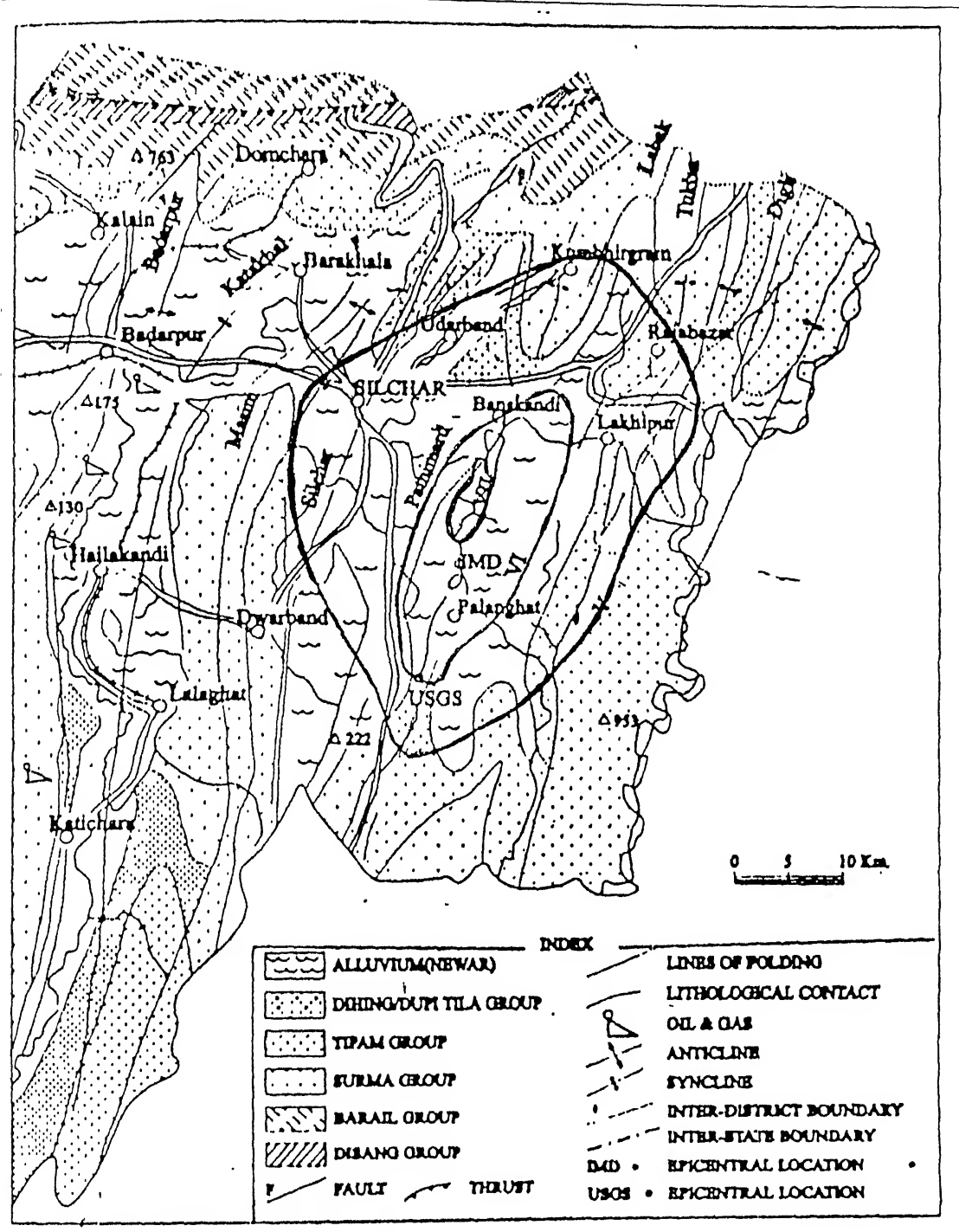


Figure 3.51 Isoseismal map of Cachar earthquake (M 5.5) of 31st December 1984 following MM scale after Narula [taken from Dasgupta *et al.* (2000)].

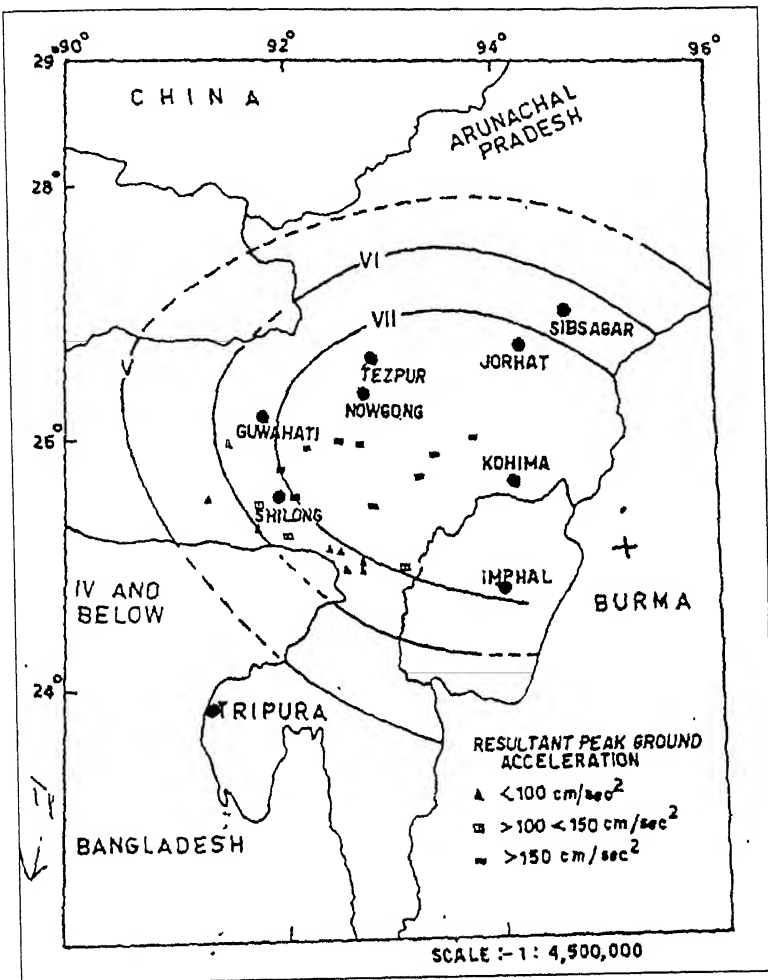


Figure 3.52 Isoseismal map of Burma earthquake (M 6.8) of 6th August 1988 following MM scale after Kumar (1992).

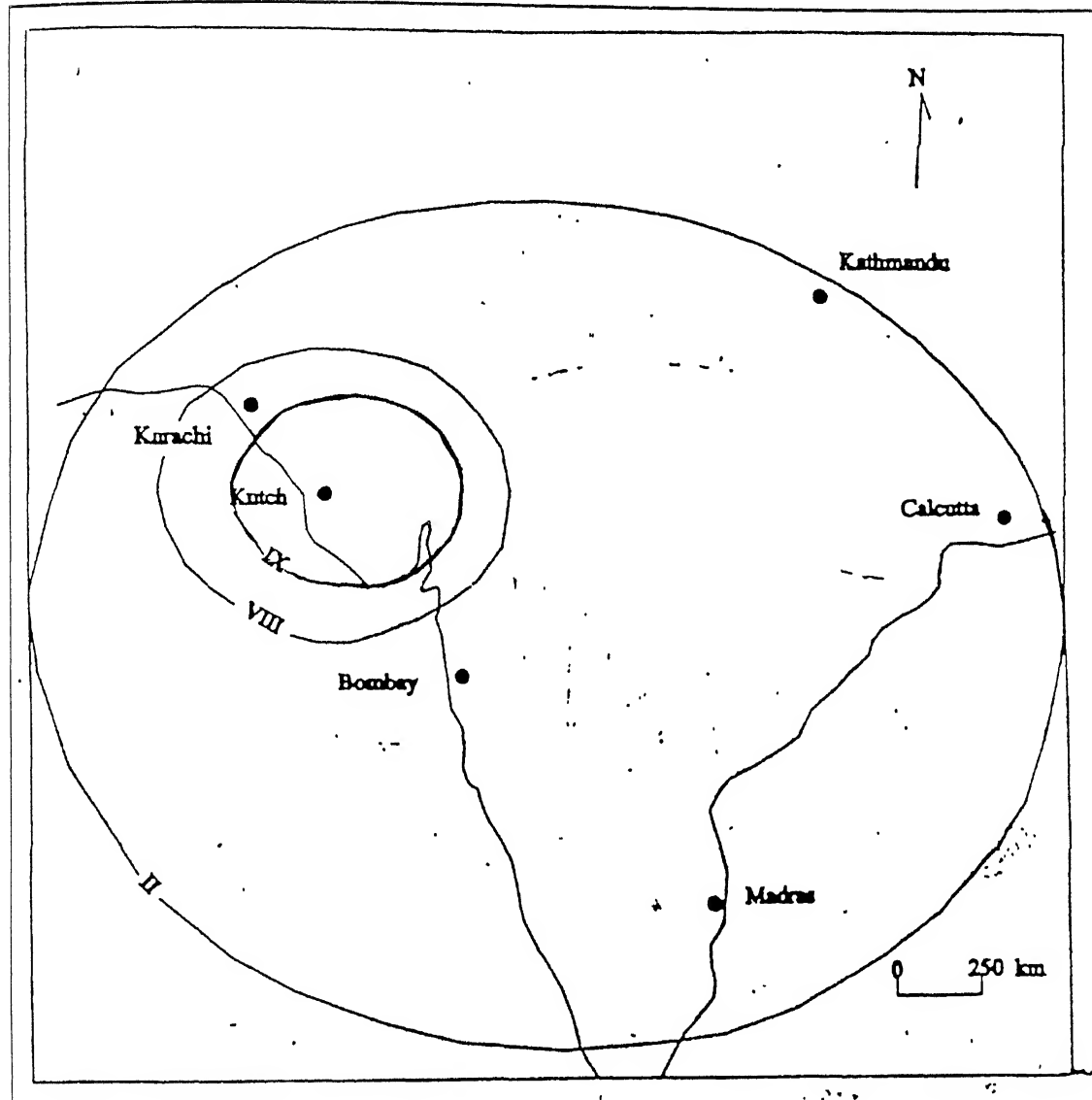


Figure 3.53 Isoseismal map of Kutch earthquake of 16th June 1819 following MM scale taken from Dasgupta *et al.* (2000).

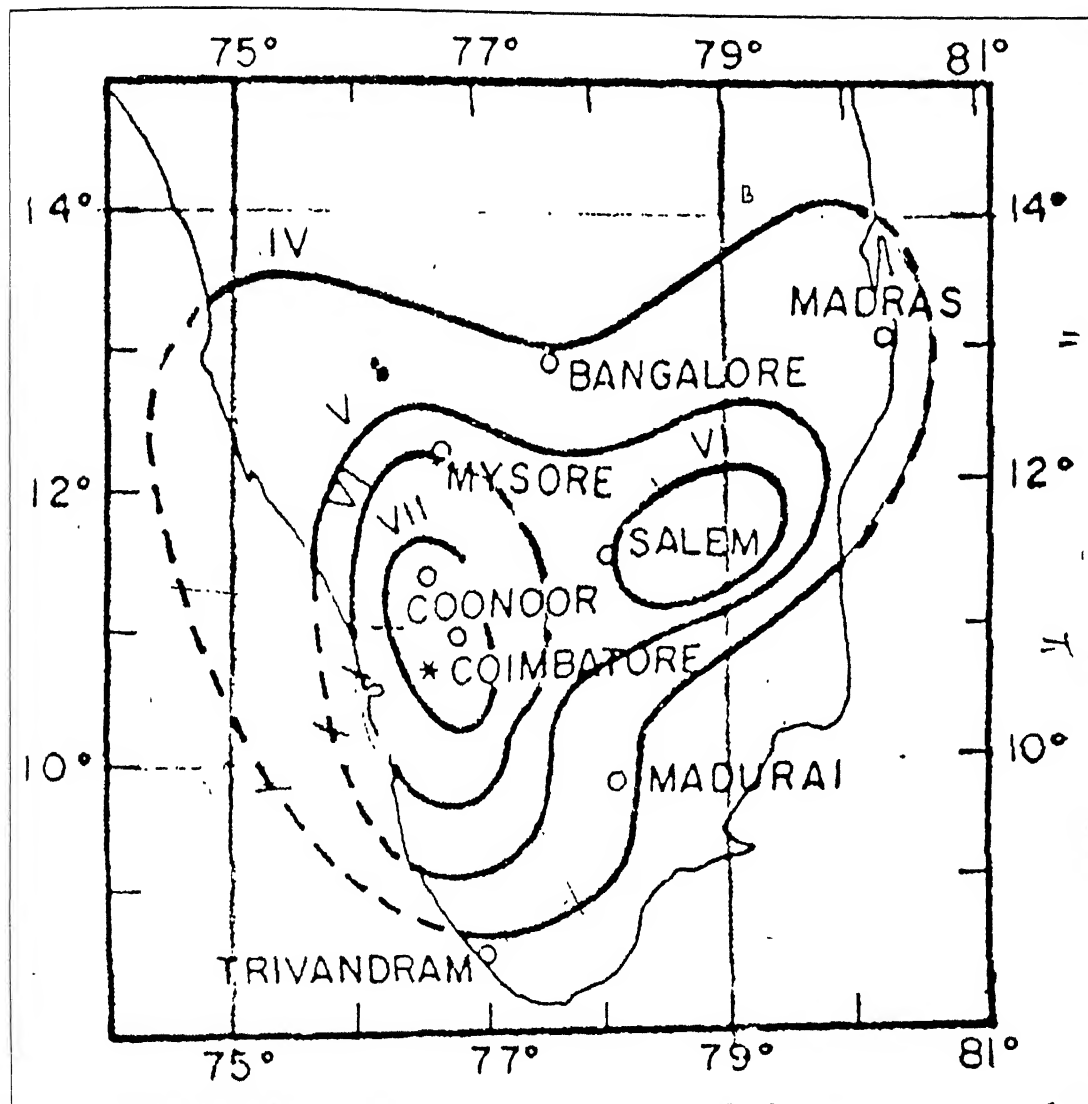


Figure 3.54 Isoseismal map of Coimbatore earthquake (M 6) of 8th February 1900 following MM scale after Basu (1964) taken from Kaila and Sarkar (1978).

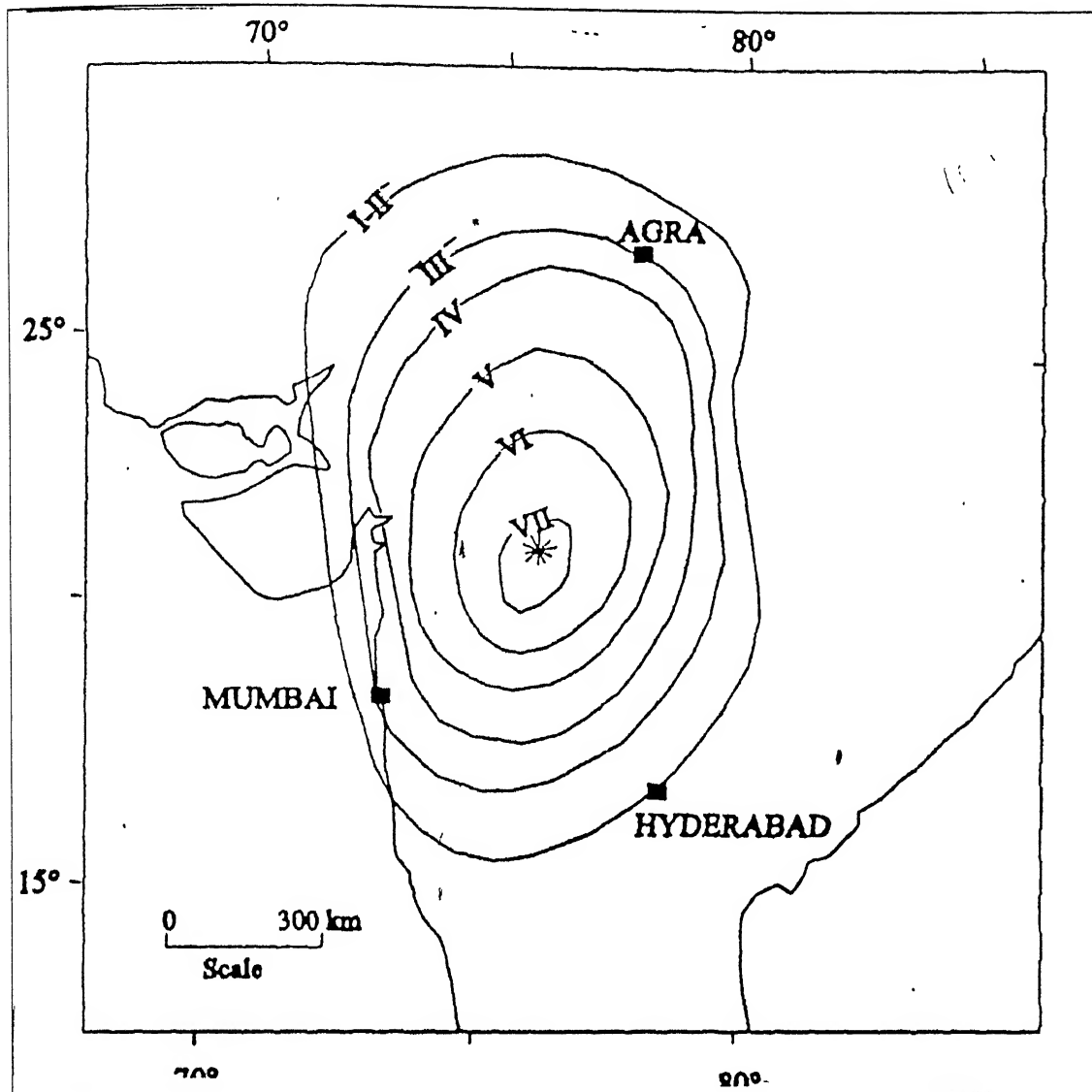


Figure 3.55 Isoseismal map of Satpura earthquake ($M 6.2$) of 14th March 1938 following MM scale after Mukherjee (1942) taken from Dasgupta *et al.* (2000).

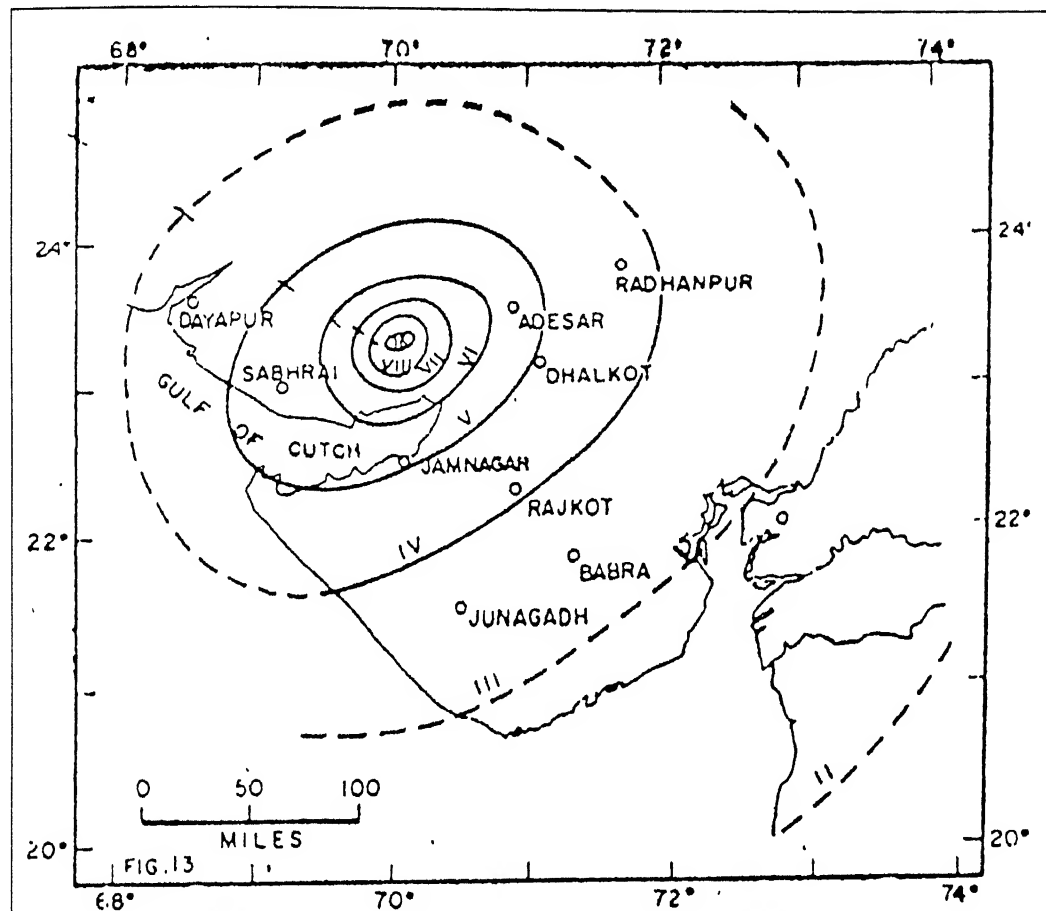


Figure 3.56 Isoseismal map of Anjar earthquake (M 7) of 21st July 1956 following MM scale after Tandon (1959).

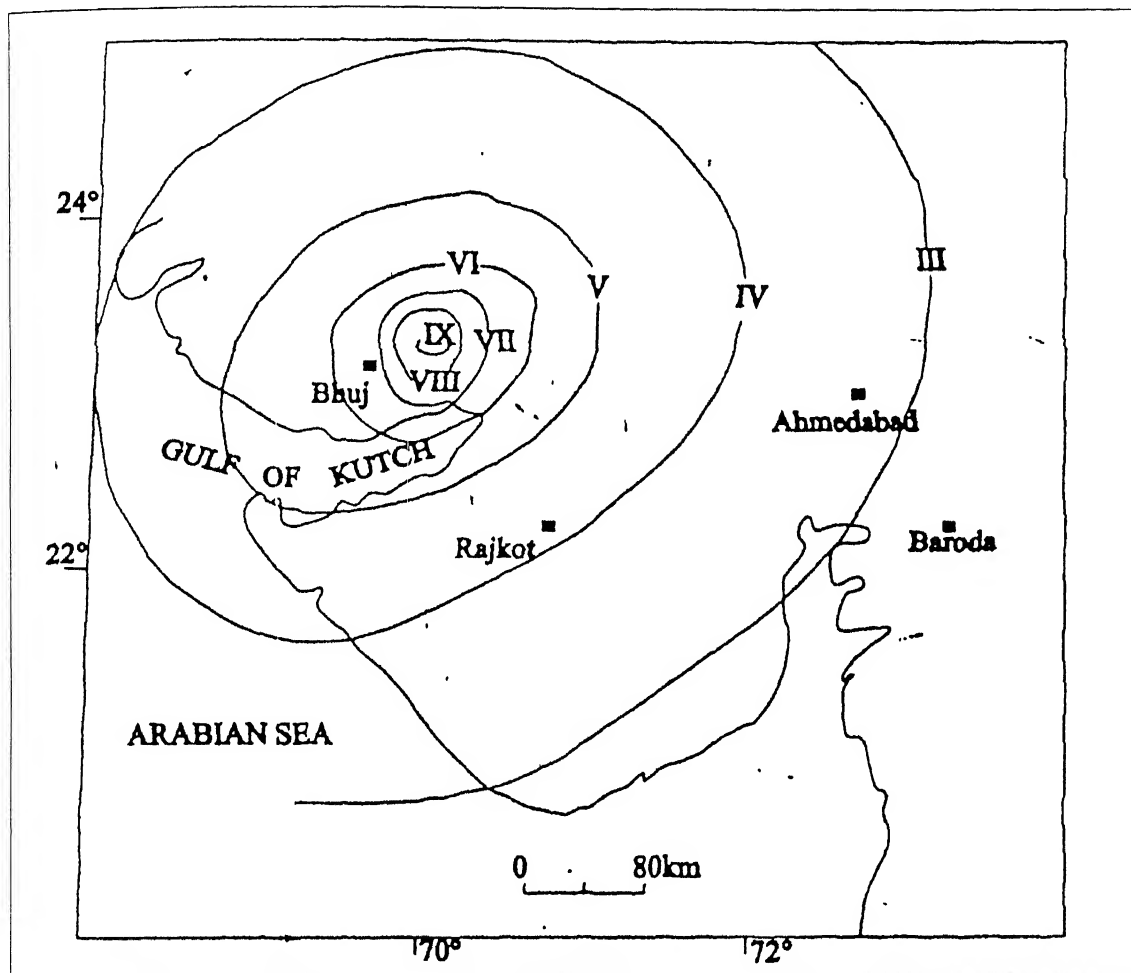


Figure 3.57 Isoseismal map of Anjar earthquake (M 7) of 21st July 1956 following MM scale taken from Dasgupta *et al.* (2000).

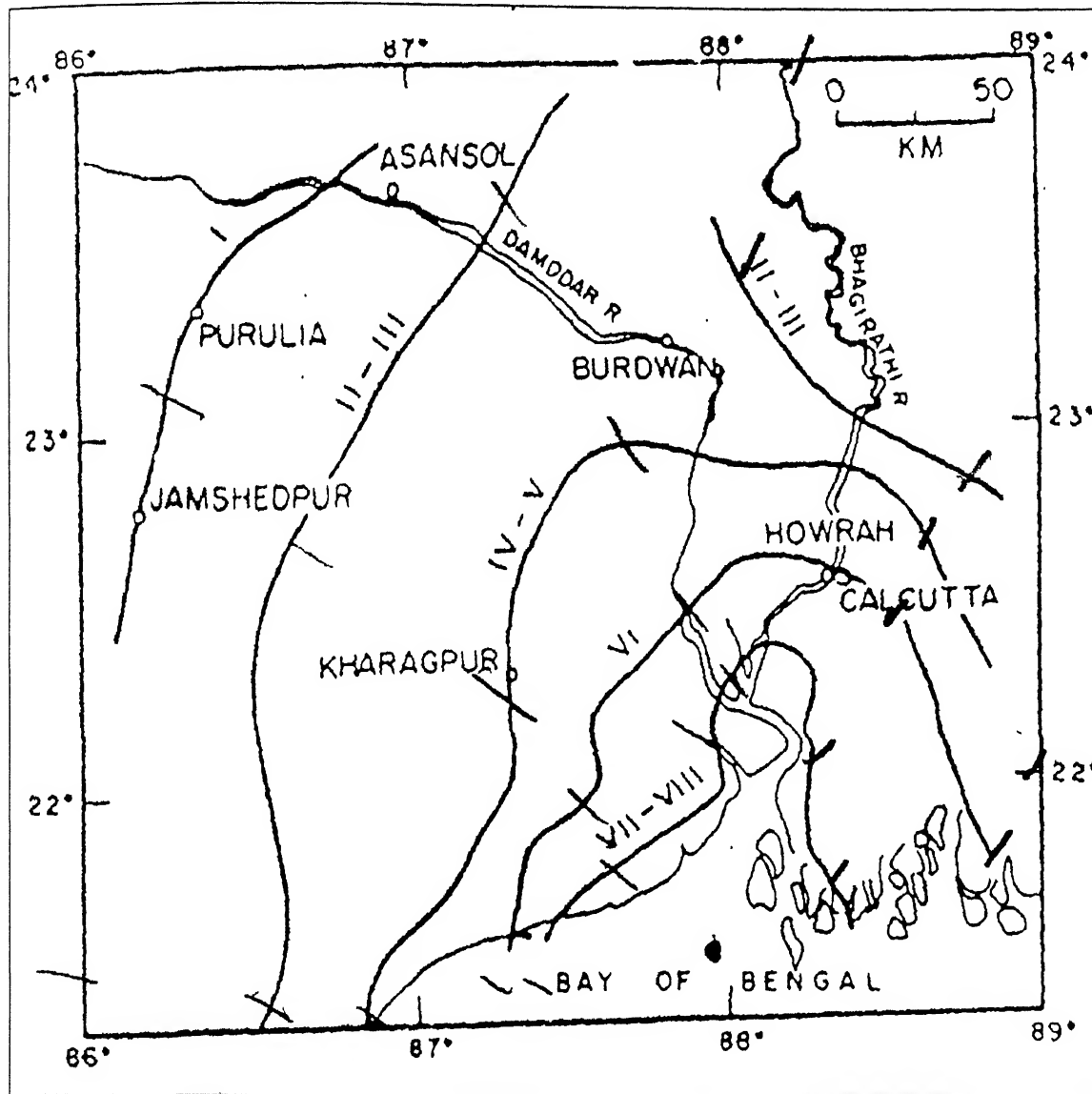


Figure 3.58 Isoseismal map of Calcutta earthquake (M 5.5) of 15th August 1964 following MM scale after Jhingran *et al.* (1969) taken from Kaila and Sarkar (1978).

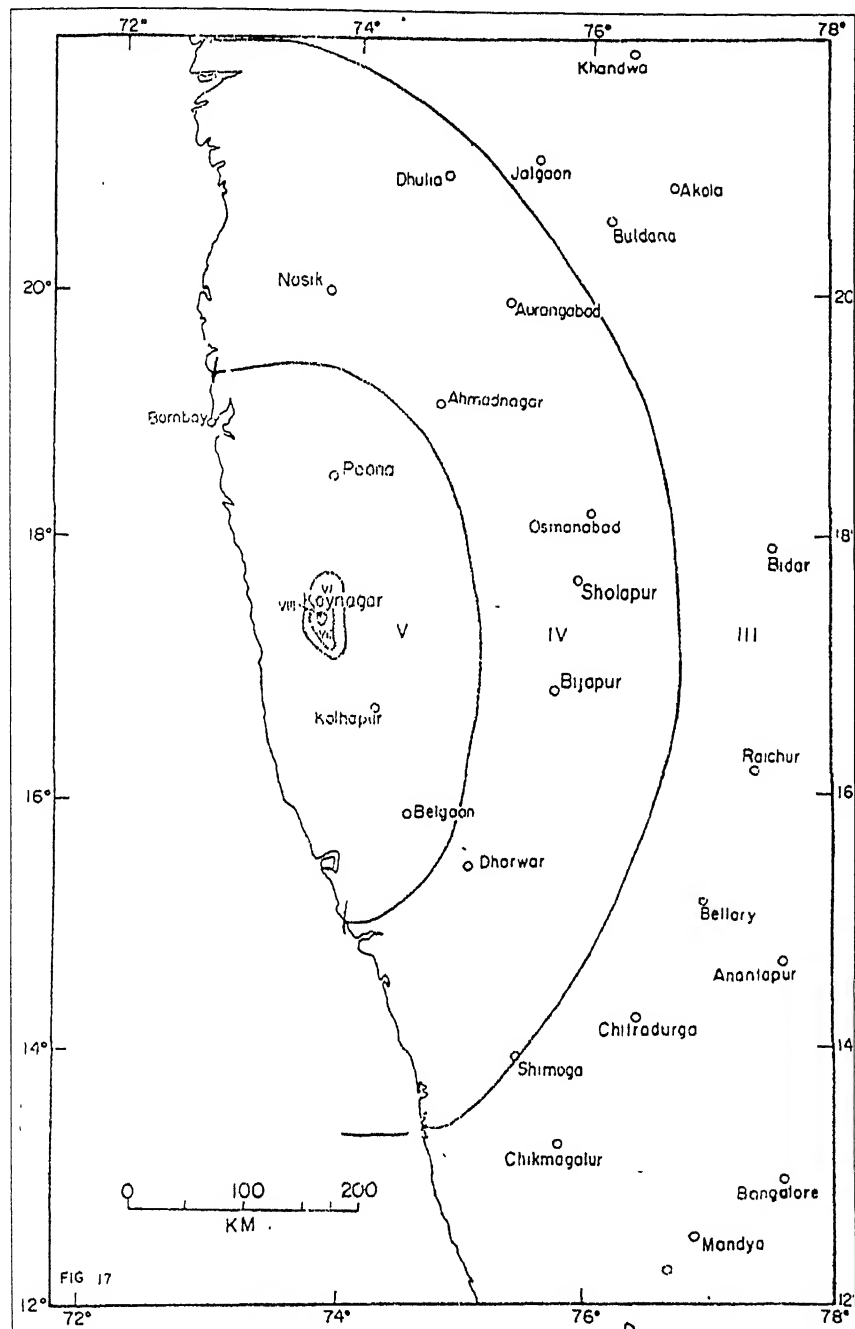


Figure 3.59 Isoseismal map of Koyna earthquake (M 5.2) of 10th December 1967 following MM scale after Chatterji *et al.* (1967) taken from Kaila and Sarkar (1978).

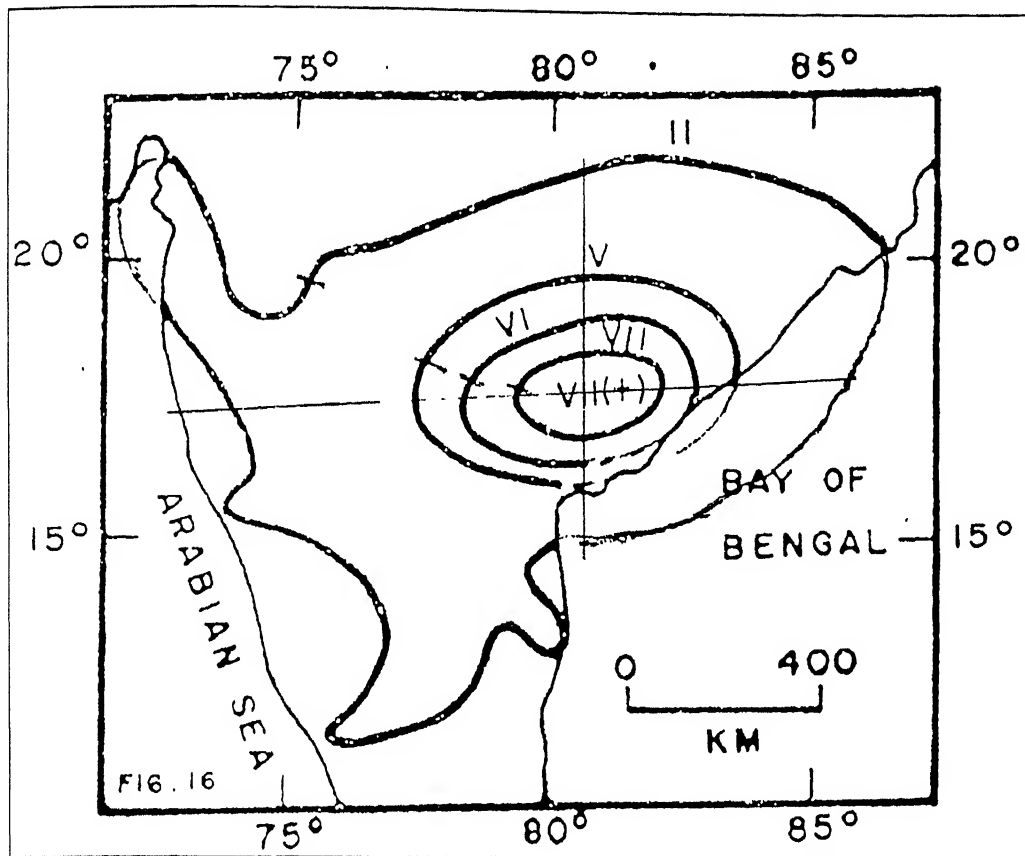


Figure 3.60 Isoseismal map of Bhadrachalam earthquake (M 6.5) of 13th April 1969 following MM scale after Mukherjee (1971) taken from Kaila and Sarkar (1978).

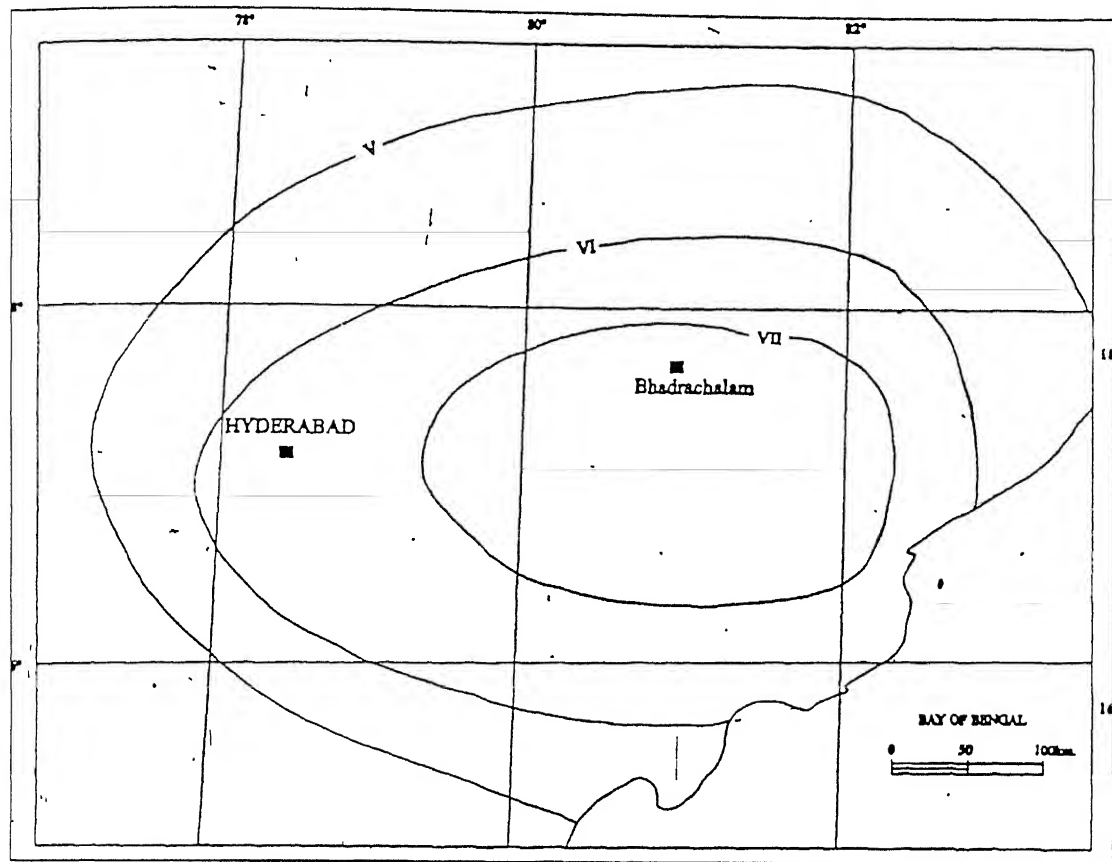


Figure 3.61 Isoseismal map of Bhadrachalam earthquake (M 6.5) of 13th April 1969 following MM scale taken from Dasgupta *et al.* (2000).

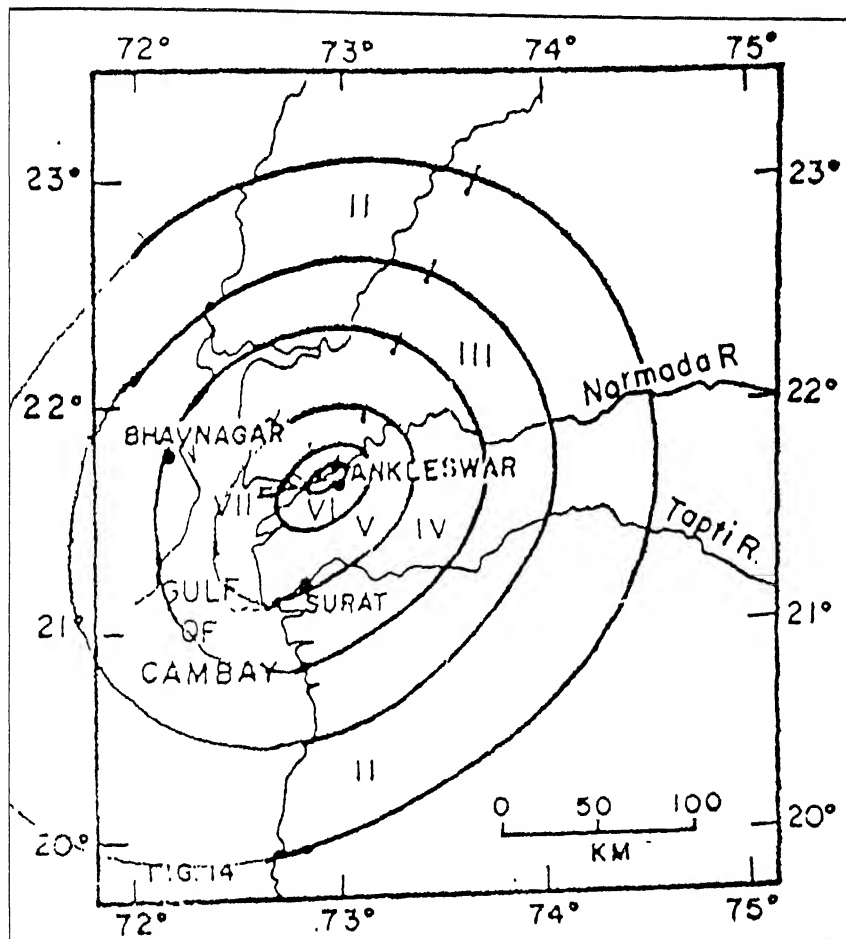


Figure 3.62 Isoseismal map of Broach earthquake (M 6.7) of 23rd March 1970 following MM scale after Chaudhury *et al.* (1970) taken from Kaila and Sarkar (1978).

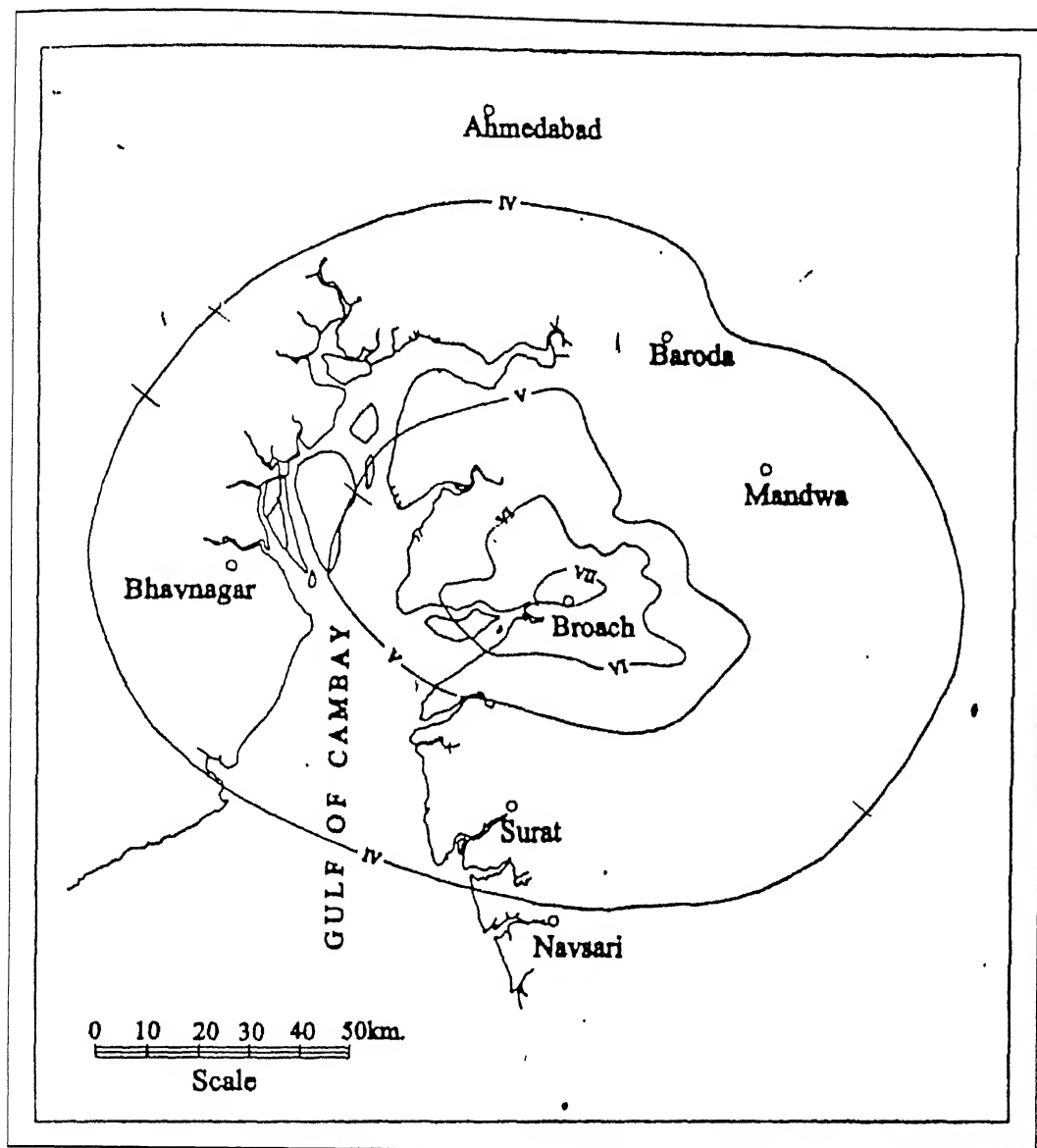


Figure 3.63 Isoseismal map of Broach earthquake (M 6.7) of 23rd March 1970 following MM scale taken from Dasgupta *et al.* (2000).

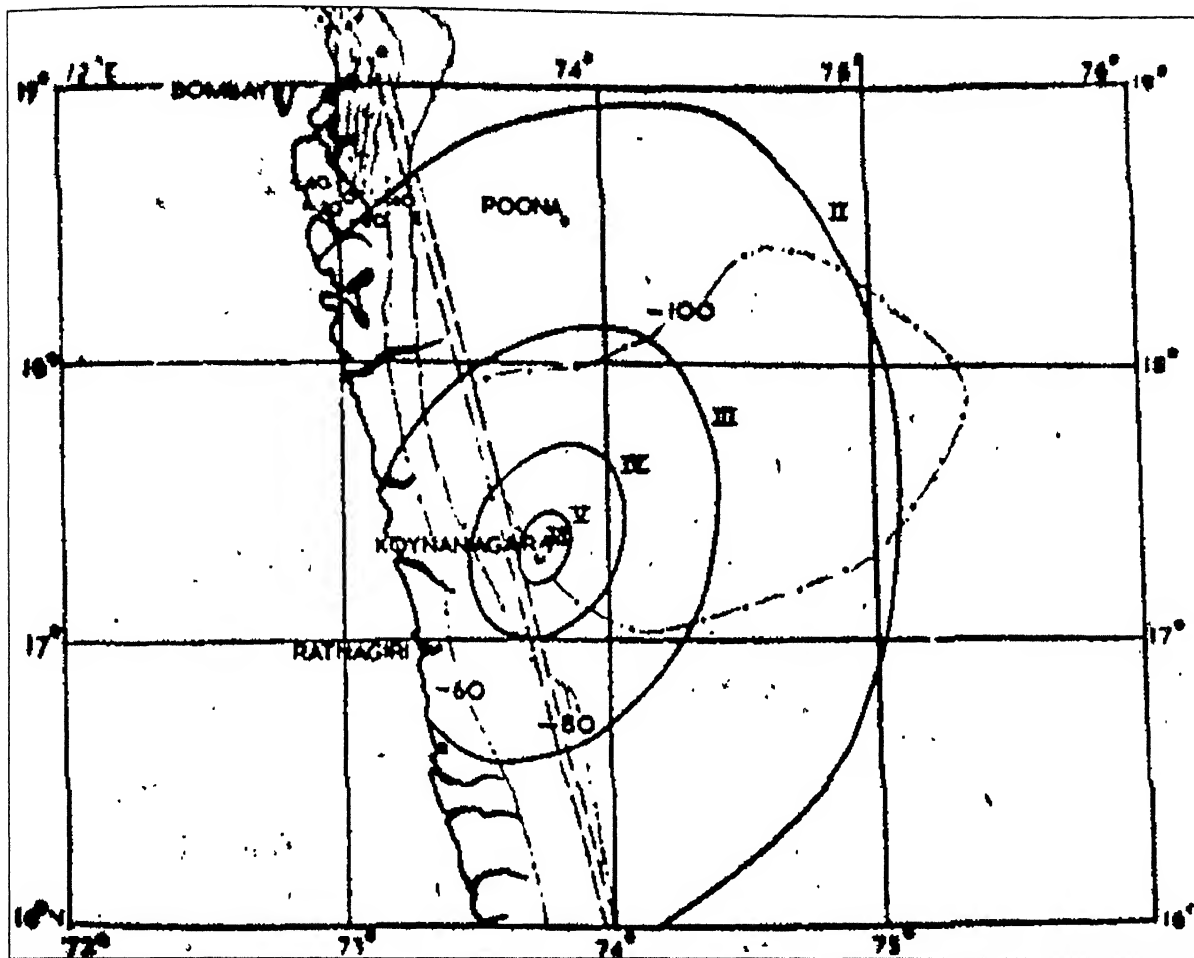


Figure 3.64 Isoseismal map of Koyna earthquake (M 5.2) of 17th October 1973 following MM scale after Gosavi *et al.* (1977).

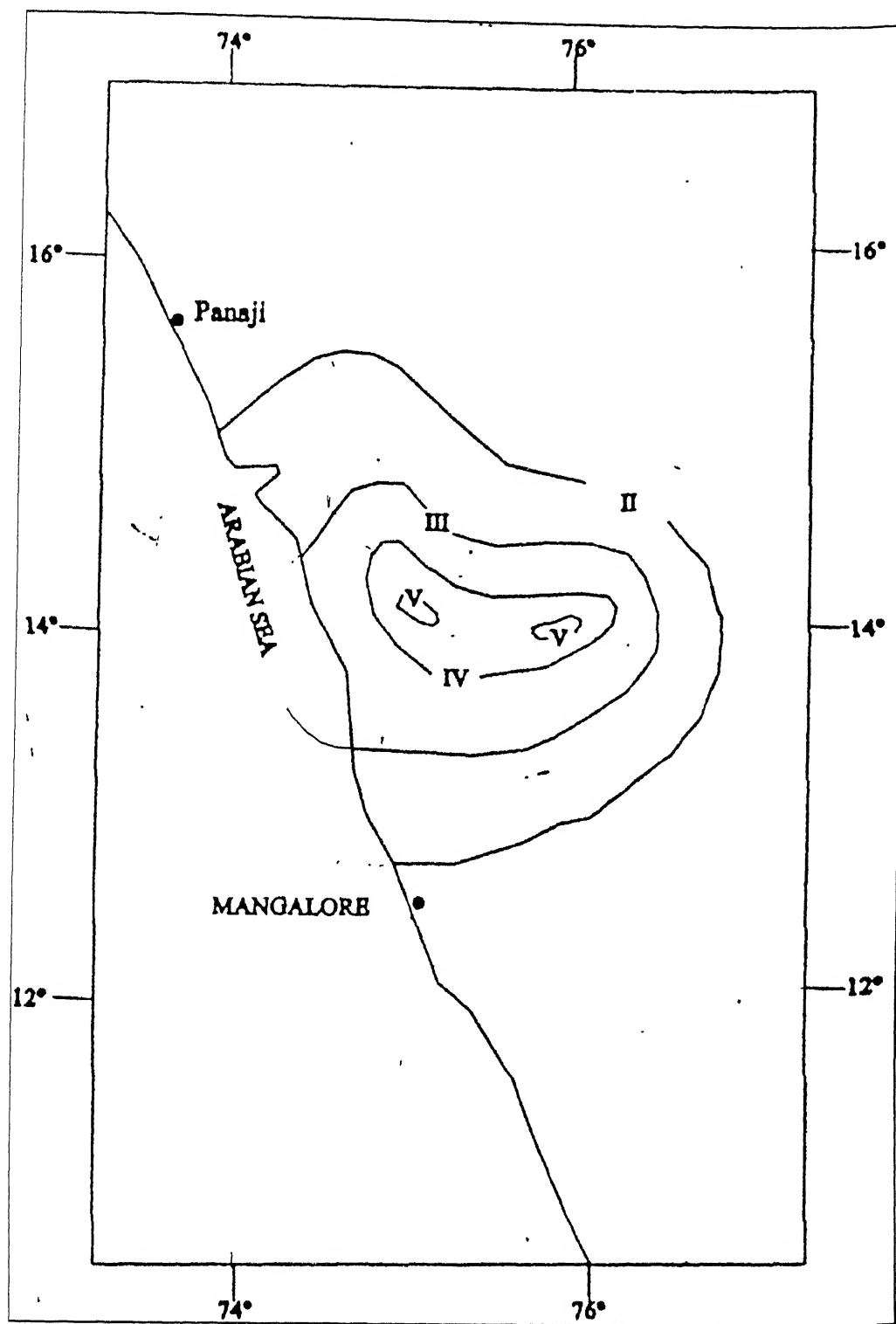


Figure 3.65 Isoseismal map of Shimoga earthquake (M 5) of 12th May 1975 following MM scale after Gosavi *et al.* (1977) taken from Kaila and Sarkar (1978).

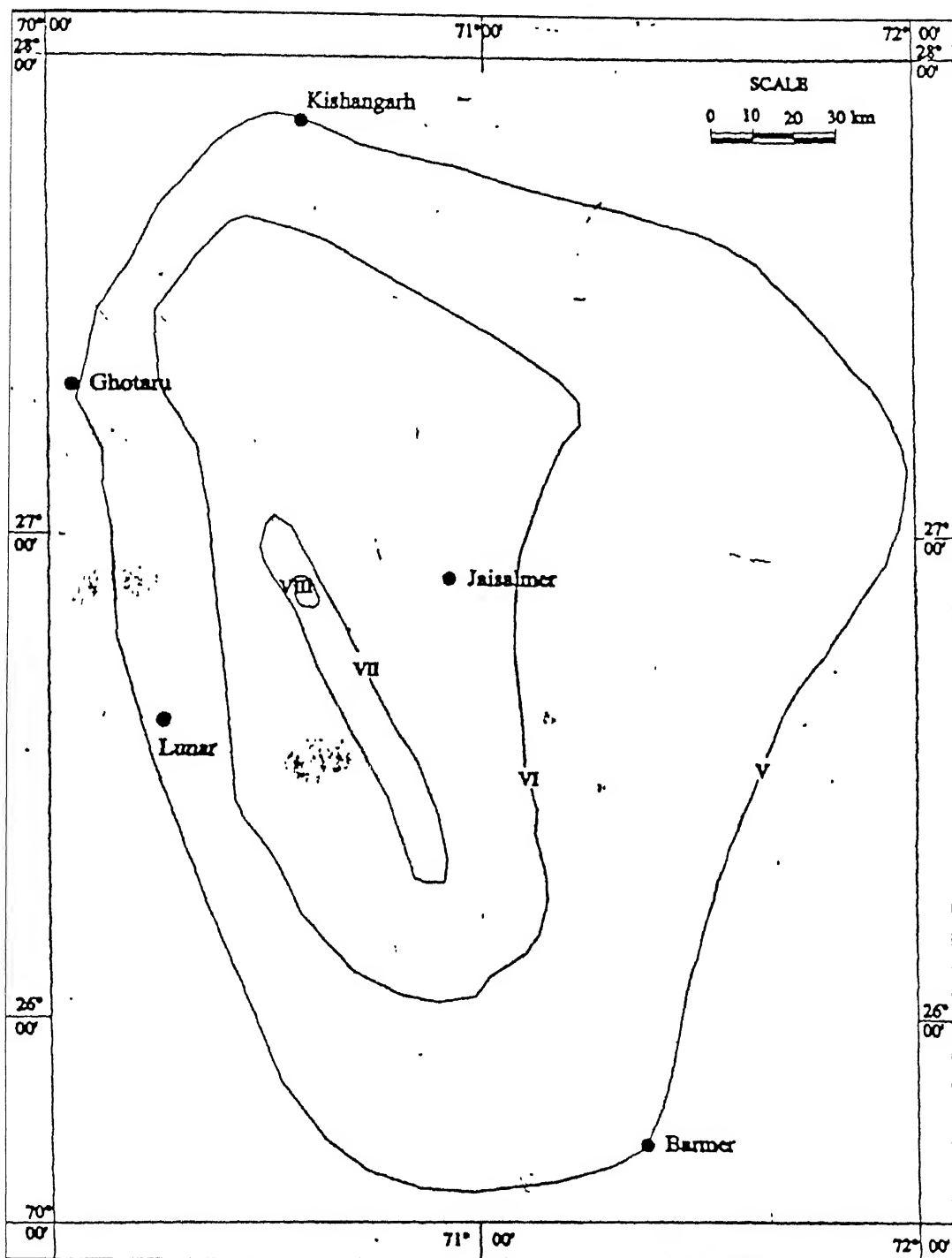


Figure 3.66 Isoseismal map of Jaisalmer earthquake (M 5.5) of 8th November 1991 following MM scale taken from Dasgupta *et al.* (2000).

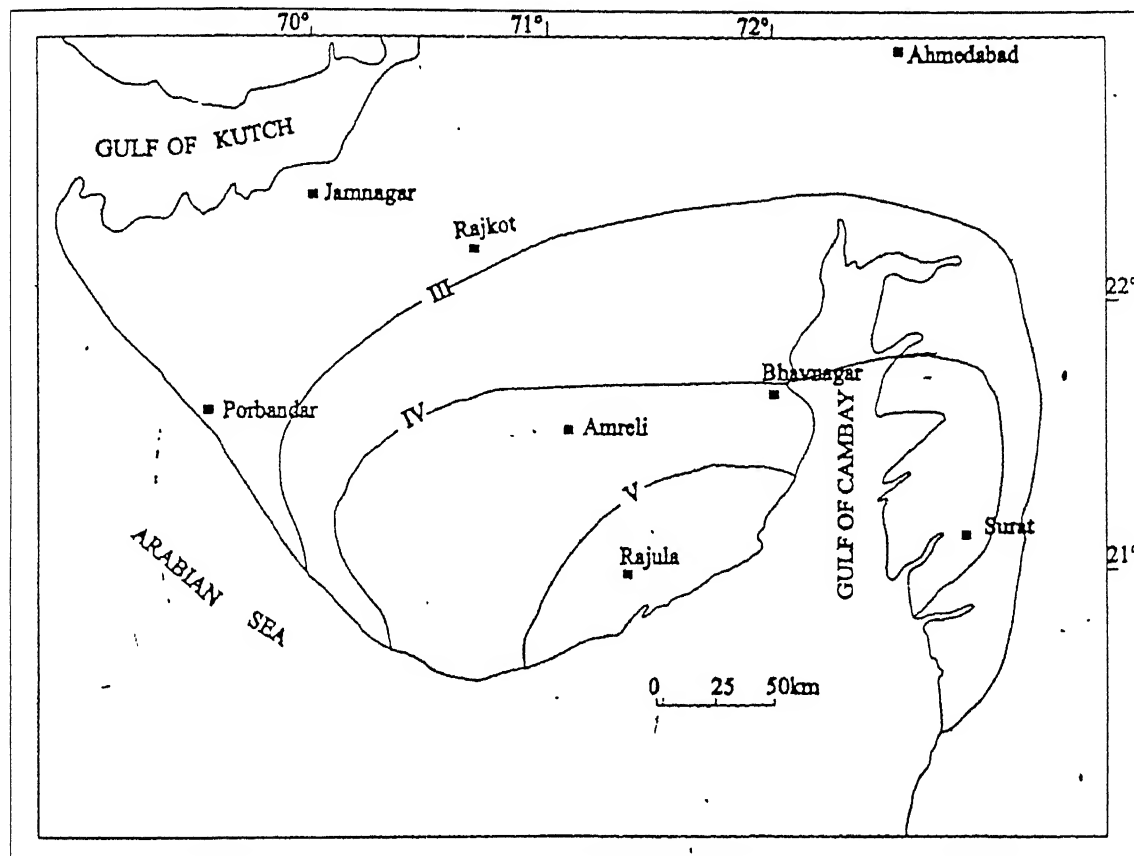


Figure 3.67 Isoseismal map of Saurashtra Coast earthquake of 24th August 1993 following MM scale taken from Dasgupta *et al.* (2000).

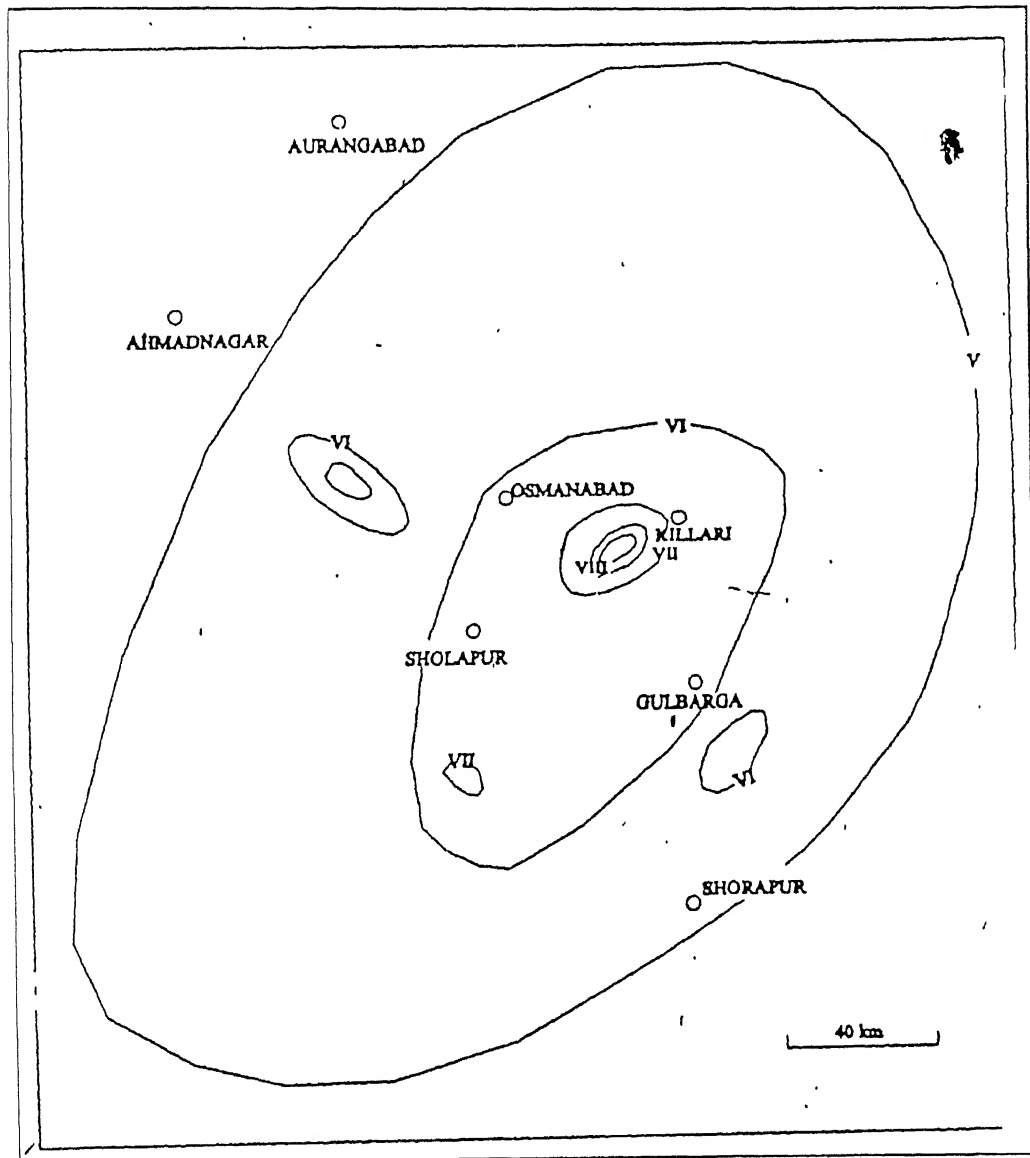


Figure 3.68 Isoseismal map of Killari (Latur) earthquake (M 6.2) of 30th September 1993 following MM scale taken from Dasgupta *et al.* (2000).

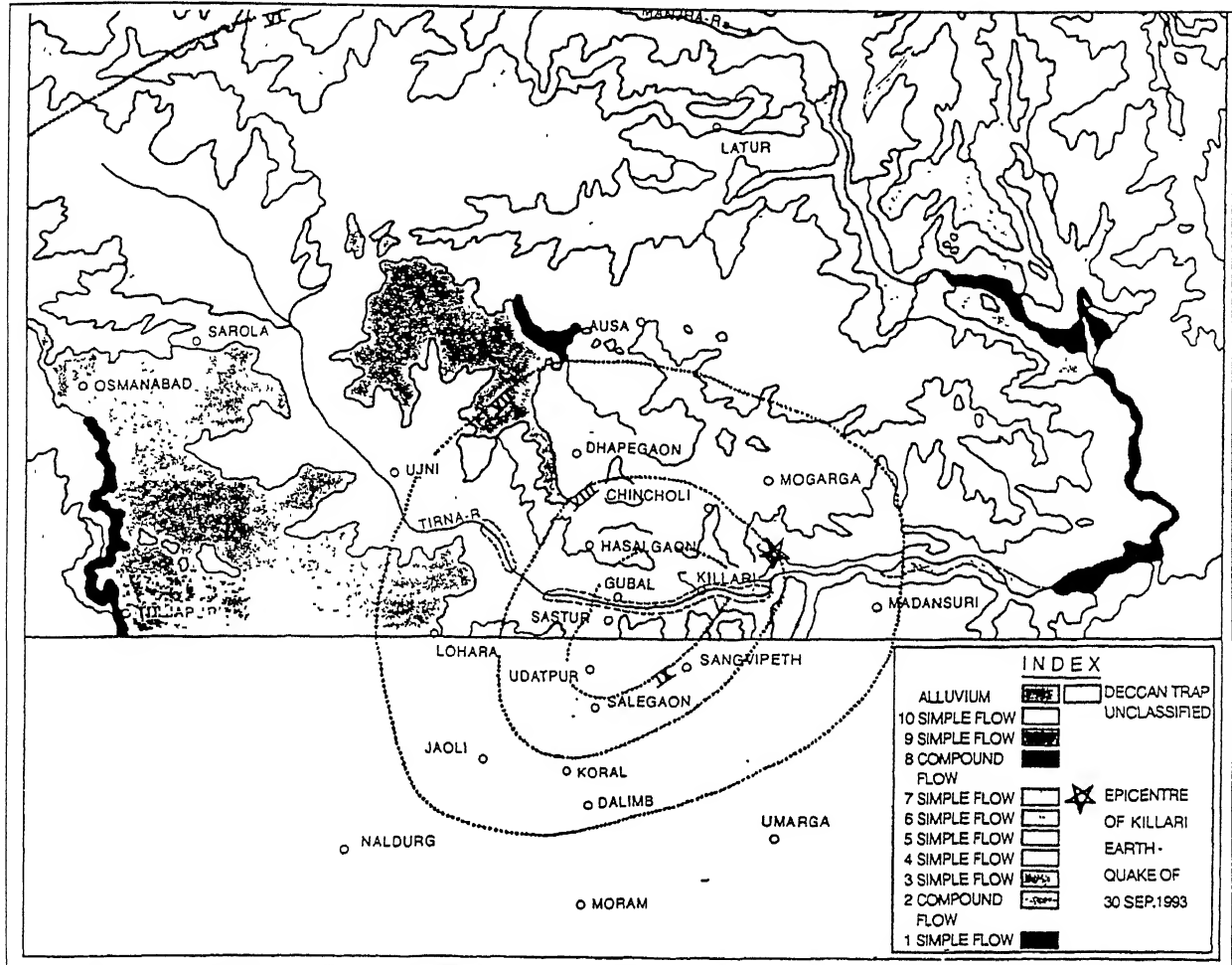


Figure 3.69 Isoseismal map of Killari (Latur) earthquake (M 6.2) of 30th September 1993 following MM scale after Narula *et al.* (1996a).

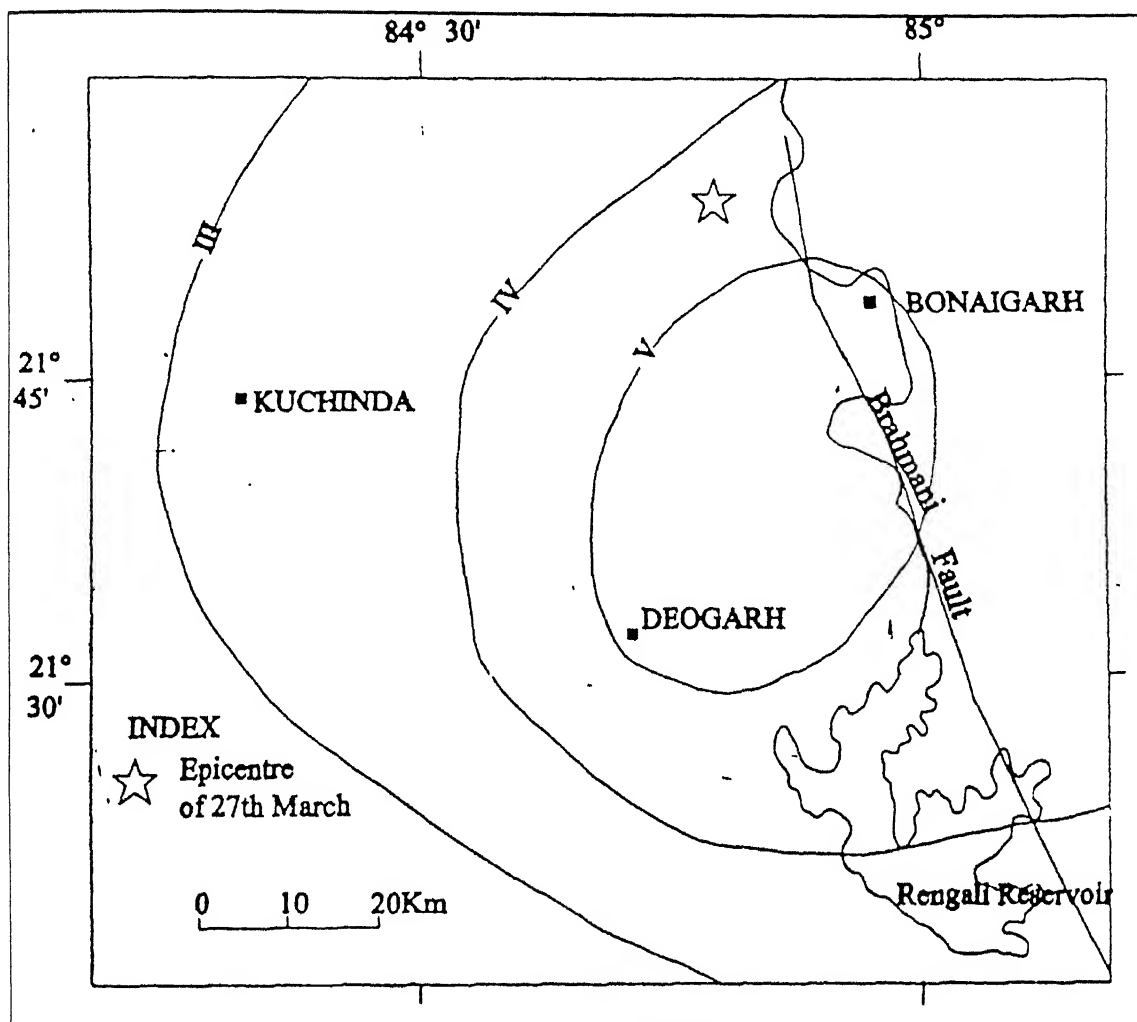


Figure 3.70 Isoseismal map of Bonaigarh earthquake (M 4.4) of 27th March 1995 following MSK scale taken from Dasgupta *et al.* (2000).

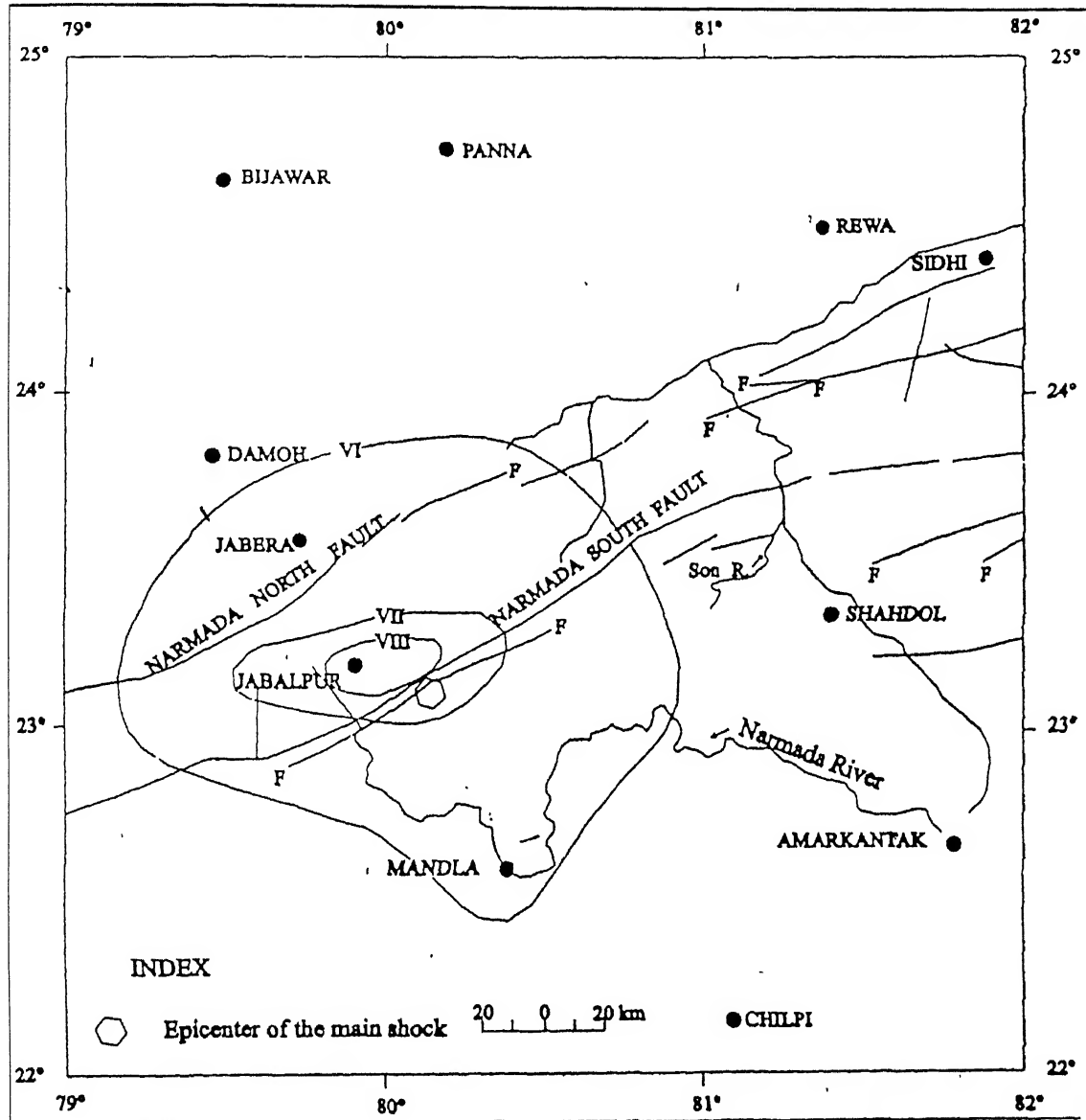


Figure 3.71 Isoseismal map of Jabalpur earthquake (M 6) of May 1997 following MSK scale taken from Dasgupta *et al.* (2000).

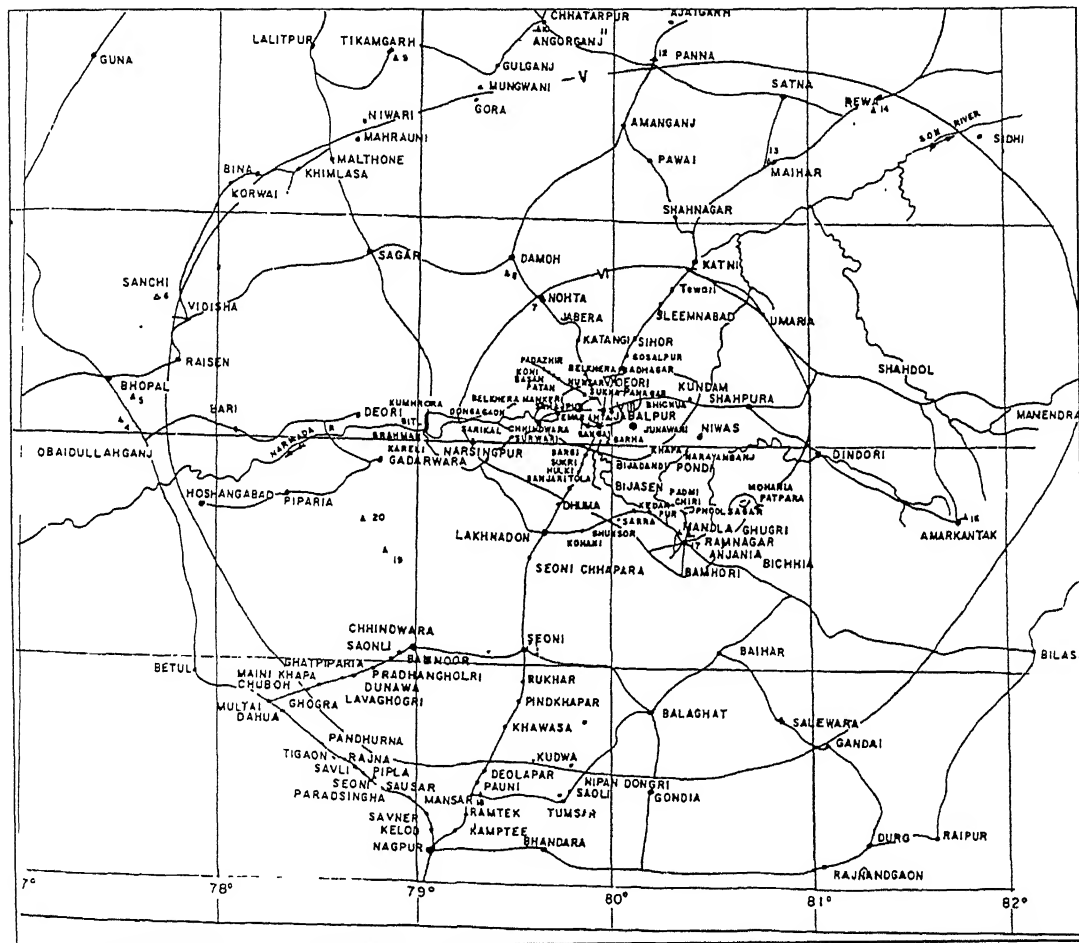


Figure 3.72 Isoseismal map of Jabalpur earthquake (M 6) of May 1997 following MSK scale after Chaturvedi *et al.* (2000).

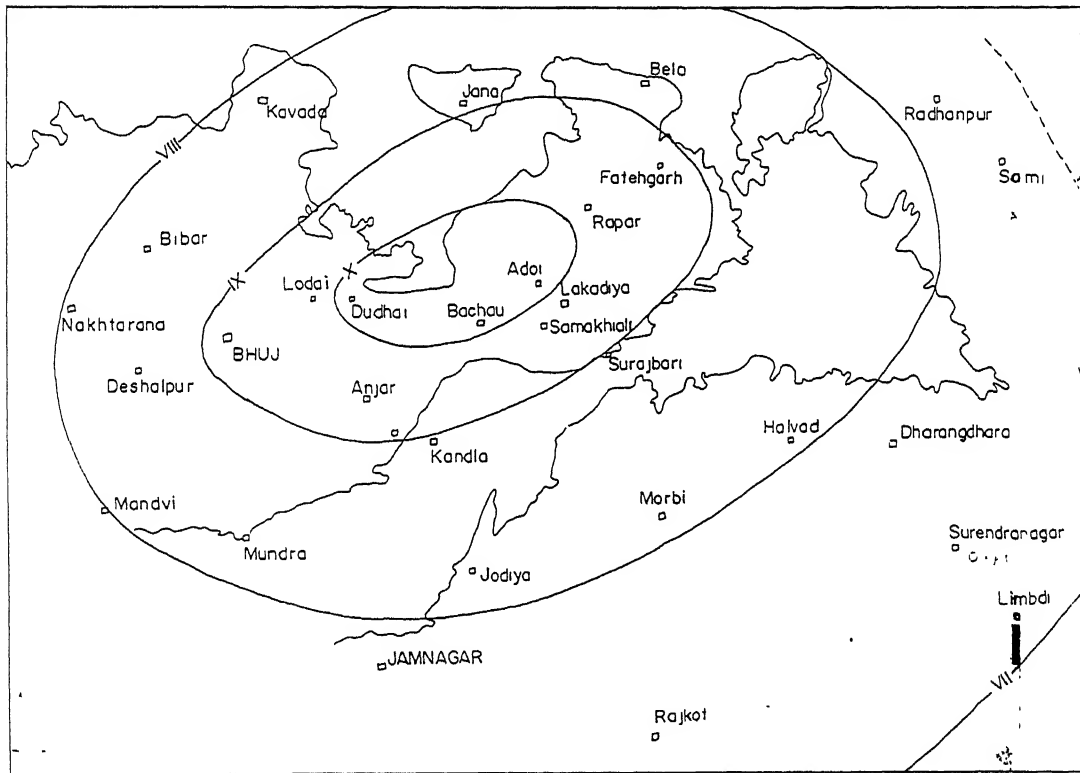


Figure 3.73 Isoseismal map of Bhuj earthquake (M 7.9) of 26th January 2001 following MSK scale after Narula and Chaubey (2001).



Figure 3.74 Isoseismal map of Bhuj earthquake (M 7.9) of 26th January 2001 following MSK scale after GSI (2001).

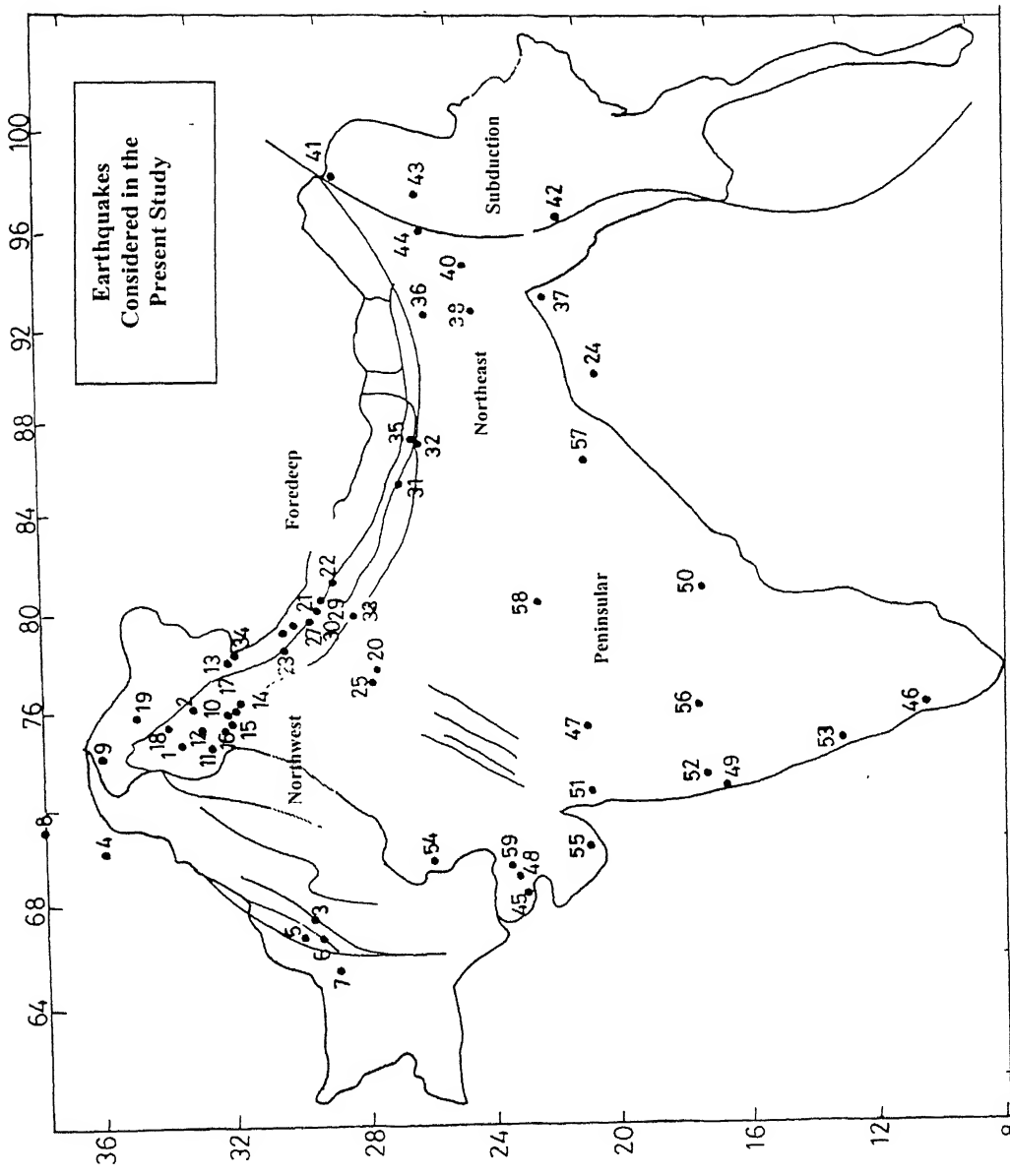


Figure 3.75 Plot of earthquakes considered in the present study

Chapter 4

Development of Attenuation Relationships

4.1 Introduction

This chapter studies the attenuation of intensity with distance from the intensity-distance data obtained from past 59 earthquakes from all over India. Depending on the regression analysis results and general geology of the region, Indian subcontinent is divided into six attenuation provinces namely Northeast, North, Northwest, Peninsular, Foredeep and Subduction province. New attenuation relationships are developed for each province and they are compared with the existing attenuation relationships available in the literature. In addition, intensity attenuation relations are developed for whole Indian subcontinent.

4.2 Modeled Shape of Isoseismal

In the literature most of the equations are developed assuming that the isoseismals represent a family of concentric circles. Radius of a particular isoseismal is taken as epicentral distance for corresponding intensity isoseist. But the shape of isoseists is elongated along the length of the fault, which gives rise to considerable difference between the attenuation along the major and minor axis of the isoseismals (Chandra *et al.*, 1979). Considering this point, two types of models are used in the present work. One representing a family of concentric circles and the other representing a family of concentric ellipses. In the first case, attenuation relations are developed for the radius of the each intensity circles while in the second case intensity attenuation relationships are developed along the major and minor axis.

4.3 Attenuation Relationships of Epicentral Intensity

The form of equation depends whether intensity is proportional to the logarithm of seismic energy density, E , at any location or is proportional to a power of the energy

density. Both approaches are used in the present study. The type of attenuation relation depends on how the intensity is related to the seismic energy density. If it is assumed that the intensity is proportional to the logarithm of seismic energy density (E) at any location, the attenuation relationships can be written as,

$$I = k_1 + k_2 \ln E. \quad (4.1)$$

where k_1 and k_2 are the proportionality constants.

Using the classical equation of energy decay

$$E = \left(\frac{E_0}{4\pi} \right) \Delta^{-d} e^{-c\Delta} \quad (4.2)$$

where E_0 is the total energy released, “ d ” is a constant representing the geometric spreading, and “ c ” is a constant representing rate of absorption, and Δ is the hypocentral distance. From Equations 4.1 and 4.2,

$$I = k_4 + k_5 \ln \left(\frac{E_0}{4\pi} \right) - k_5 d (\ln \Delta) - k_5 c \Delta \quad (4.3)$$

where k_4 , k_5 are the proportionality constants and Δ is the focal depth.

Using the abbreviations

$$a_1 = k_5 c (\ln \Delta) + k_5 d \Delta$$

$$d_1 = k_5 d$$

$$c_1 = k_5 c$$

and eliminating E_0 using Equation (4.2), we get

$$I = I_o + a_1 - c_1 \Delta - d_1 \ln \Delta \quad (4.4)$$

If the effect of exponential absorption is small compared to that of geometric spreading, this becomes equivalent to equations used by Gutenberg and Richter (1942) of the form

$$I = I_o + a_1 - d_1 \ln \Delta. \quad (4.5)$$

If geometric spreading is neglected as compared to absorption, the equation reduces to

$$I = I_o + \alpha_1 - c_1 \Delta \quad (4.6)$$

One of the simplest possible alternatives to Equation 4.4 is that intensity proportional to a power of the energy density

$$I = kE^p \quad (4.7)$$

which combined with Equation 4.2 gives

$$I = k \left(\frac{E_o}{4\pi} \right)^p \Delta^{-dp} e^{-cp} \quad (4.8)$$

At the epicenter

$$I_o = k \left(\frac{E_o}{4\pi} \right)^p H^{-dp} e^{-cpH} \quad (4.9)$$

Dividing Equation 4.8 by Equation 4.9

$$I = I_o H^{dp} e^{cpH} \Delta^{-dp} e^{-cp} \quad (4.10)$$

Taking the logarithm of both sides of this and using the abbreviations

$$\alpha_2 = d_p \ln H + c_p H$$

$$d_2 = d_p$$

$$c_2 = c_p$$

we get

$$\ln I = \ln I_o + \alpha_2 - c_2 \Delta - d_2 \ln \Delta \quad (4.11)$$

If d_2 is very small, it becomes

$$\ln I = \ln I_o + \alpha_2 - c_2 \Delta \quad (4.12)$$

If α_2 is also very small

$$\ln I = \ln I_o - d_2 \Delta \quad (4.13)$$

If α_2 and c_2 are both very small

$$\ln I = \ln I_o - d_2 \ln \Delta \quad (4.14)$$

The difference between Equations 4.4 and 4.11 lies in the curvature of the variation of intensity with distance. Taking derivative of Equation 4.4

$$\frac{dI}{d\Delta} = -\frac{d_1}{\Delta} - c_1 \quad (4.15)$$

Taking the derivative of Equation 4.11

$$\frac{dI}{d\Delta} = -I \left(\frac{d_2}{\Delta} + c_2 \right) \quad (4.16)$$

Since intensity ' I ' is itself a decreasing function of Δ , the product of I and $\left(\frac{d_2}{\Delta} + c_2 \right)$ shows that Equation 4.11 is steeper near the epicenter and flatter at larger distances than Equation 4.4.

All of the equations describe families of parallel curves whose height above the abscissa depends only on I_o . Inspection of isoseismal maps suggests that attenuation of intensity with distance is often faster for small earthquakes, so that the family of lines should diverge. To consider earthquake size effect on attenuation, two equations are proposed.

$$\begin{aligned} \ln I &= \ln I_m - c_2 (\Delta - \Delta_m) - d_2 \ln \frac{\Delta}{\Delta_m} \\ I &= I_m e^{-c_2 (\Delta - \Delta_m)} e^{-d_2 \ln \frac{\Delta}{\Delta_m}} \end{aligned} \quad (4.17)$$

The intensity attenuation equations are based on the assumption that the energy is radiated from the point source through a space of simple geometry (e.g., a uniform hemisphere only a function of depth). The equations do not give good results when distances are not large when compared to the source dimensions. An alternative approach would be to postulate that the intensity-distance relation is the sum of two attenuation rates, one more important at short distances, the other at large distances. A near-source, rapidly decreasing term should be added to the trend observed at large distances. This will

take the form of the attenuation at large distance being related to energy (magnitude) of the earthquake, and that the near-source being more closely linked to maximum intensity, that includes allowance for many factors besides energy. A simple relation of this sort is

$$I = a_3 M - b_3 \ln \Delta - c_3 \Delta + d_3 \frac{I_o}{\Delta} \quad (4.18)$$

where M is the magnitude. In this equation $a_3 M$ has been substituted for I_o and $d_3 I_o / \Delta$ replaces the constant a_1 . The d_3 term provides for a departure from the general form of Equation 4.3 at short distances.

Another family of equations similar to Equations 4.4 to 4.10 can be obtained by substituting $(1.5M-1.5)$ for I_o based on the Gutenberg and Richter's (1956) empirical relation between magnitude and MM intensity

$$M = I + \frac{2}{3} I_o \quad (4.19)$$

The equation will look like

$$I = a + b M + c \Delta + d \log_{10}(\Delta)$$

It can be assumed that magnitude is directly related to the maximum intensity (Lee and Trifunac, 1985), hence new attenuation relationships can be derived involving the maximum intensity as the earthquake parameter

$$I = a + b I_{max} + c \Delta + d \log_{10}(\Delta) \quad (4.20)$$

In all of the above equations, the coefficient "d" defines the rate of geometric spreading of the energy, the coefficient "c" defines the rate of exponential absorption and "a" and "b" terms are related to the boundary conditions at the source. Instead of the hypocentral distance, epicentral distance can also be used due to the lack of focal depth data. In the present study, both distances are used and for events whose focal depth are not available, same are suitably assumed to be equal to the average focal depth of the

region concerned. The equations involving the logarithm of intensity are not reported in the present study because they are found to be not good for Indian subcontinent [Chandra, 1982].

4.4 Attenuation Provinces

Following the general geology of the region and the standard deviations obtained from the preliminary analysis (Section 4.5.8) the Indian subcontinent is divided into six attenuation provinces viz. Northeast, Northern, Northwest Peninsular, Foredeep and Subduction provinces which conforms to the attenuation provinces of Kaila and Sarkar (1978) and Chandra (1992). Attenuation relationships have been separately analyzed and by combining all the provinces, a single equation for the whole Indian subcontinent is also derived.

4.5 Development of Attenuation Relationships

4.5.1 Selection of Parameters

The parameter, which is being predicted, is known as dependent variable and the parameters used for the predictions are called independent variables. In the present study, intensity on MM scale is taken as the dependent variable.

4.5.2 Earthquake Parameters

Seismic magnitude is one of the ideal parameters, which can be used to represent the earthquake size. But for past earthquakes, the magnitudes estimated are very approximate and are liable to be incorrect because of lack of instrumental data. Keeping this in mind, equations are developed considering other parameters like the epicentral intensity, maximum intensity and a combination of those. Maximum intensity is not frequently used as attenuation parameter (Lee and Trifunac, 1985) but it is good for practical purposes since it directly gives the damage. In literature most of the equations are based on the epicentral intensity, but is a fictitious quantity depending upon the method employed to estimate it and will differ from method to method. Hence for a

particular earthquake, what would be the exact epicentral intensity is a question and only the drop of intensity with distance can be estimated using the derived equation with epicentral intensity as the earthquake parameter. Due to the above reason the equation involving the epicentral intensity is not good in predicting the intensity for a future earthquake, in spite of smaller standard error. This equation gives the drop of intensity with distance and the drop is only due to distance parameter, while the other models have dual dependency. Hence it gives true values of the absorption and geometric spreading constants, independent of the earthquake size. In the present study, different earthquake parameters like magnitude, maximum intensity and the epicentral intensity have been used. In addition to that, equations are developed to estimate the epicentral intensity for a given magnitude.

4.5.3 Independent Variables

In the present study, equations are developed by considering different variables like magnitude of earthquake, M , maximum mapped intensity, I_{ma} , or epicentral intensity I_o . Some equations are developed by taking more than one independent variable like magnitude and maximum intensity simultaneously.

4.5.4 Source Mechanism

In the present study, isoseismals from 59 earthquakes are used as data set. Since fault mechanism of all the events are not well defined, hence the style of faulting is not included as a variable in the present study.

4.5.5 Propagation Parameters

The propagation parameters characterize the effects due to wave scattering, inelastic attenuation and geometric attenuation of intensity. Since the type and length of faulting, amount of slip etc. are not available, the distance measurements such as distance to horizontal projection of fault rupture, closest distance to rupture, distance to zone of maximum energy released etc. could not be used as the propagation parameter. In this

study epicentral distance as well as the hypocentral distance are used as the propagation parameters.

4.5.6 Site Parameters

Other than the broad classification of the site conditions [Lee and Trifunac, 1985], no detailed information is available about the local site geology. The intensity isoseists are very rough and due to the lack of information and approximation the site parameters are not included in the present study.

4.5.7 Type of Equation Used

There are many types of attenuation relationships existing in the literature involving epicentral intensity and magnitude (Howell and Schultz, 1975). Different types of equations involving magnitude and epicentral intensity have been used in the present study. Some new types of intensity attenuation relationships involving the maximum intensity and combinations of maximum intensity and magnitude have been tried, which have resulted in good correlation. The types of equation used are

Equation 1

$$I = a + b_1 M + c R$$

Equation 2

$$I = a + b_2 M + d \log_{10}(R)$$

Equation 3

$$I = a + b_3 M + c R + d \log_{10}(R)$$

Equation 4

$$I = a + b_4 I_{max} + c R$$

Equation 5

$$I = a + b_5 I_{max} + d \log_{10}(R)$$

Equation 6

$$I = a + b_1 I_{max} + c R + d \log_{10}(R)$$

Equation 7

$$I = a + b_1 I_{max} + b_2 M + c R + d \log_{10}(R)$$

Equation 8

$$I - I_o = a + c R$$

Equation 9

$$I - I_o = a + d \log(R)$$

Equation 10

$$I - I_o = a + c R + d \log(R).$$

In the above equation the constant “c” defines the rate of absorption and the constant “d” defines the loss due to geometric spreading.

4.5.8 Preliminary Analysis of the Data

Before the data is regressed to get a particular attenuation model, it is necessary to do some preliminary analysis to eliminate inconsistent data as well as the form of variables that gives a better fit for the data. The regression analysis is carried with the above models and standard deviation all each data points are calculated. The data points with relatively larger standard deviation are removed from the data set and not considered for the final regression analysis.

4.6 Development of Intensity Attenuation Relationships

Tables 4.1 to 4.20 give the coefficients of regression related to each region along with their confidence band, *t*-statistic values, σ and percentage variation explained values (R^2) of the model. Separate regression analysis has been done for the whole India, to have a single equation to describe the attenuation of whole Indian subcontinent. Earthquakes are grouped in two categories one with magnitude equal to or more than 6 and the other

with magnitude less than 6. The two categories have been separately analyzed keeping in mind that the smaller earthquake attenuates at much faster rate than that of larger earthquake hence, they have to be separated out.

4.7 Adequacy of the model

The adequacy of the model can be checked either by analyzing the residuals or by testing the significance of each coefficient derived during the analysis.

4.7.1 Analysis of Residue

The overall adequacy of the model is best assessed from an analysis of residuals. By the very nature of regression analysis, the residuals have a mean close to zero. If no apparent trend in the residuals is observed, then the model can be considered adequate. A trend indicates an inadequacy in the model in the model to predict the data and would require modification of the functional form. The residuals are plotted with respect to epicentral distance (R) as shown in Figures 4.7 to 4.10. No particular trend is shown in any plots, from which it can be ascertained that the models used in the regression analysis are adequate to represent the variation in data.

4.7.2 Significance Testing of Coefficients

The significance of the calculated coefficients can be estimated by means of a t -test. The t -statistic is defined as

$$t = \frac{\hat{b}_I - b_I}{SE(\hat{b}_I)}$$

Under the normality assumption, the variable \hat{b}_I follows t distribution with $N-P$ degree of freedom, where P is the number of coefficients in the equation. If the true value of b_I is specified in the null hypothesis, the t -statistic can be computed from the available sample and used as a test statistic.

All the coefficients are tested with a level of significance of 5% for the particular value being equal to zero. If the null hypothesis of these coefficients being equal to zero

can not be rejected when tested with a level of significance of 5%, then the values for these events should be used with caution.

4.8 Squared Multiple R

The squared multiple R represents the proportion of variation in the dependent variable, accounted for by the combination of independent variable. It is also called as the multiple correlation coefficient and defined as

$$\begin{aligned} R^2 &= \frac{\text{(Sum of Squares due to regression)}}{\text{(Total sum of squares, corrected for the mean } \bar{Y})} \\ &= \frac{\sum (\hat{Y}_i - \bar{Y})^2}{\sum (Y_i - \bar{Y})^2} \end{aligned}$$

where i is the number of data points, \hat{Y}_i is the predicted dependent variable, \bar{Y} is the mean and Y is actual value observed. The value of R^2 lies in between 0 to 1. A perfect fit of the data between \hat{Y}_i and Y would give $R^2 = 1$, while values closer to one suggest a good fit of the data for a given model. For the present study the R^2 values are calculated for each case and used to determine whether the particular model is good or not.



Table 4.1 Values of constants, confidence band, t-statistic values, standard deviation, standard error of the equation and R^2 values of the model (equation 3 with hypocentral distance).

Constant													d	S.D	Conf. Band	t-static	SD	sq. R					
A	1.222	0.371	0.610	1.834	3.294	1.360	0.055	1.269	1.451	24.727	-0.0039	0.0004	-0.0046	-0.0031	-8.9535	-1.702	0.189	-2.014	-1.390	-9.005	0.722	0.849	
L	IND	1.161	0.415	1.846	2.798	1.383	0.060	1.284	1.482	23.050	-0.0033	0.0004	-0.0039	-0.0026	-8.2000	-1.670	0.202	-2.003	-1.337	-8.267	0.782	0.823	
T		1.512	0.368	0.905	2.119	4.109	1.331	0.056	1.239	1.423	23.768	-0.0040	0.0005	-0.0048	-0.0032	-8.0200	-1.894	0.193	-2.212	-1.576	-9.813	0.744	0.839
A	2.418	0.972	0.745	4.091	2.488	1.174	0.171	0.880	1.468	6.865	-	-	-	-	-	-2.002	0.278	-2.480	-1.524	-7.201	0.772	0.658	
L	IND<6	2.031	0.973	0.356	3.706	2.087	1.249	0.174	0.950	1.548	7.178	-	-	-	-	-1.898	0.275	-2.371	-1.425	-6.902	0.788	0.644	
T		2.674	1.015	0.927	4.421	2.634	1.107	0.175	0.806	1.408	6.326	-	-	-	-	-2.044	0.296	-2.53	-1.535	-6.905	0.789	0.643	
A	1.203	0.625	0.130	2.276	1.925	1.382	0.077	1.250	1.514	17.948	-0.0038	0.0005	-0.0047	-0.0030	7.8367	-1.760	0.245	-2.181	-1.339	7.184	0.693	0.886	
L	IND>6	0.994	0.729	-0.258	2.246	1.364	1.424	0.088	1.273	1.575	16.182	-0.0033	0.0005	-0.0041	-0.0024	6.8125	-1.725	0.273	-2.194	-1.256	6.319	0.780	0.855
T		1.814	0.623	0.744	2.884	2.912	1.344	0.079	1.208	1.480	17.013	-0.0037	0.0006	-0.0047	-0.0028	6.7636	-2.103	0.246	-2.525	-1.681	8.549	0.717	0.878

Table 4.2 Values of constants, confidence band, t-statistic values, standard deviation, standard error of the equation and R^2 values of the model (equation 3 with epicentral distance).

Constant													d	S.D	Conf. Band	t-static	SD	sq. R					
A	0.877	0.397	1.656	0.099	2.209	1.334	0.062	1.455	1.213	21.631	-0.0040	0.0005	-0.0030	-0.0049	8.4468	-1.576	0.176	-1.281	-1.922	8.944	0.967	0.782	
L	IND	0.907	0.435	1.760	0.054	2.083	1.336	0.065	1.463	1.208	20.533	-0.0036	0.0004	-0.0027	-0.0044	8.1136	-1.482	0.184	-1.122	-1.842	8.071	1.017	0.758
T		0.813	0.381	1.560	0.067	2.135	1.304	0.061	1.424	1.185	21.377	-0.0044	0.0005	-0.0034	-0.0055	8.3585	-1.581	0.162	-1.263	-1.898	9.764	0.966	0.782
A	0.387	0.477	1.361	-0.587	0.812	1.393	0.071	1.537	1.249	19.732	-0.0041	0.0006	-0.0030	-0.0052	7.3214	-1.487	0.220	-1.938	-1.936	6.762	0.955	0.797	
L	IND<6	0.300	0.533	1.389	-0.789	0.562	1.415	0.076	1.570	1.260	18.587	-0.0036	0.0005	-0.0026	-0.0047	7.0000	-1.403	0.235	-0.923	-1.883	5.966	1.017	0.770
T		0.488	0.442	1.391	-0.415	1.104	1.354	0.068	1.493	1.214	19.816	-0.0044	0.0006	-0.0032	-0.0057	7.0476	-1.580	0.194	-1.183	-1.977	8.128	0.939	0.804
A	1.430	0.769	2.960	-0.100	1.859	1.262	0.108	1.476	1.048	11.729	-0.0040	0.0006	-0.0029	-0.0051	7.0000	-1.555	0.253	-1.053	-2.058	6.157	1.008	0.785	
L	IND>6	1.411	0.850	3.102	-0.281	1.660	1.272	0.116	1.503	1.041	10.969	-0.0034	0.0005	-0.0024	-0.0045	6.4340	-1.490	0.266	-0.961	-2.019	5.608	1.085	0.751
T		1.471	0.760	2.983	-0.040	1.937	1.220	0.109	1.437	1.003	11.202	-0.0045	0.0006	-0.0032	-0.0058	7.0156	-1.569	0.232	-1.108	-2.029	6.774	1.027	0.777

Table 4.3 Values of constants, confidence band, t-statistic values, standard deviation, standard error of the equation and R² values of the model (equation 6 with hypocentral distance).

EQ	Constant												SD	sq. R								
	A	S.D.	Conf. Band	t-static	b1	S.D.	Conf. Band	t-static	c	S.D.	Conf. Band	t-static	d	S.D.	Conf. Band	t-static						
IND	1.325	0.397	0.670	1.980	3.338	0.847	0.037	0.786	0.908	22.892	-0.0042	0.0005	-0.0050	-0.0035	9.1739	-0.681	0.19	-1.0011	-0.3609	3.5103	0.772	0.827
	1.139	0.434	0.423	1.855	2.624	0.866	0.039	0.802	0.930	22.205	-0.0037	0.0004	-0.0044	-0.0030	8.7381	-0.62	0.20	-0.9550	-0.2851	3.0542	0.812	0.809
	1.639	0.382	1.009	2.269	4.291	0.838	0.037	0.777	0.899	22.649	-0.0044	0.0005	-0.0053	-0.0036	8.4808	-0.909	0.19	-1.2258	-0.5922	4.7344	0.776	0.825
IND<6	3.140	0.750	1.849	4.431	4.187	0.682	0.069	0.563	0.801	9.884	-0.0032	0.0045	-0.0109	0.0046	0.7029	-1.41	0.455	-2.1931	-0.6269	3.0989	0.63	0.777
	3.004	0.747	1.718	4.290	4.021	0.715	0.068	0.598	0.832	10.515	-0.0020	0.0039	-0.0087	0.0047	0.5064	-1.418	0.451	-2.1942	-0.6418	3.1441	0.632	0.776
	3.006	0.730	1.750	4.262	4.118	0.671	0.067	0.556	0.786	10.015	-0.0073	0.0058	-0.0173	0.0027	1.2565	-1.256	0.477	-2.0769	-0.4351	2.6331	0.618	0.785
IND>6	2.489	0.639	1.392	3.586	3.895	0.769	0.049	0.685	0.853	15.694	-0.0043	0.0005	-0.0052	-0.0033	7.8889	-0.84	0.268	-1.3002	-0.3798	3.1343	0.76	0.862
	1.997	0.739	0.728	3.266	2.702	0.800	0.054	0.707	0.893	14.815	-0.0038	0.0005	-0.0047	-0.0029	7.3846	-0.669	0.294	-1.1738	-0.1642	2.2755	0.831	0.836
	3.104	0.613	2.051	4.157	5.064	0.755	0.049	0.671	0.839	15.408	-0.0042	0.0006	-0.0052	-0.0031	7.0508	-1.229	0.26	-1.6754	-0.7826	4.7269	0.765	0.861

Table 4.4 Values of constants, confidence band, t-statistic values, standard deviation, standard error of the equation and R^2 values of the model (equation 6 with epicentral distance).

EQ	Constant												SD	sq. R									
	A	S.D	Conf. Band	t-static	b1	S.D	Conf. Band	t-static	c	S.D	Conf. Band	t-static	d	S.D	Conf. Band	t-static							
A	0.606	0.383	1.356	-0.144	1.584	0.976	0.039	1.053	0.899	24.780	-0.0043	0.0005	-0.0034	-0.0053	9.2128	-0.868	0.179	-0.517	-1.219	4.845	0.798	0.858	
	L	IND	0.338	0.423	1.166	-0.491	0.800	1.004	0.042	1.086	0.922	24.086	-0.0040	0.0004	-0.0031	-0.0048	9.1860	-0.750	0.189	-0.380	-1.120	3.974	0.832
T	0.798	0.351	1.486	0.111	2.275	0.954	0.039	1.030	0.879	24.768	-0.0047	0.0005	-0.0037	-0.0057	8.8491	-1.017	0.159	-0.706	-1.328	6.409	0.787	0.862	
	A	1.028	0.658	2.371	-0.315	1.563	0.986	0.083	1.156	0.816	11.837	-0.0053	0.0022	-0.0008	-0.0097	2.4306	-1.259	0.305	-0.637	-1.881	4.131	0.588	0.860
L	IND<6	0.780	0.708	2.226	-0.666	1.101	1.015	0.089	1.197	0.833	11.398	-0.0053	0.0020	-0.0013	-0.0094	2.6834	-1.092	0.320	-0.439	-1.745	3.416	0.626	0.841
	T	1.216	0.585	2.411	0.021	2.078	0.934	0.075	1.087	0.781	12.466	-0.0063	0.0025	-0.0011	-0.0115	2.4685	-1.313	0.270	-0.762	-1.863	4.867	0.526	0.888
A	1.009	0.554	2.112	-0.094	1.820	0.904	0.053	1.010	0.798	16.913	-0.0048	0.0005	-0.0038	-0.0058	9.6400	-0.630	0.220	-0.193	-1.068	2.865	0.768	0.873	
	L	IND>6	0.504	0.645	1.787	-0.780	0.781	0.947	0.059	1.063	0.830	16.144	-0.0043	0.0005	-0.0034	-0.0053	9.0000	-0.476	0.245	0.012	-0.963	1.942	0.833
T	1.369	0.528	2.419	0.318	2.593	0.878	0.055	0.986	0.769	16.097	-0.0052	0.0006	-0.0040	-0.0063	9.0351	-0.859	0.196	-0.469	-1.250	4.378	0.787	0.866	

Table 4.5 Values of constants, confidence band, t-statistic values, standard deviation, standard error of the equation and R^2 values of the model (equation 10 with hypocentral distance).

Constant																		
EQ	a	S.D	Conf. Band	t-static	c	S.D	Conf. Band	t-static	d	S.D	Conf. Band	t-static	SD	sq. R				
A	-0.498	0.596	-1.479	0.483	0.836	-0.0037	0.00087	-0.0051	-0.0022	4.207	-1.444	0.369	-2.052	-0.836	3.912	1.682	0.473	
L	IND	-0.343	0.627	-1.376	0.689	0.547	-0.0030	0.00076	-0.0042	-0.0017	3.908	-1.477	0.373	-2.092	-0.862	3.956	1.697	0.463
T	-0.541	0.585	-1.505	0.423	0.924	-0.0040	0.00104	-0.0057	-0.0022	3.798	-1.526	0.377	-2.146	-0.905	4.051	1.732	0.441	
A	-0.853	1.346	-3.099	1.393	0.634	-0.0014	0.00915	-0.0166	0.0139	0.151	-2.162	1.110	-4.013	-0.311	1.948	1.633	0.222	
L	IND<6	0.232	1.503	-2.274	2.738	0.154	0.0063	0.01009	-0.0105	0.0232	0.626	-3.004	1.234	-5.062	-0.946	2.434	1.628	0.226
T	0.452	1.423	-1.922	2.825	0.317	0.0176	0.01473	-0.0069	0.0422	1.196	-3.696	1.298	-5.861	-1.530	2.847	1.651	0.204	
A	2.832	0.547	1.927	3.736	5.174	-0.0030	0.00066	-0.0041	-0.0019	4.545	-2.805	0.318	-3.330	-2.279	8.820	1.126	0.798	
L	IND>6	3.020	0.586	2.053	3.987	5.157	-0.0025	0.00058	-0.0035	-0.0016	4.345	-2.787	0.328	-3.329	-2.245	8.494	1.147	0.791
T	2.897	0.553	1.984	3.811	5.240	-0.0030	0.00080	-0.0044	-0.0017	3.800	-3.003	0.331	-3.551	-2.456	9.065	1.196	0.772	

Table 4.6 Values of constants, confidence band, t-statistic values, standard deviation, standard error of the equation and R^2 values of the model (equation 10 with epicentral distance).

Constant																		
EQ	a	S.D	Conf. Band	t-static	c	S.D	Conf. Band	t-static	d	S.D	Conf. Band	t-static	SD	sq. R				
A	1.179	0.199	1.568	0.790	5.939	-0.0041	0.0004	-0.0034	-0.0049	11.1892	-1.972	0.135	-1.708	-2.236	14.616	0.767	0.892	
L	IND	1.248	0.226	1.691	0.805	5.519	-0.0038	0.0004	-0.0031	-0.0044	10.7429	-1.866	0.146	-1.580	-2.152	12.801	0.825	0.875
T	0.837	0.182	1.193	0.480	4.598	-0.0047	0.0005	-0.0038	-0.0056	10.3778	-1.950	0.132	-1.692	-2.209	14.788	0.819	0.877	
A	1.637	0.365	2.352	0.923	4.491	-0.0041	0.0005	-0.0031	-0.0051	7.8846	-2.197	0.226	-1.729	-2.664	9.720	0.924	0.880	
L	IND<6	1.605	0.401	2.390	0.820	4.007	-0.0037	0.0005	-0.0028	-0.0047	7.7708	-2.031	0.238	-1.538	-2.523	8.531	0.985	0.864
T	1.250	0.341	1.918	0.582	3.667	-0.0046	0.0006	-0.0033	-0.0058	7.2540	-2.191	0.223	-1.730	-2.651	9.844	1.015	0.856	
A	1.637	0.365	2.352	0.923	4.491	-0.0041	0.0005	-0.0031	-0.0051	7.8846	-2.197	0.226	-1.729	-2.664	9.720	0.924	0.880	
L	IND>6	1.605	0.401	2.390	0.820	4.007	-0.0037	0.0005	-0.0028	-0.0047	7.7708	-2.031	0.238	-1.538	-2.523	8.531	0.985	0.864
T	1.250	0.341	1.918	0.582	3.667	-0.0046	0.0006	-0.0033	-0.0058	7.2540	-2.191	0.223	-1.730	-2.651	9.844	1.015	0.856	

Table 4.7 Values of constants, confidence band, t-statistic values, standard deviation, standard error of the equation and R^2 values of the model (equation 7 with hypocentral distance).

Constants																													
Type	EQ	a	S.D.	Conf. Band	t	b1	S.D.	Conf. Band	t	b2	S.D.	Conf. Band	t	c	S.D.	Conf. Band	t	d	S.D.	Conf. Band	t	SD	sq. R						
A	0.71	0.32	0.18	2.21	0.42	0.05	0.34	0.51	8.12	0.81	0.08	0.68	0.95	10.02	-0.0041	0.0004	-0.0047	-0.0035	11.3889	-1.32	0.17	-1.60	-1.05	7.97	0.61	0.89			
L	IND	0.55	0.36	-0.05	1.14	1.52	0.45	0.06	0.36	0.54	8.02	0.80	0.09	0.65	0.95	9.00	-0.0036	0.0003	-0.0041	-0.0030	10.5294	-1.25	0.18	-1.54	-0.95	6.96	0.66	0.87	
T		1.02	0.32	0.50	1.54	3.24	0.43	0.05	0.35	0.52	8.17	0.77	0.08	0.64	0.91	9.31	-0.0043	0.0004	-0.0050	-0.0036	10.1429	-1.53	0.17	-1.81	-1.25	9.10	0.63	0.89	
A	2.05	0.82	0.63	3.46	2.49	0.53	0.09	0.38	0.68	6.08	0.47	0.18	0.16	0.77	2.64	-0.0011	0.0044	-0.0086	0.0064	0.2460	-1.65	0.44	-2.41	-0.89	3.75	0.60	0.80		
L	IND<6	1.83	0.81	0.44	3.23	?26	0.55	0.09	0.40	0.70	6.42	0.50	0.18	0.20	0.81	2.86	-0.0002	0.0037	-0.0066	0.0062	0.0514	-1.67	0.43	-2.42	-0.93	3.87	0.59	0.81	
T		2.09	0.84	0.65	3.53	?30	0.55	0.09	0.40	0.70	6.37	0.37	0.18	0.06	0.67	2.07	-0.0053	0.0057	-0.0151	0.0046	0.9231	-1.42	0.47	-2.23	-0.61	3.03	0.60	0.80	
A	0.91	0.55	-0.04	1.85	1.65	0.37	0.07	0.26	0.48	5.66	0.87	0.11	0.68	1.07	7.71	-0.0041	0.0004	-0.0049	0.0034	9.6047	-1.38	0.23	-1.76	-0.99	6.12	0.61	0.91		
L	IND>6	0.51	0.66	-0.62	1.64	1.73	0.40	0.08	0.26	0.53	5.20	0.88	0.13	0.65	1.10	6.70	-0.0037	0.0004	-0.0044	0.0029	8.5581	-1.24	0.26	-1.69	-0.79	4.75	0.70	0.89	
T		1.57	0.55	0.63	2.51	2.86	0.38	0.07	0.26	0.49	5.61	0.82	0.12	0.63	1.02	7.16	-0.0040	0.0005	-0.0049	0.0032	8.1837	-1.74	0.23	-2.13	-1.35	7.69	0.63	0.91	

Table 4.8 Values of constants, confidence band, t-statistic values, standard deviation, standard error of the equation and R^2 values of the model (equation 7 with epicentral distance).

Constants																													
Type	EQ	a	S.D.	Conf. Band	t	b1	S.D.	Conf. Band	t	b2	S.D.	Conf. Band	t	c	S.D.	Conf. Band	t	d	S.D.	Conf. Band	t	SD	sq. R						
A	0.28	0.30	0.87	-0.32	0.91	0.62	0.05	0.72	0.52	12.08	0.57	0.08	0.72	0.41	7.21	-0.0042	0.0004	-0.0035	-0.0049	11.7222	-1.21	0.14	-0.94	-1.48	8.88	0.73	0.88		
L	IND	0.19	0.34	0.86	-0.48	0.56	0.63	0.06	0.74	0.52	11.35	0.56	0.09	0.72	0.39	6.55	-0.0039	0.0003	-0.0032	-0.0045	11.4118	-1.07	0.15	-0.79	-1.36	7.31	0.79	0.86	
T		0.28	0.28	0.83	-0.28	0.97	0.63	0.05	0.73	0.53	12.66	0.53	0.08	0.68	0.38	6.95	-0.0047	0.0004	-0.0039	-0.0054	11.9744	-1.26	0.12	-1.02	-1.50	10.3	0.71	0.88	
A	-0.11	0.35	0.60	-0.82	0.30	0.65	0.06	0.77	0.53	10.94	0.59	0.09	0.78	0.41	6.68	-0.0044	0.0004	-0.0035	-0.0052	10.6585	-1.17	0.16	-0.84	-1.50	7.26	0.69	0.90		
L	IND<6	-0.34	0.39	0.46	-1.14	0.87	0.69	0.06	0.82	0.56	10.87	0.57	0.10	0.77	0.38	6.04	-0.0040	0.0004	-0.0032	-0.0048	10.5789	-1.04	0.17	-0.68	-1.39	5.95	0.74	0.88	
T		0.06	0.32	0.73	-0.60	0.20	0.64	0.06	0.76	0.51	10.76	0.58	0.09	0.76	0.40	6.56	-0.0047	0.0005	-0.0038	-0.0057	10.3043	-1.29	0.14	-1.00	-1.59	8.96	0.68	0.90	
A	0.71	0.63	1.96	-0.54	1.12	0.60	0.07	0.75	0.45	8.04	0.51	0.13	0.77	0.26	4.00	-0.0045	0.0005	-0.0036	-0.0055	9.8696	-1.06	0.21	-0.63	-1.48	4.96	0.82	0.86		
L	IND>6	0.42	0.72	1.85	-1.01	0.59	0.62	0.08	0.79	0.46	7.40	0.50	0.14	0.78	0.21	3.48	-0.0041	0.0005	-0.0032	-0.0050	9.1333	-0.87	0.24	-0.40	-1.34	3.67	0.90	0.83	
T		0.90	0.61	2.11	-0.32	1.47	0.62	0.07	0.76	0.47	8.31	0.46	0.13	0.71	0.21	3.64	-0.0049	0.0005	-0.0039	-0.0060	9.5000	-1.18	0.19	-0.80	-1.56	6.18	0.82	0.86	

Table 4.9 Values of constants, confidence band, t-statistic values, standard deviation, standard error of the equation and R^2 values of the model (equation 3 with hypocentral distance).

Type	Pro.	Constant													SE	sq. R										
		a	S.D	Conf. Band	t-statistic	b ₂	S.D	Conf. Band	t-statistic	c	S.D	Conf. Band	t-static	d	S.D	Conf. Band	t-static									
A	g	-0.4	1.197	-1.338	2.746	0.588	1.41	0.168	1.156	1.730	8.589	-0.0053	0.0057	-0.0150	0.0044	0.9367	-1.659	0.753	-2.944	-0.374	2.203	0.674	0.781			
L	N	11.3	1.188	-1.914	2.140	0.095	1.5	0.182	1.216	1.836	8.385	-0.0052	0.0045	-0.0128	0.0025	1.1419	-1.452	0.721	-2.682	-0.222	2.014	0.703	0.762			
T		1.217	-0.800	3.352	1.048	1.3	0.163	1.112	1.668	8.528	-0.0050	0.0083	-0.0192	0.0092	0.5962	-2.007	0.881	-3.510	-0.504	2.278	0.665	0.787				
A	NE	-2.555	0.862	-4.070	-1.060	2.976	1.5	0.143	1.650	2.150	13.287	-0.0049	0.0008	-0.0063	0.0034	6.0000	-1.617	0.328	-2.190	-1.044	4.11	0.441	0.954			
L	NE	1.67	1.008	-3.527	-0.007	1.753	1.8	0.161	1.547	2.109	11.354	-0.0035	0.0008	-0.0049	0.0021	4.4430	-1.775	0.384	-2.445	-1.105	4.11	0.516	0.937			
T		-2.21	0.853	-4.449	-1.471	3.470	1.5	0.145	1.704	2.210	13.497	-0.0048	0.0008	-0.0063	0.0034	5.8780	-1.747	0.311	-2.290	-1.204	4.11	0.436	0.955			
A	NW	0.730	1.426	3.633	1.1	0.121	0.979	1.385	9.769	-0.0034	0.0009	-0.0049	0.0019	3.8111	-1.938	0.430	-2.660	-1.216	4	0.776	0.827					
L	NW	0.723	1.292	3.467	1.1	0.118	0.995	1.391	10.110	-0.0035	0.0008	-0.0048	0.0022	4.5325	-1.766	0.402	-2.441	-1.091	4	0.761	0.833					
T		2.54	0.768	1.214	3.260	1.1	0.128	0.938	1.368	9.008	-0.0040	0.0011	-0.0053	0.0022	3.7103	-1.784	0.463	-2.562	-1.006	3	0.824	0.804				
A	P	1.174	-1.133	0.725	1.4	0.131	1.206	1.650	10.884	-0.0038	0.0014	-0.0062	0.0014	2.6479	-1.657	0.514	-2.526	-0.788	3	0.747	0.882					
L	P	1.643	1	-1.622	0.394	1.4	0.139	1.193	1.662	10.291	-0.0043	0.0014	-0.0066	0.0019	3.0863	-1.345	0.528	-2.438	-0.453	2	0.785	0.869				
T		1.119	-0.973	0.821	1.4	0.129	1.216	1.652	11.124	-0.0044	0.0017	-0.0072	0.0016	2.6467	-1.804	0.505	-2.658	-0.950	3	0.733	0.886					
A	F	0.733	10.782	0.800	1.0	0.146	-0.625	1.345	7.466	-0.0047	0.0008	-0.0143	0.0033	5.7317	-0.470	0.593	-1.505	0.565	0	0.645	0.903					
L	F	1.643	-14.299	0.636	0.9	0.190	-1.323	1.241	4.784	-0.0047	0.0010	-0.0165	0.0029	4.6337	0.218	0.828	-1.228	1.664	0	0.824	0.842					
T		1.91	-9.819	1.454	1.1	0.138	-0.470	1.392	8.341	-0.0043	0.0009	-0.0144	0.0028	5.0116	-1	0.554	-2.150	-0.216	2	0.634	0.906					
A	S	1.522	-11.086	1.291	1.7	0.194	1.383	2.063	8.881	-0.007	0.0025	-0.0106	0.0019	2.5263	-0	1.803	-3.270	3.052	0	1	0.698					
L	S	1.617	-16.059	2.239	2	0.227	1.792	2.588	9.648	-0.007	0.0020	-0.0093	0.0024	3.0051	0	1.719	-2.525	3.501	0	1	0.733					
T		2.74	-7.167	0.087	1.45	0.209	1.037	1.769	6.713	-0.001	0.0042	-0.0133	0.0013	1.4399	-1	1.645	2.392	-5.813	2.573	0	1	0.857				
A	N<6	1.83	-1.741	0.893	1.1	0.467	0.347	2.001	2.514	-0.007	0.0242	-0.0487	0.0371	0.2386	-1	1.941	4.942	1.934	0	1	0.751	0.471				
L	N<6	0.772	-2.815	0.419	1.87	0.451	0.488	2.086	2.854	-0.01	0.0196	-0.0457	0.0238	0.5582	-1	1.709	4.084	1.970	0	1	0.733	0.496				
T		2.555	1.814	-0.706	1.392	0.51	0.452	0.151	1.751	2.104	-0.007	0.0243	-0.0499	0.0362	0.2827	-1	1.863	4.692	1.906	0	1	0.698				
A	NW<6	4.757	2.457	1.783	1.59	0.217	0.686	1.432	4.880	0.007	0.0445	-0.0689	0.0842	0.1718	-2	1.77	6	0.778	1.784	0	1	0.774				
L	NW<6	6.452	3.169	3.333	0.83	0.204	0.632	1.334	4.879	0.04	0.0235	0.0051	0.0861	1.9371	-5	1.519	7	2.428	3.319	0	1	0.681				
T		2.559	-1.331	1.206	1.079	0.221	0.699	1.459	4.882	-0.02	0.0620	-0.1354	0.0780	0.4624	-1	2.583	-6	2.801	2.801	0	1	0.735				
A	P<6	1.31	-6.340	0.037	1.20	0.623	0.523	2.717	2.600	-	-	-	-	-	-	1	1.744	-3	1	-0.496	2.427	0	1	0.535		
L	P<6	-1.252	4.500	0.353	1.59	0.645	0.664	2.936	2.791	-	-	-	-	-	-	1	1.777	-2	1	-0.229	2.055	0	1	0.490		
T		0.542	-5.954	0.147	1.92	0.635	0.374	2.610	2.350	-	-	-	-	-	-	1	1.797	-3	1	-0.514	2.407	0	1	0.533		
A	N>6	-0.335	1.451	-10.229	0.061	1.02	0.798	0.069	2.935	1.882	-0.0092	0.0087	-0.0248	0.0064	1.0610	-1	1.941	1.348	-3	1.365	0.783	0	1	0.758		
L	N>6	1.42	-10.303	-9.643	1	0.190	1.14	0.349	2.777	1.395	-0.0087	0.0072	-0.0215	0.0042	1.2047	-0	1.744	-3	1	1.778	0.509	0	1	0.704		
T		-1.344	4.554	-10.533	0.511	0.418	1.58	0.716	0.672	3.244	-2.735	-0.0059	0.0115	-0.0264	0.0147	0.5109	-1	1.409	-4	1	-0.229	1.548	0	1	0.807	
A	NW>6	2.72	1.451	1.11	0.71	0.17	0.353	0.131	1.153	1.412	0.0025	0.0014	-0.0113	0.0000	1.7153	-2	1.491	0.799	-3	1	-1.119	3.118	0	1	0.888	
L	NW>6	3.15	0	1.451	1.11	0.71	0.17	0.353	0.131	1.153	1.412	0.0025	0.0014	-0.0113	0.0000	2.5333	-2	0.66	0.735	-3	1	-0.804	2.811	0	1	0.892
T		1.41	1.451	1.11	0.71	0.17	0.353	0.131	1.153	1.412	0.0025	0.0014	-0.0113	0.0000	1.6311	-2	1.410	0.848	-3	1	-0.954	2.842	0	1	0.877	
A	P>6	8.40	4.849	1.479	1.8	0.195	0.920	1.553	6.451	-0.0040	0.0012	-0.0049	0.0019	3.2727	-1	1.765	0.462	-2	1	-0.964	3.820	0	1	0.955		
L	P>6	1.46	4.485	1.451	1.47	0.205	0.142	0.398	0.149	1.031	1.278	-0.0043	0.0012	-0.0049	0.0014	1.5285	-1	1.459	-2	1	-0.732	3.329	0	1	0.950	
T		1.0	4.485	1.451	1.47	0.205	0.142	0.398	0.149	1.031	1.278	-0.0043	0.0012	-0.0049	0.0014	1.965	-1	1.811	4.347	-2	1	-0.538	0.956	0	1	0.956

Table 4.10 Values of constants, confidence band, t-statistic values, standard deviation, standard error of the equation and R² values of the model (equation 3 with epicentral distance).

Constant																								
Type	Pro.	a	S.D.	Conf. Band	t-static	b2	S.D.	Conf. Band	t-static	c	S.D.	Conf. Band	t-static	d	S.D.	Conf. Band	t-static	t-statistic	SE	sq. R				
A	0.909	1.070	3.059	-1.1241	0.850	1.358	0.181	1.721	0.995	-7.515	-0.0044	0.0054	0.0064	-1.190	0.8190	-1.731	0.557	-0.613	-2.850	3.111	0.768	0.717		
L	N	0.506	1.154	2.825	-1.814	0.438	1.435	0.199	1.835	1.035	-7.210	-0.0049	0.0045	0.0041	-1.913	0.583	-1.548	0.583	-0.405	-2.690	2.656	0.819	0.679	
T		1.119	0.999	3.126	-0.888	1.120	1.261	0.171	1.604	0.918	7.387	-0.0045	0.0070	0.0095	-6.471	1.732	0.519	-0.715	-2.749	3.338	0.746	0.733		
A	0.617	-2.774	-4.758	5.538	1.956	0.102	2.179	1.734	19.156	-6.74	0.0014	-0.0033	-1.1	4.4718	-1.301	0.312	-0.621	-2.171	4.169	0.365	0.975			
L	NE	-3.389	0.111	-5.171	-5.069	4.396	1.956	0.117	1.701	1.1	-5.474	0.0018	-0.0025	-1.1	3.6286	-1.193	0.403	-0.314	-2.319	2.958	0.435	0.965		
T		-3.597	1.142	-4.597	7.769	1.948	1.175	2.113	1.782	2.3	-6.175	-0.0012	-0.0049	-1.1	6.3675	-1.264	0.206	-0.815	1	6.135	0.276	0.986		
A	2.41	-2.44	-0.548	2.746	1.166	1.1	1.419	0.913	9.2	1	-0.478	0.0009	-0.0021	-1.1	4.3596	-1.683	0.320	-1.039	1	5.256	0.980	0.755		
L	NW	1.743	1.743	0.821	3.096	1.116	1.753	1.362	0.871	6.1	-0.473	0.0008	-0.0022	-1.1	4.7125	-1.533	0.307	-0.916	1	4.997	0.975	0.757		
T		1.743	1.743	0.175	2.235	1.141	1.31	1.410	0.873	8	-0.477	0.0010	-0.0025	-1.1	4.4078	-1.475	0.321	-0.829	1	4.590	1.036	0.726		
A	1.777	1.777	-0.226	1.758	1.219	1.13	1.527	0.919	7.3	-0.475	0.0016	0.0012	1.1	1.2581	-1.943	0.439	-1.062	2	4.431	1.035	0.773			
L	P	1.659	1.659	-0.430	1.588	1.230	1.161	1.544	0.924	7.8	-0.473	0.0015	0.0015	1.1	1.6599	-1.753	0.439	-0.871	2	3.997	1.053	0.755		
T		1.74	1.74	-0.347	1.604	1.227	1.144	1.516	0.946	8	-0.477	0.0017	0.0017	1.1	1.5799	-1.864	0.359	-1.141	2	5.111	0.970	0.757		
A	1.423	1.423	0.604	2.323	0.604	2.173	1.075	0.132	2	-0.473	0.0012	0.0012	1.1	4.0902	0.051	0.723	1.560	1	4.431	1.035	0.773			
L	F	1.423	1.423	0.417	2.341	0.417	0.899	-0.066	1	-1.3	-0.066	0.0012	0.0012	1	4.2541	0.744	0.834	2.484	1	4.431	1.035	0.773		
T		1.423	1.423	0.239	2.329	0.239	1.197	0.253	3	-0.475	0.0013	0.0013	1	3.5659	-0.1	0.642	0.704	1	4.431	1.035	0.773			
A	1.553	1.553	2.703	1.74	1.192	2.107	1.340	9.494	-0.1	1.3	-0.012	0.0012	0.0012	1	5.6917	0.3	1.903	2	3.33	0.656	0.744			
L	S	1.144	1.144	0.392	3.920	1.143	2.24	2.706	1.765	10	-0.5	0.0013	0.0013	1	5.7874	1.137	1.137	3	3.33	0.656	0.744			
T		1.144	1.144	1.334	1.523	0.192	1.799	0.997	7	0.6	-0.019	0.0017	0.0017	1	4.8664	-0.545	0.898	1	4.431	1.035	0.773			
A	1.327	1.327	0.056	2.097	1.142	1.142	2.097	1.01	4	1.1	-0.016	0.0139	0.0139	1	1.7327	-0.943	1.052	1	4.431	1.035	0.773			
L	N<6	1.144	1.144	0.659	1.142	0.659	1.142	2.407	1.371	4	1.1	-0.014	0.0114	0.0114	1	1.9115	-0.615	1.038	1	4.431	1.035	0.773		
T		1.144	1.144	0.888	1.142	0.888	1.142	1.892	1.155	3	1.1	-0.0174	0.0114	0.0114	1	1.7327	-0.943	1.038	1	4.431	1.035	0.773		
A	1.434	1.434	1.845	1.540	1.142	1.142	1.845	1.91	1.1	1.3	-0.0168	0.0168	0.0168	1	5.7874	1.137	1.137	3	3.33	0.656	0.744			
L	NW<6	1.434	1.434	1.972	1.564	1.142	1.142	1.972	1.64	1.1	1.3	-0.0166	0.0166	0.0166	1	4.8664	-0.545	0.898	1	4.431	1.035	0.773		
T		1.434	1.434	1.876	1.499	1.142	1.142	1.876	1.79	1.1	1.3	-0.0166	0.0166	0.0166	1	1.7327	-0.943	1.038	1	4.431	1.035	0.773		
A	1.447	1.447	0.292	4.412	1.142	1.142	0.292	3.611	1.747	1	1.1	-0.0067	0.0067	0.0067	1	1.851	-0.851	-0.082	-0.082	1	4.431	1.035	0.773	
L	P<6	1.447	1.447	0.292	4.412	1.142	1.142	0.292	3.611	1.747	1	1.1	-0.0069	0.0069	0.0069	1	1.991	-0.851	-0.082	-0.082	1	4.431	1.035	0.773
T		1.447	1.447	0.292	4.412	1.142	1.142	0.292	3.611	1.747	1	1.1	-0.0069	0.0069	0.0069	1	1.991	-0.851	-0.082	-0.082	1	4.431	1.035	0.773
A	1.453	1.453	0.800	0.016	0.800	0.016	0.800	0.830	1.345	1.1	-0.0051	0.0051	0.0051	1	1.970	-0.481	1	1.404	1	4.431	1.035	0.773		
L	N>6	1.453	1.453	0.060	1.142	1.142	0.060	1.142	1.142	1	-0.0069	0.0069	0.0069	1	1.975	-0.104	1	3.261	0.895	0.742	0.949			
T		1.453	1.453	0.060	1.142	1.142	0.060	1.142	1.142	1	-0.0069	0.0069	0.0069	1	1.975	-0.104	1	3.261	0.895	0.742	0.949			
A	1.458	1.458	0.139	0.139	0.139	0.139	0.139	1.345	1.142	1	-0.0056	0.0056	0.0056	1	1.851	-0.851	-0.082	-0.082	1	4.431	1.035	0.773		
L	P>6	1.458	1.458	1.962	1.962	1.142	1.142	1.962	1.717	1	-0.0057	0.0057	0.0057	1	1.991	-0.441	0.441	1	4.431	1.035	0.773			
T		1.458	1.458	1.962	1.962	1.142	1.142	1.962	1.717	1	-0.0057	0.0057	0.0057	1	1.991	-0.441	0.441	1	4.431	1.035	0.773			
A	5.996	4.962	4.747	0.794	-0.364	1.753	-0.364	0.794	-0.364	1.753	-0.0046	-0.0046	-0.0046	1	1.414	-1.475	-1.475	-1.475	1	4.431	1.035	0.773		
L	NW>6	4.753	4.339	4.747	0.907	-0.280	1.712	0.907	-0.280	1.712	-0.0049	-0.0049	-0.0049	1	1.414	-0.385	-0.385	-0.385	1	4.431	1.035	0.773		
T		4.753	4.753	0.907	0.907	0.907	0.907	0.907	0.907	0.907	-0.0049	-0.0049	-0.0049	1	1.414	-0.385	-0.385	-0.385	1	4.431	1.035	0.773		
A	8.457	-1.226	1.558	1.698	0.154	1.1	1.698	0.154	1.1	-0.0071	0.0071	0.0071	1	1.642	-0.407	-0.407	-0.407	1	2.719	0.871	1			
L	P>6	3	3	8.231	-1.636	1.394	0.911	1.740	0.202	1.1	-0.0070	0.0070	0.0070	1	1.627	-0.300	-0.300	-0.300	1	2.565	0.896	1		
T		3	3	7.399	-1.655	1.324	0.986	1.706	0.265	1	-0.0070	0.0070	0.0070	1	1.643	-0.643	-0.643	-0.643	1	3.398	0.808	1		

Table 4.11 Values of constants, confidence band, t-statistic values, standard deviation, standard error of the equation and R^2 values of the model (equation 6 with hypocentral distance).

Type	Pro.	a	S.D.	Conf. Band	t-statistic	b1	S.D.	Conf. Band	Constant				SE	sq. R	
									c	S.D.	Conf. Band	t-static			
A	1.22	1.201	-0.927	3.171	0.934	0.955	0.115	0.759	1.151	8.304	-0.0115	0.0059	-0.0014	1.9444	
L	N	0.87	1.256	-1.316	2.970	0.658	0.962	0.129	0.742	1.182	7.457	-0.0093	0.0050	-0.0177	0.767
T		1.342	1.031	-0.217	3.301	1.496	0.978	0.096	0.814	1.142	10.188	-0.0141	0.0073	-0.0265	0.773
A	0.731	1.325	-1.532	3.094	0.589	0.918	0.145	0.665	1.171	6.331	-0.0065	0.0015	-0.0092	0.0039	
L	NE	1.244	1.430	-1.283	3.711	0.849	0.900	0.149	0.640	1.160	6.040	-0.0049	0.0013	-0.0072	0.0026
T	0.544	1.251	-1.530	2.838	0.523	0.944	0.144	0.693	1.195	6.556	-0.0067	0.0015	-0.0093	0.0040	
A	1.161	0.802	0.314	3.008	2.071	0.802	0.083	0.663	0.941	9.663	-0.0042	0.0009	-0.0057	0.0027	
L	NW	1.143	0.843	0.227	3.059	1.949	0.785	0.085	0.642	0.928	9.235	-0.0040	0.0008	-0.0054	0.0026
T	1.133	0.161	2.785	1.886	0.814	0.082	0.676	0.952	9.927	-0.0047	0.0010	-0.0064	-0.0030		
A	1.167	0.183	3.590	1.872	0.737	0.971	0.737	0.976	12.067	-0.0033	0.0013	-0.0055	-0.0011		
L	P	1.033	0.173	3.502	1.866	0.73	0.070	0.744	0.981	12.329	-0.0034	0.0012	-0.0054	-0.0013	
T	1.033	0.145	3.527	1.835	0.734	0.072	0.734	0.978	11.854	-0.0042	0.0016	-0.0069	-0.0015		
A	0.770	0.73	-12.863	1.613	0.242	0.15	0.186	-0.830	1.680	7.285	-0.0026	0.0009	-0.0136	-0.0009	
L	F	0.649	-14.849	2.151	0.039	0.34	0.16	-1.596	1.724	5.260	-0.0026	0.0011	-0.0158	-0.0006	
T	C 1/4	1.112	-11.713	1.941	0.772	0.11	0.11	-0.530	1.642	8.453	-0.0022	0.0009	-0.0130	-0.0006	
A	2.052	1.730	-1.310	7.604	1.058	0.6	0.16	0.680	0.912	12.061	-0.0058	0.0019	-0.0191	-0.0025	
L	S	0.533	0.710	-4.77	4.555	0.070	0.15	0.15	0.14	1.136	13.400	-0.0057	0.0014	-0.0182	-0.0032
T	7.143	0.633	0.714	13.612	1.932	0.116	0.16	0.18	0.793	8.410	-0.0049	0.0035	-0.110	-0.113	
A	0.473	0.713	-2.714	4.720	0.200	0.18	0.16	0.16	1.516	2.372	-0.0275	0.0228	-0.378	-0.129	
L	N<6	1.187	0.118	5.802	0.541	0.10	0.10	0.10	1.463	1.914	-0.0146	0.0223	-0.341	-0.141	
T	-0.115	1.712	-4.73	3.023	0.065	0.19	0.19	0.19	1.614	3.777	-0.0308	0.0164	-0.199	-0.116	
A	2.902	2.436	-1.730	7.094	1.191	0.112	0.15	0.15	0.944	5.274	-0.0223	0.0444	-0.188	-0.141	
L	NW<6	4.657	0.545	8.459	2.111	0.679	0.7	0.7	0.433	1.15	4.956	0.0141	0.0257	-0.100	-0.133
T	2.907	0.547	-4.30	7.294	1.110	0.687	0.6	0.6	0.501	0.5051	-0.0330	0.0610	:180	0.0106	
A	4.564	1.72	-1.7	7.841	2.47	0.654	0.12	0.12	0.413	0.77	0.0012	0.0076	-0.0122	0.0146	
L	P<6	4.32	0.44	7.520	2.41	0.722	0.7	0.7	0.413	0.77	0.0009	0.0063	-0.0102	0.0120	
T	3.510	0.44	1.2	7.228	2.07	0.641	0.74	0.74	0.413	0.77	-0.0031	0.0104	-0.0214	0.0152	
A	4.412	1.74	-0.410	9.374	1.67	0.609	0.268	0.268	0.413	0.77	-0.0085	0.0081	-0.0230	0.0061	
L	N>6	4.715	-0.634	10.066	1.55	0.534	0.293	0.293	0.413	0.77	-0.0084	0.0067	-0.0204	0.0037	
T	4.642	0.44	0.247	9.037	1.87	0.726	0.253	0.253	0.413	0.77	-0.0055	0.0112	-0.0256	0.0146	
A	6.83	1.57	3.916	9.710	4.07	0.487	0.113	0.113	0.413	0.77	-0.0030	0.0010	-0.0048	0.0012	
L	NW>6	6.565	3.004	10.126	3.1	0.443	0.136	0.136	0.413	0.77	-0.0034	0.0011	-0.0053	0.0016	
T	6.217	3.858	8.676	4.4	0.536	0.099	0	0	0.413	0.77	-0.0034	0.0010	-0.0051	0.0016	
A	1.31	3.480	6.206	0.41	0.863	0.238	(1.1	(1.1	0.413	0.77	-0.0045	0.0017	-0.0075	0.0016	
L	P>6	0.91	-3.770	5.718	0.3	0.889	0.239	(1.1	(1.1	0.413	0.77	-0.0045	0.0016	-0.0073	0.0017
T	0.91	-3.823	5.623	0.31	0.913	0.232	(1.1	(1.1	0.413	0.77	-0.0054	0.0020	-0.0088	0.0019	

Table 4.12 Values of constants, confidence band, t-statistic values, standard deviation, standard error of the equation and R^2 values of the model (equation 6 with epicentral distance).

Constant														SE	sq. R					
Type	Pro.	a	S.D.	Conf. Band	t-static	b*	S.D.	Conf. Band	t-statistic	c	S.D.	Conf. Band	t-static	d	S.D.	Conf. Band	t-static			
A	0.866	0.841	2.556	-0.113	1.030	1.158	0.766	9.42	-0.0105	0.0045	-11.1	-0.0194	2.3201	-0.943	0.457	-C.1	-1.862			
N	0.681	0.955	2.600	-1.19	0.713	1.201	0.754	8.3	-0.0088	0.0040	-1.1	-0.0167	2.0250	-0.787	0.503	-	-1.798			
L	0.855	0.624	2.109	-0.59	1.370	1.122	0.813	12.05	-0.0135	0.0048	-1.41	-0.0229	2.8042	-1.110	0.348	-4.1	-1.808			
T	0.836	1.269	1.929	-3.41	0.659	1.342	0.736	7.14	-0.0101	0.0033	-1.1	-0.0172	3.0762	0.124	0.673	1.1	-1.754			
A	NE	1.515	2.274	-4.45	0.677	1.380	0.730	7.1	-0.0094	0.0038	-1.1	-0.0176	2.5093	0.196	0.826	1.1	-2.017			
L	NE	-1.026	1.110	1.647	-3.12	0.696	1.335	0.782	8.71	-0.0114	0.0033	-1.1	-0.0186	3.4714	-0.964	0.541	-	-1.574		
T	NE	-0.773	0.574	3.076	0.76	3.345	0	0.940	0.679	1.1	-0.0038	0.0007	-1.1	-0.0052	5.1781	-1.109	0.246	-	-3.107	
A	NW	0.630	3.462	0.928	3.481	0	0.903	0.632	1.1	-0.0036	0.0007	-1.1	-0.0050	5.2319	-0.967	0.255	-	-4.5		
L	NW	2.195	1.540	0.552	2.648	0.431	2.791	0	0.960	0.699	1.1	-0.0043	0.0008	-1.1	-0.0059	5.3750	-1.042	0.233	-	-3
T	NW	2.389	2.192	2.043	2.046	1.161	3.815	0	0.963	0.733	1.1	-0.0019	0.0010	-1.1	-0.0039	1.9250	-1.641	0.285	-	-9
A	F	-0.902	-0.904	-0.986	-0.986	1.964	-2	0.095	0.747	1.1	-0.0025	0.0009	-1.1	-0.0044	2.6989	-1.442	0.278	-	-17.32	
L	F	-0.982	-0.418	1.463	0.952	3.463	-3	0.975	0.747	1.1	-0.0030	0.0011	-1.1	-0.0052	2.6818	-1.480	0.236	-	-1.15	
T	F	1.485	0.388	2.303	1.141	0.972	3.738	-3	0.948	0.730	1.1	-0.0030	0.0011	-1.1	-0.0047	9.9744	-1.458	0.256	-	-4
A	S	0.318	0.463	1.294	1.294	0.306	-2	1.557	1.127	1.1	-0.0039	0.0004	-1.1	-0.0047	1.9744	-1.458	0.256	-	-4	
L	S	3.122	1.389	0.653	1.91	2.248	-2	1.497	1.127	1.1	-0.0039	0.0004	-1.1	-0.0047	9.9744	-1.458	0.256	-	-4	
T	S	0.751	0.751	0.751	0.751	0.751	-2	1.517	1.841	1.1	-0.0037	0.0007	-1.1	-0.0051	5.5672	-1.154	0.522	-	-6	
A	N<6	1.310	1.518	2.086	2.086	1.616	-2	1.463	1.130	1.1	-0.0037	0.0005	-1.1	-0.0047	8.0652	-1.760	0.251	-	-17	
L	N<6	-1.616	-1.518	-1.518	-1.518	-1.700	-2	1.742	0.680	1.1	-0.0067	0.0004	-1.1	-0.0075	16.2927	-	-	-	-	
T	N<6	-1.616	-1.616	-1.616	-1.616	-1.343	-2	1.593	0.871	1.1	-0.0062	0.0004	-1.1	-0.0071	14.0227	-	-	-	-	
A	P<6	0.645	0.956	0.699	0.699	0.699	-2	0.688	0.688	1.1	-0.0023	0.0106	1.1	-0.0106	5.6496	-0.438	0.751	1.146	-2.0222	
L	P<6	2.111	2.111	2.111	2.111	2.111	-2	2.248	0.793	0.496	9.1772	-0.0077	0.0014	1.1	-0.0106	5.6496	-0.438	0.751	1.146	-2.0222
T	P<6	0.751	0.751	0.751	0.751	0.751	-2	0.751	0.751	0.751	-0.0023	0.0106	1.1	-0.0106	5.6496	-0.438	0.751	1.146	-2.0222	
A	NW>6	1.714	1.714	1.714	1.714	1.714	-2	1.652	0.800	5.9772	-0.0188	0.0113	0.0046	-0.0423	1.6634	-0.459	0.834	1.271	-2.189	
L	NW>6	1.714	1.714	1.714	1.714	1.714	-2	1.742	0.764	5.319	-0.0109	0.0102	0.0104	-0.0321	1.0625	-0.626	0.936	1.255	-2.628	
T	NW>6	1.714	1.714	1.714	1.714	1.714	-2	1.593	0.962	8.392	-0.0247	0.0099	-0.0043	-0.0451	2.5086	-0.638	0.587	0.579	-1.885	
A	N>6	4.374	4.374	4.374	4.374	4.374	-2	3.945	0.911	0.911	-0.0067	0.0004	-1.1	-0.0071	14.0227	-	-	-	-	
L	N>6	4.374	4.374	4.374	4.374	4.374	-2	3.945	0.911	0.911	-0.0067	0.0004	-1.1	-0.0071	14.0227	-	-	-	-	
T	N>6	4.374	4.374	4.374	4.374	4.374	-2	3.945	0.911	0.911	-0.0067	0.0004	-1.1	-0.0071	14.0227	-	-	-	-	
A	P>6	1.215	1.215	1.215	1.215	1.215	-2	1.864	0.841	0.841	-0.0049	0.0032	-0.0018	-0.0117	1.5552	-1.754	0.268	-1.186	-2.321	
L	P>6	1.215	1.215	1.215	1.215	1.215	-2	1.842	0.895	0.895	-0.0049	0.0032	-0.0018	-0.0117	1.5552	-1.754	0.268	-1.186	-2.321	
T	P>6	1.215	1.215	1.215	1.215	1.215	-2	1.842	0.808	0.808	-0.0049	0.0032	-0.0018	-0.0117	1.5552	-1.754	0.268	-1.186	-2.321	
A	2.717	2.675	3.655	2.717	3.316	2.689	-2	0.098	0.955	0.522	7.765	-0.0110	0.0077	0.0076	-0.0296	1.4252	-1.209	0.492	-0.019	-2.399
L	2.717	2.675	3.655	2.717	3.316	2.689	-2	0.098	0.955	0.522	8.462	-0.0280	0.0134	0.0044	-0.0605	2.0894	-1.058	0.452	0.035	-2.152
T	2.717	2.675	3.655	2.717	3.316	2.689	-2	0.098	0.955	0.522	8.462	-0.0280	0.0134	0.0044	-0.0605	2.0894	-1.058	0.452	0.035	-2.152
A	3.717	1.714	7.213	3.748	2.088	0.732	-2	1.115	0.349	4.049	-0.0026	0.0047	0.0073	-0.0125	0.5589	-0.587	0.587	0.579	-2.274	
L	3.717	1.714	7.213	3.748	2.088	0.732	-2	1.115	0.349	4.049	-0.0026	0.0047	0.0073	-0.0125	0.5589	-0.587	0.587	0.579	-2.274	
T	3.717	1.714	7.213	3.748	2.088	0.732	-2	1.115	0.349	4.049	-0.0026	0.0047	0.0073	-0.0125	0.5589	-0.587	0.587	0.579	-2.274	
A	4.374	1.714	7.213	3.748	2.088	0.732	-2	1.115	0.349	4.049	-0.0026	0.0047	0.0073	-0.0125	0.5589	-0.587	0.587	0.579	-2.274	
L	4.374	1.714	7.213	3.748	2.088	0.732	-2	1.115	0.349	4.049	-0.0026	0.0047	0.0073	-0.0125	0.5589	-0.587	0.587	0.579	-2.274	
T	4.374	1.714	7.213	3.748	2.088	0.732	-2	1.115	0.349	4.049	-0.0026	0.0047	0.0073	-0.0125	0.5589	-0.587	0.587	0.579	-2.274	
A	5.155	1.755	12.665	5.185	0.225	0.147	-2	0.963	0.652	10.906	-0.0036	0.0025	0.0018	-0.0039	1.4071	-1.574	0.315	-0.912	-2.916	
L	5.155	1.755	12.665	5.185	0.225	0.147	-2	0.963	0.652	10.906	-0.0036	0.0025	0.0018	-0.0039	1.4071	-1.574	0.315	-0.912	-2.916	
T	5.155	1.755	12.665	5.185	0.225	0.147	-2	0.963	0.652	10.906	-0.0036	0.0025	0.0018	-0.0039	1.4071	-1.574	0.315	-0.912	-2.916	
A	5.155	1.755	12.665	5.185	0.225	0.147	-2	0.963	0.652	10.906	-0.0036	0.0025	0.0018	-0.0039	1.4071	-1.574	0.315	-0.912	-2.916	
L	5.155	1.755	12.665	5.185	0.225	0.147	-2	0.963	0.652	10.906	-0.0036	0.0025	0.0018	-0.0039	1.4071	-1.574	0.315	-0.912	-2.916	
T	5.155	1.755	12.665	5.185	0.225	0.147	-2	0.963	0.652	10.906	-0.0036	0.0025	0.0018	-0.0039	1.4071	-1.574	0.315	-0.912	-2.916	
A	5.155	1.755	12.665	5.185	0.225	0.147	-2	0.963	0.652	10.906	-0.0036	0.0025	0.0018	-0.0039	1.4071	-1.574	0.315	-0.912	-2.916	
L	5.155	1.755	12.665	5.185	0.225	0.147	-2	0.963	0.652	10.906	-0.0036	0.0025	0.0018	-0.0039	1.4071	-1.574	0.315	-0.912	-2.916	
T	5.155	1.755	12.665	5.185	0.225	0.147	-2	0.963	0.652	10.906	-0.0036	0.0025	0.0018	-0.0039	1.4071	-1.574	0.315	-0.912	-2.916	

Table 4.13 Values of constants, confidence band, t-statistic values, standard deviation, standard error of the equation and R^2 values of the model (equation 7 with hypocentral distance).

Constants																		SD sq. R													
Type	EQ	a	S.D.	Conf. Band	t	b1	S.D.	Conf. Band	t	b2	S.D.	Conf. Band	t	c	S.D.	Conf. Band	t	d	S.D.	Conf. Band	t	SD	sq. R								
A	0.29	1.06	-1.51	2.11	0.27	0.43	0.17	0.21	0.80	0.82	0.26	0.38	1.27	3.17	-0.0088	0.0051	-0.0176	-0.0001	1.7232	-1.35	0.67	-2.49	-0.21	2.02	0.59	0.84					
L	N	-0.18	1.09	2.05	1.14	0.17	0.45	0.19	0.13	0.77	2.41	0.96	0.29	0.48	1.45	3.37	-0.0071	0.0042	-0.0143	0.0000	1.7000	-1.24	0.66	-2.37	-0.10	1.86	0.64	0.81			
T	0.91	-0.15	-0.71	2.12	0.96	0.15	0.37	0.89	4.14	0.61	0.23	0.23	1.00	2.72	-0.0108	0.0066	-0.0220	0.0005	1.1343	-1.72	0.69	-2.89	-0.55	2.51	0.52	0.88					
A	-3.98	-4.4	-5.28	2.12	5.35	-0.81	0.19	-1.01	-0.35	3.10	0.35	2.49	3.71	8.89	-0.0037	0.0007	-0.0049	-0.0026	1.121	-2.27	0.30	-2.80	-1.75	7.55	0.32	0.98					
L	NE	-3.05	-1.3	-4.68	-4.4	3.29	-0.1	0.25	-1.14	-0.28	2.89	3.06	0.45	2.28	3.84	6.87	-0.0025	0.0007	-0.0037	-0.0012	1.1336	-2.47	0.39	-3.16	-1.79	6.29	0.42	0.96			
T	4.26	-5.75	-2.76	4.97	-0.57	0.21	-3	-0.20	2.69	2.96	0	1	1.3	3.64	7.55	-0.0038	0.0008	-0.0052	-0.0025	1.1110	-2.27	0.32	-2.83	-1.70	7.02	0.36	0.97				
A	1.51	-1.3	0.36	2.65	2.21	0.45	0.11	0.63	4.13	0.67	0	1	0.94	4.19	-0.0037	0.0008	-0.0050	-0.0024	1.112	-1.51	0.38	-2.15	-0.86	3.94	0.66	0.88					
L	NW	1.50	-1	0.32	2.69	2.13	0.40	0.11	0.59	3.47	0.74	0	1	1.02	4.39	-0.0037	0.0007	-0.0048	-0.0025	1.1133	-1.38	0.38	-2.01	-0.75	3.68	0.68	0.87				
T	1.25	0.69	0	1.4	1.42	0	1	0.11	0.11	0.59	0	1	0.2	0.87	3.66	-0.0043	0.0009	-0.0117	-0.0028	1.136	3.39	-2.02	-0.11	3.46	0.68	0.87					
A	0.91	-0.11	-1.4	0.5	0.11	-0.1	0.11	0.5	4	0.70	0	1	1.3	1.01	3.77	-0.0037	0.0011	-0.0146	-0.0019	1.1340	-1.27	0.41	-1.96	-0.19	3.14	0.58	0.83				
L	P	0.11	0.94	-1.4	0.4	0	1	0.11	0.11	0.64	0	1	0.2	0.95	3.38	-0.0039	0.0011	-0.0167	-0.0021	1.1373	-1.09	0.40	-1.77	-0.42	2.73	0.59	0.83				
T	0.89	-0.16	-1.4	0.2	0	1	0.11	0.11	0.73	0.19	0	1	1.05	3.90	-0.0045	0.0013	-0.0188	-0.0023	1.1343	-1.37	0.41	-2.06	-0.61	3.33	0.58	0.87					
A	1.08	-1.12	1	0.45	0.52	-5.44	0	1	0.61	0.41	1.34	1.34	1.48	-0.0037	0.0012	-0.0174	-0.0016	1.1328	-1.37	0.94	-12.37	0	1.47	0.63	0.87						
L	F	0.18	1.37	-1.15	1	0.80	-8.27	0	1	0.17	0.58	0	1	1.18	1.18	1.18	0	0.0029	0.0016	-0.0222	0.0000	1.1168	-1.60	1.57	-20.06	1	1.02	0.80	0.87		
T	0.61	1.00	-1.11	1	0.43	4.33	0	1	0.43	4.33	1.71	1.71	3.73	1.21	1.21	0	0.0011	-0.0157	-0.0113	-0.0113	1.1208	-2.08	0.74	-10.78	-0.79	2.81	0.60	0.87			
A	12.11	4.61	4	-1.1	1.3	1.73	0	0.41	1.02	3.12	1.1	1.1	3.71	0.52	0	0	0	0	1.1	-1.22	1.21	-3.34	0.91	1.00	0.46	0.87					
L	S	6.30	5.05	-2	1	1.12	1.42	0.44	0.85	0	1.42	1.1	1.13	0.33	0	0.42	0.92	0	0.0014	0.0014	0.0014	0	1.1131	-0.31	1.25	-2.49	1.88	0.24	0.50	0.87	
T	1.13	6.06	8.31	29.56	-1.2	1.80	0.51	0.92	2.11	3.57	-2.53	1.1	1.1	4.56	-0.61	1.77	0	0.0036	0.0012	-0.0174	-0.0016	1.1328	-1.37	0.94	-12.37	0	1.47	0.63	0.87		
A	-7.7	1.83	-5.54	1.01	-1.2	0.26	0.42	1	0.27	0.32	0	1	0.39	0	0.58	0	0.0036	0.0012	-0.0174	-0.0016	1.1328	-1.37	0.94	-12.37	0	1.47	0.63	0.87			
L	N<6	-0.9	1.96	-6.07	0.89	-1.2	0.21	0.69	1.42	5.14	0.87	0.25	0.43	1.31	3.49	-0.0075	0.0134	-0.0311	0.0162	1.1560	-2.47	1.06	-4.32	-0.62	2.37	0.41	0.86				
T	-1.05	1.35	-4.35	0.45	-1.1	0.21	0.69	1.42	5.14	0.87	0.25	0.43	1.31	3.49	-0.0075	0.0134	-0.0311	0.0162	1.1560	-2.47	1.06	-4.32	-0.62	2.37	0.41	0.86					
A	-7.7	1.83	-5.54	1.01	-1.2	0.22	0.07	0.82	2.06	0.51	0.33	-0.06	1.08	1.53	-0.0188	0.0430	-0.0928	0.0553	1.1435	-1.43	2.15	-5.12	2.27	0.66	0.66	0.87					
L	NW<6	4.77	2.13	1.10	8.44	-1	0.23	0.00	0.78	1.74	0.52	0.33	-0.06	1.09	1.55	0.0241	0.0256	-0.0199	0.0681	1.1941	-3.56	1.68	-6.45	-0.67	2.12	0.65	0.87				
T	2.10	2.50	-2.21	6.41	0.84	0.40	0.22	0.02	0.78	1.83	0.56	0.35	-0.04	1.17	1.60	-0.0413	0.0589	-0.1427	0.0111	1.1700	-0.79	2.48	-5.11	1.49	0.32	0.69	0.75				
A	-1.0	2.48	-0.16	8.56	1.70	0.64	1.13	0.41	0.86	0.05	0.10	0.45	-0.69	0.89	0.22	0.0016	0.0081	-0.0127	0.0119	1.1200	-2.47	1.06	-4.32	-0.62	2.37	0.41	0.86				
L	P<6	-1.7	2.41	-0.48	8.02	1.56	0.69	0.12	0.49	0.90	5	0.87	0	1.78	0	0.0014	0.0067	-0.0103	0	1.1211	0.2087	-2.32	1.24	-4	14	1.87	0.51	0.88			
T	4.18	2.59	-0.38	8.74	1.62	0.65	0.13	0.43	0.88	5.15	-0.08	0.47	-0.90	0.75	0	0.0035	0.0111	-0.0230	0	1.1211	0.3126	-1.74	1.38	-4	1	1.26	0.54	0.87			
A	7.46	9.04	-8.77	23.69	0.83	0.87	0.81	0.58	2.32	1.08	-0.78	2.26	-4	83	3.27	0	0.0078	0.0087	-0.0235	0.0178	1.1897	-1.45	1.39	-5.11	1.3	1.05	0.68	0.79			
L	N>6	11.14	10.01	-6.84	29.12	1.11	1.10	0.90	-0.51	2.71	1.23	-1.69	2.51	-6.20	2.82	0	0.0076	0.0070	-0.0202	0	1.1211	0.0753	-1.18	1.40	-4	1	1.85	0.74	0.75		
T	2.19	7.61	-11.48	15.87	0.29	0.50	0.71	-0.78	1.78	0	0.68	1.98	-2.87	4.22	0.34	-0.0118	0.0118	-0.0118	0.0118	1.1211	-2.29	1.28	-4	1	1.3	1.57	0.64	0.82			
A	5.93	2.65	1.38	10.47	2.24	0.47	0.12	0.26	0.68	0	0.13	0.30	-0.39	0.65	0.44	-0.0111	0.0111	-0.0111	0.0111	1.1211	0.2830	-1.85	0.64	-4	1	0.75	2.89	0.62	0.94		
L	NW>6	4.14	2.85	-0.75	9.03	1.45	0.38	0.15	0.13	0.63	0	0.41	0.34	-0.17	0.99	1.22	0	0.0011	0.0111	-0.0111	0.0111	1.1211	0.3422	-1.38	0.70	-4	1	0.18	1.98	0.69	0.92
T	7.13	2.45	2.92	11.33	2.91	0.55	0.11	0.37	0.74	1.16	-0.12	0.28	-0.60	0.36	0.43	-0.0111	0.0111	-0.0111	0.0111	1.1211	0.2812	-1.97	0.57	-2.95	-1.00	3.47	0.56	0.95			
A	4.32	2.03	0.80	7.84	2.13	-0.53	0.36	-1.15	0.09	1.7	1.80	0.41	1.08	2.52	4.36	-0.0012	0.0012	-0.0012	0.0012	1.1211	0.3256	-2.43	0.64	-3.53	-1.33	3.83	0.52	0.96			
L	P>6	3.20	2.09	-0.43	6.82	1.53	-0.39	0.38	-1.04	0.26	3	1.69	0.44	0.93	2.45	3.84	-0.0012	0.0012	-0.0012	0.0012	1.1211	0.3093	-1.95	0.62	-3.02	-0.89	3.17	0.57	0.95		
T	4.01	1.97	0.60	7.43	2.04	-0.54	0.36	-1.17	0.08	1.50	1.90	0.42	1.16	2.63	3.84	-0.0017	0.0017	-0.0017	0.0017	1.1211	0.2906	-2.70	0.66	-3.84	-1.56	4.11	0.52	0.96			

Table 4.15 Values of constants, confidence band, t-statistic values, standard deviation, standard error of the equation and R^2 values of the model (equation 10 hypocentral distance).

Type	Pro.	Constant										SE	sq. R						
		a	S.D.	Conf. Band	t-static	c	S.D.	Conf. Band	t-static	t	S.D.	Conf. Band	t-static						
A	1.721	0.607	0.697	2.745	2.838	-0.0058	0.00325	-0.0113	-0.0003	1.785	-33	0.482	-3.91	-2.290	6.443	0.500	0.912		
L	N	2.781	0.969	1.145	4.416	2.870	0.0014	0.00487	-0.00668	0.0096	0.283	-37	0.741	-5.1	-2.615	5.216	0.792	0.779	
T	3.344	1.057	1.560	5.129	3.163	0.0072	0.00913	-0.0082	0.0226	0.788	-1.1	0.932	-6.4	-3.294	5.223	0.773	0.789		
A	1.949	0.318	1.399	2.499	6.129	-0.0032	0.00058	-0.0042	-0.0022	5.500	-1.1	0.205	-2.8	-2.254	12.728	0.319	0.985		
L	NE	2.451	0.508	1.573	3.328	-0.0021	0.00072	-0.0034	-0.0009	2.931	-15	0.311	-3.3	-2.297	9.121	0.470	0.966		
T	1.750	0.271	1.281	2.219	6.448	-0.0031	0.00056	-0.0041	-0.0021	5.518	-16	0.179	-2.9	-2.336	14.751	0.299	0.986		
A	3.249	0.441	2.513	3.986	7.370	-28	0.00079	-0.0041	-0.0015	3.557	-16	0.295	-4.3	-3.344	13.024	0.626	0.948		
L	NW	3.290	0.525	2.444	4.167	6.269	-27	0.00079	-0.0040	-0.0013	3.354	-11	0.336	-4.2	-3.131	10.996	0.733	0.928	
T	2.751	0.475	1.957	3.545	5.788	-16	0.00099	-0.0053	-0.0020	3.646	-9	0.329	-4.1	-3.079	11.018	0.696	0.935		
A	3.382	0.324	2.841	3.923	10.443	-29	0.00060	-0.0039	-0.0019	4.850	-18	0.203	-3.8	-3.847	3.169	17.291	0.392	0.965	
L	P	3.412	0.343	2.839	3.986	9.941	-5	0.00057	-0.0040	-0.0021	5.421	-13	0.208	-3.7	-3.701	3.004	16.084	0.403	0.960
T	3.412	0.343	2.839	3.986	9.941	-5	0.00057	-0.0040	-0.0021	5.421	-13	0.208	-3.7	-3.701	3.004	16.084	0.403	0.963	
A	4.531	0.554	3.584	5.478	8.184	-0.0028	0.00051	-0.0036	-0.0019	5.431	-12	0.309	-2.3	-2.314	9.203	0.431	0.973		
L	F	4.418	0.596	3.398	5.438	7.410	-0.0027	0.00048	-0.0036	-0.0019	5.708	-12	0.325	-2.9	-2.096	8.167	0.437	0.973	
T	5.111	0.671	3.963	6.260	7.618	-0.0022	0.00071	-0.0034	-0.0010	3.141	-10	0.382	-2.7	-2.726	8.846	0.551	0.956		
A	0.230	1.022	-1.543	2.003	0.225	-0.0062	0.00060	-0.0072	-0.0051	10.317	-8	0.500	-2.2	-2.234	0.501	2.737	0.301	0.985	
L	S	-2.801	2.038	-6.335	0.733	1.374	-0.0061	0.00094	-0.0077	-0.0045	6.468	-9	0.960	-1.4	-1.486	1.845	0.187	0.560	0.948
T	3.423	1.966	0.014	6.831	1.741	-0.0057	0.00159	-0.0094	-0.0039	4.189	-115	1.012	-4.8	-4.871	1.360	3.078	0.545	0.951	
A	1.119	0.405	0.424	1.874	2.766	-0.0150	0.00229	-0.0189	-0.0110	1.13	-9	0.320	-3	-3.019	-1.919	7.710	0.290	0.977	
L	N<6	0.307	1.337	-1.988	2.602	0.230	-0.0262	0.01054	-0.0443	-0.0081	1.16	-8	1.148	-3.4	-3.470	0.473	1.305	0.777	0.833
T	1.351	1.388	-1.033	3.735	0.973	-0.0290	0.01637	-0.0571	-0.0009	1.70	-7	1.318	-4.9	-4.921	-0.393	2.015	0.764	0.838	
A	-1.256	0.794	-2.605	0.092	1.583	-0.0191	0.01190	-0.0393	-0.0012	1.691	-3	0.799	-4.0	-4.051	-1.336	3.372	-1/4	0.867	
L	NW<6	-1.139	0.691	-2.313	0.034	1.650	-0.0090	0.00713	-0.0211	0.0031	1.235	-7	0.630	-3.8	-3.834	-1.693	4.386	-1/49	0.881
T	-1.457	1.063	-3.262	0.349	1.370	-0.0292	0.02132	-0.0654	0.0070	1.0	-40	1.164	-4.5	-4.538	-0.583	2.199	-1/18	0.796	
A	'86	0.652	0.564	2.809	2.587	-0.0061	0.00389	-0.0128	0.0006	1.3	-7	0.517	-3.4	-3.407	-1.627	4.866	-1/32	0.935	
L	P<6	'404	0.730	1.147	3.660	3.293	-0.0030	0.00340	-0.0089	0.0028	1.14	-7	0.546	-3.8	-3.837	-1.957	5.303	-1/70	0.940
T	'60	0.613	-0.194	1.915	1.404	-0.0115	0.00490	-0.0200	-0.0031	1.15	-5	0.517	-3.8	-3.834	-1.693	4.386	-1/49	0.881	
A	'83	0.678	1.883	4.283	4.550	0.0080	0.00338	0.0020	0.0140	'1	'1	0.543	-3.1	-3.396	0.809	'1	'1	0.966	
L	N>6	'89	0.557	1.702	3.676	4.824	0.0025	0.00207	-0.0012	0.0062	1/3	3	0.410	-3.4	-3.410	-2.917	8.883	'25	0.976
T	'29	1.438	0.582	5.675	2.176	0.0116	0.00982	-0.0058	0.0290	'0	'0	1.236	-3	-3.514	3.804	'4	'4	0.872	
A	'48	4.181	6.915	6.839	-0.0031	0.00083	-0.0044	-0.0017	1/5	'5	0.459	-4	-4.459	2.998	8.215	'1/6	0.953		
L	NW>6	'61	3.121	7.000	4.396	-0.0032	0.00102	-0.0049	-0.0014	1/8	4	0.633	-4	-4.440	-2.307	5.329	'1/1	0.912	
T	'49	3.736	6.362	6.480	-0.0038	0.00091	-0.0053	-0.0022	1/1	1	0.452	-4	-4.438	-2.815	7.912	'3	0.952		
A	'32	0.304	4.118	5.145	15.211	0.0020	0.00049	-0.0028	-0.0011	1/0	0	0.185	-4	-4.185	-3.842	22.466	'62	0.986	
L	P>6	'31	4.900	10.653	-0.0027	0.00058	-0.0037	-0.0017	1/0	0	0.235	-4	-4.140	-3.338	15.903	'3	0.976		
T	'04	0.391	3.746	5.063	-0.0030	0.00080	-0.0043	-0.0017	0/0	0	0.247	-4	-4.131	-3.719	16.745	0.3/0	0.976		

Table 4.16 Values of constants, confidence band, t-statistic values, standard deviation, standard error of the equation and R^2 values of the model (equation 10 with epicentral distance).

Type	Pro.	a	S.D	Conf. Band	t-static	c	S.D	Conf. Band	Constant			SE	sq. R
									t-static	d	S D		
A	N	1.351	0.509	2.349	0.353	2.653	-0.0010	0.0045	0.0078	-0.0097	0.2192	-2.265	0.464
L	N	1.249	0.639	2.501	-0.004	1.954	-0.0023	0.0041	0.0058	-0.0103	0.5474	-1.960	0.530
T	N	0.796	0.416	1.611	-0.019	1.915	-0.0033	0.0059	0.0083	-0.0149	0.5635	-2.059	0.440
A	NE	0.600	0.497	1.575	-0.374	1.207	-0.0039	0.0024	0.0009	-0.0086	1.6033	-1.538	0.393
L	NE	0.663	0.590	1.820	-0.495	1.122	-0.0039	0.0025	0.0010	-0.0088	1.5458	-1.454	0.451
T	NE	0.402	0.410	1.205	-0.401	0.981	-0.0041	0.0027	0.0011	-0.0093	1.5318	-1.570	0.352
A	P	1.740	0.327	2.382	1.099	5.320	-0.0038	0.0007	-0.0024	-0.0053	5.2329	-2.515	0.245
L	NW	1.755	0.348	2.436	1.073	5.048	-0.0040	0.0007	-0.0027	-0.0053	6.0303	-2.318	0.246
T	NW	1.150	0.326	1.789	0.511	3.526	-0.0045	0.0009	-0.0027	-0.0063	4.9341	-2.279	0.262
A	F	1.438	0.325	2.075	0.801	4.426	-0.0043	0.0008	-0.0028	-0.0058	5.7333	-2.045	0.210
L	P	1.353	0.343	2.025	0.682	3.949	-0.0042	0.0008	-0.0028	-0.0057	5.5789	-1.959	0.228
T	P	0.913	0.267	1.437	0.389	3.417	-0.0049	0.0009	-0.0030	-0.0067	5.1809	-2.019	0.200
A	S	1.731	0.305	2.328	1.133	5.679	-0.0033	0.0003	-0.0026	-0.0039	9.5588	-2.345	0.182
L	S	1.962	0.430	2.805	1.119	4.561	-0.0032	0.0004	-0.0024	-0.0039	7.9000	-2.280	0.246
T	S	1.605	0.420	2.428	0.781	3.820	-0.0029	0.0006	-0.0018	-0.0040	4.9828	-2.597	0.261
A	N<6	1.645	1.856	5.282	-1.992	0.886	-0.0064	0.0012	-0.0039	-0.0088	5.1626	-1.528	0.392
L	N<6	0.467	2.513	5.392	-4.458	0.186	-0.0058	0.0013	-0.0034	-0.0083	4.6480	-0.767	1.206
T	N<6	1.801	2.421	6.546	-2.944	0.744	-0.0078	0.0024	-0.0030	-0.0125	3.2199	-1.891	1.298
A	NW<6	0.671	0.895	2.425	-1.082	0.751	-0.0137	0.0130	0.0118	-0.0392	1.0515	-1.496	0.935
L	NW<6	0.884	1.128	3.094	-1.326	0.784	-0.0063	0.0121	0.0174	-0.0300	0.5190	-1.671	1.078
T	NW<6	0.705	1.19	2.054	-0.645	1.024	-0.0132	0.0137	0.0137	-0.0400	0.9606	-1.813	0.798
A	P<6	1.119	1.317	-0.246	1.343	-0.0244	0.0110	-0.0029	-0.0459	2.2222	-1.103	0.505	
L	P<6	1.115	1.45	1.660	-0.085	1.769	-0.0137	0.0074	0.0009	-0.0282	1.8448	-1.267	0.480
T	P<6	1.118	1.8	0.988	-0.337	0.962	-0.0300	0.0150	-0.0006	-0.0595	1.9967	-1.132	0.569
A	N>6	1.41	1.5	0.035	2.073	-0.0028	0.0014	1.1111	-0.0056	1.9930	-1.667	0.243	
L	N>6	1.13	1.4	1.121	1.619	-0.0033	0.0014	1.1111	-0.0059	2.3971	-1.486	0.262	
T	N>6	1.11	1.1	0.207	1.066	-0.0041	0.0016	1.1111	-0.0072	2.5000	-1.547	0.203	
A	NW>6	1.74	1.4	0.998	4.064	-0.0032	0.0006	1.1111	-0.0043	5.3559	-2.443	0.290	
L	NW>6	1.3	1.2	0.799	3.242	-0.0033	0.0006	1.1111	-0.0046	5.3871	-2.247	0.360	
T	NW>6	1.13	1.2	0.406	2.877	-0.0033	0.0007	1.1111	-0.0047	4.4521	-2.387	0.290	
A	P>6	1.4	1.4	1.323	3.813	-0.0029	0.0011	1.1111	-0.0050	2.7358	-3.241	0.451	
L	P>6	1.4	1.4	0.843	3.270	-0.0036	0.0009	1.1111	-0.0053	3.9888	-2.693	0.397	
T	P>6	1.4	1	0.634	2.721	-0.0031	0.0014	1.1111	-0.0060	2.1806	-3.148	0.547	
A	P>10	1.427	1	2.052	6.763	-0.0020	0.0009	1.1111	-0.0038	2.1957	-3.131	0.309	
L	P>10	0.441	1	1.763	5.962	-0.0032	0.0009	1.1111	-0.0049	3.7558	-2.716	0.305	
T	P>10	0.420	1	0.943	4.208	-0.0040	0.0013	1.1111	-0.0065	3.0938	-2.564	0.325	

Table 4.17 Values of the regression constants of the equation $I_{\max} = e + f M$ considering all earthquakes of magnitude more than or equal to 6.

Province	e	σ_e	f	σ_f	σ
Northern	1.328	1.38	1.070	0.216	1.100
Northwest	1.729	0.809	0.947	0.138	0.804
Northeast	-4.011	2.294	1.718	0.336	1.050
Peninsular	-0.670	1.730	1.345	0.291	1.010
Indian sub.	0.526	0.839	1.125	0.133	1.006

Table 4.18 Values of the regression constants of the equation $I_{\max} = e + f M$ considering all earthquakes of magnitude less than 6.

Province	a	σ_a	b	σ_b	σ
Northern	1.711	1.807	0.913	0.350	0.706
Northwest	0.854	2.795	1.158	0.530	0.874
Peninsular	-4.733	7.425	2.176	1.501	0.832
Indian sub.	0.359	1.662	1.198	0.323	0.7198

Table 4.19 Values of the regression constants of the equation $I_o = e + f M + g I_{\max}$ considering all earthquakes of magnitude more than or equal to 6.

Province	e	σ_e	f	σ_f	g	σ_g	σ
Northern	-4.430	1.399	0.321	0.170	1.403	0.196	0.83
Northwest	5.776	2.217	1.41	0.338	-0.275	0.175	1.22
Northeast	-2.728	2.364	1.203	0.610	0.436	0.315	0.88
Peninsular	2.183	2.557	0.531	0.520	0.450	0.279	1.37
Indian sub.	1.472	1.000	0.202	0.270	0.704	0.140	0.70

Table 4.20 Values of the regression constants of the equation $I_o = e + f M + g I_{\max}$ considering all earthquakes of magnitude less than 6.

Province	e	σ_e	f	σ_f	g	σ_g	σ
Northern	1.206	1.300	0.731	0.350	0.357	0.270	0.51
Northwest	0.123	0.605	0.023	0.148	0.963	0.081	0.27
Peninsular	5.08	0.878	-0.603	0.900	0.8787	0.240	0.69
Indian sub.	1.472	1.000	0.202	0.270	0.704	0.140	0.70

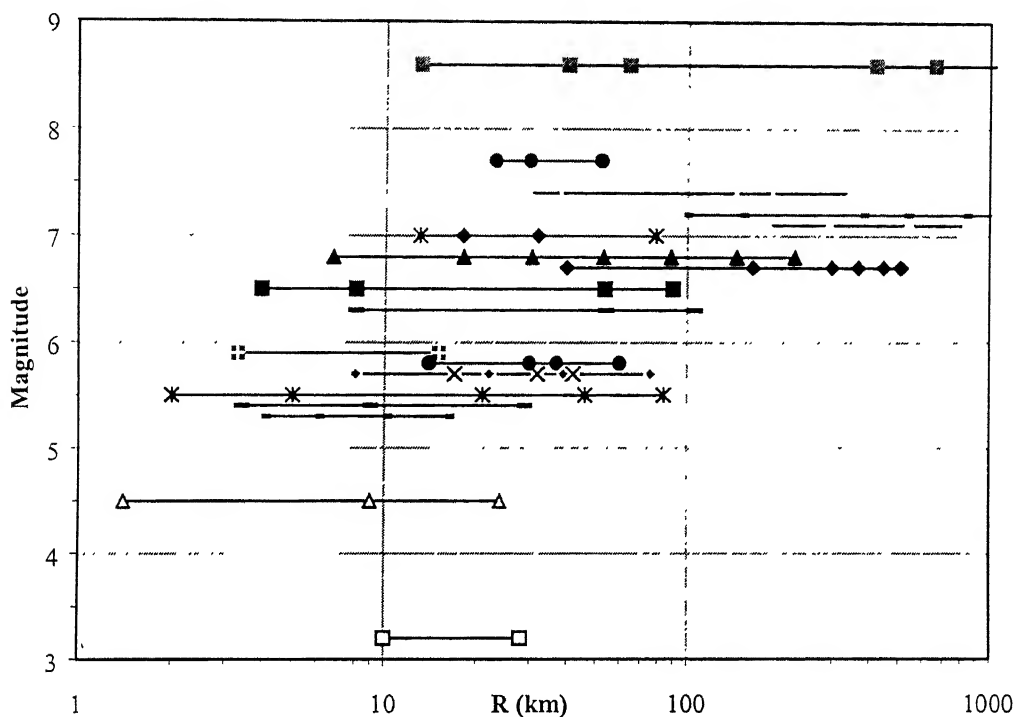


Figure 4.1 Data plots for Northwest province earthquakes.

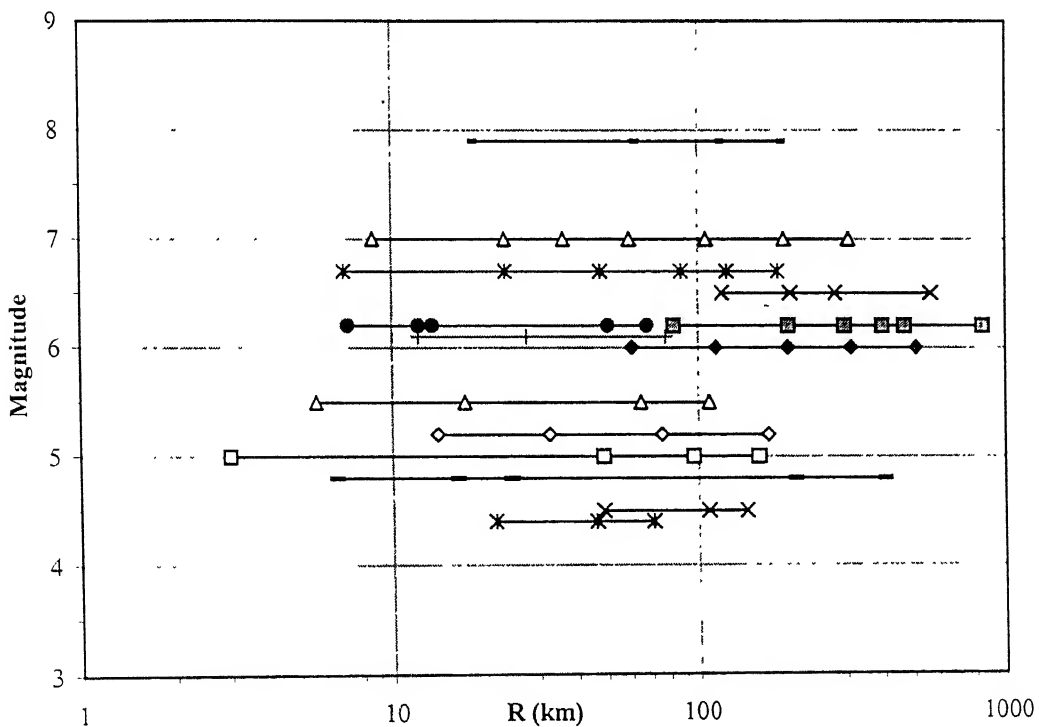


Figure 4.2 Data plots for peninsular province earthquakes.

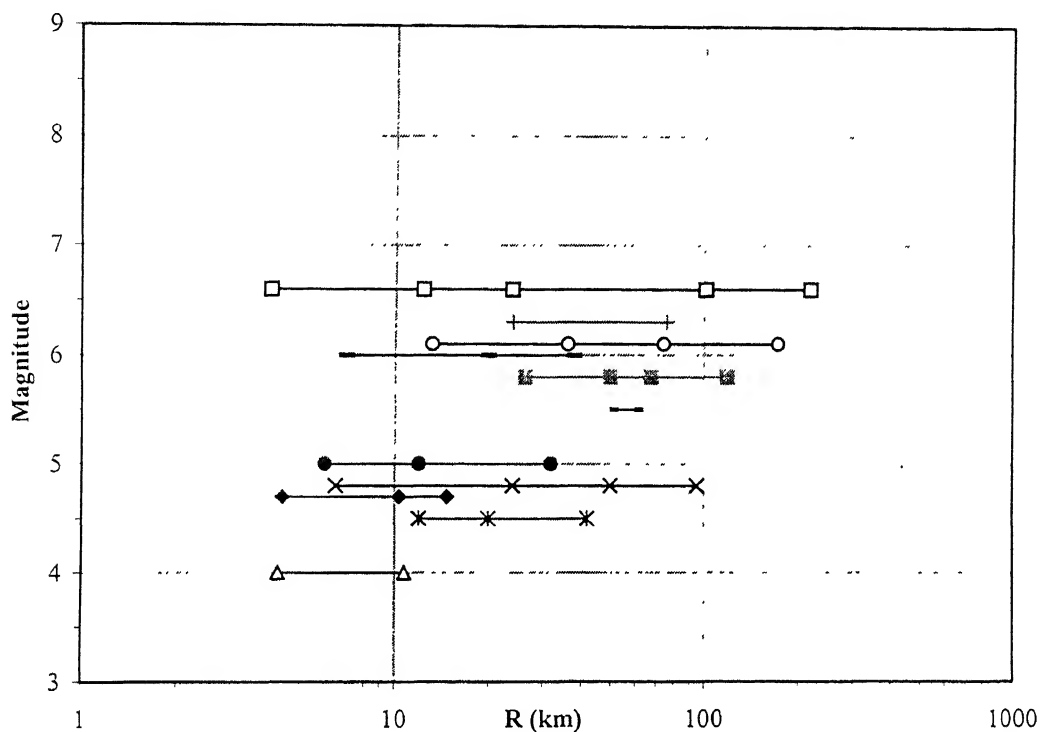


Figure 4.3 Data plots for North earthquakes.

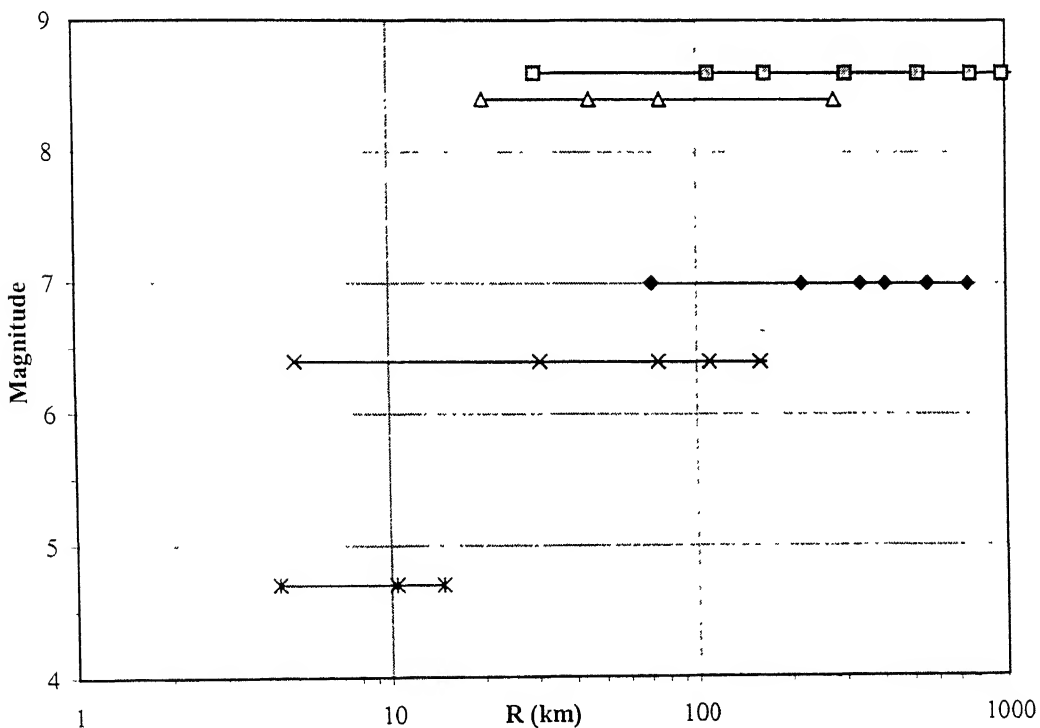


Figure 4.4 Data plots for Foredeep earthquakes.

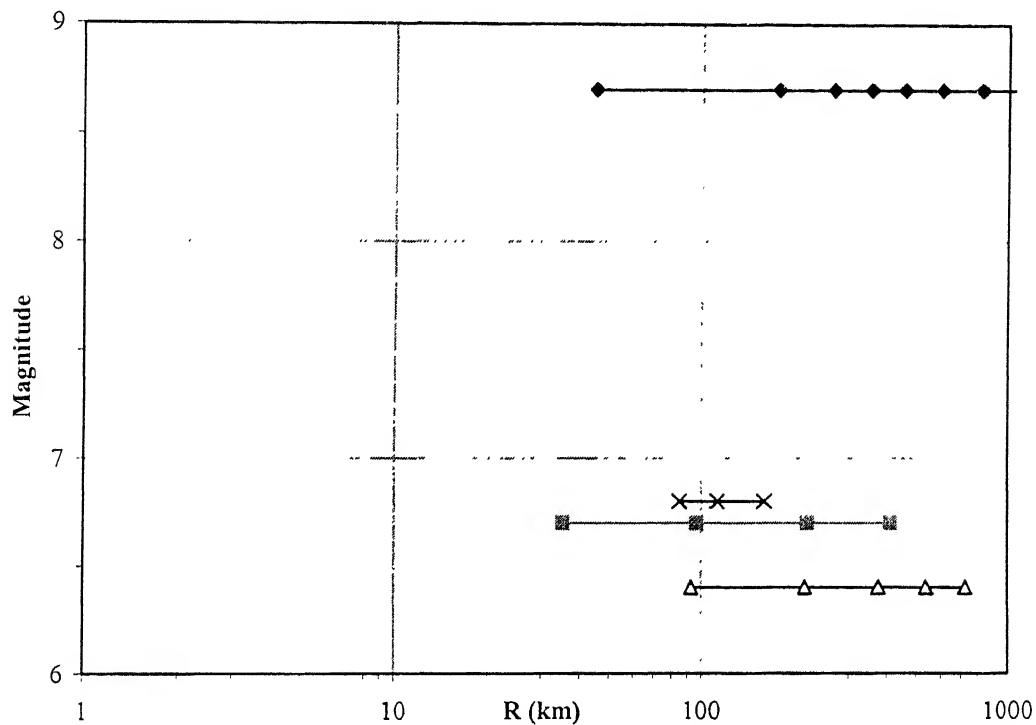


Figure 4.5 Data plots for Subduction earthquakes.

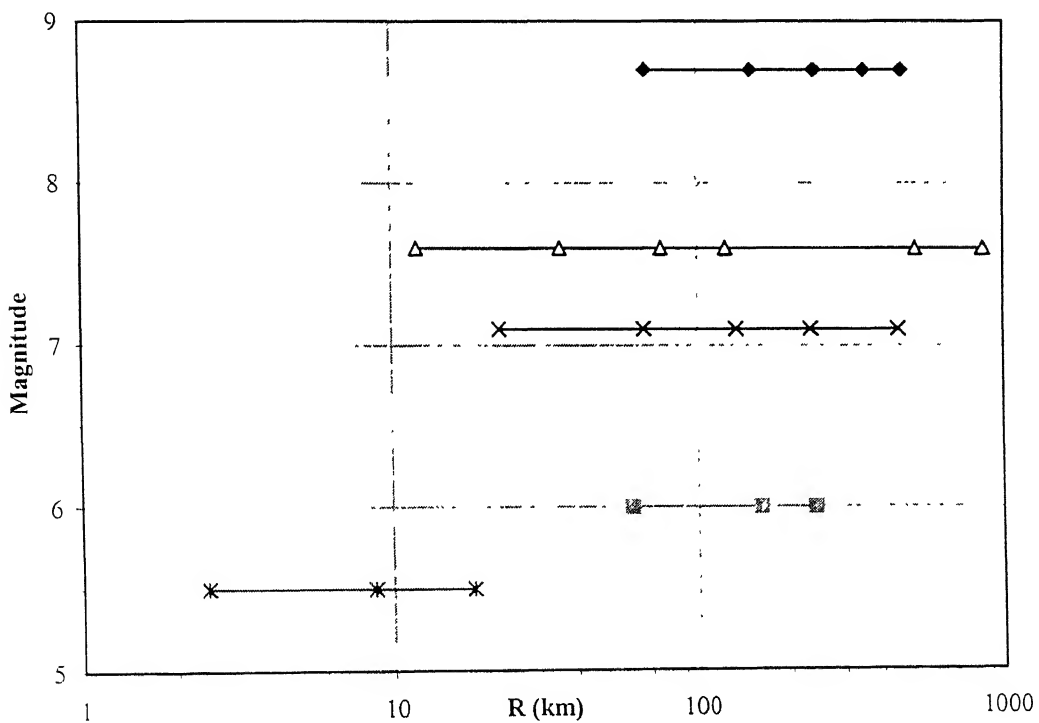


Figure 4.6 Data plots for Northeast province earthquakes.

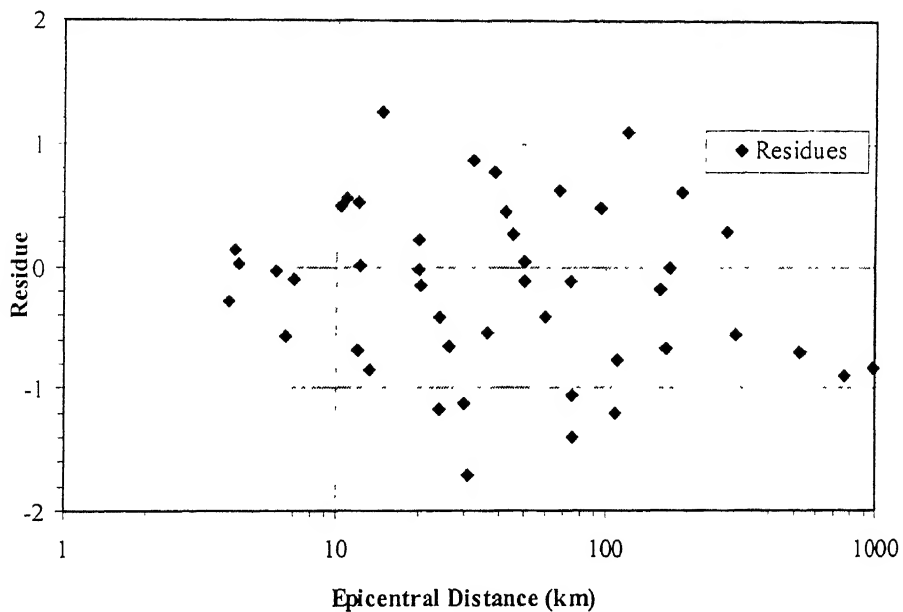


Figure 4.7 Plot of residues of the regression analysis for Northern province considering all earthquakes.

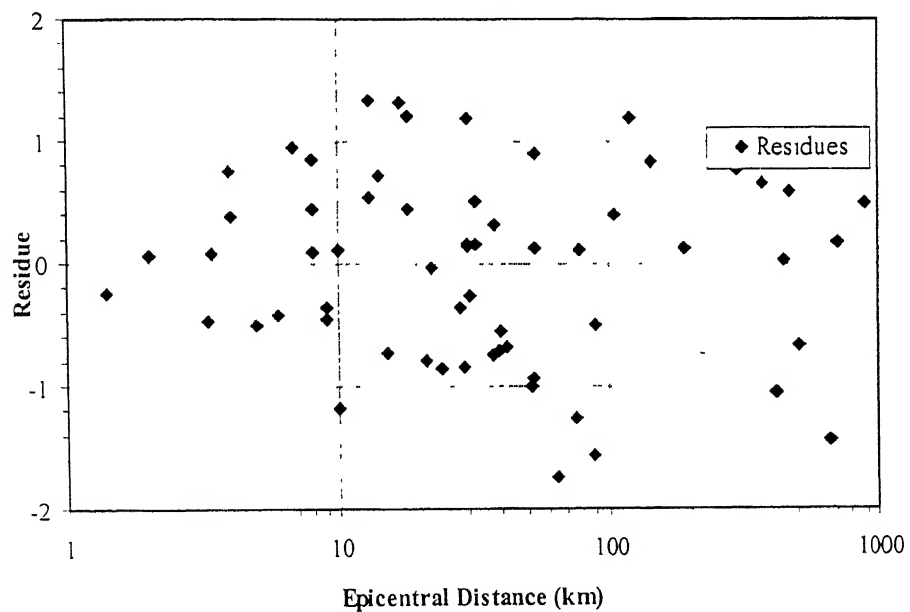


Figure 4.8 Plot of residues of the regression analysis for Northwest province considering all earthquakes.

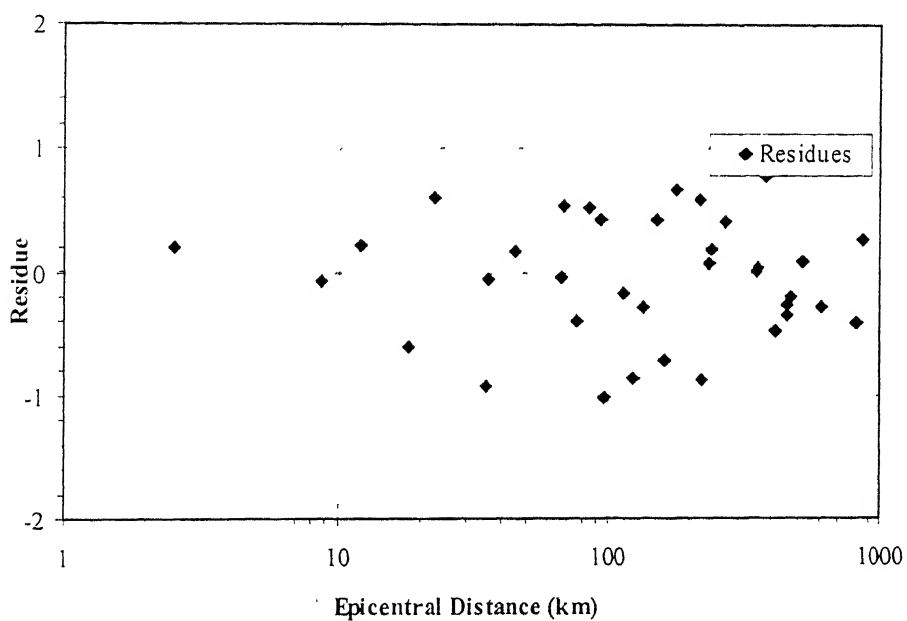


Figure 4.9 Plot of residues of the regression analysis for Northeast province considering all earthquakes

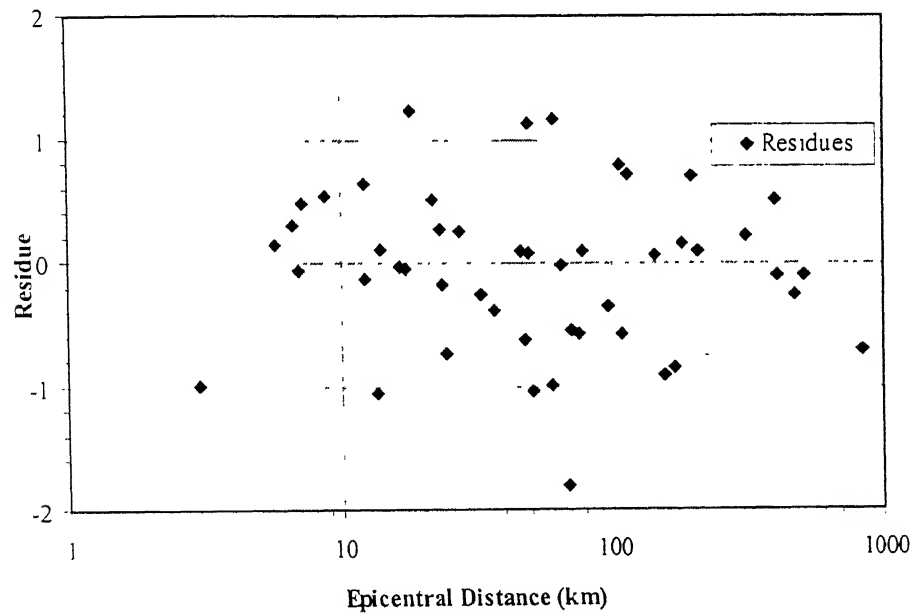


Figure 4.10 Plot of residues of the regression analysis for Peninsular province considering all earthquakes.

Chapter 5

Discussion and Conclusions

5.1 Introduction

India has experienced a large number of earthquakes in the past. But very few strong motion records have been obtained from these earthquakes. On the other hand, the intensity isoseismals are available for a substantial number of earthquakes and it is prudent to use these for development of attenuation relationships.

In this study, 59 earthquakes from different parts of the country have been considered. The isoseismals are collected from Memoirs of Geological Survey of India and some other publications. All the isoseismals along with their intensity area data have been compiled. Considering the regional geology and tectonics, and the standard deviation obtained from the regression analysis, the Indian subcontinent is divided into six intensity attenuation province, *viz.*, Northwest, North, Northeast, Peninsular, Foredeep, and Subduction Provinces. Apart from these, a single attenuation relationship has also been derived for the entire Indian subcontinent treating it as a single region. The earthquakes are divided into two categories, one with magnitude greater than or equal to 6.0 and the other with magnitude less than 6.0. These two categories and their combinations have been separately analyzed.

5.2 Discussion of Results

5.2.1 Type of Equations and Earthquake Parameters Used

In this study three different earthquake parameters (M , I_{max} , I_o) are used. The ten different equations used are described in the Section 4.5.7. Equations 3 (involving magnitude and both the linear and logarithmic distance term), 6 (involving maximum intensity and both the linear and logarithmic distance term), 7 (involving maximum intensity, magnitude and both the linear and logarithmic distance term) and 10 (involving

epicentral intensity and both the linear and logarithmic distance term) have two terms, cR and $d \log_{10}(R)$, for distance while others have only one of these terms for distance. This is to find the predominance of either of the distance terms indicating whether logarithmic or linear attenuation with distance dominates a particular region, discussions here are made only for Equations 3, 6, 7, and 10 since they involve both distance terms.

Equation 7 contains both maximum intensity (I_{max}) and magnitude (M), and fits better than equations 3 and 6. Equations 7 and 10 are used to study the regional dependency for intensity attenuation.

5.2.2 Selection of the Best Equation

Equations 10, involving epicentral intensity (I_o), fits best for the available data. The estimation of epicentral intensity (I_o) involves a graphical and iterative method wherein the value of I_o depends on the database of intensity and distance. Hence, I_o is really not an independent variable indicating size of earthquake or maximum intensity of shaking. On the other hand, magnitude and maximum intensity are independent variables. Therefore, it is reasonable to expect that regression analysis will give higher standard deviation values when using magnitude or maximum intensity as a variable.

The estimation of epicentral intensity for future earthquake is not possible since it is a hypothetical intensity. Hence, Equation 10 is not very useful for seismic risk estimation studies even though it gives smaller values of standard deviation. Equations 3 and 6 are better suited for attenuation estimation of future earthquakes as they involve magnitude and maximum intensity, which may be assumed for a given seismic risk scenario. In the present study, a regression analysis has also been performed to estimate epicentral intensity (I_o) from given magnitude and maximum intensity (Tables 4.17 to 4.20). The standard deviation in this case is quite high. Hence, Equation 3 or 6 is better than Equation 10 for seismic risk estimation studies.

5.2.3 Regional Dependency

The Indian subcontinent is divided into six attenuation provinces. Performing the *t*-test (*t*-static) on the coefficients of the proposed equations, the possibility of combining the different attenuation provinces can be obtained. Table 5.1 shows the possibility of combining the different provinces. The *t*-test performed on the coefficients of Equation 10 suggests that north, northeast and subduction zone earthquakes can be combined into one set, and northwest and peninsular earthquakes can be combined into another set. As per Equation 7, northwest, north and peninsular earthquakes can be combined into one set. Therefore peninsular and northwest region can be combined in either of the cases, but Figures 5.1 to 5.3 show that they have different attenuation rate. Moreover large standard deviation of northwest earthquakes may have given the positive *t*-test. Hence in the present study these have been treated separately.

5.2.4 Magnitude Dependency

Keeping in mind that the smaller earthquakes attenuate more rapidly than the large earthquakes, the earthquakes are divided into two groups: those with $M < 6$ and those with $M \geq 6$. The *t*-test performed on these groups shows that both exhibit different characteristics (Table 5.2) and could not be combined. Figures 5.4 to 5.6 show attenuation trend of smaller and larger earthquakes for different provinces, both indicating quite different attenuation trends.

5.2.5 Choice of Distance

In the present study, both hypocentral distance and epicentral distance have been used. Hypocentral distance fits better for Equations 3 and 10, while epicentral distance fits better for Equation 6. Equation 7 involves both maximum intensity and magnitude and hence, hypocentral distance and epicentral distance both fit well for Equation 7 depending upon the dependence on magnitude and maximum intensity respectively.

Equation 6 involves maximum intensity, which includes the effect of focal depth, and hence, use of hypocentral distance does not give better results in this case (Table 5.3).

Plot of intensity versus hypocentral distance, and intensity versus epicentral distance, are shown in Figure 5.7. For large distances both curves give similar result. Subduction earthquakes show considerable difference as they have large focal depth.

5.2.6 Effect of Isoseismal Modeling

The isoseismals can be modeled as a family of concentric circles or ellipses. In case of ellipses, relationships for intensity decay have been developed both along the major and minor axes of the isoseists. Figure 5.8 shows the average, longitudinal and transverse attenuation for different attenuation provinces. There is considerable difference in the attenuation rate for longitudinal and transverse directions, as large as one to two intensity units. Average attenuation will overestimate the attenuation in the longitudinal direction and underestimate that in the transverse direction. Hence, where it is possible to estimate the fault direction and therefore, the direction of major axis, one should use the longitudinal and transverse attenuation for estimation of seismic risk.

Subduction zone earthquakes show very large difference in the attenuation rate in the longitudinal and transverse directions, as large as two to three intensity units, and hence, one should be very careful in using the appropriate equation for the subduction region.

5.2.7 Approximate Decay Pattern

The attenuation relationships contain two terms for distance, cR representing material absorption and $d \log_{10}(R)$ representing geometric spreading. Figures 5.9 to 5.15 compare predominance of either of these two terms for different provinces. Tables 5.4 to 5.6 give the standard deviation and R^2 values for Equations 8, 9 and 10. In all the regions except subduction zone, the logarithmic decay term dominates. The subduction zone earthquakes are dominated by the linear term.

Figure 5.9 shows the plot of attenuation of intensity with different distance terms, cR , $d \log_{10}(R)$ and both, for different provinces. North, northeast, peninsular, foredeep and Indian subcontinent earthquakes show logarithmic decay for first 200, 500, 450, 600 and 500 km, respectively, and after that both distance terms dominate equally. On the other hand, northwest and subduction earthquakes show more or less logarithmic and linear decay, respectively. The results are presented in Table 5.1.

5.3 Attenuation for Different Provinces

The Indian subcontinent is divided into six attenuation provinces *viz.*, north, Northeast, Northwest, Peninsular, Foredeep and Subduction zone. It is found that earthquakes in different province follow different attenuation depending upon the type of equation used. Hence attenuation of different provinces is described as per the type of equation used.

5.3.1 Equation Involving Magnitude

Equation 3 has magnitude as the earthquake parameter. The attenuation of each province varies according to the magnitude dependency (constant b_2). It is found that the earthquakes of northeast province have the maximum magnitude dependency. The value of constant b_2 is close to 2 *i.e.*, an increase in magnitude by one unit can cause an increase in intensity by about two units, while the values of constant b_2 for other provinces are around one unit.

Foredeep and subduction earthquakes exhibit quite different characteristics than the other provinces. They show very slow attenuation for first 100 km (Figure 5.16) and fast decay after 100 km. The other provinces show more or less similar attenuation rates.

5.3.2 Equation Involving Maximum Intensity

Equation 6 has maximum intensity as the earthquake parameter and the attenuation of earthquakes in different provinces depends upon the maximum intensity

dependency (constant b_1). It is found that the subduction and foredeep earthquakes have the highest dependency on maximum intensity.

Subduction zone earthquakes show slow attenuation rate for first 100 km (Figure 5.17) and then rapid decay rate. Foredeep earthquakes show the slowest decay, while northern earthquakes have the fastest decay.

5.3.3 Equation Involving Epicentral Intensity

Equation 10 gives drop of intensity from epicentral intensity with distance. It has only distance dependency. The attenuation is only due to distance irrespective of the size of earthquake.

Figures 5.1 to 5.3 give the attenuation of different province earthquakes with distance. The smaller earthquakes attenuate very fast and earthquakes in northwest province have fastest decay while peninsular earthquakes have smallest decay. Among larger earthquakes, subduction zone earthquakes have slowest decay for first 400 km and after that northeast earthquakes have slowest decay. Northern earthquakes have fastest decay for first 200 km and after that peninsular earthquakes have fastest decay.

5.4 Comparison of Attenuation Pattern of Whole India Subcontinent with United States

For the seismic risk analysis, the attenuation relationships developed in United States are often used for Indian projects. Hence, it is interesting to compare the intensity attenuation trend of Indian earthquakes with those of United States. Figures 5.18 to 5.20 compare the Indian attenuation relationships with that of United States, and it is found that the intensity attenuation pattern of Indian earthquakes matches very well with that of San Andreas province of United States. Hence, it is suggested that the strong motion attenuation relationships could be used for Indian earthquakes.

5.5 Comparison with the Bhuj 2001 Earthquake (M 7.9, Imax 10)

Equations 3, 6, 7 and 10 of peninsular province and Indian subcontinent have been compared with the recent Bhuj earthquake of January 26, 2001 (Figures 5.21 to 5.24). It is found that Equations 10 (involving epicentral intensity and both the linear and logarithmic distance term) for Indian subcontinent fits best. The Equations 3, 6 and 7 of Indian subcontinent fits better than that of peninsular. In any of the case, Equations of Indian subcontinent fit better than the peninsular region, the probable cause could be the non-availability of intensity data for large earthquakes in peninsular province.

5.6 Conclusions

1. Out of different attenuation Equations, Equation 10 (involving epicentral intensity and both the linear and logarithmic distance term) fit best of all the provinces but Equation 3 (involving magnitude and both the linear and logarithmic distance term) or 6 (involving maximum intensity and both the linear and logarithmic distance term) can be used for seismic risk evaluation.
2. The northeastern earthquakes have very large dependence on magnitude, and the attenuation pattern changes significantly with slight increase in the values of magnitude.
3. Hypocentral distance fits best for Equation 3 (involving magnitude and both the linear and logarithmic distance term) and Equation 10 (involving epicentral intensity and both the linear and logarithmic distance term), while epicentral distance fits best for Equation 6 (involving maximum intensity and both the linear and logarithmic distance term).
4. Subduction and foredeep earthquakes show different characteristics than the rest. They have relatively high epicentral tract than that of others indicating maximum damage areas. Subduction earthquakes have linear attenuation, while the other provinces follow a logarithmic decay. Northern, northeastern, peninsular and foredeep

- earthquakes show logarithmic decay for first 200, 500, 450 and 600 km respectively, after which both distance term dominates equally.
5. Small intensity earthquakes attenuate faster than large intensity earthquake, and hence, can be separated out.
 6. Among the smaller earthquakes, northwestern earthquakes attenuate fastest, while the peninsular earthquakes have the slowest decay rate.
 7. It is found that the attenuation along the transverse direction of the isoseismal is faster than that along the longitudinal direction. The difference is as high as one to two intensity units. Assuming equivalent circles for isoseismals introduce approximation, and hence, separate attenuation relationships have been developed along the minor and major axis of the isoseismals.
 8. The attenuation trend of India matches very well with that of San Andreas region and hence it is suggested that the strong motion attenuation relationships of San Andreas could be used for Indian earthquakes.

5.7 Scope for Future Studies

1. Equations involving magnitude (and maximum intensity) as the earthquake parameter, have dual dependency, both on magnitude (and maximum intensity) and distance. Hence, it is not possible to get intensity decay independently as a function of distance. One can develop relationships separating their dependency.
2. For the present study the method of least square is used in the regression analysis. The two-stage regression method or the method of maximum likelihood, which are reported to be most robust, can be used.



Table 5.1 Possibility of combining the regions as per t-test values for the comparison of constants of equation 10 for hypocentral distance (in bracket are those of equation 7).

Province	North	Northeast	Northwest	Peninsular	Fooredeep	Subduction
North						
Northeast	✓(✗)					
Northwest	✗(✓)	✗(✗)				
Peninsular	✗(✓)	✗(✗)	✓(✓)			
Foredeep	✗(✗)	✗(✗)	✗(✗)	✓(✗)		
Subduction	✓(✗)	✓(✗)	✗(✗)	✗(✗)	✗(✗)	

Table 5.2 Possibility of combining the smaller and larger earthquakes group, as per t-test values for the comparison of constants, of equation 10 for hypocentral distance (in bracket are those of equation 7).

Province	North	Northwest	Peninsular
North			
Northwest	✗(✗)		
Peninsular	✗(✗)	✗(✗)	

Table 5.3 Best distance parameter for different type of equations.

Equation No.	Best distance parameter
1, 2, 3 (M)	Hypocentral
4, 5, 6 (I_{max})	Epicentral
7 (M, I_{max})	Hypocentral or Epicentral
8, 9, 10 (I_o)	Hypocentral

Table 5.6 Table showing standard deviations and R^2 values for different provinces as per equation 8, 9 and 10 respectively, for transverse attenuation.

Province	R (Eq-8)		Log(R) (Eq-9)		With Both (Eq-10)	
	S.D.	R^2	S.D.	R^2	S.D.	R^2
North	1.037	0.610	0.769	0.785	0.773	0.789
Northwest	1.170	0.815	0.758	0.922	0.696	0.935
Northeast	1.107	0.803	0.495	0.960	0.299	0.986
Peninsular	0.976	0.780	0.581	0.922	0.403	0.963
Subduction	0.674	0.919	0.778	0.892	0.545	0.951
Foredrip	1.170	0.794	0.653	0.936	0.551	0.956
North ($M < 6$)	0.82	0.804	0.804	0.811	0.764	0.838
Northwest($M < 6$)	0.628	0.758	0.597	0.781	0.588	0.796
Peninsular($M < 6$)	0.521	0.832	0.441	0.879	0.396	0.908
North ($M \geq 6$)	0.782	0.687	0.533	0.854	0.524	0.872
Northwest($M \geq 6$)	1.101	0.867	0.737	0.929	0.613	0.952
Peninsular($M \geq 6$)	1.083	0.790	0.431	0.967	0.370	0.976

Table 5.7 General trend of attenuation pattern for different attenuation provinces.

Sl. No	Province	Average	Longitudinal	Transverse
1	North	Logarithmic	Logarithmic	Logarithmic
2	Northwest	Logarithmic	Logarithmic	Logarithmic
3	Northeast	Logarithmic	Logarithmic	Logarithmic
4	Peninsular	Logarithmic	Logarithmic	Logarithmic
5	Foredrip	Logarithmic	Logarithmic	Logarithmic
6	Subduction	Linear	Linear	Linear
7	North($M < 6$)	Both	Both	Both
8	Northwest($M < 6$)	Logarithmic	Logarithmic	Logarithmic
9	Peninsular($M < 6$)	Logarithmic	Logarithmic	Logarithmic
10	North($M \geq 6$)	Logarithmic	Logarithmic	Logarithmic
11	Northwest($M \geq 6$)	Logarithmic	Logarithmic	Logarithmic
12	Peninsular($M \geq 6$)	Logarithm	Logarithmic	Logarithmic

Table 5.8 Approximate pattern of type of attenuation patterns with distance.

Sl. No	Province	Smaller distance	Larger distance
1	North	$\leq 200\text{km}$ Log	≥ 200 Both
2	Northwest	Logarithmic	Logarithmic
3	Northeast	$\leq 500\text{km}$ Log	≥ 500 Both
4	Peninsular	$\leq 450\text{km}$ Log	≥ 450 Both
5	Foredeep	$\leq 600\text{km}$ Log	≥ 600 Both
6	Subduction	Linear	Linear
7	North($M < 6$)	$\leq 120\text{km}$ Log	≥ 120 Both
8	Northwest($M < 6$)	$\leq 90\text{km}$ Both	≥ 90 Both
9	Peninsular($M < 6$)	$\leq 120\text{km}$ Log	≥ 120 Both
10	North($M \geq 6$)	Logarithmic	Logarithmic
11	Northwest($M \geq 6$)	Logarithmic	Logarithmic
12	Peninsular($M \geq 6$)	Logarithm	Logarithmic

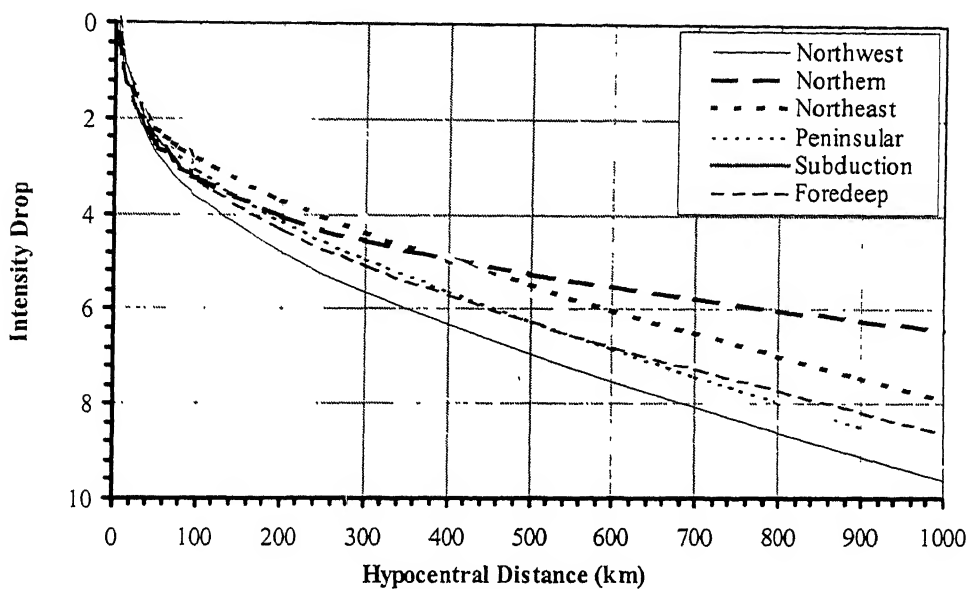


Figure 5.1 Attenuation of intensity with hypocentral distance for different provinces using equation 10 considering all earthquakes.

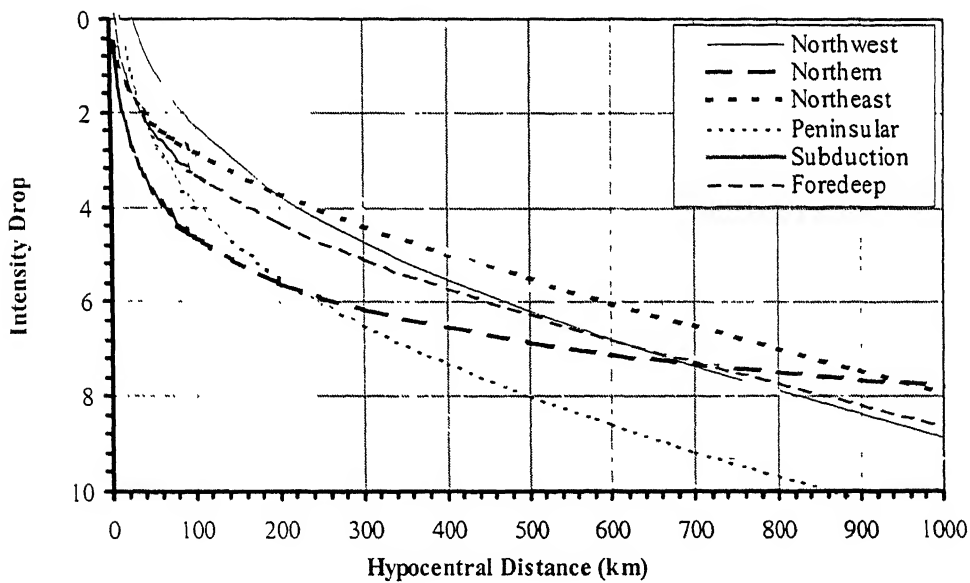


Figure 5.2 Attenuation of intensity with hypocentral distance for different provinces using equation 10 considering earthquakes of magnitude greater than or equal to 6.

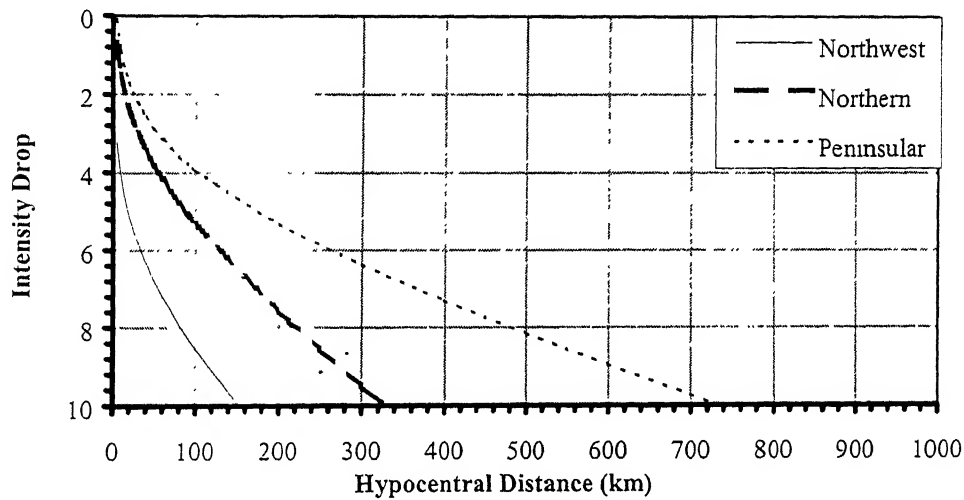


Figure 5.3 Attenuation of intensity with hypocentral distance for different provinces using equation 10 considering earthquakes of magnitude less than 6.

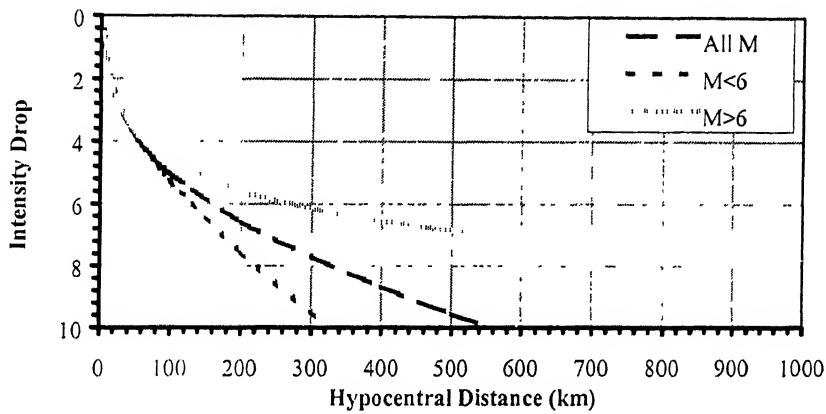


Figure 5.4 Plot of attenuation rates of different earthquake group for northern province as per equation 10.

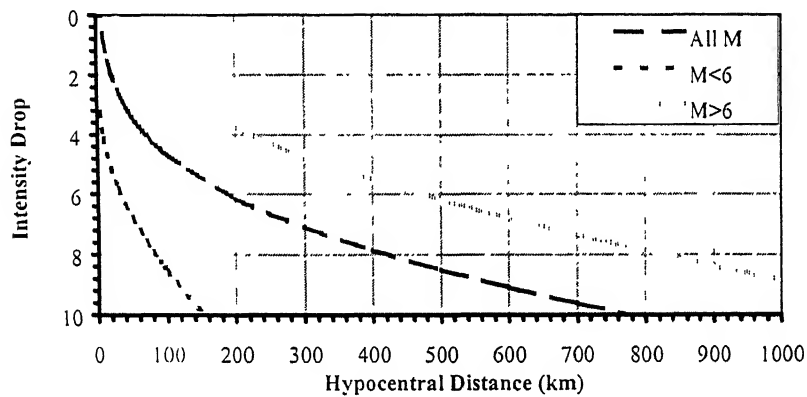


Figure 5.5 Plot of attenuation rates of different earthquake group for northwest province as per equation 10.

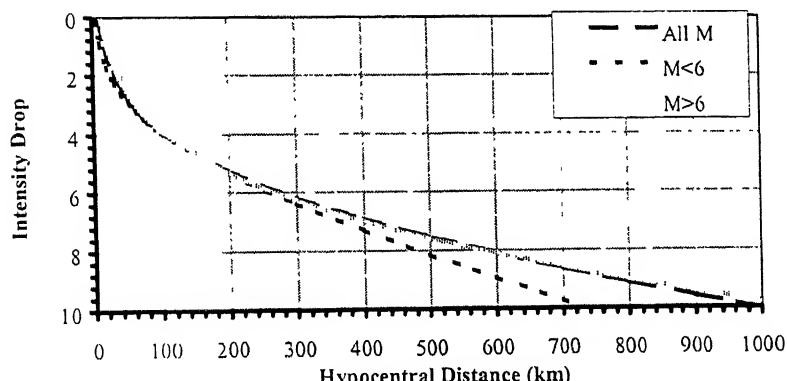


Figure 5.6 Plot of attenuation rates of different earthquake group for peninsular province as per equation 10.

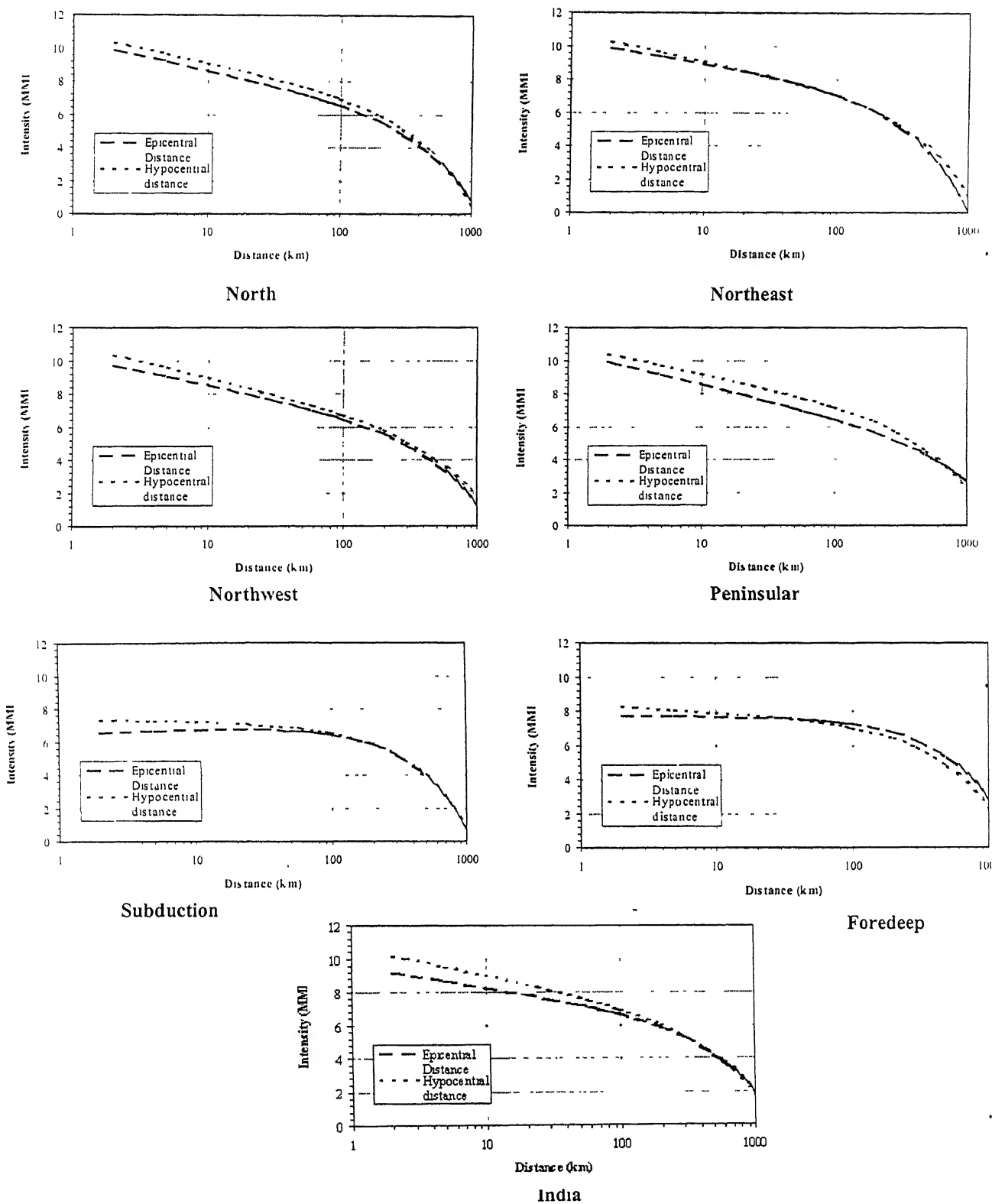


Figure 5.7 Attenuation pattern for different provinces with epicentral and hypocentral distance for M7.0

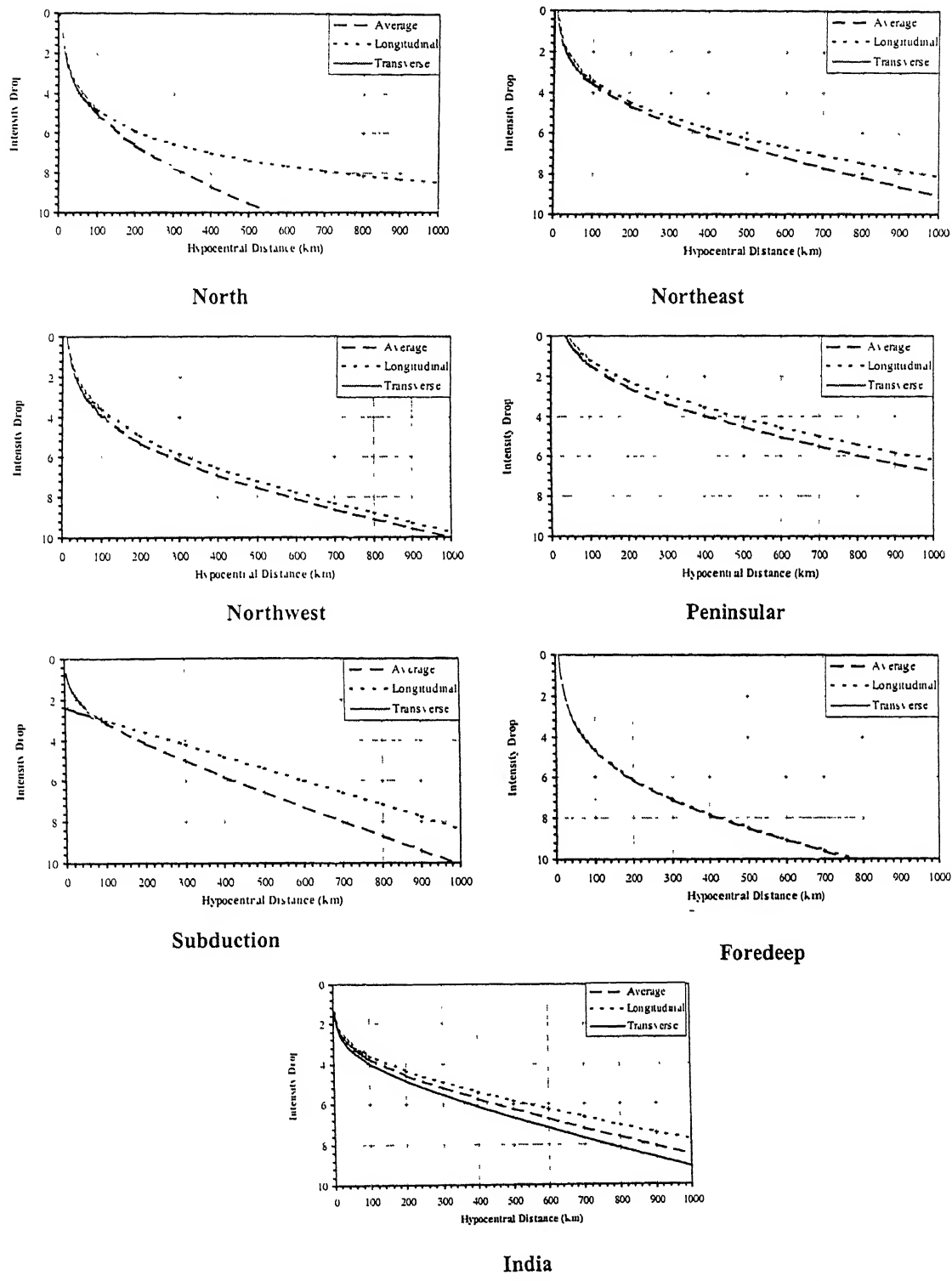


Figure 5.8 Plot of attenuation along average, longitudinal and transverse direction for different provinces as per equation 10.

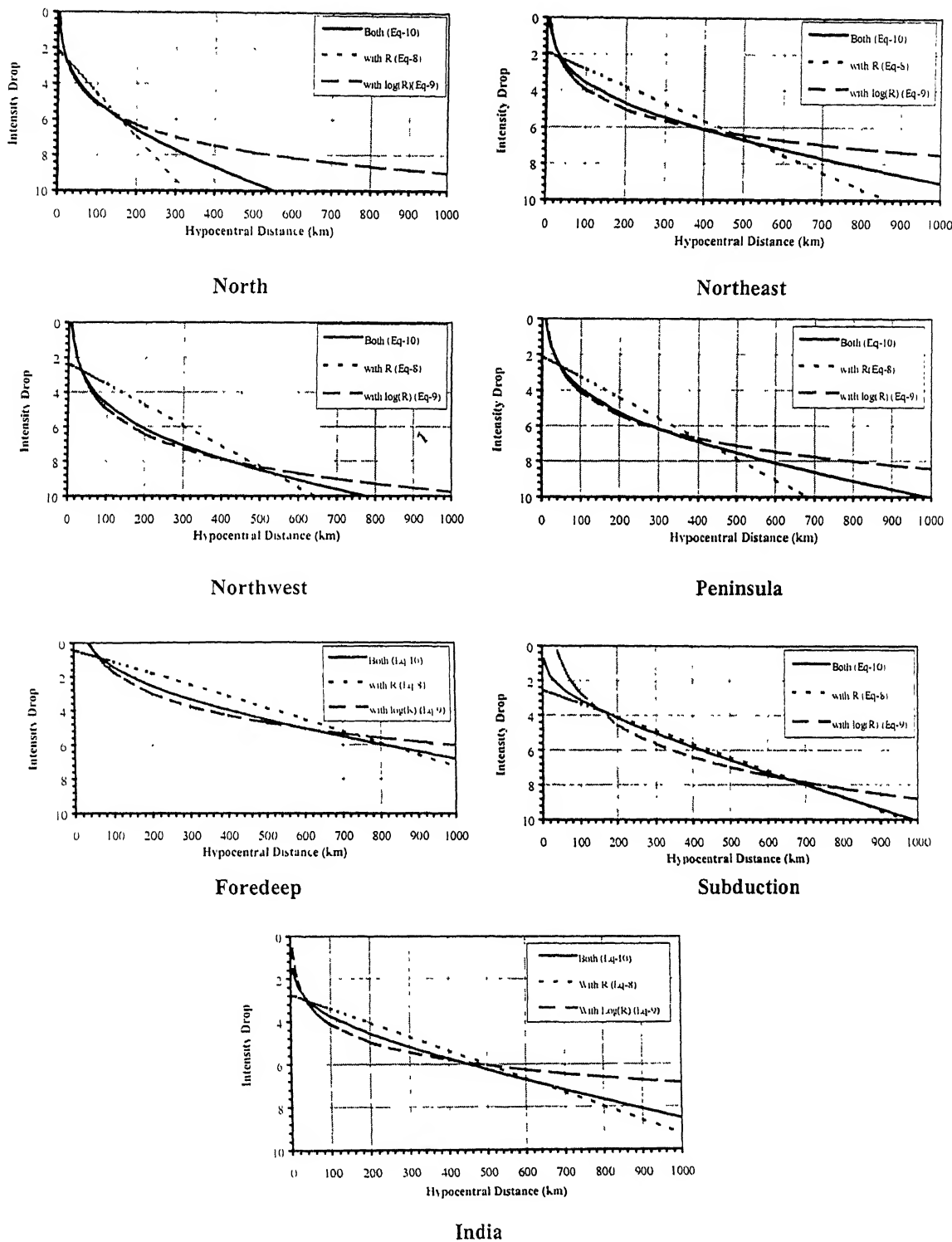


Figure 5.9 Attenuation pattern for different attenuation provinces with distance as parameter (equations 8, 9 and 10)

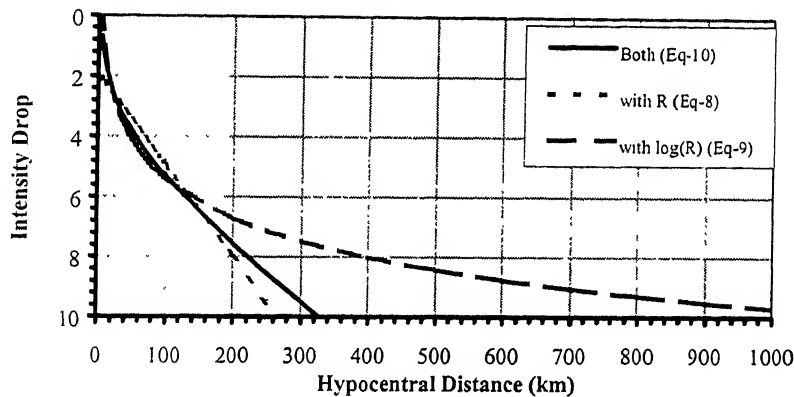


Figure 5.10 Plot of attenuation with different distance parameters for north province considering earthquakes of $M < 6$ (equations 8, 9 and 10).

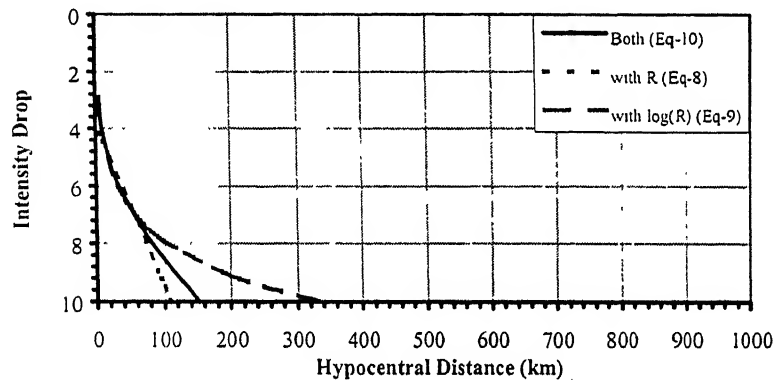


Figure 5.11 Plot of attenuation with different distance parameters for northwest province considering earthquakes of $M < 6$ (equations 8, 9 and 10).

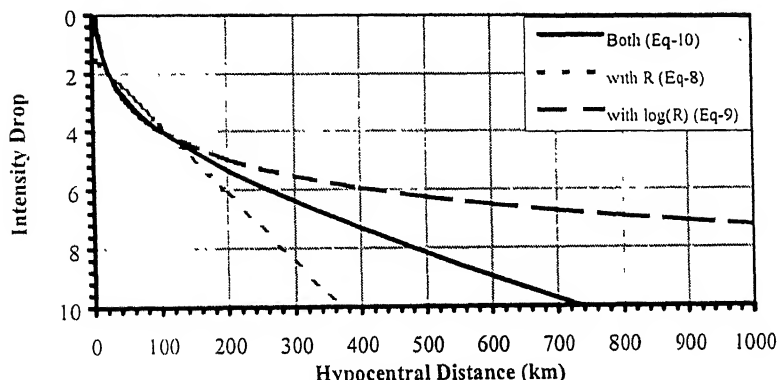


Figure 5.12 Plot of attenuation with different distance parameters for peninsular province considering earthquakes of $M < 6$ (equations 8, 9 and 10).

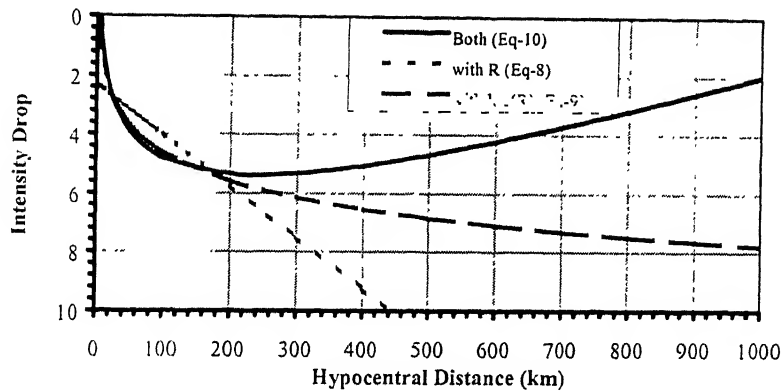


Figure 5.13 Plot of attenuation with different distance parameters for north province considering earthquakes of $M \geq 6$ (equations 8, 9 and 10).

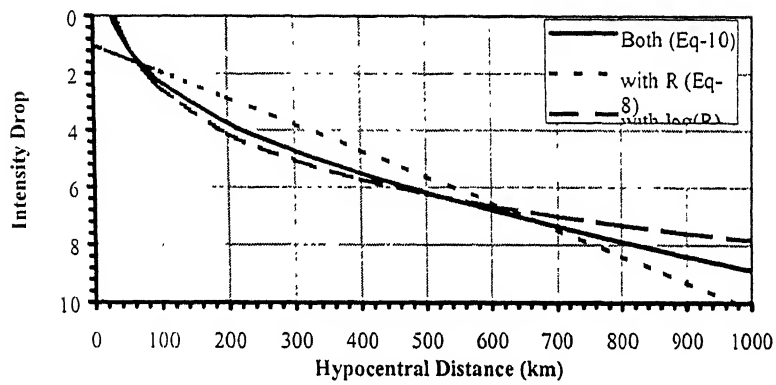


Figure 5.14 Plot of attenuation with different distance parameters for northwest province considering earthquakes of $M \geq 6$ (equations 8, 9 and 10).

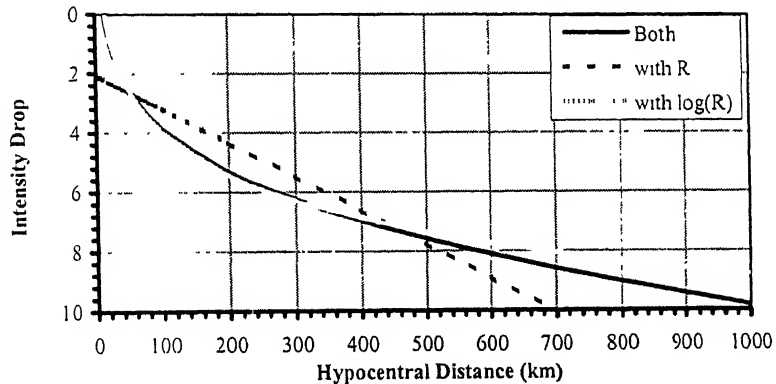


Figure 5.15 Plot of attenuation with different distance parameters for peninsular province considering earthquakes of $M \geq 6$ (equations 8, 9 and 10).

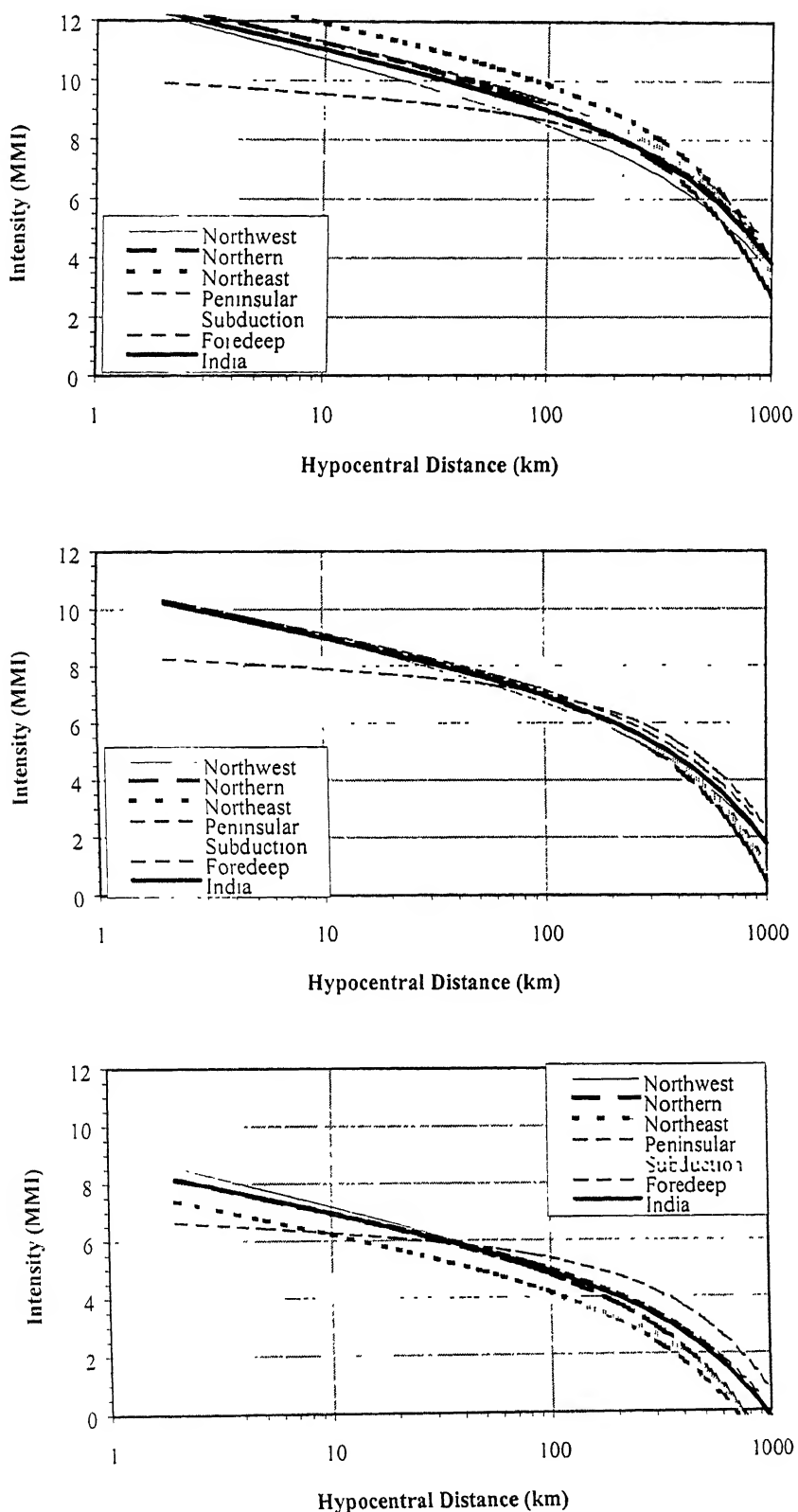


Figure 5.16 Plot of average attenuation for different provinces for magnitude 8.5, 7.0 and 5.5 using equation 3.

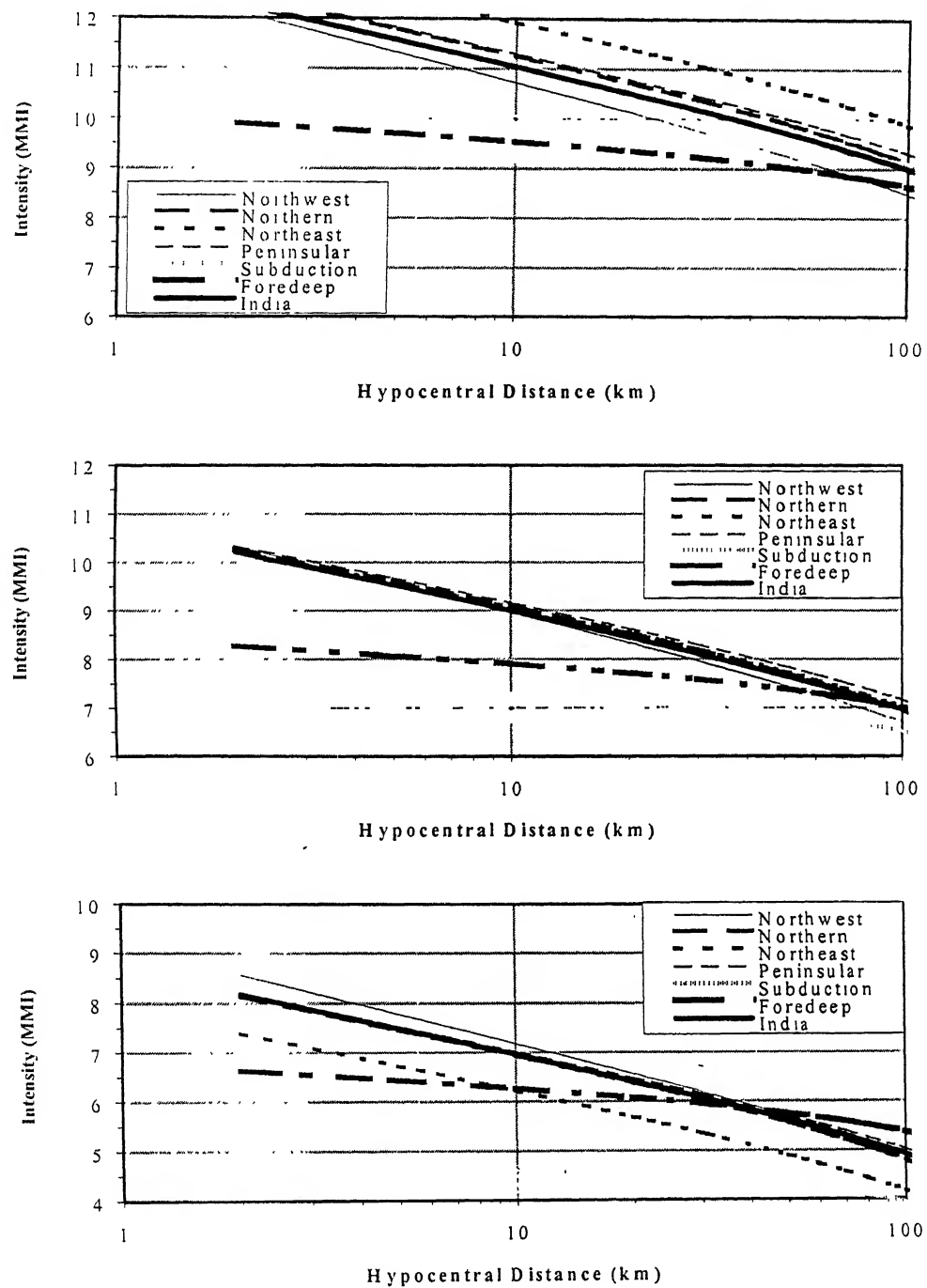


Figure 5.16 Plot of average attenuation for different provinces for magnitude 8.5, 7 and 5.5 using equation 3.

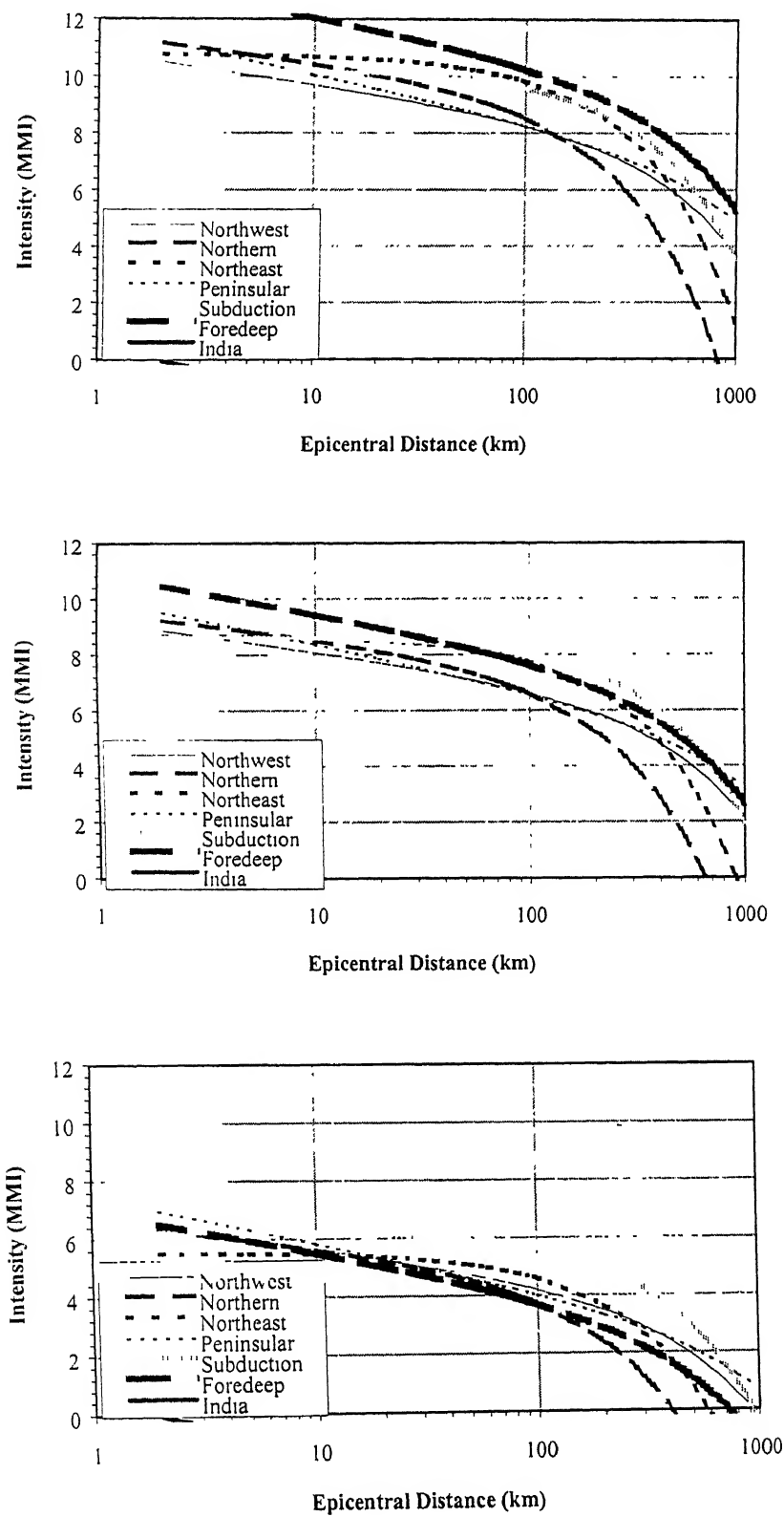


Figure 5.17 Plot of average attenuation for different provinces for maximum intensity 11, 9 and 6.

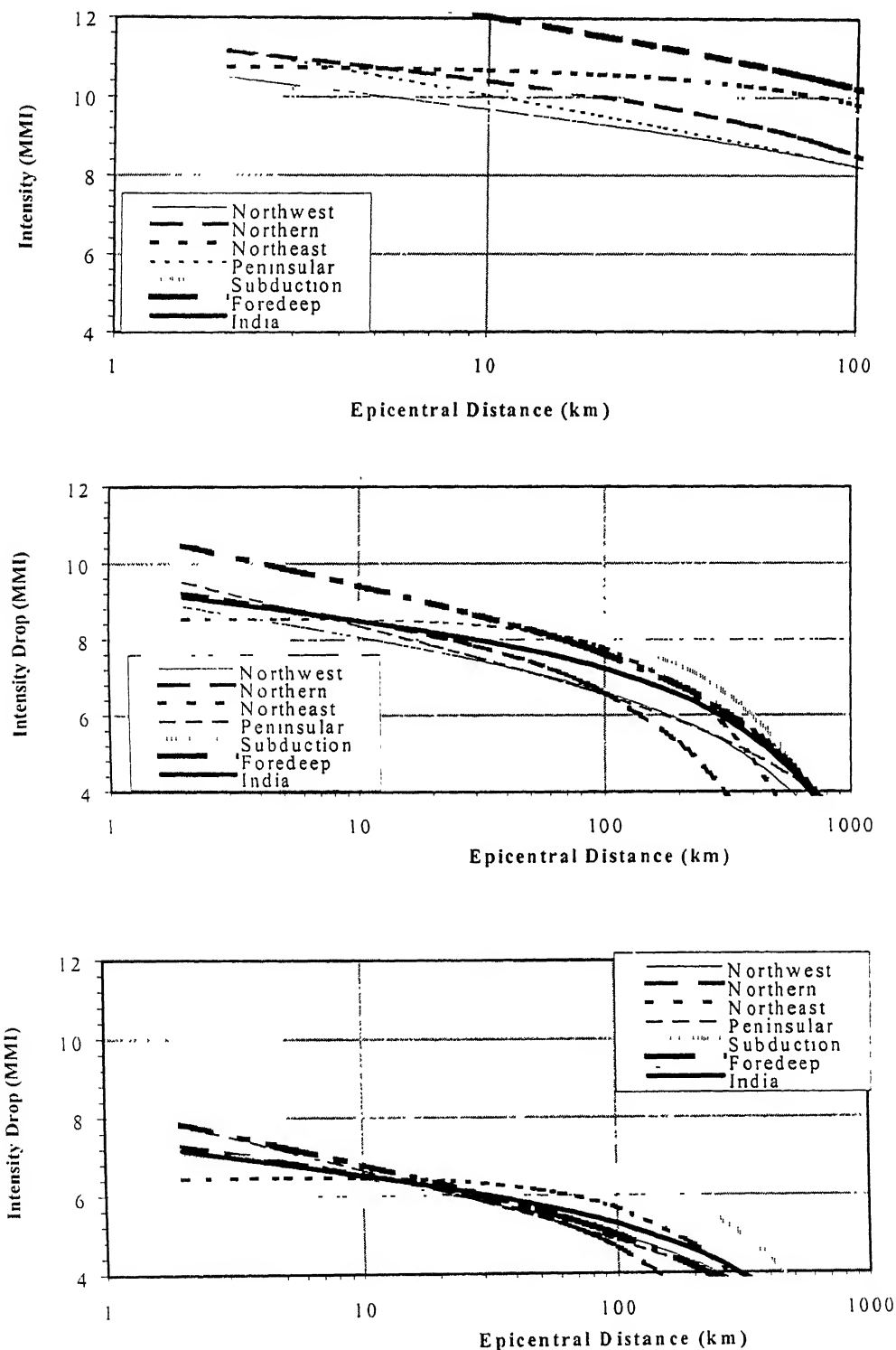


Figure 5.17 Plot of average attenuation for different provinces for maximum intensity 11, 9 and 7.

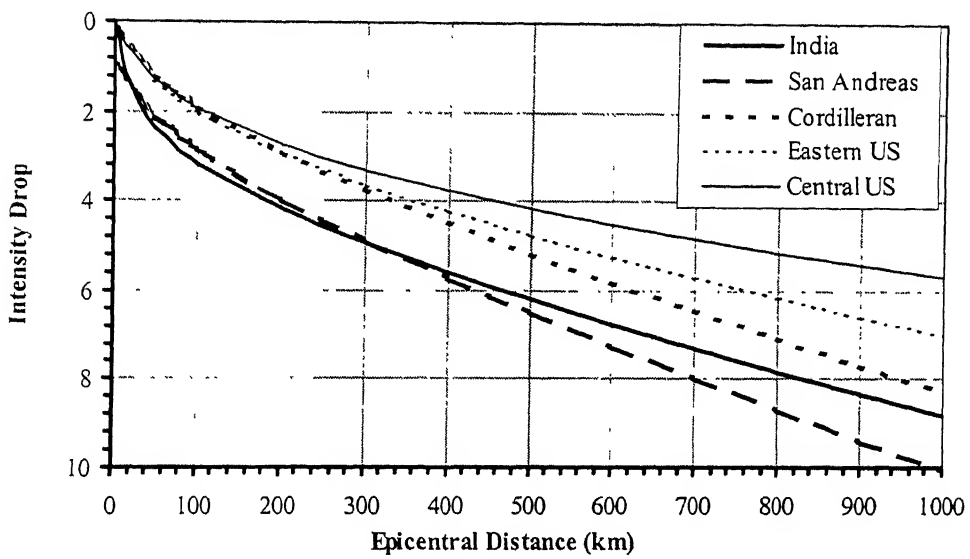


Figure 5.18 Comparison of attenuation pattern of India to that of United States as given by Chandra (1979).

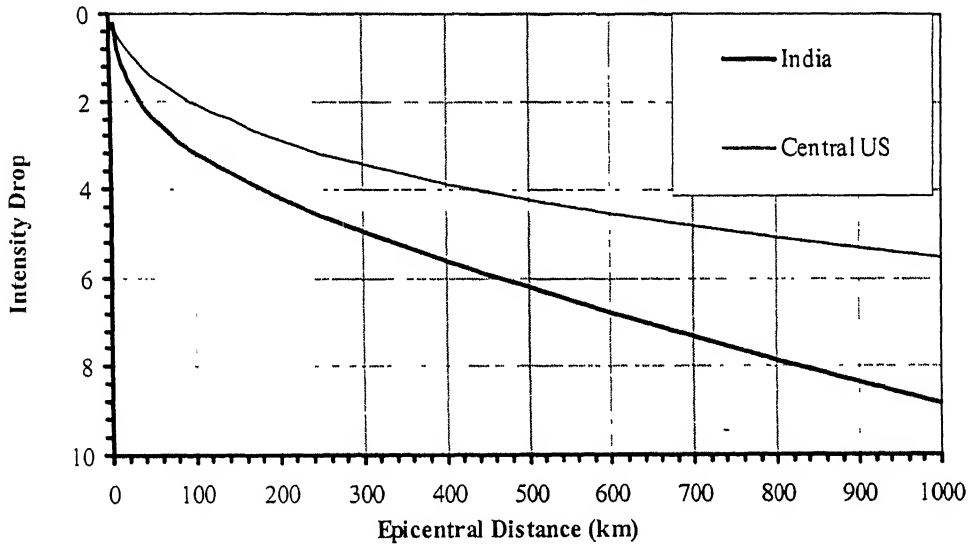


Figure 5.19 Comparison of attenuation pattern of India to that of others as given by Gupta and Nuttli (1976).

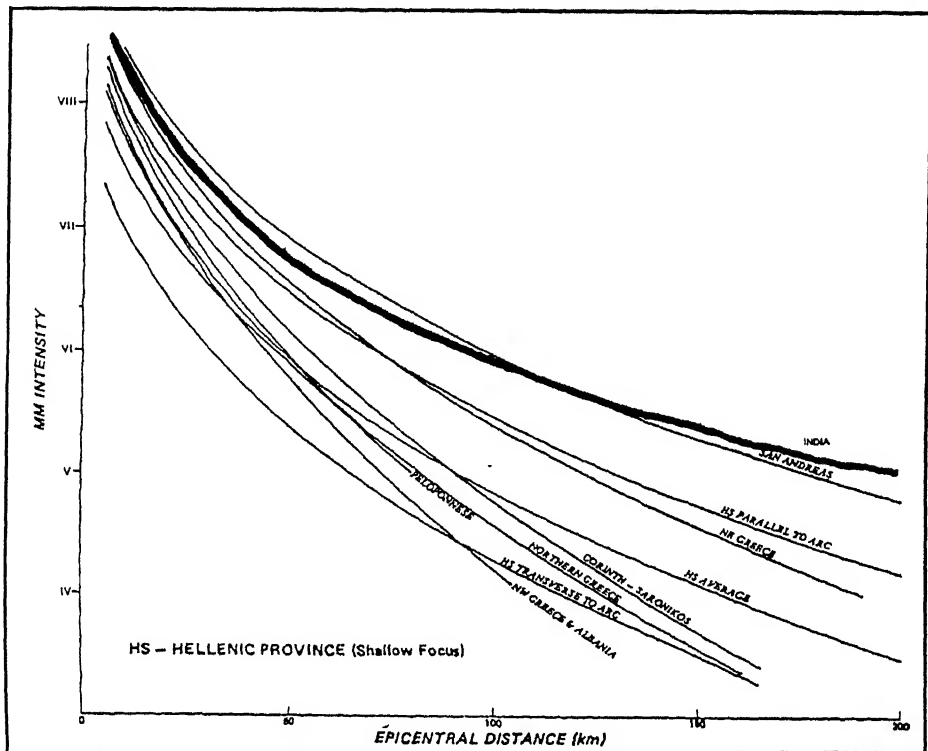


Figure 5.20 Comparison of intensity patterns of India with that of United States (Chandra 1982).

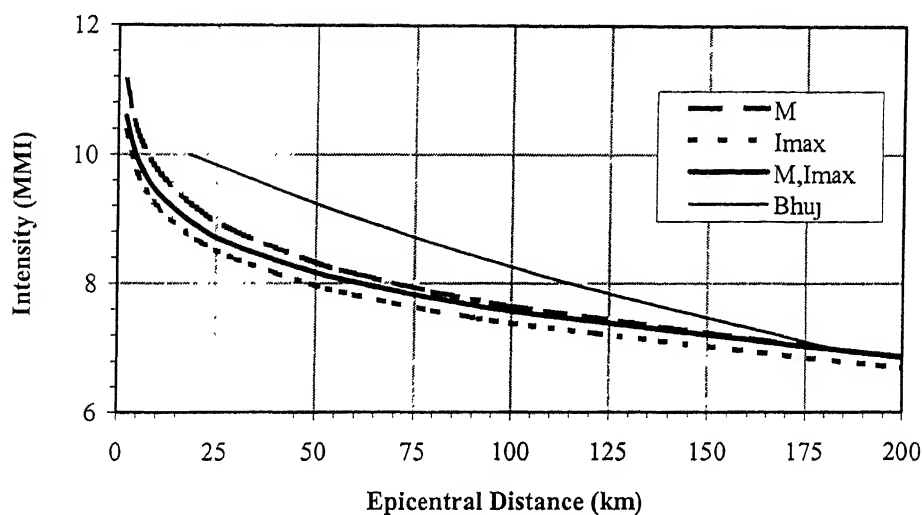


Figure 5.21 Comparison of Bhuj 2001 earthquake data with that of derived equation for Peninsular province (Equations 3, 6, and 7).

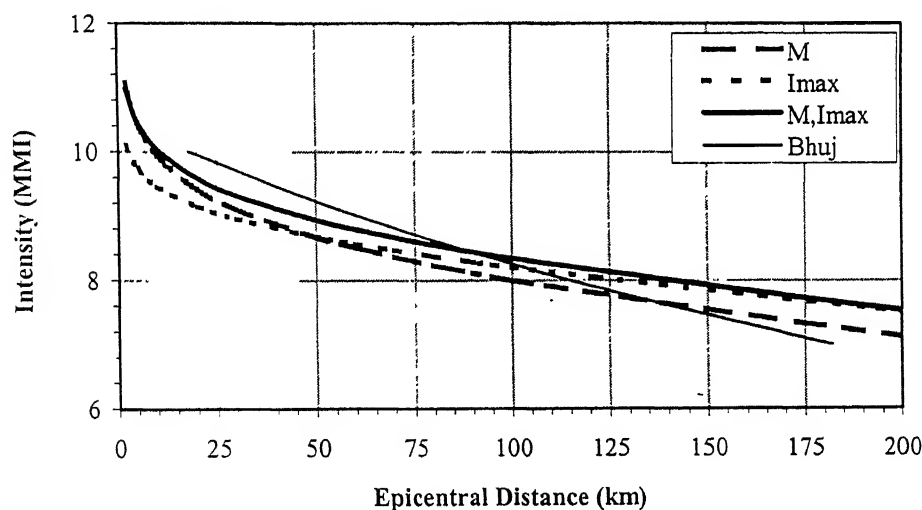


Figure 5.22 Comparison of Bhuj 2001 earthquake data with that of derived equation for Indian Subcontinent (equations 3, 6, and 7).

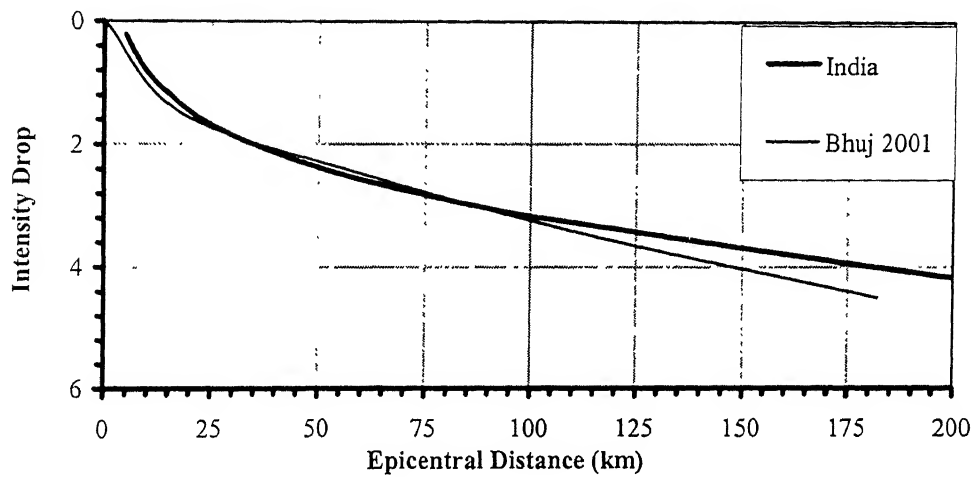


Figure 5.23 Comparison of Bhuj 2001 earthquake data with that of derived equation for Indian Subcontinent (equation 10).

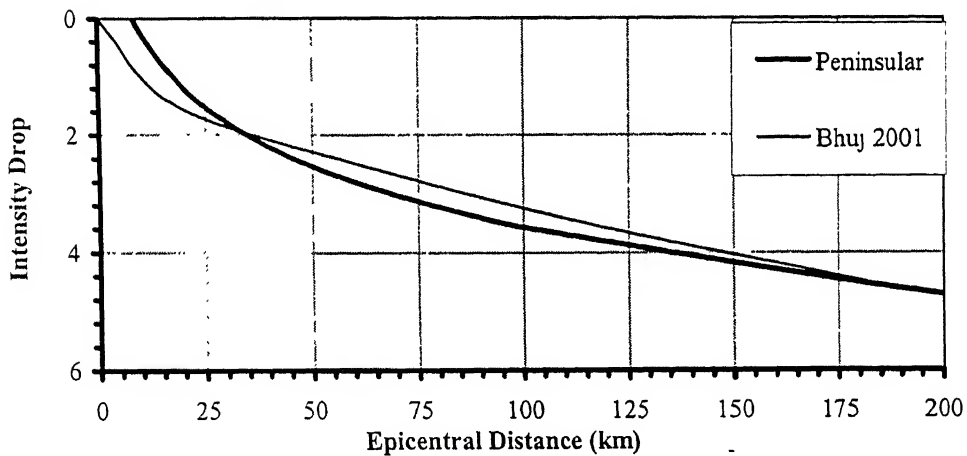


Figure 5.24 Comparison of Bhuj 2001 earthquake data with that of derived equation for Peninsular region (equation 10).

References

- Agrawal, P. N. (1985): "Damage to Buildings during December 31, 1984 Cachar Earthquake, Northeast India", *Records of Geological Survey of India*, Paper No. 241, Vol. 22, No. 2, June 1985, pp. 53-72.
- Ambraseys, N. (1985): "Intensity-Attenuation and Magnitude-Intensity Relationships for Northwest European Earthquakes", *Earthquake Engineering and Structural Dynamics*, Vol. 13, 733-778 (1985).
- Anand, P. S. (1956): "Two Proposed Measure of Seismicity", *Bulletin of the Seismological Society of America*, Vol. 46, pp. 41-45, 1956.
- Anderson, J. H. (1978): "On the Attenuation of Modified Mercalli Intensity with Distance in the United States", *Bulletin of the Seismological Society of America*, Vol. 68, No. 4, pp. 1147-1179, August 1978
- Arya, A. S., Singh, S., Sinvhal, H., Prakash, R., Agarwal, P. N., Khattri, K. N., Prakash, B., and Sinvhal, A. (1977): "A Macroseismic Study of November 6, 1975 Roorkee Earthquake, India". Preprints; *6th World Conference of Earthquake Engineering, New Delhi, January 1977*, Vol. 1, pp. 1:67-1:71.
- Auden, J. B. and Ghosh A. M. N. (1934): "Preliminary Account of Earthquake of 15th January 1934 in Bihar-Nepal", *Memoir of Geological Survey of India*, Vol. 68, Part 2, pp. 177-239.
- Banghar, A. N. (1984): "Kinnur Earthquake of January 19, 1975", *Journal of Association of Exploration and Geophysics*, Vol. 4, No. 4, pp. 1-10.
- Basu, K. L. (1964): "A Note on the Coimbatore Earthquake of Feb. 8, 1900", *Indian Journal of Meteorology and Geophysics*, Vol. XV, No. 2. 1964.
- Brazee, R. J. (1980): "Reevaluation of Modified Mercalli Intensity Scale for Earthquake Using Distance as Determinant (NUREG/CR-1804)", *Washington, D. C., Division of Reactor Safety Research, U.S. Nuclear Regulatory Commission, 1980*, 170 pages.
- Brazee, R. J. (1972): "Attenuation of Modified Mercalli Intensities with Distance for the United States East of 106° W", *Earthquake Notes*, Vol. XLIII, No. 1., March, 1972.
- Kumar, B. (1990): "Preliminary Isoseismal Map of Bihar-Nepal Earthquake of August 21, 1988", *Bulletin of Indian Society of Earthquake Technology*, Paper No. 290, Vol. 27, No. 3, Sept. 1990, pp. 59-63.
- Kumar, B. (1992): "Isoseismal of Burma-India Region Earthquake of August 6, 1988", *Bulletin of Indian Society of Earthquake Technology*, Paper No. 316, Vol. 29, No. 1, March 1992, pp. 57-67.

- Bufaliza, M. A. (1986): "Attenuation of Seismic Intensities with Distance for Mexican Earthquakes", *Laboratorio Nacional De Engenharia Civil, Proceedings of the 8th European Conference on Earthquake Engineering*, pp. 3.1/47-3.1/53, 1986.
- Bulsari, B. S. and Thakkar, M. C. (1970): "Response of Structures in Broach Earthquake", Paper No. 101, ", *Bulletin of Indian Society of Earthquake Technology*, Vol. VII, No. 4, pp. 197-206, Dec. 1970.
- Burton, P. W., McGonigle, R., Neilson, G., and Musson, R. M. W. (1985): "Macroseismic Focal Depth and Intensity Attenuation for British Earthquakes", *Earthquake Engineering in Britain*, Paper 8, Burton et al.
- Campbell K. W. (1997): "Empirical Near Source Attenuation Relationships for Horizontal and Vertical Components of Peak Ground Acceleration, Peak Ground Velocity, and Pseudo-Absolute Acceleration Response Spectra", *Seismological Research Letters*, Vol. 68, No. 1, pp. 154-177, Jan./Feb. 1997.
- Chandra, M., McWhorter, J. G., and Ali A. N. (1979): "Attenuation of Intensities in Iran", *Bulletin of the Seismological Society of America*, Vol. 69, No. 1, pp. 237-250, February 1979.
- Chandra, U. (1977): "Earthquake in Peninsular India-A Seismotectonic study", *Bulletin of the Seismological Society of America*, Vol. 67, No. 5, pp. 1387-1413, October 1997
- Chandra, U. (1979): "Attenuation of Intensities in the United States", *Bulletin of the Seismological Society of America*, Vol. 69, No. 6, pp. 2003-2024, December 1979.
- Chandra, U. (1980): "Attenuation of Intensity in India, Istanbul", *Turkish National Committee on Earthquake Engineering et al., Proceedings of the Seventh World Conference on Earthquake Engineering*, pp. 521-524.
- Chandra, U. (1982a): "Attenuation of Intensity with Distance in Greece", *Proceedings of the Third International Microzonation Conference Seattle*, June 28-July 1, 1982, Place of Publication and Publisher unknown, 1982, Volume 2, pp. 542-552.
- Chandra, U. (1982b): "Attenuation of Strong Ground Motion in India and Neighboring Regions", *VII Symposium on Earthquake Engineering, University of Roorkee*, Nov. 10-12, 1982 Vol. I.
- Chandra, U. (1982): "Attenuation of Strong Motion in India and Neighboring Regions", *VII Symposium on Earthquake Engineering, University of Roorkee*, Nov. 10-12, 1982 Vol. 1.
- Chaturvedi et al. (2000): "Macroseismic Study, Jabalpur earthquake, 22 May, 1997", *A Geoseintific Study, Geological Survey of India Special Publication*, No. 51, July 2000.

- Chavez, M., and Castro, R. (1988): "Attenuation of Modified Mercalli Intensity with Distance in Mexico", *Bulletin of the Seismological Society of America*, Vol. 78, No. 6, pp. 1875-1884, December 1988.
- Coulson, A. L. (1929): "The Epicenter of the Northwest Himalaya Earthquake of the 1st February, 1929", *Records of Geological Survey of India*, Vol. 63, Part 4, pp. 434-443.
- Coulson, A. L. (1938): "The Hindukush Earthquake of the 14th November 1937", *Records of Geological Survey of India*, Vol. 73, Part 1, pp. 135-144.
- Coulson, A. L. (1940): "An Earthquake in the Great Pamir", *Records of Geological Survey of India*, Vol. 75, Professional Paper No. 12, pp.1-11.
- Dasgupta, A., Srivastava, H. N. and Basu M. S. (1982): "Source Mechanism of Earthquake in Kangra-Chamba Regions of UP, India", *Bulletin of Indian Society of Earthquake Technology*, Vol. 19, No. 3. pp. 102-116.
- Dasgupta, S. (1993): "Tectonologic Framework of the Eastern Gangetic Foredeep Bihar-Nepal Earthquake, August 20, 1988", *Geological Survey of India Special Publication*, No. 31, pp.61-69.
- Dasgupta, S. et al. (2000): "Seismotectonic Atlas of India and its Environs", *Book Publised by Geological Survey of India*.
- Drakopoulos, J. and Stamelou I. (1986): "Intensity-Distance Relations Along Maximum and Minimum Axis of a proposed Elliptical Isoseismal Maps in Western Greece", *Proceedings of the 8th European Conference on Earthquake Engineering, Lisbon Portugal, Sep. 7-12, 1986. Lisbon, Laboratprio Nacional de Engenharia Civil, 1986*, pp. 3-1/79-3-1/86.
- Draper, N. R. and Smith, H. (1998): "Applied Regression Analysis", *John Wiley & Sons*.
- Duggal, R. and Sato. N. (1989): "Damage Report of the Bihar-Nepal Earthquake of August 21, 1988", *Earthquake Disaster Mitigation Engineering Laboratory, Institute of Industrial Science, University of Tokyo, March 1989*.
- Ergin, K. (1969): "Observed Intensity-Epicentral Distance Relations in Earthquakes", *Bulletin of the Seismological Society of America*, Vol. 59, No. 3, pp. 1227-1238, June, 1969.
- Evernden, J. F. (1975): "Seismic Intensities, Size of Earthquake and Related Parameters", *Bulletin of the seismological society of America*, Vol. 65, No. 5, pp. 1287-1313, October 1975.
- Geological Survey of India (1992): "Uttarkashi Earthquake, October 21, 1991", *Geological Survey of India Special Publication*, No. 30, 1992.

- Gosain, N. and Arya, A. S. (1967): "A Report on Anantnag Earthquake of February 20, 1967.", *Bulletin of Indian Society of Earthquake Technology*, Vol. 4, No. 3, pp. 11-39, Sept. 1967.
- Gosavi, P. D., Bapat A. V. and Guha, S. K. (1977): "Macroseismic Studies of Four Recent Indian Earthquakes". *Preprints: VI World Conference Earthquake Engineering*, New Delhi 1977, Vol. 1, pp. 1:49-1:54.
- Grandori, G., Perotti, F. and Tagliani, A. (1987): "On the attenuation of Macroseismic Intensity with Epicentral Distance", *Ground Motion and Engineering Seismology*, pp. 581-594.
- Grandori, G., Drei, A., Garavaglia, E., and Molina, C., (1988): "A New Attenuation Law of Macroseismic Intensity", *Proceedings of Ninth World Conference on Earthquake Engineering*, August 2-9, 1988, pp. II-391-II-396.
- Geological Survey of India GSI (1939): "The Bihar-Nepal Earthquake of 1934", *Memoir of Geological Survey of India*, Vol. 73.
- Guha, S. K. and Gosavi, P. D. (1974): "A Short Note on the Nagaland Earthquake of July 29, 1970, " *Bulletin of Indian Society of Earthquake Technology*, Vol. 11, No. 4, Paper No. 150, Dec. 1974, pp. 116-124.
- Gupta H. K. (1994): "The Deadly Latur Earthquake", *Memoir of Geological Survey of India*, No. 35. pp. 1-5.
- Gupta I. D., Joshi R. G., Rambabu V. and Gowda B. M. R. (1999): "Attenuation of MMI with Distance in Peninsular India", *European Earthquake Engineering 1999*.
- Gupta, I. D., and Trifunac, M. D. (1988): "Attenuation of Intensity with Epicentral Distance in India", *Soil Dynamics and Earthquake Engineering*, 1988, Vol. 7, No. 3, pp. 162-169.
- Gupta, I. D. (1986): "On Using Modified Mercalli Intensity Data for Evaluating Engineering Seismic Risk in Northern India", *Records of Geological Survey of India*, Paper No. 247, Vol. 23, No. 1, March 1986, pp. 17-33.
- Gupta., I. N., and Nuttli, O. W. (1976): "Spatial Attenuation of Intensities for Central U.S.", *Bulletin of the Seismological Society of America*, Vol. 66, No. 3, pp. 743-751, June
- Gupta, K. H., Mohan I., and Narin, H. (1972): "The Broach Earthquake of March 23, 1970", *Bulletin of the Seismological Society of America*, Vol. 62, No. 1, pp. 47-61, February, 1972.
- Gupta, S. K., Kumar, S., Jalote, P. M., Sharan, R. B. and Relan, A. K. (1986): "A macroseismic study of Dharamsala Earthquake of 26th April, 1986", *Proceeding VIII symposium on Earthquake Engineering, Roorkee*, Vol. 1, pp. 31-38.

- Gupta, S. K. and Sharda, Y. P. (1996): "A Geotechnical Assessment of Delhi Earthquake of July 28, 1994", *Proceeding International Conference on Disasters and Mitigation, Madras, January 1996*, Vol. 1, pp. AI/26-AI/31.
- Gupta, S. K., Kumar, S., Jalote, P. M., Sharan, R. B. and Relan, A. K. (1986): "A Microseismic Study of Dharamsala Earthquake of 26th April, 1986", *Proceeding VIII Symposium on Earthquake Engineering, Roorkee*. Vol. 1, pp.31-38.
- Gutenberg, B. and Richter, C. F. (Second Paper) (1956): "Earthquake Magnitude, Intensity, Energy, and Acceleration", *Bulletin of the seismological society of America*, Vol. 46, pp. 105-145, 1956.
- Gzovsky, M. V. (1962): "Tectonophysics and Earthquake Prediction", *Bulletin of the Seismological Society of America*, Vol. 52, No. 3, July, 1962, pp. 485-505.
- Haron, A. M. (1912): "The Baluchistan Earthquake of 21st October 1909", *Records of Geological Survey of India*, 41 (Part 1).
- Howell, B. F. Jr. and Schultz T. R. (1975): "Attenuation of Modified Mercalli Intensity with Distance from the Epicenter", *Bulletin of the Seismological Society of America*, Vol. 65, No. 3, pp. 651-665, June 1975.
- Iyanger, R. N. and Meera, K. (1984): "Earthquakes in South India on 20th March 1984", Paper No. 233, *Bulletin of Indian Society of Earthquake Technology*, Vol. 21, No. 2, June 1984, pp. 49-61.
- Jain, S. K. (1988): "Indian Earthquakes: An Overview", *The Indian Concrete Journal*, Vol. 72, No. 11, November 1998.
- Jones, E. J. (1885): "Notes on the Kashmir Earthquake of 30th May, 1885", *Records of Geological Survey of India*, Vol. 18, Part 3, pp. 153-155.
- Kaila, K. L. and Sarkar, D. (1978): "Atlas of Isoseismal Maps of Major Earthquakes in India", *Geophysical Research Bulletin*, Vol. 16, No. 4.
- Kaila, K. L. and Narin, H. (1971): "A New Approach for Preparation of Quantitative Seismicity Maps as Applied to Alpide Belt-Sunda Arc an Adjoining Areas", *Bulletin of the seismological society of America*, Vol. 61, pp. 1275-1291, October, 1971.
- Kaila, K. L. and Sarkar, D. (1978): "Atlas of Isoseismal Maps of Major Earthquakes in India", *Geophysical Research Bulletin*, Vol. 16, No. 4.
- Kaila, K. L., Gaur, V. K. and Narain, H. (1972): "Quantitative Seismicity Maps of India", *Bulletin of the seismological society of America*, Vol. 62, pp. 1119-1132, October 1972.
- Kaila, K. L., and Rao, N. M. (1975): "Seismic Zoning Maps of Indian Sub-Continent", *Geophysical Research Bulletin*, Vol. 17, No. 4, pp. 293-301.

- Kapila, I. P. (1959): "Aseismic Design of Bhakra Dam Project", *Proceeding First Symposium Earthquake Engineering, Roorkee*.
- Karnik, V., and Algermissen, S. T., (1978): "Seismic Zoning, The Assessment and Mitigation of Earthquake Risk", *UNESCO*, pp. 11-47, 1978.
- Khattri, K. N., Rogers, A. M., and Perkins, D. M. (1983): "Estimates of Seismic Hazard in Northwestern India and Neighborhood", *Paper No. 226, Bulletin of Indian Society of Earthquake Technology*, Vol. 20, No. 1, March 1983, pp. 1-22.
- Krishna, J. (1964): "Engineering Aspects of Badgom Earthquake of 2nd Sept. 1963". *Proceeding III World Conference on Earthquake Engineering*, Vol. 3, pp. V-113.
- Krishnaswamy, V. S. (1962): "Probable Correlation of the Structural and Tectonic Features of the Punjab-Himachal Pradesh Tertiary Re-entrant with the Patterns of Seismity of the region", *Proceeding 2nd Symposium Earthquake Engineering, Roorkee*, pp. 437-464.
- Kumar, A., Agarwal, P. N. and Chandrashakaren, A. R (1981): "A Study of Indo-Nepal Earthquake of May 21, 1979", *Proceeding Symposium on Earthquake Disaster Mitigation, Roorkee*, Vol. I, pp. 43-51.
- Kumar, S, Gupta, S. K., and Jalote, P. M. (1981): "A Macroseismic Study of 14th June 1978, Dharamsala Earthquake, Himachal Pradesh", *Records of Geological Survey of India*, Vol. 12, No. 8, pp.84-88.
- Lee, V. W., and Trifunac, M. D. (1985): "Attenuation of Modified Mercalli Intensity for Small Epicentral Distance in California", *University of Southern California, Department of Civil Engineering*, Report No. CE 85-01, Oct. 1985.
- Makjanic, B. (1982): "On the Generalized Exponential Distribution of Earthquake Intensity and Magnitude", *Bulletin of the seismological society of America*, Vol. 72, No. 3, pp. 981-986, June 1982.
- Malone, S. D., and Bor, S. (1979): "Attenuation Pattern in the Pacific Northwest Based on Intensity Data and the Location of the 1872 North Cascades Earthquake", *Bulletin of the Seismological Society of America*, Vol. 69, No. 2, pp. 531-546, April 1979.
- Maugeri, M., and Motta, E. (1993): "Attenuation Laws of Seismic Intensity in the Regions of Sicily and Calabria", *Soil Dynamics and Earthquake Engineering 12* (1993) 25-35.
- Middlemiss, C. S. (1905): "Preliminary Account of the Kangra Earthquake of 4th April 1905", *Records of Geological Survey of India*, Vol. 32, Part 4, pp. 258-294.

- Middlemiss, C. S. (1910): "The Kangra Earthquake of 4th April 1905". *Memoir of Geological Survey of India*, Vol. 38, pp. 1-409 (Reprint: 1981).
- Mohammadi, J. and Suen, S. J. (1986): "Effects of Source Parameters on Seismic Risk Analysis", *Proceedings of the 8th European Conference on Earthquake Engineering*, pp. 2.4/47-2.4/53, 1986.
- Mohan, I. and Rao, M. N. (1994): "A field Study of Latur (India) Earthquake of 30th September 1993", *Memoir Geological Society of India*, No. 35, 1994, pp. 7-32.
- Molnar, P. (1987): "The Distribution of Intensity Associated with the 1905 Kangra Earthquake and Bounds on the Extent of Rupture Zone", *Journal of Geological Survey of India*, Vol. 29, pp. 221-229.
- Mortgat, C. P., Lawrence H. W., and Don L. B. (1981): "Seismic Hazard Analysis: A Methodology for the Eastern United States", *Earthquakes and Earthquakes Engineering: The Eastern United States*, Vol. 2, pp. 883-893. 1981.
- Mukherjee, S. M. (1942): "Seismological Features of Satpure Earthquake of the March 14, 1938", *Proceedings of the Indian Academy of Sciences*, Vol. 16, pp. 167-175, 1942.
- Mukherjee, S. M. (1950): "Remarks on Two Hindukush Earthquake Shocks", *Indian Journal of Meteorology and Geophysics*, Vol. 1, No. 4, pp. 297-302.
- Muktinath, K. N. and Srivastave, J. P. (1968): "The Delhi Earthquake of 27th Aug., 1960", *Records of Geological Survey of India*, Vol. 65, No. 2, pp. 367-382.
- Narula P. L. and Shome, S. K. (1992): "Macroseismic Studies of Recent Earthquakes in Northwest Himalayas", *Current Science*, Vol. 62, No. 1&2, pp. 24-33.
- Narula, P. L., Shome, S. K., Kumar, S. and Pande, P. (1995): "Damage Patterns and Delineation of Isoseismals of Uttarkashi Earthquake of 20th Oct. 1991", *Memoir of Geological Survey of India*, Vol. 30, pp. 1-17.
- Narula, P. L., Pande, P., Gupta, S. K., Venkatramana, N. V. and Harendranath, L. (1996): "Geotechnical Assessment of Isoseists, Killari Earthquake", *Geological Survey of India, Special Publication 37*, 1996, pp. 149-164.
- Narula, P. L. and Chaubey, S. K. (2001): "Macroseismic Surveys for the Bhuj (India) Earthquake of 26th January 2001", www.nicee.org.
- Nuttli, O. W. (1973): "The Mississippi Valley Earthquakes of 1811 and 1812: Intensities, Ground Motion and Magnitudes", *Bulletin of the Seismological Society of America*, Vol. 63, No. 1, pp. 227-248, February 1973.
- Oldham, R. D. (1899): "Report on the Great Earthquake of 12th June, 1897", *Memoir of Geological Survey of India*, Vol. 29 (Reprint 1981).

- Oldham, R. D. (1926): "The Kutch Earthquake of 16th June 1819 with A Revision of the Earthquake of 12th June 1897", *Memoir of Geological Survey of India*, Vol. 46, Part 2.
- Oldham, T. (1882): "The Cachar Earthquake of 10th January 1869", *Memoir of Geological Survey of India*, Vol. 19, Part 1, pp. 1-98.
- Oldham, T. (1883): "A Catalogue of Indian Earthquakes from the Earliest To the End of AD 1869", *Memoir of Geological Survey of India*, Vol. 19, Part, 3.
- Pande, P., Gupta, S. K., Sharda, Y. P., Joshi, K. C. Babu, P. A. R. and Uppadhyay, M. C. (1994): "Geoseismological Study of Bhind Earthquake of September 1, 1994", *Records of Geological Survey of India*,
- Pantea, A., (1994): "Macroseismic Intensity Attenuation for Crustal Source on Romanian Territory and Adjacent Areas, Natural Hazards", *Journal of the International society for the Prevention and Mitigation of Natural Hazards*, Vol. 10, Pp.65-71, 1994.
- Pietrafesa, M., Termo, A. and Bottari, A. (1990): "A Comparison of Different Attenuation Models for Macroseismic Intensity", *Bollettino Di Geofisica Teorica Ed Applicata*, Vol. 32, N. 127-128-September-December 1990, pp. 743-751.
- Poddar, M. C. (1952): "Preliminary Report on the Assam Earthquake of 15th August 1950", *Bulletin Geological Survey of India*, Sec. B, No. 2, pp. 1-40.
- Prasad, Y. J. J. (1991): "Attenuation Characteristic of Strong Seismic Ground Motion in India", *Thesis report submitted at IIT Kanpur, 1991*.
- Rai, D. C., Narayan, J.P., Pankaj and Kumar, A. (1997): "Jabalpur Earthquake of May 22, 1997", *Reconnaissance Report, Department of Earthquake Engineering, University of Roorkee*.
- Ramakrishnan, M., Rastogi, B. K., Narula, P. L., Kamble, V. P., and Gupta, G. D. (1995): "Workshop on Killari Earthquake of 30 September 1993 at Hyderabad", *Geological Survey of India, Special Publication No. 27*. pp. 1-6.
- Rao, R. B., Rao, P. T. S. K., and Rao, S. P. (1982): "A Relationship of Intensity, Epicentral Distance, Focal Depth, Magnitude and Acceleration", *Geophysical Research Bulletin*, Vol. 20, No. 4, pp.191-204.
- Rao, C. (1989): "On Applying the Concept of Rupture Propagation to Deduce the Location of 1905 Kangra Earthquake Epicenter", *Journal of Geological Survey of India*, Vol. 33, pp. 150-158.
- Rastogi, B. K. and Chadha, R. K. (1995): "Intensity and Isoseismals of Uttarkashi Earthquake of October 20, 1991", *Memoir 30, Geological Survey of India*, 1995, pp. 19-24.

- Reiter, L. (1991): "Earthquake Hazard Analysis", *Columbia University Press*, New York.
- Richter C. F. (1969): "Elementary Seismology", *Eurasia Publishing House (Pvt Ltd.)*, 1st edition, 1969.
- Sharma, M. L., and Agrawal, P. N. (1994): "A Comparative Study of Few Attenuation Relationships", *Proceedings of Tenth Symposium on Earthquake Engineering*, Nov. 16-18, 1994, Roorkee.
- Shanker, R. and Narula, P. L. (1999): "Chamoli Earthquake of 29th March", 1999-A Preliminary Appraisal, Volume 52, No. 1 & 2, (January-June, 1998), pp. 141-150.
- Sinvhal, A., Bose, P. R. and Dubey, R. N. (1994): "Damage Report of the Latur-Osmanabad Earthquake of September 30, 1993", *Bulletin of Indian Society of Earthquake Technology*, paper No. 339, Vol. 31, No. 1, March 1994, pp. 15-54.
- Singh, S., Jain, A. K., Singh, V. N. and Srivastava, L. S. (1977): "Damage During Kinnaur Earthquake of January 19, 1975 in Himachal Pradesh, India", Reprints: VI World Conference of Earthquake Engineering, New Delhi 1977, pp. 1:01 - 1:06.
- Sinha, K. K., (1993): "Isoseismal Studies of Bihar-Nepal Earthquake: August 20, 1988", *Geological Survey of India Special Publication*, No. 31, pp. 49-57.
- Srivastava, H. N. (1993): "National and International Status of Seismological Observations over Last 25 Years", *Bulletin of the Seismological Society of America*, Vol. 30, No. 2, pp. 61-76, June 1993.
- Srivastava, V. K., Singh, B. K., Narayan, S. and Jayapaul, D (1981): "Note on Earthquake of 29th July, 1980 Around Dharchula Area, Pithoragarh District, Utterpradesh", *Indian Minerals*, Vol. 35, No. 1, pp. 27-28.
- Stuart, M. (1918): "Preliminary Note on the Srimangal Earthquake of July 8th, 1918", *Records of Geological Survey of India*, Vol. 49. Part 3, pp. 173-189.
- Stuart, M. (1926): "The Srimangal Earthquake of 8th July 1918", *Memoir of Geological Survey of India*, Vol. 46, pp. 1-70.
- Kumar, S., Srivastava, M. S., Sinha, P., Srivastava, D., Srivastava, V. B. and Nagar, M. (1989): "A Macro-Seismic Study on the Effects of Indo-Nepal Border Earthquake of 21st August, 1988 in the Eastern Districts of UP", *Records of Geological Survey of India*, Vol. 122, Part 8, pp. 207.
- Tandon, A. N. and Chaudhury, H. M. (1968): "Koyna Earthquake of Dec. 1967", *Scientific Report No. 59, Indian Meteorological Department, New Delhi, April, 1968*.
- Tandon, A. N. (1972): "Anantnag Earthquakes (February To April, (1967))", *Indian Journal of Meteorological Geophysics*, Vol. 23, pp. 491-502.

- Tandon, A. N. (1975): "Some Typical Earthquakes of North and West Uttarpradesh", *Bulletin of Indian Society of Earthquake Technology*, Vol. 12, No. 2, pp. 74-85.
- Tao, X., and Zheng (1991): "Intensity Attenuation Relationships for Seismic Zonation of China", *Proceedings of Fourth International Conference on Seismic Zonation August 25th -29th, 1991*, pp. 431-437.
- Teramo, A., Stillitani, E., and Bottari, A. (1995): "On an Anisotropic Attenuation Law of the Macroseismic Intensity", *Journal of the International Society for the Prevention and Mitigation of Natural Hazards*, Vol. 11, pp. 203-221, 1995.
- Thakar, S. K., Paul, D. K., Mukerjee, S., Bandyopadhyay, S., Kumar, A., and Lavania, B. V. K. (1988): "Damage Survey Report on Bihar-Nepal Earthquake of August 21, 1988", *Department of Earthquake Engineering*, University of Roorkee.
- Tilford, N. R., and Chandra, U. (1985): "Attenuation of Intensities and Effect of Local Site Conditions on Observed Intensities During the Corinth, Greece, Earthquakes of 24 and 25 Feb. and 4 Mar. 1981", *Bulletin of the Seismological Society of America*, Vol. 75, No. 4, pp. 923-937, August 1985.
- Timiovska, L. S. (1992): "A Note on Attenuation of Earthquake Intensity in Macedonia", *Soil Dynamics and Earthquake Engineering* 11 (1992) 457-463.
- Timiovska, L. S. (1992): "Determination of Intensity Attenuation of Earthquakes Based on the Probability Approach", *Tenth World Conference on Earthquake Engineering*, pp. 305-310, 1992.
- Trifunac, M. D. and Brady, A. G. (1975): "On the Correlation Os Seismic Intensity Scale with the Peaks of Recorded Strong Motion", *Bulletin of the Seismological Society of America*, Vol. 65, No. 1, pp. 139-162, February 1975.
- Varma, M. M., Gosavi, P. D. and Guha, S. K. (1970): "Kothagudam (Andhra Pradesh) Earthquake of April 13, 1969, Broach (Gujarat) Earthquake of March 23, 1970 and Seismcity of Peninsular India", *Bulletin of Indian Society of Earthquake Technology*, Vol. 4, No. 4, Dec. 1970.
- Varma, G. S. (1975): "Seismicity of North-East India, Paper No. 156", *Bulletin of Indian Society of Earthquake Technology*, Vol. 12, No. 3, pp. 113-119 Sep. 1975.
- Vanmarcke, E. H., and Lai, S. P. (1980): "Attenuation of Intensity with Epicentral Distance in the Phillipines", *Bulletin of the Seismological Society of America*, Vol. 70, No. 4, pp. 1287-1291, August 1980.
- Wakhloo, G. L, (1977): "The Badgom Earthquake of Sep. 2, 1963, Srinagar District, Jammu and Kashmir". *Records of Geological Survey of India*, Vol. 108, Pt. 2, pp. 112-123.

- Wakhaloo, G. L, and Rastogi, S. P. (1977): "The Anantnag Earthquake of Feb. 20, 1967, Anantnag District, Jammu and Kashmir", *Records of Geological Survey of India*, Vol. 108, Pt. 2, pp. 124-135.
- Wang, F., Rachel D. and Bendimerad, F., (1995): "Attenuation of Intensity with Epicentral Distance in Jamaica", Proceedings of the Fifth International Conference on Seismic Zonation, Nice, France, Oct. 17-18-19, 1995. Nantes France, Ouest Editions, 1995, Vol. 2. pp. 1197-1204.
- West, W. D. (1934): "The Baluchistan Earthquakes of August 25th and 27th, 1931", *Memoir of Geological Survey of India*, Vol. 67, Part 1, pp. 1-82.
- West, W. D. (1937): "Earthquakes in India, Presidential Address, Proceeding 24th Session", *Indian Science Congress*, Sec. 3, pp. 189-227.
- Wood, H. O. and Neuman, F. (1931): "Modified Mercalli Intensity Scale of 1931". *Bulletin of the Seismological Society of America*, Vol. 21, No. 21, No. 4, pp. 277-283.
- Yarar, R., Ergunay, O., Erdik, M., and Eren, K. (1984): "Attenuation of Intensities in Turkey", *Proceedings of Eight World Conference on Earthquake Engineering*, July 21-28, 1984, Vol. 2, pp. 343-350.

